

CONTAMINANT LEACHING FROM  
CEMENT-BASED WASTE FORMS  
UNDER ACIDIC CONDITIONS

By  
PIERRE COTE

A Thesis  
Submitted to the School of Graduate Studies  
In Partial Fulfilment of the Requirements  
for the Degree  
Doctor of Philosophy

McMaster University

February 1986 ©

Appendix Tables of a thesis (1986)

Contaminant leaching from cement-based  
waste forms under acidic conditions.

By Pierre Coté  
McMaster University  
Civil Engineering Department

This diskette contains the following files,  
part of the thesis Appendices I and II:

- TableI3 : Source code of the program LEEQ.
- TableI4 : Definition of the input data requirement for  
the program LEEQ.
- TableI5 : Source code of the program LEEEX.
- TableI6 : Definition of the input data requirement for  
the program LEEEX.
- TableII3 : Sample input data file: S27.
- TableII4 : Sample output data file: S27.
- TableII5 : Sample input data file: S28.
- TableII6 : Sample output data file: S28.

# LEACHING FROM CEMENT-BASED WASTE FORMS

DOCTOR OF PHILOSOPHY (1986)  
(Civil Engineering)

McMASTER UNIVERSITY

TITLE: Contaminant Leaching From Cement-based  
Waste Forms under Acidic Conditions

AUTHOR: Pierre Côté B. Ing. (Université de Montréal)  
M. Sc. A. (Université de Montréal)

SUPERVISOR: Professor Andrew Benedek

NUMBER OF PAGES: xvii , 295

## Abstract

### CONTAMINANT LEACHING FROM CEMENT-BASED WASTE FORMS UNDER ACIDIC CONDITIONS.

by Pierre Côté

A waste form can be prepared by mixing a hydraulic cement and, if needed, a bulking agent with an aqueous waste to cause it to solidify. A mechanistic leaching model was developed based on describing the chemistry of the waste form-leachant system and the flow regime of the leachant and assuming that transport takes place via diffusive exchanges through the waste form-leachant interface. This model was successful in predicting leaching from simple waste matrices and in identifying important containment mechanisms effective in the more complex matrices.

The cement-based waste forms studied had porosities ranging from 40 to 60%. Portland cement provided acid neutralization capacity to maintain the high pH environment where the waste form is stable; a typical waste form contains enough cement to neutralize between 2000 to 3000 times its volume of a pH 3 leachant.

In a mild environment, leaching was controlled by the diffusion of the soluble fraction of a contaminant present in the connected pores of the matrices. Immobile species instantaneously solubilized to maintain chemical equilibrium between the soluble and insoluble

fractions. In tests conducted over a period of almost 2 years, less than 1% of the initial amount of cadmium, chromium and lead contained in a specimen leached out.

In an acidic environment, the leaching rates were limited by the availability of acid to dissolve the matrix. The leaching process was similar to a surface corrosion process. However, since waste matrices are not completely soluble in a mild acid, a leached layer develops, eventually protecting the core of the waste form from direct contact with aggressive groundwaters. Contaminants solubilized at the leaching front are subjected to concentration gradients that force them to diffuse both inward and outward. Only a fraction of the total concentration therefore leaches out.

The mechanistic knowledge developed through the experimental programme and the modelling effort was used to develop eight long term leaching scenarios covering a wide range of waste form and groundwater conditions. In addition to allowing the prediction of leaching rates for periods of up to 100 years, these scenarios were useful in developing recommendations to prepare more efficient waste forms and design better landfills.

## ACKNOWLEDGMENTS

This research was conducted at the Wastewater Technology Centre and supported financially by Environment Canada. My gratitude goes to the following:

Dr Andrew Benedek for his stimulating role and encouragement in directing the research;

Mr Trevor Bridle and Dr Bruce Jank for their moral and financial support;

Mr Trevor Bridle, Dr Thomas Constable and Mrs Julia Stegemann for their comments and suggestions in editing the thesis;

Messrs Alan Moreira, Daniel Langlais, Donald Hamilton, Daniel Cossette, Michel Lebeuf and Steve Sawell for their assistance with the laboratory experiments;

Dr Philip Malone, Mr Jesse Connor and Mr William Webster for their stimulating advices;

Mr Jim Fraser and the personnel of the Wastewater Technology Centre Analytical Section for performing the chemical analyses;

and Mrs Sonya Perrone for her help in typing the thesis.

♥  
Merci de tout coeur à mon amie  
et compagne Pascale Vignani pour  
son appui et sa patience!

## TABLE OF CONTENTS

	<u>Page</u>
Abstract	iii
Acknowledgments	v
List of Figures	x
List of Tables	xiii
List of Symbols	xv
1. INTRODUCTION	1
2. OBJECTIVES	3
3. BACKGROUND	4
3.1 Waste Stabilization/Solidification Technology	4
3.2 Physical Containment of the Waste	7
3.2.1 Hydraulic Cements	8
3.2.2 Hydration of Portland Cement	10
3.2.3 Latent Hydraulic Cements	16
3.2.4 Hydration in an Aqueous Waste Environment	17
3.2.5 Durability of Hydrated Cement	19
3.3 Chemical Fixation of Contaminants	20
3.3.1 Precipitation as Metal Hydroxides	21
3.3.2 Precipitation as Metal Carbonates	24
3.3.3 Precipitation as Metal Sulfides	26
3.3.4 Formation of Metal Silicates	27
3.3.5 Adsorption	30
3.4 Current Data on Waste Form Characteristics	32
3.4.1 Physical and Engineering Properties	32
3.4.2 Leachability	34
4. FORMULATION OF A MODEL	49
4.1 Formalization of the Leaching Phenomenon	49



	<u>Page</u>
4.1.1 Morphology of the Matrix	50
4.1.2 Transport Mechanisms	52
4.1.3 Initial and Boundary Conditions	54
4.1.4 Chemical Reactions	57
4.2 Numerical Solution	59
4.2.1 Equilibrium Chemistry	60
4.2.2 General Flow Diagram	62
5. VALIDATION OF THE NUMERICAL SOLUTION	71
5.1 Criteria for Stability and Convergence	72
5.2 Mass Balance in the Aqueous Solution	73
5.3 Profile in the Porous Matrix for Constant Surface Concentration	74
5.4 Desorption Following a Linear Isotherm	75
5.5 Metal Hydroxide Dissolution	80
5.5.1 Profiles Calculated Using Equilibrium Chemistry (LEEQ)	81
5.5.2 Profiles Calculated Using Titration and Solubility Curves (LEEX)	84
6. EXPERIMENTAL METHODS	88
6.1 Preparation of Waste Form Specimens	88
6.1.1 Materials	88
6.1.2 Mixing and Molding	91
6.2 Characterization of the Specimens	92
6.2.1 Mercury Intrusion Porosimetry	93
6.2.2 Equilibrium Leaching	93
6.2.3 Titration and Solubility (low liquid-to-solid ratio)	94
6.2.4 Titration and Solubility (high liquid-to-solid ratio)	96
6.2.5 Static Leaching	96
6.2.6 Dynamic Leaching (Continuous Flow)	97
6.2.7 Dynamic Leaching (Intermittent Flow)	98

	<u>Page</u>
7. RESULTS AND DISCUSSION	101
7.1 Microstructure of the Waste Forms	102
7.1.1 Particle Size Distribution of Insoluble Powdery Additives	102
7.1.2 Moisture-density Characteristics	102
7.1.3 Mercury Intrusion Porosity	104
7.2 Chemical Containment of Contaminants	107
7.2.1 Distribution of Chemical Species In the Matrix	107
7.2.2 Titration and Solubility	113
7.3 Mechanisms of Leaching	120
7.3.1 Soluble Contaminants	122
7.3.2 Insoluble Contaminants	129
7.4 Long Term Leaching Results	144
7.4.1 Data History	145
7.4.2 Semi-empirical Modelling	150
8. INFERENCE OF LONG TERM LEACHABILITY	159
8.1 Long Term Inference of Leaching Rates	159
8.1.1 Assumptions about Landfilling Conditions	160
8.1.2 Assumptions about the Waste Form	162
8.1.3 Long Term Leaching Scenarios	163
8.2 From Leaching Rates to Concentrations	169
8.3 Practical Implications	171
8.3.1 Preparation of Better Waste Forms	171
8.3.2 The Design of Better Landfills	174
9. CONCLUSIONS	176
9.1 Microstructure	176
9.2 Mechanisms of Containment	177
9.3 Mechanisms of Leaching	179
9.4 Long Term Leachability	180

	<u>Page</u>
10. RECOMMENDATIONS	183
10.1 Modelling	183
10.2 Laboratory Evaluation	184
10.3 Minimization of Field Leaching Rates	186
REFERENCES	188
APPENDICES	196
I Mathematical Model	196
II Simulation Runs	201
III Solidification Additives	206
IV Chronology of the Experimental Programme	210
V Results of Mercury Intrusion	212
VI Results of Total Metal Analysis	219
VII Results of Equilibrium Leaching	223
VIII Results of Titration and Solubility (low L/S)	226
IX Results of Titration and Solubility (high L/S)	236
X Results of Static Leaching	241
XI Results of Dynamic Leaching (continuous flow)	246
XII Results of Dynamic Leaching (intermittent flow)	259
XIII Long Term Leaching Scenarios	283

## LIST OF FIGURES

<u>Figure</u>	<u>Title</u>	<u>Page</u>
3.1	Typical limits of oxide content for several cementing materials.	9
3.2	Diagrammatic representation of the sequence of hydration of cement.	14
3.3	Material balance in the hydration of portland cement.	15
3.4	Theoretical solubility of metal hydroxides.	23
3.5	Conceptual leaching model.	38
3.6	Dependency of the leach rate on the leachant velocity.	40
4.1	Distribution of a chemical element in the waste form matrix.	51
4.2	Representation of the aqueous solution hydraulic regime.	56
4.3	General numerical solution flow diagram.	63
4.4	Representation of the porous matrix for numerical solution.	65
6.1	Set-up for the titration and solubility experiments.	95
6.2	Experimental set-up to obtain kinetic leaching data.	97
6.3	Target and actual leachant velocities for the intermittent flow dynamic leaching test.	100
7.1	Corrected cumulative porosity from mercury intrusion.	106

		<u>Page</u>
7.2	Fraction available for leaching under acidic conditions.	110
7.3	Comparison of measured solubility and hydroxide solubility for Batches A&B.	115
7.4	Comparison of measured solubility and hydroxide solubility for Batches C&D.	115
7.5	Simulation of lithium leaching from the powdered silica matrix (Batch B).	123
7.6	Simulation of lithium leaching from the fly ash-cement matrix (Batch C).	125
7.7	Simulation of lithium leaching from the fly ash-cement matrix (Batch D).	128
7.8	Simulation of cadmium leaching from the powdered silica matrix (Batch A).	130
7.9	Simulation of the reactor's pH in the leaching of the powdered silica matrix (Batch A).	131
7.10	Simulation of cadmium leaching from a powdered silica-cement matrix (Batch B).	133
7.11	Simulation of static leaching from a fly ash-cement matrix (Batch C).	135
7.12	Soluble metal profile as a function of time.	140
7.13	Leaching efficiency of cadmium under acidic conditions for various waste form matrices.	144
7.14	Fraction of the total mass leached in the long term dynamic leaching tests.	146
7.15	pH histories for the long term dynamic leaching tests.	148
7.16	Modelling the leaching of arsenic from the dynamic leaching tests.	154

		<u>Page</u>
7.17	Modelling the leaching of cadmium from the dynamic leaching tests.	154
7.18	Modelling the leaching of chromium from the dynamic leaching tests.	155
7.19	Modelling the leaching of lead from the dynamic leaching tests.	155
8.1	Layout of a waste form in a landfill.	160
8.2	Inference of leaching rates following different disposal scenarios.	165
8.3	Simplified groundwater mixing model.	170
8.4	Groundwater contaminant concentration based on the simple mixing model represented by Figure 8.3.	170

# LIST OF TABLES

<u>Table</u>	<u>Title</u>	<u>Page</u>
3.1	Stabilization/solidification systems for hazardous wastes.	6
3.2	Typical mineral composition of various portland cements.	11
3.3	Principal chemical reactions in the hydration of portland cement.	12
3.4	Metal hydroxide equilibrium chemistry.	22
3.5	Metal carbonate equilibrium chemistry.	25
3.6	Metal sulfide equilibrium chemistry.	28
5.1	Comparison of the model to an analytical solution for desorption following a linear isotherm.	78
5.2	Initial composition of the waste form pore solution.	81
5.3	Evaluation of the relative precision of the numerical solution.	84
6.1	Summary of the experimental testing programme.	89
6.2	Chemical analysis of the solidification additives.	91
6.3	Molds used to prepare specimens for leaching tests.	92
7.1	Moisture-density relationships of the specimens prepared in the laboratory.	103
7.2	Results of the equilibrium leaching experiment.	109
7.3	Acid neutralization capacity of waste forms.	119

		<u>Page</u>
7.4	Analysis of the dynamic leaching tests.	141
7.5	Mass of contaminants leached after 665 days in the dynamic leaching tests.	149
7.6	Coefficients for the leaching model represented by Equation 7.3.	153



# LIST OF SYMBOLS

$dz$	: thickness of a slice in the numerical solution [L]
$f$	: leachant renewal frequency [1/T]
$i$	: indices used in the numerical solution for nodes or slices
$j$	: indices used for chemical species
$l$	: indices used for chemical components
$m_0$	: initial mass of a chemical species in a specimen [M]
$\Delta m$	: mass leached between time $t$ and $t+\Delta t$
$n_i$	: number of nodes
$n_j$	: number of chemical species
$n_l$	: number of chemical components
$t$	: time [T]
$\Delta t$	: time step in the numerical solution [T]
$u$	: network dissolution velocity [L/T]
$v$	: leachant velocity (Equation 4.6) [L/T]
$w$	: connected pore water content of the porous matrix [M/M;wet weight basis]
$z$	: distance [L]
$\Delta z$	: slice thickness for the numerical solution [L]
$A$	: geometrical surface area of the specimen in contact with the aqueous solution [L <sup>2</sup> ]
$C_0$	: initial concentration in the pore solution [M/L <sup>3</sup> ]

- C : concentration of one soluble species in the leachant ( $C_L$ ),  
in the pore solution ( $C_P$ ) or in the aqueous solution ( $C_W$ )  
[M/L<sup>3</sup>]
- CAL : cumulative amount leached [M]
- C<sub>e</sub> : equilibrium concentration [M/L<sup>3</sup>]
- C<sub>t</sub> : total soluble concentration in the leachant ( $C_{tL}$ ), in  
the pore solution ( $C_{tP}$ ) or in the aqueous solution ( $C_{tW}$ ),  
all species included [M/L<sup>3</sup>]
- C<sub>T</sub> : total concentration available for leaching in terms of mass  
per unit volume of total matrix [M/L<sup>3</sup>]
- D : molecular diffusion coefficient [L<sup>2</sup>/T]
- D<sub>e</sub> : effective diffusion coefficient [L<sup>2</sup>/T]
- D<sub>s</sub> : molecular diffusion coefficient corrected for matrix  
tortuosity [L<sup>2</sup>/T]
- F : cumulative fraction leached [ ]
- H<sub>c</sub> : cumulative amount of acid added to one slice in terms of  
weight of acid per wet weight of porous matrix [ ]
- L : leaching rate in term of mass per unit geometrical surface  
area [M/L<sup>2</sup>·T], or space dimension
- K : linear adsorption isotherm coefficient [ ]
- M : mass dimension
- M<sub>o</sub> : waste specimen mass [M]
- M<sub>s</sub> : mass of one slice of matrix in the numerical solution [M]
- Q : leachant flow rate [L<sup>3</sup>/T]
- R : reaction rate [M/L<sup>3</sup>·T]

$T$  : time dimension or diffusion coefficient correction factor  
 $V$  : volume of the aqueous solution [ $L^3$ ], Equation 4.3 or  
       volume of the leaching specimen [ $L^3$ ], Equation 3.4  
 $V_w$  : amount of interconnected water in one slice [ $L^3$ ]  
 $W$  : molecular weight  
 $B$  : specimen geometrical surface area-to-leachant volume  
       ratio [ $1/L$ ]  
 $\gamma_b$  : bulk density of the porous matrix [ $M/L^3$ ]  
 $\gamma_w$  : density of water [ $M/L^3$ ]  
 $\phi$  : connected porosity [ $]$   
 $\theta$  : duration of a leaching period [ $T$ ]

## 1. INTRODUCTION

Present hazardous waste management alternatives can be grouped, based on the nature of the waste. Concentrated organic wastes can be detoxified through biological or chemical oxidation and even destroyed by incineration. Inorganic wastes can sometimes be chemically rendered less toxic but ultimately need to be disposed of by concentration and safe storage. Toxic organics are often present in low concentrations in inorganic matrices and need to be safely disposed of with inorganic wastes.

Large volumes of hazardous wastes are produced as aqueous solutions or suspensions of contaminants. These wastes can be isolated from the environment through inclusion in a waste form. A cement-based waste form consists of a skeletal structure of insoluble, non-toxic substances, with the pores impregnated by the waste.

Toxic metals and other contaminants are physically contained in a waste form and are often also immobilized through various chemical mechanisms. These contaminants can be released to the environment if the waste form comes into contact with natural waters. Of particular interest are the leaching situations where the waste form is contacted with acidic waters since several contaminants become more mobile in a low pH environment.

Proper management strategies for waste forms or solidified wastes could be established provided the mechanisms of contaminant containment

were known and the long term leaching behavior could be inferred. Little information of a mechanistic nature has been generated on the subject of pollutants immobilization in cement-based waste forms. Existing leaching tests are empirical and their results do not lend themselves to extrapolation over long periods of time.

Therefore, there is a need to develop a mechanistic understanding of contaminant containment in cement-based waste forms and to formulate mathematical models to help estimate their long term leachability. This fundamental understanding will be useful in designing better landfills and in selecting more appropriate leaching tests for the evaluation of waste forms.

## 2. OBJECTIVES

The objectives of this thesis are:

- i) to determine the mechanisms of containment of inorganic contaminants in cement-based waste forms,
- ii) to determine the mechanisms of leaching in neutral and acidic environments, and
- iii) to identify the rate-limiting leaching mechanisms to allow inference of long term leachability.

These were achieved by first conducting a thorough review of the literature. The mechanisms of containment were studied by characterizing the microstructure of typical waste forms and by doing equilibrium leaching tests. A mechanistic leaching model was developed to interpret the results of kinetic leaching tests and to determine the rate-limiting leaching mechanisms. Long term leaching scenarios are proposed based on the information gathered and on various groundwater conditions.

The research program generated fundamental information to allow:

- i) preparation of more durable waste forms,
- ii) design of landfills with the appropriate levels of environmental protection,
- iii) identification of relevant laboratory testing methods to evaluate cement-based waste forms, and
- iv) development of mathematical models for the long term inference of leachability.

### 3. BACKGROUND

This chapter starts with a review of waste stabilization and solidification technology, focusing on cement-based waste forms applied to inorganic aqueous wastes. The mechanisms of contaminant containment are then examined, from a physical (Section 3.2) and from a chemical (Section 3.3) point of view. Finally, the engineering and leaching properties of waste forms are reviewed in Section 3.4.

#### 3.1 Waste Stabilization/Solidification Technology

The stabilization/solidification technology comprises unit operations to transform a hazardous waste into a waste form suitable for land disposal. Stabilization refers to those aspects of the technology which result in detoxifying the waste through destruction or fixation of the contaminants that it contains. Solidification is related to those operations which improve the physical and handling characteristics of the waste.

A historical development of the technology was presented by Conner (1979). Prior to 1970, residues were solidified to improve their physical characteristics. These include radioactive wastes that were solidified in drums for transportation, mine tailings that were treated to be used as backfill and fly ash-lime mixtures used as a base for road construction. In the early seventies, fly ash and lime started being

used to solidify flue gas desulphurization sludges and a process based on soluble silicates and cement was applied to a variety of sludges from manufacturing, metal producing and metal finishing operations. During the seventies, the implementation of more stringent environmental laws stimulated the development of several new processes. In the same period, the emphasis of the benefits of the technology went from "production of a solid mass" to "reducing the leachability of the waste".

Several state-of-the-art reviews of the technology have been published (Conner, 1979; Pojasek, 1979b; Environmental Laboratory (WES), 1980; Poon et al, 1983). Stabilization/solidification processes are often classified based on the principal additives used to obtain a solid matrix. Various systems based on inorganic or organic additives are listed in Table 3.1. The systems based on inorganic additives all use some kind of hydraulic cement. Portland cement is most frequently used but other types of cement have also been used: aluminous cement, natural cement, slag cement, pozzolanic cement and gypsum cement. Those processes will hereafter be referred to as cement-based processes. Most of the organic-based processes involve mixing a waste with a prepolymer and adding a catalyst to produce a solid mass.

Organic-based processes are normally hydrophobic; they are therefore best suited for organic waste streams such as hydrocarbons or pesticides. When used with aqueous wastes, water is either evaporated in thermosetting processes (e.g. bitumen) or encapsulated within the polymer matrix in catalyst-based processes. In the latter case, contaminated weep water is often produced since polymerization takes



place at low pH (e.g. urea-formaldehyde process). Organic-based waste forms normally show low contaminant leachability since the matrices are impervious. However, there is usually no reaction between the waste constituents and the polymer. Since the system does not destroy, detoxify or insolubilize the hazardous constituents, the long term stability of the waste form depends entirely on its physical integrity. Organic-based processes are energy intensive, requiring high cost additives and sophisticated blending equipment. Their use has been practically limited to high hazard, low volume wastes such as radioactive wastes. They will not be considered further in this study.

Table 3.1 Stabilization/solidification systems for hazardous wastes (adapted from Conner (1979)).

Cement-based Systems

cement  
lime-cement  
pozzolan-lime  
pozzolan-cement  
clay-cement  
soluble silicate-cement  
gypsum

Organic-based Systems

urea formaldehyde  
polybutadiene  
polyester  
epoxy  
acrylamide gel  
bitumen

Cement-based processes are well suited to the treatment of aqueous waste since cement needs water for hydration. A cement-based waste form is a porous matrix whose permeability is a function of the pore structure and the amount of water originally present in the waste. The leachability of a contaminant thus depends on whether it remains in

solution in the pore system or is immobilized through chemical reaction. Cement-based processes create an alkaline environment suitable to the containment of heavy metals. The additives, which are often themselves waste materials, are inexpensive and can be blended with the waste using simple equipment. Cement-based processes have been widely used commercially (Pojasek, 1979a).

The applicability of cement-based solidification has been documented and several vendors have published lists of waste streams on which their processes have been used (Pojasek, 1979a). The most common waste streams comprise inorganic materials in aqueous solution or suspension which contain appreciable amounts of toxic heavy metals and/or inorganic salts. It is often necessary to pretreat the waste to render it suitable for cementation (neutralization of acidic wastes), to decrease the mobility of contaminants (oxidation or reduction, precipitation) or to reduce its volume (dewatering). The solids content of the waste can also be adjusted through addition of a water absorbant (ashes, slags, clays) to minimize the amount of cementitious material required. Secondary additives are sometimes used to reduce the leaching of otherwise mobile contaminants (activated carbon, zeolites, high cation exchange capacity clays) or to control the setting properties of cement. The latter will be discussed in the next section.

### 3.2 Physical Containment of the Waste

The most evident benefit of a stabilization/solidification process is the creation of a waste form which has a reduced surface of

contact with the leaching medium. The environmental stability of this waste form is a function of the physical and chemical properties of the cementing materials used to create the solid matrix.

### 3.2.1 Hydraulic Cements

Cement can be defined as a finely powdered, calcareous material that, when mixed with water, forms a plastic paste that sets and eventually hardens to a rock-like consistency (Double and Hellowell, 1977). Figure 3.1 shows the oxide composition of several cementing materials. The cementing property results from high temperature activation of otherwise non-reactive materials.

Portland cement is the most commonly used hydraulic binder. It is a mixture of calcium silicate and calcium aluminate minerals produced by the calcination of limestone and clay (Popovics, 1979).

Alumina cement is fabricated by calcining a mixture of limestone and bauxite (Popovics, 1979). Alumina cement has several properties which make it suited for waste solidification. It uses up about twice as much water for hydration as ordinary portland cement and is more resistant to sulphate and weak acid attack. It has not been used intensively for construction purposes because it tends to weaken with time.

Some of the areas shown on Figure 3.1 define latent hydraulic cements: natural pozzolans, fly ash and blast furnace slag. These

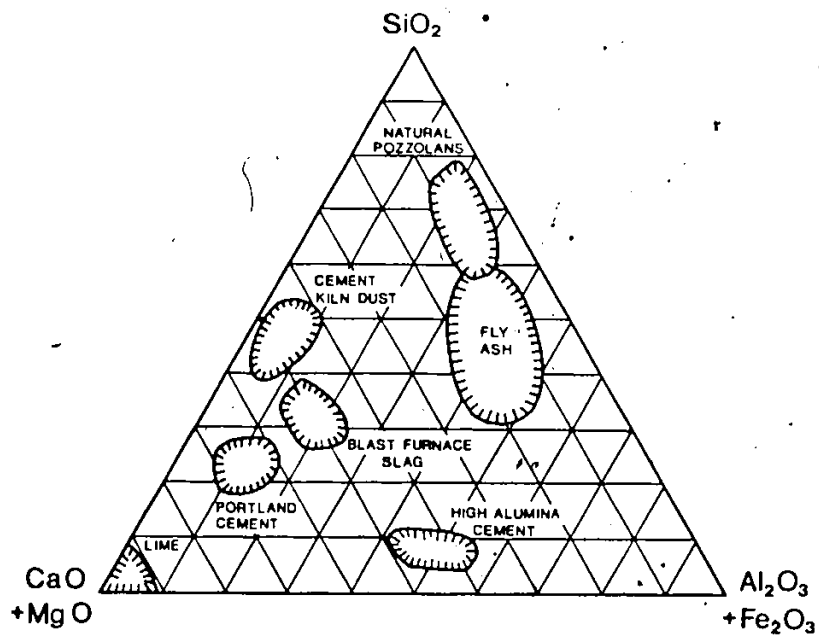


Figure 3.1 Typical limits of oxide content for several cementing materials. Each point in the triangular diagram represents a composition: the perpendicular distance from a point to any side gives the proportion of the component(s) occupying the opposite corner (Adapted from Popovics, 1979).

materials are not cementitious in themselves but contain constituents that combine with lime in the presence of water, at ordinary temperatures, to form compounds of low solubility with cementing properties (Lea, 1970).


Granulated blast furnace slag is a glassy nonmetallic product, consisting of silicates and aluminosilicates of calcium, that is developed simultaneously with iron in a blast furnace and is granulated by quenching the molten slag material in water or steam and air. The slag can be used as an aggregate or ground to increase its reactivity.

The latent hydraulic cements known as pozzolans can be of natural or industrial origin (Popovics, 1979). Naturally occurring pozzolans include volcanic tuffs, diatomaceous earth, opaline cherts and some shales. The most important industrial pozzolan is fly ash, which is the finely divided residue resulting from the combustion of ground or powdered coal. It should be noted that pozzolans have a much lower CaO content than blast furnace slag.

We will briefly review the cementing chemistry and hydrated matrix properties of the cementing materials most relevant to waste solidification.

### 3.2.2 Hydration of Portland Cement

In addition to several textbooks (Lea, 1970; Popovics, 1979), information on the subject of cement chemistry can be obtained from the proceedings of a series of International Conferences on the Chemistry of Cement (Tokyo, 1968; Moscow, 1974; Paris, 1980).



Portland cement contains approximately 65% by weight of calcium oxide but typically less than 1% is present as free CaO. Different types of portland cement can be produced by altering the mineral composition of the raw materials. The mineral composition of the five main types of portland cement in use in North America is presented in Table 3.2. Type I or ordinary portland cement is the general-purpose cement used when the special properties of the other types are not required. Of special interest for waste solidification are Type II and V which show better resistance to sulphate attack. A small amount of gypsum (3 to 5%) is normally mixed with portland cement to control the rate of setting.

Table 3.2 Typical mineral composition of various portland cements (adapted from Popovics, 1979).

<u>Cement</u>	<u>Compound Concentration [%]</u>				<u>Comment</u>
	C <sub>3</sub> S	C <sub>2</sub> S	C <sub>3</sub> A	C <sub>3</sub> AF	
Type I	49	25	12	8	ordinary portland cement
Type II	46	29	6	12	moderate sulfate resistance
Type III	56	15	12	8	high early strength
Type IV	30	46	5	13	low heat of hydration
Type V	43	36	4	12	high sulfate resistance

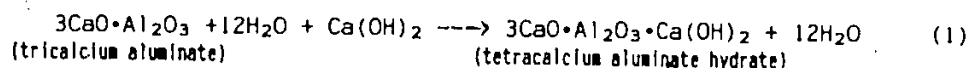
Legend

C<sub>3</sub>S : tricalcium silicate ( $3\text{CaO} \cdot \text{SiO}_2$ )  
 C<sub>2</sub>S : dicalcium silicate ( $2\text{CaO} \cdot \text{SiO}_2$ )  
 C<sub>3</sub>A : tricalcium aluminate ( $3\text{CaO} \cdot \text{Al}_2\text{O}_3$ )  
 C<sub>3</sub>AF : tricalcium aluminoferrite ( $3\text{CaO} \cdot \text{Al}_2\text{O}_3 \cdot \text{Fe}_2\text{O}_3$ )

Table 3.3 lists the principal hydration reactions which take place when portland cement is mixed with water. The compounds formed are complex and are a function of several factors including water-to-cement

ratio and temperature. The different compounds hydrate at various rates, over several months.

Table 3.3 Principal chemical reactions in the hydration of portland cement.



dosed against the amount of calcium aluminate. If it is too small, calcium aluminate hydrate and/or calcium monosulphate aluminate hydrate are produced (Table 3.3, Reaction 1 and 3) in the shape of large tabular crystals which cause quick setting. If the sulphate supply is too great, secondary gypsum precipitates, also causing quick setting.

The hydration of tricalcium silicate and dicalcium silicate, which account for approximately 75% of the dry cement weight, is responsible for the strength development of the cement paste (Table 3.3, Reactions 4 and 5). Hydration results in the formation of calcium silicate hydrate gel (tobermorite gel) and crystalline calcium hydroxide (portlandite).

Double et al (1980) proposed a model for the hydration of the calcium silicates which involves the sequence of events illustrated in Figure 3.2. When cement is contacted with water, there is an initial leaching of lime from the calcium silicate structure through hydrolysis. The calcium ions released into solution then recombine with the hydrosilicate residues left on the surface of the cement grains to precipitate a calcium silicate hydrate (CSH) gel membrane. This membrane allows inward diffusion of water and outward diffusion of  $\text{Ca}^{+2}$  and  $\text{OH}^-$  ions but prevents the outward diffusion of larger ions of hydrolysed silicates. As a result, the concentration of  $\text{Ca}^{+2}$  and  $\text{OH}^-$  ions increases above the solubility product of lime in the solution (the pH might reach 13) and calcium hydroxide is precipitated. Concurrently, the preferential diffusion process leads to the development of an osmotic pressure across the membrane coating the cement grains. This pressure



causes rupture of the membrane and extrusion of hydrosilicate material which combine with calcium ions in solution to precipitate CSH gel as excrescences on the surface of the grains. Interlocking of those tubular excrescences provide dimensional stability to the hydrated mass. The rate of the hydration reaction decreases with time as the thickness of the gel layer through which reactants have to diffuse becomes larger.

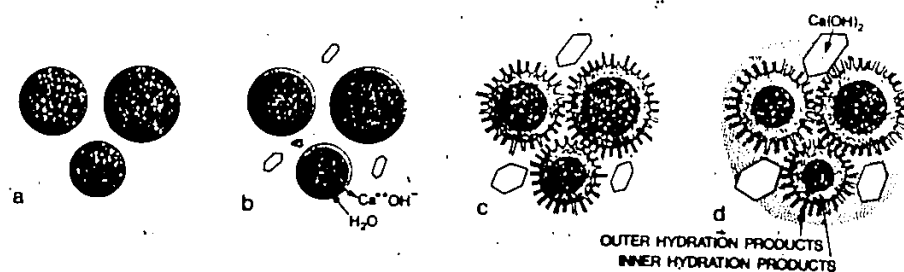


Figure 3.2 Diagrammatic representation of the sequence of hydration of cement. (a) Cement grains in water, (b) initial gel coatings around the cement grains, (c) secondary growth of C-S-H gel after osmotic rupture of gel coatings and (d) long term infilling and consolidation of microstructure (from Double et al, 1980).

A major factor which determines the morphology of the hydrated cement paste is the water-to-cement ratio (W/C). During the process of hydration, the volume of a cement paste specimen remains approximately constant. The relative volume distribution between the different phases, before and after hydration, is presented in Figure 3.3 for two water-to-cement ratios, 0.32 and 0.48 (on a weight basis). At  $W/C=0.32$ , the initial volume is equally split between water and cement. Hydration

proceeds until all the water has been used up. This leaves some cement unhydrated and 7.5% (by volume) of air voids since the volume of water decreases by chemical combination. A  $W/C=0.48$  permits full hydration of the cement leaving 18% of free water and air in the pores.

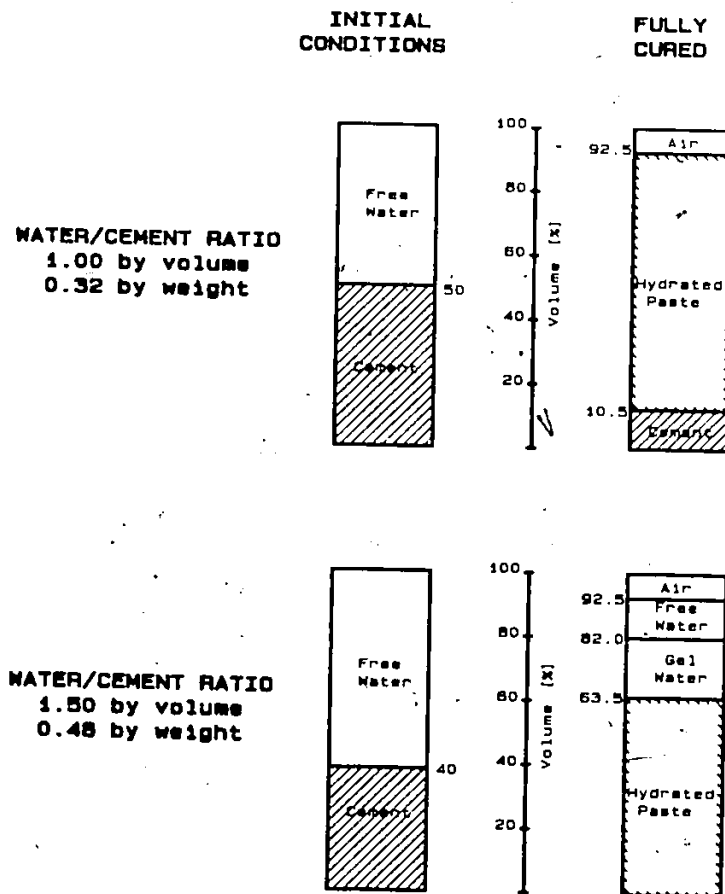


Figure 3.3 .Material balance in the hydration of portland cement when curing conditions are applied where neither access to water nor evaporation are possible (Adapted from Popovics, 1979).

The examples given above show that the volume of cement approximately doubles upon hydration creating a network of gel pores of very small diameter (15-30 Å) (Popovics, 1979). The volume originally occupied by free water forms a void system of much larger pores, the capillary pores. The contribution of these pores to the total porosity increases rapidly with the water-to-cement ratio. As a result, the permeability of the cement paste, which is essentially zero for  $W/C=0.32$ , increases exponentially as  $W/C$  reaches 0.6 to 0.7.

The amount of lime produced as a result of cement hydration is of special importance to waste solidification since it provides acid neutralization capacity. Based on the stoichiometry of Reactions 4 and 5 (Table 3.3) and on a typical cement composition of 50% tricalcium silicate and 25% dicalcium silicate, it can be estimated that full hydration of 1 gram of cement produces 0.3 gram of  $Ca(OH)_2$ . This corresponds to an acid neutralization capacity of 8 meq/g of dry cement. The pH in the pore solution, controlled by the solubility of lime, should be in the range of 12 to 13.

### 3.2.3 Latent Hydraulic Cements

The hydraulic reactivity of slag and pozzolans is mainly a function of the amorphous compounds that they contain (Smolczyk, 1980). Crystalline compounds will also hydrate but at a much slower rate. Modern slags have a glassy content of more than 90% (Smolczyk, 1980). Studies of different fly ashes indicate that the glass content ranges from 70 to 90% (Minnick, 1967). Granulated blast furnace slag can be

activated with a variety of alkalis including soda, lime and gypsum (Daimon, 1980). Fly ash is normally activated with lime. The products of hydration are similar to those of portland cement (e.g. calcium silicate hydrate gel, crystalline aluminate hydrate) without the liberation of  $\text{Ca(OH)}_2$ . If sulphate is present, ettringite will also be formed. The reactions are much slower than that of portland cement; Regourd (1980) observed that hydration of several slag mixtures only started after 28 days. There is no direct method of measuring pozzolanic reactivity other than preparing specimens by mixing with lime or portland cement and measuring the strength development as a function of time (ASTM C618-72 and C595-74).

When mixed with portland cement, the activators for slag and fly ash hydration are the gypsum contained in cement and the lime produced from hydration of the calcium silicates. The resulting cement paste normally has a higher strength than portland cement alone since the  $\text{Ca(OH)}_2$  crystals in a portland cement paste form weak bonds in the hydrated matrix (Popovics, 1979).

#### 3.2.4 Hydration In an Aqueous Waste Environment

Aqueous wastes might contain large concentrations of inorganic electrolytes and soluble organics which can interfere with the hydration of cementing materials. These interferences can be evaluated by studying the effects of admixtures on the properties of cement (Franklin, 1976; Popovics, 1979; Gatcho, 1980). Admixtures are special chemicals added to cement to impart certain desirable properties to the concrete. Of

relevance to our topic are the admixtures which are used to accelerate or retard the hydration of cement.

Most inorganic electrolytes behave as hydration accelerators of tricalcium silicate (the main strength developing compound of portland cement) with the exception of fluorides, phosphates and those cations that precipitate as hydroxides (Skalny and Young, 1980). The most widely used and best studied accelerator is  $\text{CaCl}_2$ . Little is known on the mechanisms of hydration acceleration (Ramachandran, 1976). Kondo et al (1977) compared the acceleration effect of several potassium salts and found that the effect increased with the ionic mobility (diffusivity) of the anion. They postulated that the accelerating effect was related to the inward diffusion of the anion through the calcium silicate hydrate gel coating the cement particles, forcing  $\text{Ca}^{+2}$  to diffuse out in order to maintain electroneutrality. According to the osmotic hydration model presented in Section 3.2.2, this would speed up the formation of calcium silicate hydrate gel.

There are two categories of compounds that will retard or even inhibit the hydration of calcium silicates. The first category comprises compounds which have the potential of forming precipitates on the cement grains. Gypsum is purposely mixed with portland cement to control the rate of setting. As described in Section 3.2.2, it does so by causing the precipitation of ettringite on the calcium silicate grains. Several researchers have reported that heavy metal salts retard the setting of cement by precipitating hydroxides or other insoluble salts on the cement particles (Longuet and Bellina, 1980; Skalny and Young, 1980;

Alford et al, 1981; Thomas et al, 1981; Arliguie et al, 1982). The second category includes compounds (many of them are organic) which tend to adsorb to the cement grains, hindering reactions between cement and water (Skalny and Young, 1980).

### 3.2.5 Durability of Hydrated Cement

The long term containment of a waste incorporated in a cement matrix depends primarily on the ability of the matrix to maintain its integrity. Durability refers to the resistance of the matrix to chemical interactions in an aqueous environment (Calleja, 1980).

Because cement paste and concrete normally have low permeabilities, the chemical attacks are interfacial phenomena which take place via diffusive exchanges of soluble species. Deterioration takes place through complex mechanisms which include ion exchange, dissolution of hydrated solids or formation of new insoluble compounds (Calleja, 1980). The most destructive chemical compounds are sulphates which react with the aluminates to form expansive sulfoaluminates and acids which dissolve the cement hydrates. The latter class of compounds is of more interest for the present topic.

All compounds of cement hydration are insoluble in neutral water with the exception of  $\text{Ca(OH)}_2$  (Lea, 1970). It has been shown that lime will leach easily from ordinary hydrated portland cement until 10 to 15% of the original wet weight of cement has dissolved. This corresponds roughly to the amount of lime produced from the hydration of tricalcium and dicalcium silicate as estimated in Section 3.2.2. The leaching of

lime occurs without significant reduction of the cement strength (Lea, 1970). Mixtures of portland cement and pozzolan or blast furnace slag show much lower lime leachability, as could be expected considering that lime reacts to form less soluble hydrates.

The matrix of hydrated cement can be completely dissolved by strong acids (Demoulian et al, 1980). Portland cement will resist pH values as low as 5 or 6 while alumina cement does not dissolve until the pH reaches 4. The resistance of alumina cement to acidic water is attributed to alumina gel which coats and protects the calcium aluminate matrix (Lea, 1970).

### 3.3 Chemical Fixation of Contaminants

The main objective of a stabilization/solidification operation is to immobilize contaminants contained in a waste by taking them out of solution. Those contaminants (or the fraction of them) which remain in solution in the pores of the waste form are directly available for leaching.

The chemical mechanisms which can effectively fix contaminants in waste forms were reviewed by Malone and Larson (1982):

- production of insoluble compounds,
- adsorption/chemisorption,
- passivation of waste particles,
- production of substitution in insoluble, crystalline materials.

Not all of these mechanisms will play an equally important role in the containment of actual complex wastes. Passivation or armoring will occur when a chemical reaction between species in solution forms a precipitate

on the surface of waste particles, isolating them from the bulk of the solution. Substitution in crystalline matrices such as clay particles can effectively immobilize metals. This is one of the major systems that remove elements from the environment in natural geochemical cycles. These mechanisms however will only occur incidentally when wastes are solidified using cement-based processes as described in Section 3.1. Based on the state-of-the-art treatment technology for wastewater (Patterson, 1975) and on the chemical environment created in cement-based matrices (high pH, high specific surface area), a more detailed review is presented below for hydroxide, carbonate and sulfide precipitation, formation of metal silicates and adsorption of hydrous metal oxides.

### 3.3.1 Precipitation as Metal Hydroxides

Precipitation via lime addition is the most common treatment process for the removal of metals including cadmium, chromium, copper, lead, nickel and zinc from industrial wastewater (Patterson, 1975).

The hydroxide chemistry of metals is summarized in Table 3.4. It is assumed that no polymeric species are formed and that speciation can be treated at equilibrium. In addition to being in equilibrium with the precipitated phase (Table 3.4, Expression 1), the metals hydrolyze to form several species (Table 3.4, Expression 3). The concentration of hydrolyzed species increases as the pH increases and thus explains the amphoteric nature of the metals (they are soluble at low and high pH).

The total soluble metal concentration can be expressed as a

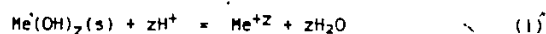


function of pH and the stability constants of the various species by replacing the expressions for the stability constants (Table 3.4, Equations 2 and 5) in the summation of all soluble species (Table 3.4, Equation 6). The result is shown on Figure 3.4 for cadmium, chromium and lead. It illustrates several important facts:

- the pH at which precipitation occurs (e.g. in a base titration) varies with the metal and its actual concentration,
- the optimal precipitation pH is unique to each metal and
- if excess alkalinity is present, the metal starts resolubilizing.

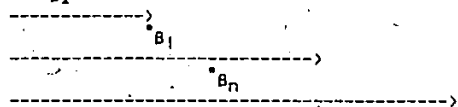
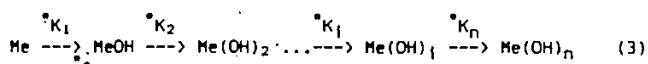
Table 3.4 Metal hydroxide equilibrium chemistry (adapted from Stumm and Morgan, 1981).

- Hydroxide solid.



$$K_{\text{so}} = \frac{[\text{Me}^{+z}]}{[\text{H}^+]^z} \quad (2)$$

- Hydroxide soluble species

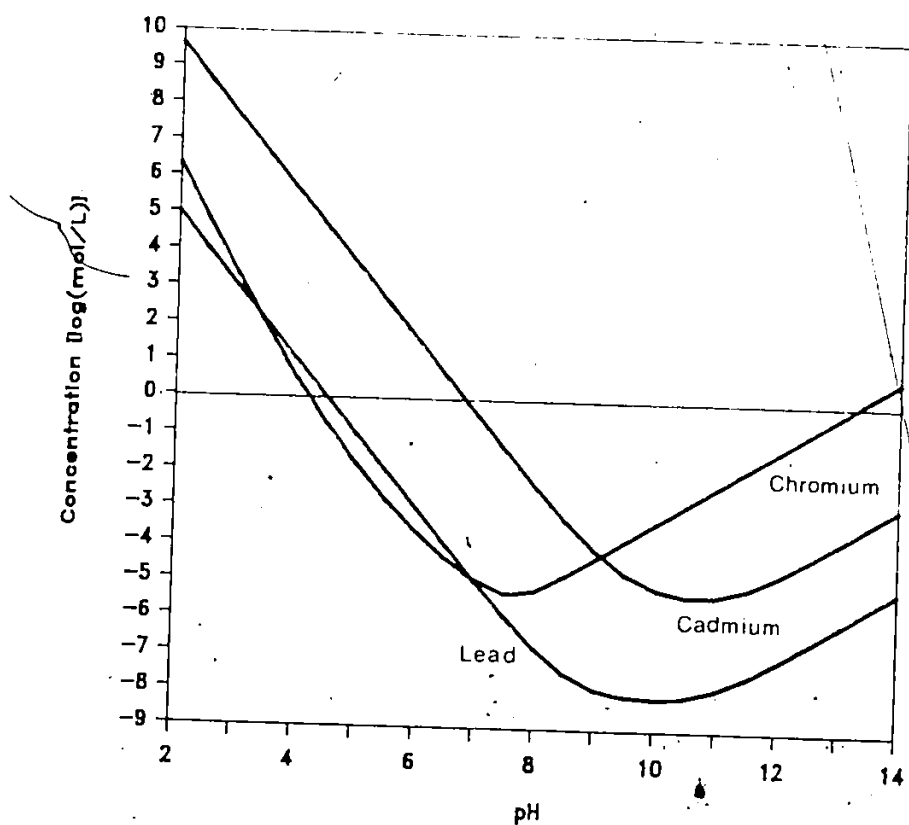


$$K_i = \frac{[\text{H}^+] [\text{Me}(\text{OH})_i]}{[\text{Me}(\text{OH})_{i-1}]} \quad (4)$$

$$B_i = \frac{[\text{H}^+]^i [\text{Me}(\text{OH})_i]}{[\text{Me}]} \quad (5)$$

- Total soluble metal concentration

$$\text{Me}_T = [\text{Me}^{+z}] + \sum_{i=1}^n [\text{Me}(\text{OH})_i^{z-i}] \quad (6)$$



Using convention of Table 3.4 (constants from Westall et al, 1976)

	Log of stability constant				
	$^*K_{SO}$	$^*K_1$	$^*B_2$	$^*B_3$	$^*B_4$
Cadmium	13.6	-9.0	-19.1	-30.4	-47.4
Chromium (+3)	12.3	-4.2	-10.3	-----	-25.6
Lead	9.0	-8.2	-17.2	-28.1	-----

Figure 3.4 Theoretical solubility of metal hydroxides.

The stability constants used to prepare Figure 3.4 are typical of freshly precipitated metal hydroxide. These values however change upon aging of the precipitates (Stumm and Morgan, 1981), resulting in lower solubilities. The decrease in solubility is explained by the formation of an active form of the precipitate (very fine crystalline matrix) when obtained from strongly oversaturated solutions. This precipitate is slowly converted into a more stable inactive form (amorphous) upon aging. Characterization studies of fresh and aged hydroxide sludges using X-ray diffraction did not reveal the presence of crystalline phases (Malone et al, 1978; Meredith, 1980).

### 3.3.2 Precipitation as Metal Carbonates

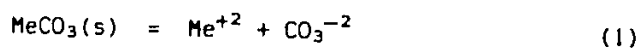
Metal carbonate precipitates are often more stable than their hydroxide counterparts (Stumm and Morgan, 1981). Carbonate precipitation, using a salt such as soda ash ( $\text{Na}_2\text{CO}_3$ ), has not been widely used for industrial wastewater treatment, except in some cases for the purpose of metal recovery (Patterson, 1975). Formation of metal carbonates can, however, be significant in the disposal environment, where the waste form can be exposed to relatively high partial pressures of  $\text{CO}_2$  resulting from microbial respiration. The chemical changes taking place at the waste form groundwater interface, called "carbonation" by cement and concrete chemists (Calleja, 1980), involve neutralization and formation of metal carbonates.

Expression of metal carbonate solubility requires consideration of three independent variables, e.g. metal concentration, pH and partial

pressure of  $\text{CO}_2$ . The equilibrium relationships of Table 3.5 illustrate that the carbonate ion concentration,  $[\text{CO}_3]$ , depends on both  $\text{CO}_2$  partial pressure (Table 3.5, Equation 3) and  $\text{OH}$  (Table 3.5, Equations 4 and 5). Based on the values of the equilibrium constants  $K_1$  and  $K_2$  (Table 3.5, Equations 8 and 9), the  $\text{CO}_3$  species dominates at pH larger than 10.3 ( $\text{CO}_3$  is 10% of  $C_T$  at  $\text{pH}=9.3$ ).

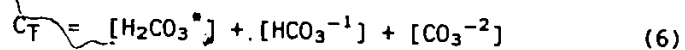
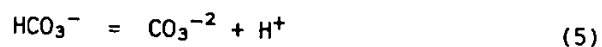
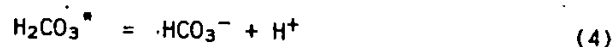
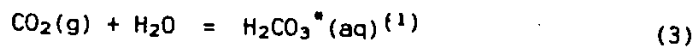
Table 3.5 Metal carbonate equilibrium chemistry  
(adapted from Stumm and Morgan, 1981).

- Carbonate solid



$$K_{\text{sp}} = [\text{Me}^{+2}] [\text{CO}_3^{-2}] \quad (2)$$

- Carbonate soluble species



$$K_H = \frac{[\text{H}_2\text{CO}_3^*]}{P_{\text{CO}_2}} \quad (7)$$

$$K_1 = \frac{[\text{H}^{+1}] [\text{HCO}_3^{-1}]}{[\text{H}_2\text{CO}_3^*]} \quad (8)$$

$$K_2 = \frac{[\text{H}^{+1}] [\text{CO}_3^{-2}]}{[\text{HCO}_3^-]} \quad (9)$$

$$^{(1)} \quad [\text{H}_2\text{CO}_3^*] = [\text{CO}_2(\text{aq})] + [\text{H}_2\text{CO}_3]$$

The carbonation process can be described by the following chemical equation



The condition under which a phase change from hydroxide to carbonate will occur can be approximated by combining Equations 2 from Table 3.4 and Equation 2 from Table 3.5:

$$[\text{CO}_3] [\text{H}^+]^2 = \frac{K_{\text{sp}}}{K_{\text{so}}}$$

This relationship illustrates that the pH at which carbonation occurs depends on the solubility products of the carbonate and hydroxide and on the actual  $\text{CO}_3$  concentration. This relationship, along with the equilibrium expressions of Tables 3.4 and 3.5, can be used to construct solubility diagrams for different metals, at various pH levels and carbonate concentrations.

The solubility of several metal hydroxides and carbonates was compared by Patterson et al (1977). It was found that formation of hydroxide precipitates controlled the solubility of zinc and nickel throughout the range of tested pH, while carbonate precipitates controlled the solubility of cadmium and lead in an intermediate pH range.

### 3.3.3 Precipitation as Metal Sulfides

Metal sulfides have solubilities which are several orders of magnitude lower than hydroxides or carbonates throughout the pH range. Furthermore their solubility is not as sensitive to a change in pH

(Stumm and Morgan, 1981). Metal sulfides will resolubilize in an oxidizing environment. Their use for wastewater treatment has been limited by a high operating cost and the problem of hydrogen sulfide gas generation (Patterson, 1975).

The equilibrium chemistry of sulfide in a reducing environment (Table 3.6) shows that metal sulfides will be formed at low pH.  $\text{H}_2\text{S}(\text{aq})$  has a low solubility. Therefore, if a metal solution is treated with a highly soluble sulfide salt (e.g.  $\text{Na}_2\text{S}$ ),  $\text{H}_2\text{S}(\text{g})$  will readily escape solution. As a consequence, no excess sulfide can be added to buffer the system. If hydrogen sulfide pressure is allowed to build up over the solution (i.e. forcing sulfide ion into solution) metals will tend to resolubilize as thio complexes  $(\text{Me}(\text{SH})^{(2-n)})$ . These problems can be resolved by using a slightly soluble sulfide salt as the treatment additive. The SULFEX process makes use of iron sulfide which has a higher solubility product than most metals (Scott, 1977). This limits generation of  $\text{H}_2\text{S}(\text{g})$  and also allows addition of excess sulfide ions (in the form of undissociated  $\text{FeS}$ ) to buffer the system at a low redox value by providing a source of electrons.

#### 3.3.4 Formation of Metal Silicates

Metal silicates are non-stoichiometric compounds where the metal is coordinated to silanol groups ( $\text{SiOH}$ ) in an amorphous polymerized silica matrix (Iler, 1979). It has been postulated that formation of metal silicates is the effective immobilization mechanism in several waste stabilization/solidification processes (Conner, 1972; Societe

Internationale de publicite et d'Agences Commerciales, 1975; Falcone et al, 1984) although it is difficult to positively identify metal silicates. The main advantage of forming metal silicates is that the silica matrix is relatively insoluble in a pH range from 2 to 11 (Iler, 1979).

Table 3.6 Metal sulfide equilibrium chemistry (under reducing conditions).

- Sulfide solid

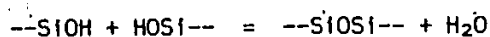


$$K_{\text{sp}} = [\text{Me}] [\text{S}] \quad (2)$$

- Sulfide soluble species



The silica in solutions of soluble silicates is present as a complex distribution of polymeric silicate anions. These anions are in a metastable equilibrium state which slowly tends to produce more polymerized species. The polymerization of silicic acid ( $\text{Si(OH)}_4$ ) involves the condensation of silanol groups (Iler, 1979):



The condensation of silicate anions is enhanced by the addition of mineral acid and/or acidic salts (relative to silicate anions). The gelling reaction is sensitive to pH, with a minimum at pH 2 and maximum

In the neutral range. In highly alkaline environments, silica is soluble.

When a soluble silicate is mixed with solutions of salts of metals other than the alkali metal group, insoluble amorphous metal silicates can be precipitated. The process is very sensitive to variables such as pH and energy of mixing. The resulting precipitate may vary from relatively homogeneous colloidal aggregates of very small units of polysilicic acids and metal hydroxide, to heterogeneous masses in which either silica or metal hydroxide is present as discrete colloidal units, held together by the other component (Iler, 1979).

One commercial silicate-based solidification process involves mixing the waste with soluble silicates (e.g.  $\text{Na}_2\text{O} \cdot \text{SiO}_2$ ) and a setting agent (Conner, 1972). Use of soluble silicates, however, produces an alkaline environment where the rapid precipitation of metal hydroxide will be in competition with the slow formation of the silica matrix. In another process, a silicate bearing material (e.g. blast furnace slag) is first dissolved in acid to promote the formation of low molecular weight silicic acid. The waste is then added to this solution and polymerization is promoted by raising the pH (Societe Internationale de Publicite et d'Agences Commerciales, 1975).

In a recent attempt to positively identify metal silicates, Petit and Rouxhet (1980) used infrared spectroscopy and X-ray diffraction to demonstrate that nickel and zinc formed chemical bonds with a silica gel matrix carefully prepared in the laboratory. They also observed that the pH at which these metals were incorporated in the silica matrix was



slightly lower than the pH of hydroxide precipitation.

### 3.3.5 Adsorption

Atoms and molecules are held together by cohesive forces that range in magnitude from strong valence bonds to weak van der Waals forces of attraction. Atoms and molecules located at surfaces suffer from an imbalance of these forces which produces the phenomenon of adsorption (Wagner and Julia, 1981).

Adsorbents relevant to waste stabilization/solidification technology include the metal hydrous oxides which form cement and pozzolanic matrices, as well as materials such as activated carbon or clay which can be added for the specific purpose of immobilizing contaminants. There is abundant literature on the use of activated carbon for removing organic and inorganic contaminants from wastewater (Cheremisinoff and Ellerbusch, 1980; Perrick, 1981; Suffet and McGuire, 1981), and on the sorptive properties of clays and waste materials (Theis et al, 1976; Chan et al, 1980; Benson, 1980; Travis et Etnier, 1981).

The forces of attraction responsible for adsorption on an activated carbon surface are predominantly of a physical nature (e.g. van der Waals forces). Physical adsorption is characterized by a low heat of reaction, relative ease of desorption and a significant temperature dependence upon equilibrium (Wagner and Julia, 1981). Activated carbon has mainly been used for organics adsorption but its capacity for adsorbing inorganics such as Cd, Cr, Hg, Cu and CN has also

been demonstrated (Huang, 1978).

The metal ions in the surface layer of metal oxides have a reduced coordination number. In water, they coordinate  $H_2O$  molecules which dissociate to produce a hydroxylated surface (Schindler, 1981). Oxides of iron, aluminum, silicon and manganese are strongly hydrolyzed in aqueous solution and thus have a net positive surface charge at low pH and a net negative charge at high pH. Metal oxides therefore tend to adsorb cations at a pH higher than their pH of zero point charge. It has been observed that adsorption invariably occurs before the initiation of bulk precipitation from solution and that saturation of the surface sites takes place over a narrow pH range (Kinniburgh and Jackson, 1981). This phenomenon is reversible and occurs at a very rapid rate. Equilibrium models have thus been developed where the surface is considered as a ligand interacting with soluble species (Anderson and Rubin, Eds, 1981). Adsorption models can thus be included into the general scheme of aqueous equilibrium calculations (Morel et al, 1981).

Cation adsorption by phyllosilicate clays differs from that of the simple oxides because the surface charge on clays (usually negative) is largely controlled by the amount of isomorphous substitution within the clay structure, rather than by the adsorption of  $H^+$  or  $OH^-$  from solution. The planar surfaces of most phyllosilicates (Si-O-Si) are relatively inactive compared to iron or aluminum oxide surfaces and the adsorptivity tends to be dominated by the energetics of fitting exchangeable cations into interlayer space. This phenomenon is not as reversible as simple surface adsorption (Kinniburgh and Jackson, 1981).

### 3.4 Current Data on Waste Form Characteristics

Waste forms have been evaluated to determine their acceptability for transportation and landfilling operations and to assess their leaching characteristics. Published information on hazardous waste form characteristics is available from vendors of processes (Pojasek, 1979a), independent laboratories evaluating commercial processes (Maloch et al, 1976; Bartos and Palermo, 1977; Meric, 1979; Bruce et al, 1981; Rousseaux and Craig, 1981) and research laboratories working with synthetic wastes processed in the laboratory (Mahoney et al, 1981; Cote and Hamilton, 1983; Bishop et al, 1984; Poon et al, 1985). A wealth of information is also available for radioactive waste forms (McCarthy, 1979; Oak Ridge National Laboratory, 1980; Mendel et al, 1981).

#### 3.4.1 Physical and Engineering Properties

A waste form, depending on the solidification additives used and their dosage, can be granular soil-like material or a monolithic concrete-like mass (Environmental Laboratory, 1980). Testing methods adapted from the soil and concrete fields have therefore been used to characterize their physical properties (Bartos and Palermo, 1977).

A solidification operation increases the weight and volume of the waste. Volume increase factors (final/initial volume) of three different aqueous wastes solidified using five processes ranged from 1.29 for a dewatered sludge solidified with soluble silicates and cement, to 2.35 for a liquid waste solidified with fly ash and lime

(Côté and Hamilton, 1983).

The bulk density of a variety of cement-based waste forms was reported to vary between 1.25 and 1.75 g/cm<sup>3</sup> (Environmental Laboratory, 1980; Côté and Hamilton, 1983). The water content of the same samples varied between 0.14 and 0.50 (weight by weight; wet weight basis). Low bulk densities were associated with high water contents. The specific gravity of the matrix skeleton can be used along with the water content and the bulk density to calculate the waste form porosity (Peck et al, 1974). Porosity values reported by Bartos and Palermo (1977) and van der Sloot and Wijkstra (1984) for a wide variety of cement-based waste forms ranged from 0.25 to 0.75 (voids/total volume). Comparisons between porosity and water content for any of the waste forms indicate that the voids are only partially filled with water.

Unconfined compressive strength data of waste forms reported by the U.S. Army Corps of Engineers (Environmental Laboratories, 1980) vary from 100 to 1000 kPa while various aqueous sludges solidified using cement-based processes at the Wastewater Technology Centre (Cote and Hamilton, 1983) had strengths ranging between 68 and 5200 kPa. Sugl et al (1980) reported that it was possible to increase the physical strength of a waste form by a factor of up to 10 relative to ordinary portland cement by using the right combination of cement, slag and gypsum. The improved performance was attributed to the formation of ettringite.

Permeability coefficients reported by Bartos and Palermo (1977) and van der Sloot and Wijkstra (1984) ranged from  $10^{-9}$  to  $10^{-7}$  m/sec and

are comparable to those of clay.

The resistance of waste forms to weathering, either freezing/thawing or wetting/drying cycles is low. The sample tested by Bartos and Palermo (1977) and by Bruce et al (1981) typically disintegrated after less than 10 cycles when ASTM standard methods for soil-cement mixtures were used. The waste forms which showed the best performance were based on pozzolan-lime additives and had the lowest water content.

Several researchers have reported that the water-to-cement ratio is the single most important factor to influence the morphology of the matrix and its physical and engineering properties (Environmental Laboratory, 1980; Poon et al., 1984; Bishop et al, 1984). For obvious economical reasons, the minimum amount of binder is added to aqueous waste to obtain solidification. A higher matrix water content results in lower strength, higher permeability, lower resistance to weathering and, as will be shown in next section, higher leachability. In fact, the matrix of actual cement-based waste forms might be quite different from the idealized situation pictured on Figure 3.2. When cement is mixed with a waste and a filler in lean proportions, hydration produces a thin film of cement gel on the surface of the particles and does not fill the voids between them (Bruce et al, 1981).

#### 3.4.2 Leachability

Most of the leaching data available has been generated in the laboratory using leaching tests. A few field investigations of

solidified waste landfills have been reported (Environmental Laboratory, 1981 and 1983)

The conduct of a laboratory leaching test consists in contacting a waste sample with a leachant, separating the liquid from the solid and analyzing the liquid. This can be done in a number of ways which have been classified as dynamic or static leaching tests (Mendel et al, 1981). A dynamic leaching test is one in which the specimen is exposed to a leachant that is either continuously or periodically renewed, e.g., a flow-through system. In a static test, the leachant is not renewed and its composition changes until eventually, if the test is run for long enough, equilibrium is attained.

Most of the tests in use for regulatory purposes are batch leaching tests e.g. the U.S. EPA Extraction Procedure (U.S. EPA, 1980), in which chemical equilibrium is often attained (Côté and Constable, 1982). For solidified wastes, which are normally crushed to accelerate attainment of equilibrium, the results of these tests can be used to evaluate whether the contaminants were effectively insolubilized. When the leachant is distilled water or a slightly acidic medium, the pH at the end of the test is controlled by the waste. For cement-based waste forms, the pH is usually high and contaminant concentrations are solubility limited.

In order to gain an understanding of the rate at which contaminants leach, a kinetic test must be used. When conducting this type of test, the integrity of the waste form is respected (i.e., no crushing) since formation of a solid mass is an important rate limiting

factor. Because of the low permeability of cement-based waste forms, tests aiming at measuring interface exchanges are more appropriate than those, such as column tests, which attempt to simulate convective transport.

Individual mechanisms that can control leaching rates under various conditions or at different times during a leaching process include bulk diffusion, chemical reactions and surface transfer phenomena. Mechanisms are normally studied by developing mathematical models that describe release patterns observed in laboratory leaching tests. Consideration of simple models, for which an analytical solution is available, provides an understanding of the role played by individual mechanisms in complex leaching phenomena.

Before reviewing selected leaching models, simplifying assumptions that allow derivation of simple analytical solutions will be presented.

#### 3.4.2.1 Conceptual Leaching Model

A cement-based waste form consists of several solid phases, a liquid phase (pore solution) and air voids. Prior to being contacted with an aqueous leaching solution, the different chemical species in the solid phases and in the pore solution are in a state of chemical equilibrium (Machiels and Pescatore, 1982). Upon contact, the difference in chemical potential of species in the aqueous phase and in the solid leads to fluxes of mass between the surface and the solution. These surface exchanges create concentration gradients inducing bulk diffusion

within the waste form matrix. Species from the solid and from the leachant also interact to form new species both in the aqueous solution and in the solid. These principles apply to species initially present in the leachant and in the solid:

Several transport mechanisms and chemical reactions which would be part of a comprehensive mechanistic leaching model are presented on Figure 3.5. This conceptual model represents, in unidimensional geometry, the interactions and transport of several species as a function of distance and time. The superscripts represent concentrations in the bulk of the waste matrix (b), in the leachant (l) and in the aqueous solution (w). The term leachant is used to describe the leaching liquid prior to any interaction with the waste while aqueous solution refers to the liquid in contact with the waste form.

The chemical species of interest in leaching are initially present in the waste matrix in an immobile form ( $C_{im}$ ) or in a mobile form, i.e., in solution in the pore solution ( $C_{mo}$ ). The immobile form is subject to mobilization if the local equilibrium is disrupted as a result of the mobile form being transported by diffusion or convection.

Leaching is normally expressed as a leach rate or as a cumulative fraction leached (Mendel, 1981). The leach rate (L) is defined as the mass of a species crossing the waste form-aqueous solution interface per unit area per unit time:

$$L \equiv \left[ \frac{\text{mass}}{\text{area} \cdot \text{time}} \right]$$

L is positive for species leaving the solid. It is normally expressed based on the geometrical surface area of the waste form.



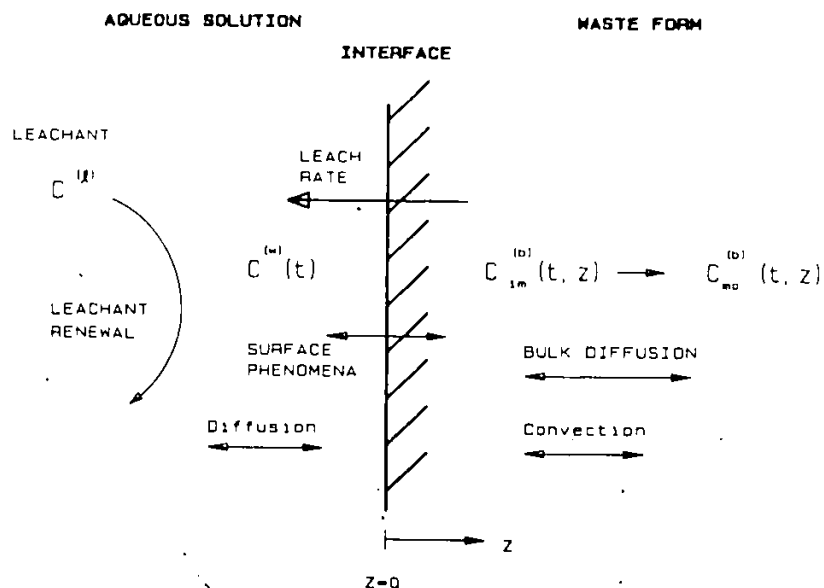


Figure 3.5 Conceptual leaching model (adapted from Cote, 1983).

Leaching data obtained from laboratory experiments are often expressed as a cumulative fraction leached ( $F$ ). The relationship between the leach rate and the cumulative fraction leached is as follows,

$$L = \frac{m_0}{A} \frac{dF}{dt} \quad (3.1)$$

where  $A$  is the geometrical surface area of the waste form specimen and  $m_0$  is the initial amount present in the specimen.

The chemical composition of the aqueous solution, next to the waste form, establishes the driving forces for the surface phenomena. It is determined by the rate of renewal of the leachant. Leachant velocity,  $v$ , is defined herein as the volume of leachant contacted with the waste

per unit waste surface area per unit time,

$$v \equiv \left[ \frac{\text{volume}}{\text{area} \cdot \text{time}} \right] \equiv \left[ \frac{\text{distance}}{\text{time}} \right]$$

The leachant velocity can be related to the movement of aquifers or infiltrating water under field disposal conditions. It can be used to examine the effect of the hydraulic regime of the leachant on the leach rate (Figure 3.6). The slope of the curve in Figure 3.6 has concentration units. The curve has two asymptotical limits where the slope can be interpreted as the concentration of the leached species near the interface. Limit 1, the maximum leach rate, is reached when the leachant velocity tends toward infinity. Under such flow conditions, there is no accumulation of leached species in the leachate (the slope of the curve tends toward zero) and the leaching driving forces are maximum. Limit 2 represents the saturation concentration of a species under specific leaching conditions. This limit can be approached for tests conducted with sufficiently low leachant velocity.

#### 3.4.2.2 Model Based Bulk Diffusion

If a species is present in the matrix in its mobile form only,  $C_{mo}$ , a mass balance shows that the net rate of transport is expressed by Fick's second law of diffusion:

$$\frac{\delta C}{\delta t} = D_e \frac{\delta^2 C}{\delta z^2} \quad (3.2)$$

where  $C$  is used for  $C_{mo}(t,z)$  and  $D_e$  is an effective diffusion coefficient. The diffusion coefficient is referred to as effective

because diffusion takes place in the liquid filling the interstices of the porous matrix. The liquid path length can therefore be much longer than that assumed in the formulation of Fick's law (i.e. a straight line).

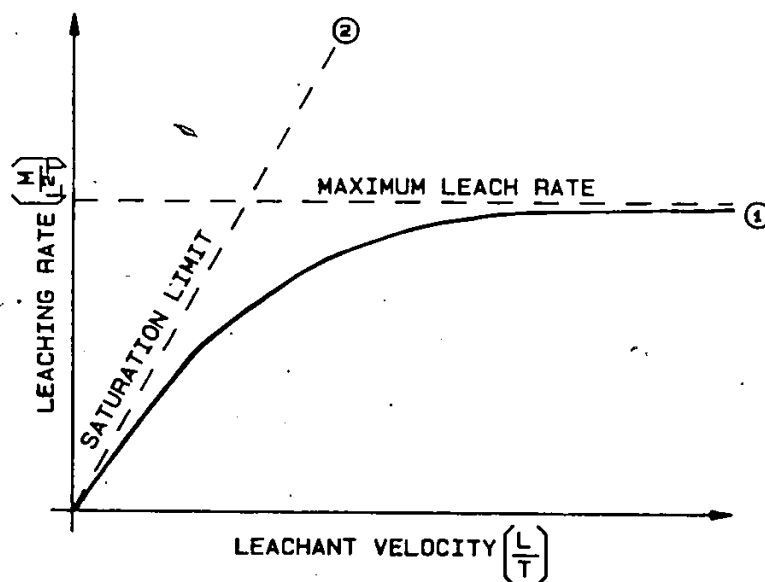


Figure 3.6 Dependency of the leach rate on the leachant velocity.

A solution of Equation 3.2 for the case where the leachant velocity is high enough to maintain zero surface concentration (i.e.,  $C(w)(t)=0$ , Figure 3.5), was presented by Crank (1956):

$$L(t) = C_T \left( \frac{D_e}{\pi t} \right)^{1/2} \quad (3.3)$$

where  $L(t)$  is the leach rate and  $C_T$  is the initial uniform concentration.

(on a volume basis) throughout the matrix.

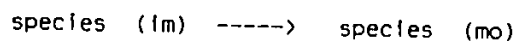
The release can also be expressed as a cumulative fraction leached by substituting Equation 3.3 into Equation 3.1 and integrating:

$$F(t) = \frac{A}{V} \frac{D_e t^{1/2}}{\pi} \quad (3.4)$$

where  $A/V$  is the ratio of the specimen geometrical surface area to volume.

#### 3.4.2.3 Models Based on Bulk Diffusion and Chemical Reaction.

For the case where a species is present in both an immobile and a mobile form initially in a state of chemical equilibrium, leaching of the mobile form will establish a difference in chemical potential to drive the following reaction:



If the reaction is fast, compared to the diffusion rate, the two forms of the species could be considered to be in a state of constant chemical equilibrium. If on the other hand, the reaction is slow, the kinetics of production of the mobile form have to be taken into account. The two cases will be discussed separately.

##### a) Instantaneous Chemical Reaction

A simple analytical solution to the mass balance equation can be obtained if the chemical equilibrium is represented by a linear adsorption isotherm:

$$K_D = \frac{C_{im}}{C_{mo}} \quad (3.5)$$

A mass balance across a differential section leads to:

$$\frac{\delta C_{mo}}{\delta t} = D_e \frac{\delta^2 C_{mo}}{\delta z^2} + \frac{\delta C_{im}}{\delta t} \quad (3.6)$$

which can be reduced to a form similar to Equation 3.2 by replacing  $C_{im}$  by  $K_D C_{mo}$  (from Equation 3.5):

$$\frac{\delta C_{mo}}{\delta t} = \frac{D_e}{(1 + K_D)} \frac{\delta^2 C_{mo}}{\delta z^2} \quad (3.7)$$

The effect of the chemical equilibrium is thus to slow down the diffusion process. The solutions to Equation 3.7 are given by Equations 3.3 and 3.4 where  $D_e$  is replaced by:

$$D_e' = \frac{D_e}{(1 + K_D)} \quad (3.8)$$

These equations show that the leach rate and cumulative fractions leached are reduced by a factor of  $(1 + K_D)^{1/2}$  when a fraction equal to  $1/(1 + K_D)$  of the initial concentration  $C_T$  is in a mobile form (Moore et al, 1975).

#### b) Kinetically Controlled Chemical Reaction

If the mobile species of initial concentration  $C_{mo}(0,z)$  is being produced at a rate  $k [C_{mo}(0,z) - C_{mo}(t,z)]$ , a mass balance

across a differential section leads to:

$$\frac{\delta C}{\delta t} = D_e \left( \frac{\delta^2 C}{\delta z^2} \right) + k (C_e - C) \quad (3.9)$$

where, in order to simplify the notation,  $C$  represents  $C_{mo}(t, z)$  and  $C_e$ , an equilibrium concentration, represents  $C_{mo}(0, z)$ . A solution of this differential equation was presented by Godbee and Joy (1974) for the semi-infinite medium of uniform initial concentration  $C_e$  and zero surface concentration. The leaching rate is expressed as:

$$L(t) = C_T (D_e' k)^{1/2} \left[ \text{erf}(kt)^{1/2} + \frac{e^{-kt}}{(\pi kt)^{1/2}} \right] \quad (3.10)$$

where  $C_T$  is the total initial concentration ( $C_{im} + C_{mo}$ ),  $\text{erf}$  is the error function (whose values are tabulated in most mathematical handbooks) and the effective diffusion coefficient  $D_e'$  is now defined as follows:

$$D_e' = \frac{D_e}{(1 + K_d)^2} \quad (3.11)$$

where  $K_d$  is the initial value of the distribution coefficient given by Equation 3.5. Substituting Equation 3.10 into Equation 3.1 and integrating, an expression for the cumulative fraction leached is obtained:

$$F(t) = \frac{A}{V} (D_e' k)^{1/2} \left[ \left( t + \frac{1}{2k} \right) \text{erf}(kt)^{1/2} + \left( \frac{t}{\pi k} \right)^{1/2} e^{-kt} \right] \quad (3.12)$$

Asymptotic analysis can be used to simplify Equations 3.10 and 3.12 for short and long time (Godbee and Joy 1974; Nathwani and

Phillips, 1980). For small values of  $kt$  (for a short time or for  $k \rightarrow 0$ ), Equation 3.10 reduces to the simple diffusion model represented by Equation 3.3. For large values of  $kt$ ,  $\text{erf}(kt)$  approaches unity and the leach rate as defined by Equation 3.10 reaches a steady state:

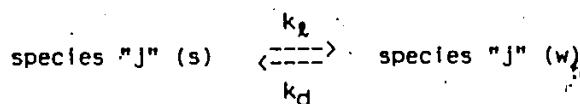
$$L(t) = C_T (D_e k)^{1/2} \quad (3.13)$$

This analysis shows that if a chemical species is initially present in an immobile form which is slowly transformed to a mobile form, a steady state leach rate will eventually be reached.

#### 3.4.2.4 Models Based on Interface Mass Resistance.

##### a) Using a Chemical Kinetics Approach

Pescatore et al (1982) presented a complex leaching model for glass waste forms where surface phenomena were described based on the kinetics of exchanges of a species between the surface of the solid (s) and the aqueous solution (w):



where  $k_s$  and  $k_d$  are phenomenological rate constant coefficients describing the kinetics of all elementary processes involved in releasing or attaching species "j" from or onto the surface, respectively;  $k_s$  and  $k_d$  may be complex functions of the physical and chemical properties of the surface and the aqueous solution. Their model indicated that, at short times, the surface processes dominate leaching rather than bulk diffusion, regardless of the leachant flow conditions. With simplifying assumptions which apply at short times, it is possible

to derive the following expression for the leaching rate:

$$L(t) \sim e^{-(k_g + \beta k_d)t} \quad \text{for small values of } t \quad (3.14)$$

where the constant  $\beta$  is equal to the ratio of the solid surface area to the aqueous solution volume. The initially rapid decrease of the leach rate predicted by Equation 3.14 is due to the rapid release of surface species into the aqueous solution. Integrating the leach rate expression leads to an equation of the following form for the cumulative fraction leached:

$$F(t) = k_1 [1 - e^{-(k_g + \beta k_d)t}] \quad (3.15)$$

When the kinetics of surface phenomena are fast as compared to other factors which can rapidly become rate limiting, Equation 3.15 can be simplified by dropping the exponential term. The remaining constant term is referred to as "initial fraction leached" and the surface phenomena are called initial wash-off.

#### b) Using a Mass Transfer Coefficient

The surface phenomena can be expressed in terms of an overall mass-transfer coefficient  $K$  (Treybal, 1968):

$$L(t) = K [C_{\text{sat}}^{(w)} - C^{(w)}(t)] \quad (3.16)$$

where  $C_{\text{sat}}^{(w)}$  is the saturation concentration in the aqueous solution. Since  $C_{\text{sat}}^{(w)}$  is the aqueous concentration when the system is at equilibrium, it represents the chemical potential of the surface species. The leach rate will reach a maximum value when  $C^{(w)}(t)$  tends towards zero:

$$L_0 = K C_{\text{sat}}^{(w)} \quad (3.17)$$



Replacing the value of  $K$  obtained from Equation 3.17 into Equation 3.16, we obtain:

$$L(t) = L_0 \left[ 1 - \frac{C^{(w)}(t)}{C_{sat}^{(w)}} \right] \quad (3.18)$$

If the leaching species is structurally a major component of the waste form, its release into the aqueous solution leads to a structural breakdown of the matrix, a process which is referred to as corrosion. The kinetics of the process can be represented by a network dissolution velocity  $u$  [L/T], defined as the volume of solid material being dissolved per unit time, per unit surface area of solid exposed:

$$u(t) = \frac{L(t)}{C_T} \quad (3.19)$$

Substituting Equation 3.18 into 3.19 and defining the maximum network velocity as  $u_0 = L_0/C_T$ , we obtain:

$$u(t) = u_0 \left[ 1 - \frac{C^{(w)}(t)}{C_{sat}^{(w)}} \right] \quad (3.20)$$

To derive an expression for the cumulative fraction leached for network dissolution controlled leaching using Equations 3.1 and 3.19, the time dependency of  $C^{(w)}(t)$  would have to be substituted into Equation 3.20. For the simple case where  $C_{sat}^{(w)} \gg C^{(w)}(t)$ ,  $u(t) = u_0$  and we obtain:

$$F(t) = \frac{A}{V} u_0 t \quad (3.21)$$

which expresses that the cumulative fraction leached of any species is independent of the concentration of that species in the waste form.

#### 3.4.2.5 Models Involving Interacting Species

So far, the discussion has been limited to single chemical species. When several species undergo transport and chemical reactions, there are no analytical solutions available. The following is a brief review of modelling efforts of these phenomena.

The phenomena taking place when acid diffusion in a porous reactive solid is controlled by dissolution/precipitation reactions have been studied by Cussler (1982) for several chemical systems. Qualitative results show that i) the diffusing acid dissolves the metals which in turn diffuse in and out of the porous solid, and ii) depending on the number of competing reactions, the concentration of each reactant and the stoichiometry of the reaction, the solubilized metals will reprecipitate farther in the solid.

In recent years, several models have been developed to describe the transport and chemical reactions of chemical species in soils (Miller and Benson, 1983; Kirkner et al, 1984). As outlined by Jennings et al (1982), there are two distinct techniques for modelling multicomponent systems. The first technique consists of inserting all of the interaction chemistry directly into the transport equations and reducing the problem to one set of equations. The alternative technique involves solving by iteration between the transport and chemical sets of equations.

The first technique has been extensively used for simple adsorption problems where the Langmuir or Freundlich Isotherm were substituted into the transport equation (Crank, 1956; Lindstrom and

Boersma, 1970; Van Genuchten et al, 1974). Berner (1980) demonstrated the application of this technique to the dissolution of a binary salt from the pores of a solid. The development was pursued by Jennings et al (1982) and Miller and Benson (1983) who generalized the technique to include several transport mechanisms and chemical reactions. A disadvantage of the method is that it is not flexible since the equations have to be modified to handle a new chemical system.

The second technique allows treatment of the chemical system completely separately from transport considerations. In a finite difference solution, at each time step, the transport equations are solved ignoring the chemical interactions. The concentrations are then corrected by solving the chemical interaction relationships using equilibrium or kinetic expressions. This technique can take advantage of the availability of powerful computer programs to solve chemical equilibrium problems (Nordstrom et al, 1979).

#### 4. FORMULATION OF A MODEL

In this Chapter, a mathematical model for the leaching of contaminants from waste forms will be formulated based on the information available in the literature as reviewed in Chapter 3. The system will be qualitatively described, making the simplifying assumptions which will allow formalization into a model. A numerical solution method will then be presented.

##### 4.1 Formalization of the Leaching Phenomenon

This model is intended to be used for the simulation of the results of laboratory leaching experiments for the purpose of determining the mechanisms of contaminant containment and leaching. This purpose is reflected in the simplifying assumptions and numerical solution methods described below. The model is not intended to be used as a long term predictive tool for complex field leaching processes.

A mechanistic leaching model must consider several interacting chemical species. This model will focus on contaminant mobilization resulting from protonation reactions. The model must, therefore consider, directly or indirectly, all the species which play an important role in the balance of the hydrogen ion ( $H^+$ ) in addition to the contaminants of interest.

The formulation of simplifying assumptions and the mathematical description of the model is broken down into four parts: 1)

the morphology of the matrix, 2) the transport mechanisms, 3) the initial and boundary conditions, and 4) the method of handling the chemical reactions..

#### 4.1.1 Morphology of the Matrix

The waste form is represented as a system consisting of several solid phases and a liquid phase. The solid phases include an insoluble skeleton capable of adsorption and a number of chemical precipitates that can dissolve. The skeleton of cement-based waste forms, typically made of hydrated cement, fly ash or clay particles, is essentially insoluble in natural waters. This skeleton provides a high surface area of hydrous metal oxides which have the potential of immobilizing contaminants through reversible adsorption. The chemical precipitates which are part of the matrix include the waste and the soluble parts of the solidification additives (e.g. calcium hydroxide from portland cement).

The water contained in the matrix is distributed between pore water, water absorbed in the matrix particles and water of hydration. The fraction of interest to modelling is the water contained in interconnected pores.

For modelling purposes, the total concentration of a species contained in the waste form is divided into several fractions (Figure 4.1). The total concentration is identified either with the aqueous phase of the waste (soluble) or with the solid phase (insoluble). The insoluble fraction is in turn classified as available or unavailable for leaching.

"Available for leaching" is defined as soluble in a leaching medium when an equilibrium leaching test is conducted at infinite liquid-to-solid ratio. The leaching medium can have any desirable properties. Specification of an infinite liquid-to-solid ratio ensures that 1) the interactions of the solid with the leaching medium does not change the leaching environment and 2) there are no solubility limitations.

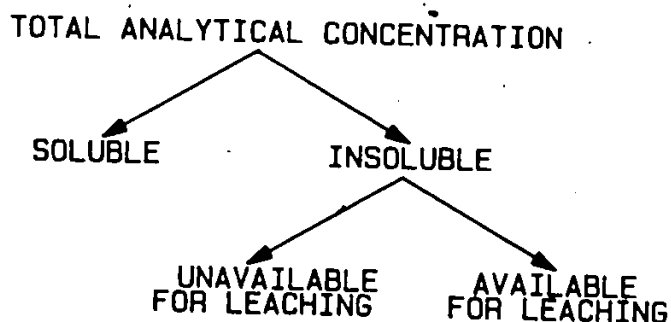


Figure 4.1 Distribution of a chemical element in the waste form matrix.

The fraction unavailable for leaching includes those contaminants which are immobilized through irreversible reactions with the matrix. Examples of such reactions in the context of leaching under mild acidic conditions are substitution in crystal lattices, formation of insoluble metal silicates and migration of ions between layers of clay particles. Included in the unavailable fraction are also those contaminants which, irrespectively of their chemical speciation, do not have access to the interconnected pore system.

#### 4.1.2 Transport Mechanisms

Transport of contaminants within the waste form can take place through convection or diffusion. Given the low permeability of solidified wastes, the laboratory tests will be conducted by immersing a specimen in a leaching medium. Because of the nature of the tests, convective transport can be neglected. In the absence of convective transport, the only effective diffusion process is caused by the random motion of individual ions or molecules. This process, called molecular diffusion, can occur within the solid, on the surface of the solid or in the pore solution. Only pore solution molecular diffusion will be considered here (Berner, 1980).

In order to simplify the mathematical treatment, it is assumed that the waste form is isotropic and that a unidimensional geometry can be used. The first assumption can easily be justified since, during the solidification process, wastes are blended with additives and homogenized before being disposed of and allowed to set. The assumption of unidimensional geometry implies that the layer at the surface of the waste form which is affected by leaching is small compared to the overall size of the waste form. This has proved to be true for the leaching of radionuclides from glass waste forms (American Nuclear Society, 1980; Machiels and Pescatore, 1982).

Taking the aqueous solution/waste form interface as the origin, a mass balance for a soluble species "j" on a slice of the solid perpendicular to the axis z leads to the following equation:

$$\frac{\delta C_p(j)}{\delta t} = D_e(j) \frac{\delta^2 C_p(j)}{\delta z^2} + \Sigma R(j) \quad (4.1)$$

where,  $C_p(j)$  = concentration of soluble species "j" in the pore solution in terms of mass per unit volume of pore solution  $[M/L^3]$ ,

$D_e(j)$  = effective diffusion coefficient  $[L^2/T]$ ,

$\Sigma R(j)$  = the net effect of all reactions that affect concentration  $C_p(j)$  in terms of mass per unit volume of pore solution per unit time  $[M/L^3 \cdot T]$ ,

$t$  = time  $[T]$ ,

$z$  = distance from the interface  $[L]$ .

The concentration  $C_p(j)$  is, of course, a function of time ( $t$ ) and distance ( $z$ ). These have been dropped to simplify the notation. The diffusion term of Equation 4.1 has the familiar form of Fick's law applied to an aqueous solution. However, in its derivation for porous solids, presented in Table I-1 (Appendix I), assumptions were made about the porosity and tortuosity of the matrix and about the diffusion coefficient.

In considering that porosity is independent of position (see derivation in Table I-1), it was indirectly assumed that leaching does not change the volume and structure of the pore solution system. The fact that the matrix porosity,  $\phi$ , does not appear in Equation 4.1 means that, for a given value of the diffusion coefficient, the profile developed in a porous solid is identical to the one that would develop in an aqueous solution. Porosity, however, appears in the flux equation (Equation 6, Table I-1) indicating that the leaching rate is



proportional to the actual cross-sectional area of diffusion.

The effective diffusion coefficient  $D_e(j)$  presented in Equation 4.1 is a molecular coefficient corrected for the tortuosity of the matrix and neglecting ionic-assisted diffusion. The diffusion coefficient of ions in aqueous solution can be calculated directly using the Nernst Equation, from their limiting equivalent conductivity (Li and Grégory, 1974). The coefficient of several ions, calculated assuming infinite dilution, are listed in Table I-2. In more concentrated solutions, the condition that electroneutrality must be respected at all points affects the diffusion fluxes. Lasaga (1979) studied this effect for diffusion in sediments and concluded that it was negligible for most ions.

#### 4.1.3 Initial and Boundary Conditions

Equation 4.1 is a non-linear partial differential equation of order two. Its solution requires specification of initial and boundary conditions.

The initial condition must specify the concentration at all points along the axis:

$$t = 0, z \geq 0 \longrightarrow C_p(j) = C_0(j)$$

$C_0(j)$  is the initial pore soluble concentration in equilibrium with the solid phases.

To have sufficient boundary conditions for solving partial differential equations, the value of the dependent variable must be specified at some value of one independent variable and at every value

of the other independent variable. Furthermore, the number of boundary conditions for one dependent variable in terms of the independent variables equals the order of the highest derivative with respect to the given independent variable. For Equation 4.1, these requirements mean that the concentration  $C_p(j)$  must be specified at two locations along the axis  $z$  for all values of time  $t$ .

The first boundary condition can be formulated by assuming that the solid is semi-infinite:

$$t > 0, z = \infty \longrightarrow C_p(j) = C_o(j)$$

The second boundary condition describes the situation at the liquid/solid interface. It is assumed that the aqueous solution in contact with the waste form is an extension of the pore solution system and that there is no mass transfer limitation at the interface. This allows us to formulate the second boundary condition as:

$$t > 0, z = 0 \longrightarrow C_p(j) = C_w(j)$$

where  $C_w(j)$  is the concentration in the aqueous solution close to the interface.

The waste form specimen is represented as being completely and continuously immersed in a finite volume of aqueous solution (Figure 4.2). The specimen geometrical surface area to aqueous solution volume ratio,  $B$ , is known and constant. The leachant is renewed at a constant frequency  $f$ . Since transport processes in aqueous solution are much faster than in the solid, it is assumed that there is no concentration gradient in the reactor. A mass balance on a species "j" in the reactor leads to:

$$\frac{\delta C_w(j)}{\delta t} = B L(j) + f [C_l(j) - C_w(j)] + \Sigma R_w(j) \quad (4.2)$$

where:

- $C_l(j)$  = concentration of species "j" in the fresh leachant  $[M/L^3]$ ,
- $C_w(j)$  = concentration of species "j" in the aqueous solution  $[M/L^3]$ ,
- $L(j)$  = leaching rate of species "j" in terms of mass per unit geometrical area of waste form per unit time  $[M/L^2 \cdot T]$ ,
- $\Sigma R_w(j)$  = the net effect of all reactions that affect concentration  $C_w(j)$  in terms of mass per unit volume per unit time  $[M/L^3 \cdot T]$ ,
- $B$  = specimen surface area to aqueous solution volume ratio  $[1/L]$ ,
- $f$  = leachant renewal frequency  $[1/T]$ .

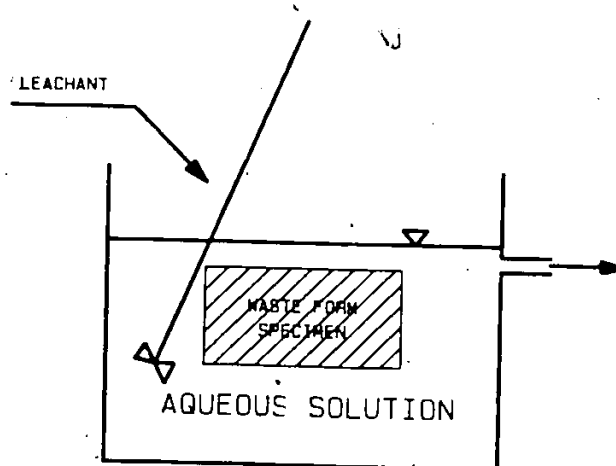


Figure 4.2 Representation of the aqueous solution hydraulic regime.

The specimen surface area-to-aqueous solution volume ratio defines a physical characteristic of the leaching system:

$$B = \frac{A}{V} \quad (4.3)$$

where A is the geometrical surface area of the waste form in contact with the volume V of the aqueous solution. The leachant renewal frequency can be further defined for intermittent flow or continuous flow conditions. For intermittent flow,

$$f = \frac{1}{\theta} \quad (4.4)$$

where  $\theta$  is the duration of the leaching period. For continuous flow conditions,

$$f = \frac{Q}{V} \quad (4.5)$$

where Q is the flow rate [ $L^3/T$ ] and V is the volume of the aqueous solution [ $L^3$ ].

The leachant velocity, defined in Section 3.4, can be expressed as a function of the parameters defined earlier,

$$v = \frac{f}{B} \quad (4.6)$$

#### 4.1.4 Chemical Reactions

The reaction terms of Equations 4.1 and 4.2 include all the processes that have the potential of modifying the concentration of a

soluble species "j". With reference to Figure 4.1, these reactions involve species which belong to the fraction "available for leaching". They include reactions of speciation within the aqueous solution, precipitation/dissolution and adsorption/desorption on/from the matrix surface.

The question arises whether these reactions should be treated using a kinetic or equilibrium approach. Equilibrium is not a necessary assumption. Kinetic expressions could be replaced for the reaction terms of Equations 4.1 and 4.2. However, if chemical reactions are so rapid that equilibrium is essentially maintained in the face of advection and diffusion, then a thermodynamic approach is possible and simpler. Ionic reactions involving proton transfer are usually very fast with half-lives less than milliseconds (Stumm and Morgan, 1981, page 121). In modelling transport and adsorption of a variety of chemicals in soils, an equilibrium approach has always been successful whenever the convective transport term was small or zero (Jennings et al, 1984; Travis and Etnier, 1981). An equilibrium approach has been successful in modelling diagenesis processes (Berner, 1980) and leaching of radionuclides from glass waste forms (Machiels and Pescatore, 1982). Of course, strictly speaking, no net reaction can occur at equilibrium, but the assumption is that there is so little kinetic impediment to the reactions that they occur rapidly with very small departures from equilibrium.

In the model outlined earlier, molecular diffusion is the sole transport mechanism and the chemical reactions of interest are

protonation reactions. It is therefore assumed that the chemical reaction term can be handled using a chemical equilibrium approach. The mathematical description of chemical reactions has been included in the next section since it depends upon the method chosen to solve the transport/reaction system.

#### 4.2. Numerical Solution

Since the reaction term of Equation 4.1 is a function of the independent variables  $C_p(j)$  (i.e., the composition of the pore solution), the equation is non-linear and must be solved numerically. In describing an interacting multicomponent transport system, one equation (such as Equation 4.1) has to be written for each soluble species. Furthermore, the chemical interactions, assumed to be at equilibrium in this case, are expressed as stability constants, solubility products or adsorption isotherms. The result is a set of differential equations coupled to a set of algebraic equations. A solution technique consisting of solving the chemical interactions separately from the transport equations will be used (see discussion in Section 3.4.2.5). A description will first be given of two methods selected to handle the equilibrium chemistry: 1) use of chemical equilibrium model and 2) use of experimentally determined titration and solubility curves. The different elements of the solution pertaining to the transport equations, the mass balances in the aqueous solution and the chemical equilibrium are then presented in an integrated manner. Two computer programs, LEEQ (LEaching and Equilibrium model) and LEEX (LEaching and

Experimental data), developed to implement the two methods of handling the equilibrium chemistry, are described in Appendix I.

#### 4.2.1 Equilibrium Chemistry

In this section, two methods of handling the chemical equilibrium calculations are presented. If the chemical system can be well characterized in terms of its composition and interactions among components, then a chemical equilibrium model can be used. If, on the other hand, the system is too complex, another approach is proposed in which the equilibrium composition of the pore solution is determined experimentally as a function of pH.

##### 4.2.1.1 Chemical Equilibrium Model: MINEQL

The problem of finding the equilibrium composition of an aqueous solution consists of minimizing the Gibbs free energy of the system subject to the constraints of mass balance. One approach, called the equilibrium constant approach, begins with an initial guess for a set of components from which the minimum Gibbs free energy composition is readily calculated from equilibrium constants, then the mass balance equations are solved by iteration (Westall et al., 1976). This approach is perfectly suited for interfacing with the transport problem in a numerical solution since the initial guess can be taken as the composition at the previous time step, thus minimizing the number of iterations required to find the equilibrium composition. It is worth noting that the only components that are included in the mass balance

are those that are involved in chemical reactions. It is therefore possible to leave non-reacting components (such as  $\text{Na}^+$  and  $\text{Cl}^-$ ) out of the calculations even if that results in a system which is not apparently neutral.

From the available computer programs which can be used to solve aqueous equilibrium problems (Nordstrom et al., 1979), MINEQL (Westall et al., 1979) was selected because it includes all the basic features to facilitate its interfacing with the transport equations: 1) It has one of the most complete libraries of thermodynamic data, 2) It can handle precipitation/dissolution of solids, 3) It can be adapted to model adsorption on hydrous metal oxide surfaces (Morel et al., 1981), 4) It allows correction of the thermodynamic data for the ionic strength of the solution, and 5) It is written as a FORTRAN subroutine which facilitates its insertion in the general model.

MINEQL uses a special terminology to describe a chemical system. The components are a set of chemical entities such that every species can be represented as the product of a reaction involving only these components, and no component can be represented as the product of a reaction involving only the other components. A species is the product of a chemical reaction involving the components as reactants. The species can be soluble (the components themselves and the complexes) or precipitated. MINEQL contains a library of complexes and precipitates. New components or species can easily be added to this library along with the thermodynamic data which describe their interactions.



#### 4.2.1.2 Experimental Equilibrium Data: Titration and Solubility Curves

Complex waste forms contain a large number of chemical components whose interactions can not always be described by stoichiometric chemical reactions (e.g. hydration of portland cement). Even if that was possible, the numerical burden of repeatedly calculating the equilibrium composition as transport proceeds could be too heavy. An alternative approach consists of measuring experimentally the equilibrium soluble concentration using pH as a master variable. This approach is best suited to systems where mobilization is primarily due to protonation reactions.

The pore solution of the waste form is considered a completely mixed reactor in contact with the porous matrix. The pH and soluble contaminant concentration of the pore solution as a function of cumulative amount of acid added can be expressed using titration and solubility curves.

This approach does not distinguish among the various soluble species of a component (e.g.  $\text{Cd}^{++}$ ,  $\text{CdOH}^+$ ,  $\text{CdCl}^+$ , etc). All the species are included in the analytical determination of the soluble concentration of the contaminant. This concentration is the same as the one which is considered in the definition of conditional stability constants (Stumm and Morgan, 1981).

#### 4.2.2 General Flow Diagram

The different elements of the numerical solution are integrated as illustrated in Figure 4.3. The following description encompasses the

two versions of the solution implemented using MINEQL (computer program LEEQ) and using titration and solubility curves (computer program LEEX). The reader is referred to Appendix I for a description of the two computer programs. In this section, after presenting the data input and simulation initialization, the numerical calculations are described, for a time step from " $t$ " to " $t+\Delta t$ ".

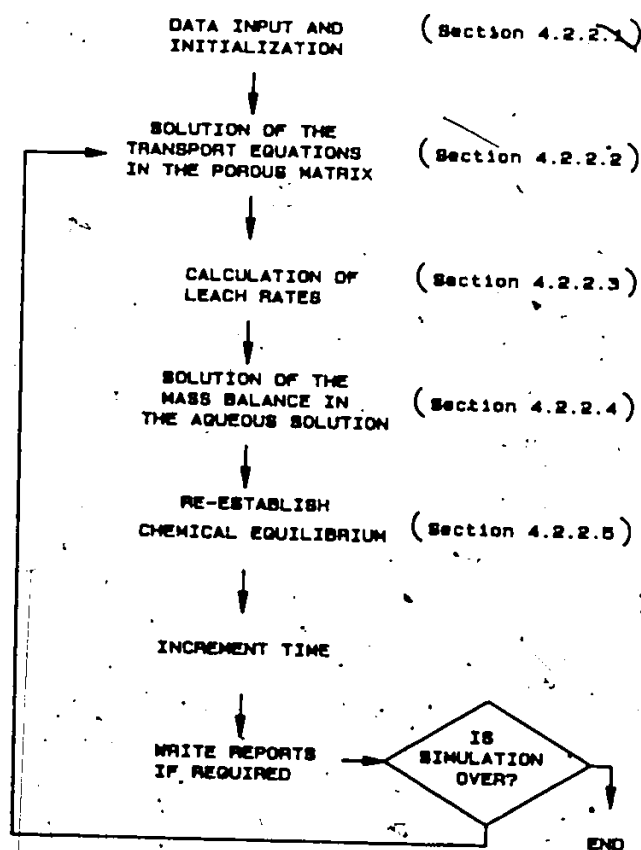


Figure 4.3 General numerical solution flow diagram.

#### 4.2.2.1 Data Input and Initialization.

Input data must first be provided to describe the waste form specimen and the aqueous solution flow regime. The required quantities include the specimen mass ( $M_0$ ), bulk density ( $\gamma_D$ ), connected pore water content ( $\phi$ ) and geometrical surface area ( $A$ ). The aqueous solution volume ( $V$ ) and leachant flow rate ( $Q$ ) must also be specified.

The porous matrix is divided into " $n_l$ " slices of equal thickness " $dz$ ". The numerical solution proceeds through calculation of concentration at nodes " $i$ " located at the middle of each slice (as such, the first slice is half the thickness of the other slices). An analogy can be made between the slices of the porous matrix and a series of completely mixed chemical reactors (Figure 4.4). Each reactor contains a homogeneous mixture composed of the pore water and the solid phases of the matrix. The volume of that mixture in each reactor corresponds to the volume of a slice. It can be pictured that diffusive transport takes place in the porous matrix while chemical reactions occur in the reactors.

The chemical system is described through consideration of " $n_j$ " soluble species. When MINEQL is used to calculate the equilibrium composition, the " $n_j$ " species are divided into two groups: " $n_l$ " components and " $n_j - n_l$ " complexes (see Section 4.2.1.1). For each of the " $n_j$ " species, the following concentrations must be specified:

- $C_l(J)$  : concentration in the leachant [ $M/L^3$ ],
- $C_w(J)$  : initial concentration in the aqueous solution [ $M/L^3$ ]
- $C_p(I,J)$  : initial soluble pore concentration at node " $i$ " expressed on a pore volume basis [ $M/L^3$ ].

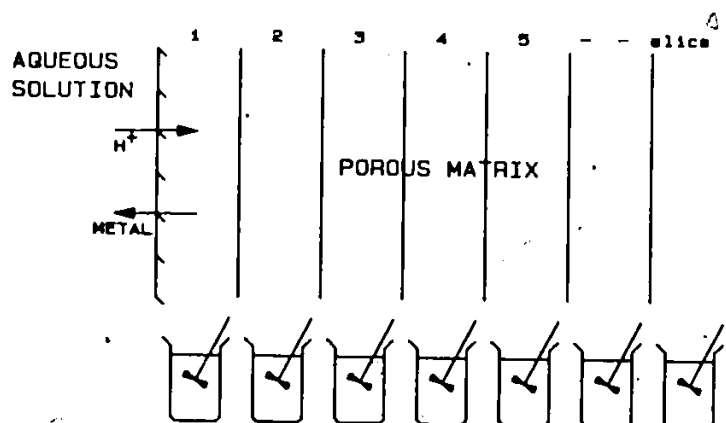


Figure 4.4 Representation of the porous matrix for numerical solution.

In addition  $C_T(i,j)$ , the total concentration available for leaching (see Figure 4.1) expressed on the basis of the total matrix volume, must be provided.  $C_T(i,j)$  includes both the mobile and immobile fractions of a component. For a component which is entirely mobile, the following equation holds:

$$C_T(i,j) = \frac{\gamma_b w}{\gamma_w} C_p(i,j) \quad (4.7)$$

where  
 $\gamma_b$  : bulk density of the porous matrix [ $M/L^3$ ],  
 $\gamma_w$  : density of water [ $M/L^3$ ]  
 $w$  : water content of the matrix [weight by weight; wet weight basis]

For a component which is only partly mobile,

$$C_T(i,j) > \frac{\gamma_b w}{\gamma_w} C_p(i,j) \quad (4.8)$$

The initial value of  $C_p(i,j)$  is determined based on the equilibrium chemistry of the pore solution (see Section 4.2.2.5).

When experimental titration and solubility curves are used to calculate the equilibrium composition, the "nj" species are composed of "nl" components and  $H^+$  (i.e.,  $n_j = n_l + 1$ ). The soluble concentration of a component is now expressed as  $C_t$  and includes the component itself and all the soluble species that it forms. The concentrations  $C_{t_l}(j)$ ,  $C_{t_w}(j)$  and  $C_{t_p}(i,j)$  must be specified.  $C_T(i,j)$  is defined as before for each of the "nl" components. For  $H^+$  however, a new quantity is introduced. The variable  $H_c(i)$ , initialized with the value zero, is used to keep track of the cumulative amount of  $H^+$  added to each slice.

The initial values of  $C_{t_p}(i,j)$  are determined based on the titration and solubility curves when no acid has been added.

For simplicity the concentration  $C$  (as opposed to  $C_t$ ) will be used in the remainder of this section whenever it is not explicitly necessary to distinguish them.

#### 4.2.2.2 Solution of the Transport Equations in the Porous Solid

The boundary condition at the interface requires that the concentration at node one of the porous solid be assigned the value of the aqueous solution concentration. Thus for each of the "nj" soluble species :

$$C_p(i,j) = C_w(j) \quad (4.9)$$

The other boundary condition specifies that the matrix be considered

semi-infinite. This is achieved by considering a depth of simulation (i.e., number of slices) such that the concentration in the last few slices remains equal to the initial concentration for the duration of the simulation. In the computer programs, the number of slices is incremented as the simulation time increases to respect this criterion. The concentrations of all components at the fifth to last node are compared to the initial concentrations. Whenever a difference larger than 0.1% is observed, the number of nodes is increased.

Since the solution method selected involves alternating between transport and chemical reactions, Equation 4.1 must be redefined to include only the transport term:

$$\frac{\delta C_p(j)}{\delta t} = D_e(j) \frac{\delta^2 C_p(j)}{\delta z^2} \quad (4.10)$$

This equation is numerically solved for each of the "nj" soluble species using the central-difference Crank-Nicholson method (Gerald, 1980). The dimensionless ratio

$$r(j) = \frac{D_e(j) \Delta t}{\Delta z^2} \quad (4.11)$$

where  $\Delta z$  = slice thickness [L],  
 $D_e$  = diffusion coefficient [ $L^2/T$ ],  
 $\Delta t$  = time step [T].

used in the finite difference equations is different for each species (j) since the diffusion coefficients are different and the same values of  $\Delta t$  and  $\Delta z$  are used in the computer programs. The magnitude of  $r(j)$  determines the accuracy of the solution as discussed in Chapter 5.

#### 4.2.2.3 Calculation of Leach Rates

The leach rate of a species "j" is defined as the mass leached per unit time per unit geometrical area of contact with the aqueous solution:

$$L(j) = \frac{1}{A} \frac{dm(j)}{dt} \quad (4.12)$$

In a numerical solution where the time step is  $\Delta t$ , the leach rate can be approximated as

$$L(j) = \frac{1}{A} \frac{\Delta m(j)}{\Delta t} \quad (4.13)$$

The incremental mass leached  $\Delta m(j)$ , which is positive for species that leach out, can be calculated by numerical integration over all slices between the profiles at time  $t$  and  $t+\Delta t$ :

$$\Delta m(j) = \sum_{i=1}^{n1} [C_p(i,j)_t - C_p(i,j)_{t+\Delta t}] V_w \quad (4.14)$$

where  $V_w$  is the amount of interconnected pore water in a slice.

#### 4.2.2.4 Solution of the Mass Balance in the Aqueous Solution

Similarly to the transport equation in the porous matrix, the mass balance in the aqueous solution, Equation 4.2, must be rewritten without the reaction term to accommodate the iterative solution technique:

$$\frac{\delta C_w(i)}{\delta t} = BL(i) + f[C_s(i) - C_w(i)] \quad (4.15)$$

This equation is solved numerically using a Runge-Kutta fourth-order method (Gera, 1980).

#### 4.2.2.5 Re-establish Chemical Equilibrium

Prior to re-establishing chemical equilibrium at each node, the total concentrations  $C_T(i,j)$  must be updated since components have been transported in and out of the matrix. This is done differently if MINEQL or experimental titration and solubility curves are used.

When using MINEQL (program LEEQ), the total concentration of each of the "n1" components must be updated at each node "i" of the matrix:

$$C_T(i,1)_{t+\Delta t} = C_T(i,1)_t - \frac{\gamma_D w}{\gamma_w} \sum_{j=1}^{n_j} (S(j,1) [C_p(i,j)_{t+\Delta t} - C_p(i,j)_t]) \quad (4.16)$$

The new concentration is thus taken as the concentration at time "t" corrected by the amount leached of all species which include component "1".  $S(j,1)$  is the stoichiometric coefficient of component "1" in species "j". The ratio  $\gamma_D w / \gamma_w$  ensures conversion of the concentration from the pore water to the total matrix basis (see Equation 4.7).

After the total concentrations have been adjusted, the MINEQL program, used as a subroutine, is called to calculate the new soluble equilibrium concentrations at time  $(t+\Delta t)$  at each node of the porous solid,  $C_p(i,j)$  and in the aqueous solution,  $C_w(j)$ . The initial "guess composition" transmitted to MINEQL is the set of concentrations  $C_p(i,j)$  or  $C_w(j)$  at time "t".



When using titration and solubility curves, the total concentration of each of the "n" components are updated as follows:

$$C_T(i,1)_{t+\Delta t} = C_T(i,1)_t - \frac{Y_b W}{Y_w} [C_{p(i,1)}_{t+\Delta t} - C_{p(i,1)}_t] \quad (4.17)$$

Here, concentration  $C_{p(i,1)}$  already includes all soluble forms of component "1". In addition, the cumulative amount of acid which has penetrated to a certain node "i" is calculated as

$$H_c(i)_{t+\Delta t} = H_c(i)_t + \frac{V_w(i)}{M_s(i)} [C_{p(i,H^+)}_{t+\Delta t} - C_{p(i,H^+)}_t] \quad (4.18)$$

where  $V_w(i)$  and  $M_s(i)$  are the volume of pore water and weight of a slice respectively. The value of  $H_c(i)$  is used with the titration curve to determine the  $H^+$  concentration in the pores at each node. The  $H^+$  concentration is then used with solubility curves to re-establish the equilibrium concentration  $C_{p(i,j)}$  for the "n" components.

## 5. VALIDATION OF THE NUMERICAL SOLUTION

In this chapter, the numerical solution of the leaching model implemented in the computer programs LEEQ and LEEX will be evaluated to determine its characteristics of stability and convergence, to establish its limits of applicability and to ensure that the codes are error-free. Three simple cases for which an analytical solution is available will first be studied: mass balance in the aqueous solution (Section 5.2), the profile developed in the porous matrix for constant surface concentration (Section 5.3) and desorption from the porous matrix following a linear isotherm for constant surface concentration (Section 5.4). The third case is especially important since it involves a chemical reaction and can thus be used to validate the technique of iteration between transport and chemical reactions. Finally, in Section 5.5, the dissolution of a metal hydroxide will be studied to compare the use of titration and solubility curves (in LEEX) against the use of equilibrium chemistry (in LEEQ). An analytical solution is not available for this case and therefore, validation will be effected by comparison to experiments (Chapter 7).

The input data for all simulations are listed in Table II-1. A complete set of results is not presented for each simulation. Rather, the useful information was extracted and incorporated into the text. The computer output of two simulations, 27 (LEEQ) and 28 (LEEX), are included in Tables II-3 and II-4 as typical examples. The waste form

characteristics used in the validation correspond to the simplest matrix prepared for experimentation (Batch A, Chapter 6).

### 5.1 Criteria for Stability and Convergence

A numerical method can be evaluated based on its stability and convergence (Gerald, 1980). Stability signifies that the errors made at one stage of the calculations do not cause increasingly large errors as the computations are continued. Convergence means that the results of the method approach the analytical values as the finite independent variable step approaches zero.

The leaching model described in Chapter 4 is based on two coupled differential equations for which a numerical solution is implemented using the same time step. The mass balance in the aqueous solution (Equation 4.15) is solved using a Runge-Kutta fourth order method in which the error is proportional to the fourth power of the time step. The porous matrix diffusion equation (Equation 4.10) is solved using the Crank-Nicholson method for which convergence and stability is evaluated based on the first power of the time step and the second power of the distance step. The time step required for the later equation will therefore control the overall precision of the numerical solution.

The dimensionless ratio  $r$  defined by Equation 4.11 is used to assess the accuracy of the numerical solution. As pointed out by Gerald (1980), the Crank-Nicholson method is stable for a wide range of  $r$  values but it converges as  $r$  is made smaller. This criterion does not account for the concentration changes resulting from re-establishing

chemical equilibrium at each time step. The stability of the overall solution will be studied in the next sections by comparing numerical to analytical solutions for a wide range of slice thicknesses and time steps. When an analytical solution is not available, convergence and stability will be assessed by measuring the relative change in the model response as smaller slice thicknesses and time steps are used.

## 5.2 Mass Balance in the Aqueous Solution

The mass balance in the aqueous solution (Equation 4.15) becomes linear and has an analytical solution (Thomas, 1969) if the variables  $f$ ,  $L$ ,  $f$  and  $C_L$  are considered independent of the concentration  $C_w$ . The analytical solution can be expressed as:

$$C = \frac{h}{f} + \left(C_0 - \frac{h}{f}\right) e^{-ft} \quad (5.1)$$

where:  $h = (BL + fC_L)$   
 $C_0 = \text{Initial concentration}$

Simulation 1 was performed to validate the numerical solution. It considers a sample of surface area equal to  $69.4 \text{ cm}^2$  immersed in a 2 litre completely mixed reactor. The initial concentration  $C_0$  of a chemical component in the reactor is  $10^{-3} \text{ mol/L}$ . The leachant flow is  $2.85 \text{ L/d}$  and has the same component concentration ( $C_L = 10^{-3} \text{ mol/L}$ ). It is assumed that the constant leach rate  $L$  is equal to  $-10^{-5} \text{ mol/cm}^2 \cdot \text{d}$ . Note that a negative leach rate means that the chemical component is being absorbed into the matrix. The calculated aqueous solution concentration after 1 day using Equations 4.3, 4.5 and 5.1 is  $5.8566 \times 10^{-5} \text{ mol/L}$ . The numerical solution of Simulation 1 gives an identical result.

### 5.3 Profile in the Porous Solid for Constant Surface Concentration

The mass balance equation for diffusion in a porous matrix has an analytical solution for soluble chemical components provided simple boundary conditions are stipulated. Solution of Equation 4.10 for a semi-infinite medium with uniform initial concentration and constant surface concentration was presented by Crank (1956):

$$\frac{C_p - C_1}{C_0 - C_1} = \text{erf} \left( \frac{z}{2 (D t)^{1/2}} \right) \quad (5.2)$$

where:  $C_p$  = concentration at a distance  $z$  from the interface,  
 $C_1$  = surface concentration,  
 $C_0$  = initial uniform concentration throughout the porous matrix, and  
 erf = error function whose value is available from mathematical tables.

In the model, constant surface concentration (e.g. concentration in the aqueous solution) can be forced by modifying the computer program or by specifying a very high leachant flow rate so that the leaching process does not significantly affect the mass balance in the aqueous solution. The latter technique was used to generate the profiles presented in Figure 5.1 for a component being absorbed in the matrix or leaching out of the matrix. The profiles generated with the model (Simulations 2 and 3) are superimposed on the profiles obtained from the analytical solution.

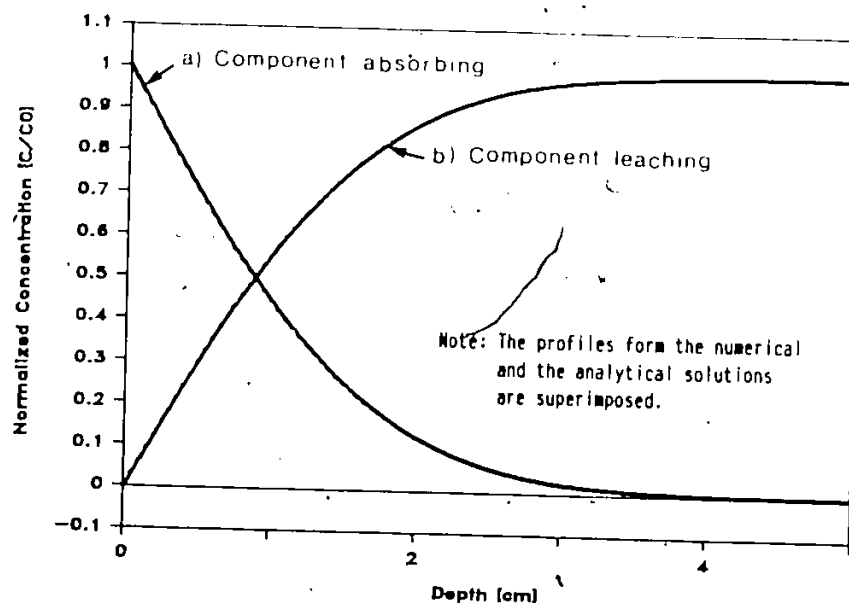


Figure 5.1 Profile developed in the porous matrix at 1 day for constant surface concentration (soluble species).

#### 5.4 Desorption Following a Linear Isotherm

For the purpose of evaluating the technique of iteration between transport and chemical reaction we consider that the distribution of a chemical component between the pore solution (mobile) and the solid matrix (immobile) is subject to a linear isotherm:

$$K = \frac{C_{im}}{C_{mo}} \quad (5.3)$$

where

$C_{im}$  = immobile concentration,  
 $C_{mo}$  = mobile concentration,  
 $K$  = constant.

A mass balance across a differential section of the matrix leads to

$$\frac{\partial C_{mo}}{\partial t} = D \frac{\partial^2 C_{mo}}{\partial z^2} - \frac{\partial C_{im}}{\partial t} \quad (5.4)$$

where  $-\partial C_{im}/\partial t$  represents the reaction term of Equation 4.1. Replacing  $C_{im}$  from Equation 5.3 into Equation 5.4, we obtain:

$$\frac{\partial C_{mo}}{\partial t} = \frac{D}{1+K} \frac{\partial^2 C_{mo}}{\partial z^2} \quad (5.5)$$

The effect of the adsorption reaction can thus be taken into account by redefining the diffusion coefficient:

$$D' = \frac{D}{1+K} \quad (5.6)$$

Equation 5.5 is similar to Equation 4.10 and an analytical solution is thus available with the boundary conditions described in Section 5.3. This solution, represented by Equation 5.2, can be integrated for the zero surface concentration case ( $C_s=0$ ) to yield (Crank, 1956):

$$M_t = 2 A C_T \left( \frac{D' t}{\pi} \right)^{1/2} \quad (5.7)$$

where  $M_t$  is the total mass leached at time  $t$ . This form of the solution is more convenient for the evaluation of the numerical method.

The numerical method of iteration will be validated in the following way. An analytical solution is first obtained using  $D'$ , the coefficient of diffusion corrected for adsorption (Equation 5.6). The

numerical solution is then used with the diffusion coefficient  $D$  for transport and Equation 5.3 to adjust the mobile concentration  $C_{mo}$  at each node of the matrix and at each time step. The two methods are compared by defining the departure from the analytical solution as.

$$e = 100 \left( \frac{M_{T,n} - M_{T,a}}{M_{T,a}} \right) \quad (5.8)$$

where  $e$  = error of the numerical solution with respect to analytical solution, [%],  
 $M_{T,a}$  = total mass leached at time  $t$  using the analytical solution [M]  
 $M_{T,n}$  = total mass leached at time  $t$  using the numerical solution [M]

The simulation runs described in Table 5.1 were performed with a diffusion coefficient  $D = 10^{-6} \text{ cm}^2/\text{s}$  and for two values of  $K$ , 9 and 999. In addition, several combinations of slice thickness and time step were used to yield  $r$  values ranging from 0.5 to 1920. Each simulation was run for 24 hours and the error with respect to the analytical solution, calculated using Equation 5.8, is presented in the two last columns of Table 5.1 for  $t=12$  and  $t=24$  hours.

Evaluation of stability and convergence must take into account the number of slices into which the porous matrix was subdivided. Although the actual number of slices is increased in the computer program as the simulation proceeds, to respect the semi-infinite hypothesis (see Section 4.2.2.2); we can compare the number of slices at  $t=24$  hours as a relative precision criterion. Defining depth of penetration as the depth where the concentration has changed by 2%, the number of slices for each combination of  $K$  value and slice thickness is



given in Table 5.1 (number in bracket in column 3). This corresponds to depths of penetration of respectively 10000  $\mu\text{m}$  and 1000  $\mu\text{m}$  for  $K=9$  and  $K=999$ .

Table 5.1 Comparison of the model to an analytical solution for desorption following a linear isotherm.

Simulation Run	Ads. Coeff. K	Slice Thickness [ $\mu\text{m}$ ]	Time Step [min]	Ratio (Eq. 4.11)	Error [%] 12 hrs	Error [%] 24 hrs
15	9	400(25)	120.00	45.00	unstable	
14	9	400(25)	80.00	30.00	-2.73	-3.62
13	9	400(25)	60.00	22.50	-0.07	-1.31
12	9	400(25)	40.00	15.00	1.75	0.33
11	9	400(25)	20.00	7.50	2.01	0.87
10	9	400(25)	10.00	3.75	1.27	0.57
9	9	400(25)	5.00	1.88	0.72	0.32
8	9	100(100)	20.00	120.00	-12.94	-7.34
4	9	100(100)	10.00	60.00	-4.09	-2.46
7	9	100(100)	5.00	30.00	-1.18	-0.86
5	9	100(100)	1.00	6.00	-0.17	-0.30
6	9	100(100)	0.10	0.60	-0.17	-0.30
17	999	100(10)	20.00	120.00	98.90	50.05
18	999	100(10)	5.00	30.00	65.31	32.18
19	999	100(10)	6.00	6.00	19.64	8.97
20	999	100(10)	1.00	1.00	3.41	1.45
21	999	100(10)	0.50	0.50	1.89	0.71
22	999	25(40)	20.00	1920.00	-40.27	-48.87
23	999	25(40)	5.00	480.00	-20.98	-23.44
24	999	25(40)	1.00	96.00	-3.65	-4.37
25	999	25(40)	0.10	9.60	0.39	-0.11
26	999	25(40)	0.01	0.96	0.25	-0.11

Note: The numbers in bracket in Column 3 indicate the number of slices affected by leaching.

Examination of Table 5.1 reveals that the numerical solution is stable even for large values of the ratio  $r$ . For all simulation runs, except 15, the error at  $t=24$  hours is usually the same or less than the error at  $t=12$  hours showing that the error does not increase as the simulation proceeds. In Simulation 15, the model was taken to a limit as

the 24 hour simulation period was divided into only 12 time steps of 120 minutes each. The solution was then unstable, generating a negative amount leached.

The numerical solutions converge as the slice thickness and the time step are reduced and stabilize when reaching a value of  $r=1$ . For all conditions studied, using a value of  $r=1$  resulted in a numerical response which is within  $\pm 1\%$  of the analytical response. For a given value of the slice thickness, reducing the time step so that  $r$  becomes much smaller than 1, does not reduce further the error. The accuracy of the numerical solution is controlled by the slice thickness as the depth of the solid affected by leaching is divided into a larger number of slices (Table 5.1). The use of smaller slices is, however, limited by the fact that the time step has to be reduced concurrently to keep  $r$  low (Equation 4.11). Since the time step is proportional to the second power of the slice thickness, the computational burden of using thinner slices increases rapidly (e.g. halving the slice thickness results in a time step which is four times smaller and thus roughly quadruples the computation time).

Increasing  $K$ , the fraction which is adsorbed on the solids, reduces the depth affected by leaching. Therefore, for the same slice thickness (e.g. 100  $\mu\text{m}$ ) and time step (e.g. 1 min) the precision drops rapidly as  $K$  increases (compare runs 5 and 20). It is however possible to obtain the same precision with  $K=999$  as with  $K=9$  provided the depth affected by leaching is divided into a larger number of slices (compare runs 5 and 25).

### 5.5 Metal Hydroxide Dissolution

It was shown that the numerical method of iterating between transport and chemical reactions yields accurate results when compared to an analytical solution for a linear adsorption isotherm (Section 5.4). In that case, the chemical reaction affected in a similar manner the concentration at all nodes within the porous matrix. However, when several mobile species are interacting, local discontinuities can occur that will affect the behavior of the numerical solution. This phenomenon will be studied by considering a waste form containing a precipitated metal contacted with an acidic aqueous solution.

The waste form under consideration is composed of 76% inert solids and 24% interconnected pore solution (on a weight basis). It is contacted with a pH=3 aqueous solution using an area-to-solution volume ratio  $B$  of  $0.1375 \text{ cm}^{-1}$ . The simulation is fully described in Table II-1, Run 27.

The waste form pore solution contains 0.01 mol/L of  $\text{Cd}(\text{NO}_3)_2$  and 0.02 mol/L of KOH. These react to form a cadmium hydroxide precipitate,  $\text{Cd}(\text{OH})_2(\text{s})$ , in equilibrium with the following soluble species:  $\text{Cd}^{+2}$ ,  $\text{Cd}(\text{OH})^+$ ,  $\text{Cd}(\text{OH})_2$ ,  $\text{Cd}(\text{OH})_3$ ,  $\text{H}^+$  and  $\text{OH}^-$ . Table 5.2 describes the composition of the pore solution based on information extracted from Figure 3.4.

When the waste form is contacted with the aqueous solution, at time zero, driving forces exist for  $\text{H}^+$  to diffuse into the porous solid and for the various cadmium species to diffuse out. However the

progression of  $H^+$  is retarded by its reaction with  $Cd(OH)_2(s)$  which solubilizes cadmium. A layer depleted of precipitated cadmium, called the leached layer, thus increases in thickness as the reaction front progresses inward. The profiles of the various species at time  $t=24$  hours, as simulated with the programs LEEQ and LEEEX, will be examined.

Table 5.2 Initial composition of the waste form pore solution (Simulation 27).

Chemical components added: 0.01 mol/L  $Cd(NO_3)_2$   
0.02 mol/L KOH

Equilibrium composition calculated using MINEQL (Westall et al., 1976):

pH	= 9.42			
$[Cd^{+2}]$	= $5.70 \times 10^{-6}$	mol/L pore solution		
$[Cd(OH)^{+1}]$	= $1.50 \times 10^{-5}$	"	"	"
$[Cd(OH)_2]$	= $3.20 \times 10^{-6}$	"	"	"
$[Cd(OH)_3^{-1}]$	= $4.20 \times 10^{-8}$	"	"	"
$[Cd(OH)_2(s)]$	= $9.98 \times 10^{-3}$	"	"	"

$NO_3^-$  and  $K^+$  do not form complexes or precipitates and therefore remain in solution in the pores.

#### 5.5.1 Profiles Calculated Using Equilibrium Chemistry (LEEQ)

The profiles in the porous solid at time  $t=24$  hours indicate that the leaching front has progressed from the interface to 4800  $\mu m$  (Figure 5.2). In the leached layer, all  $Cd(OH)_2(s)$  has been solubilized. Since the aqueous solution is static and  $B$  is relatively small, the leaching phenomena affect the concentrations in the aqueous solution and at the same time, the interface concentration. For instance, at  $t=24$  hours,  $H^+$  diffuses into the porous solid under a driving force corresponding to

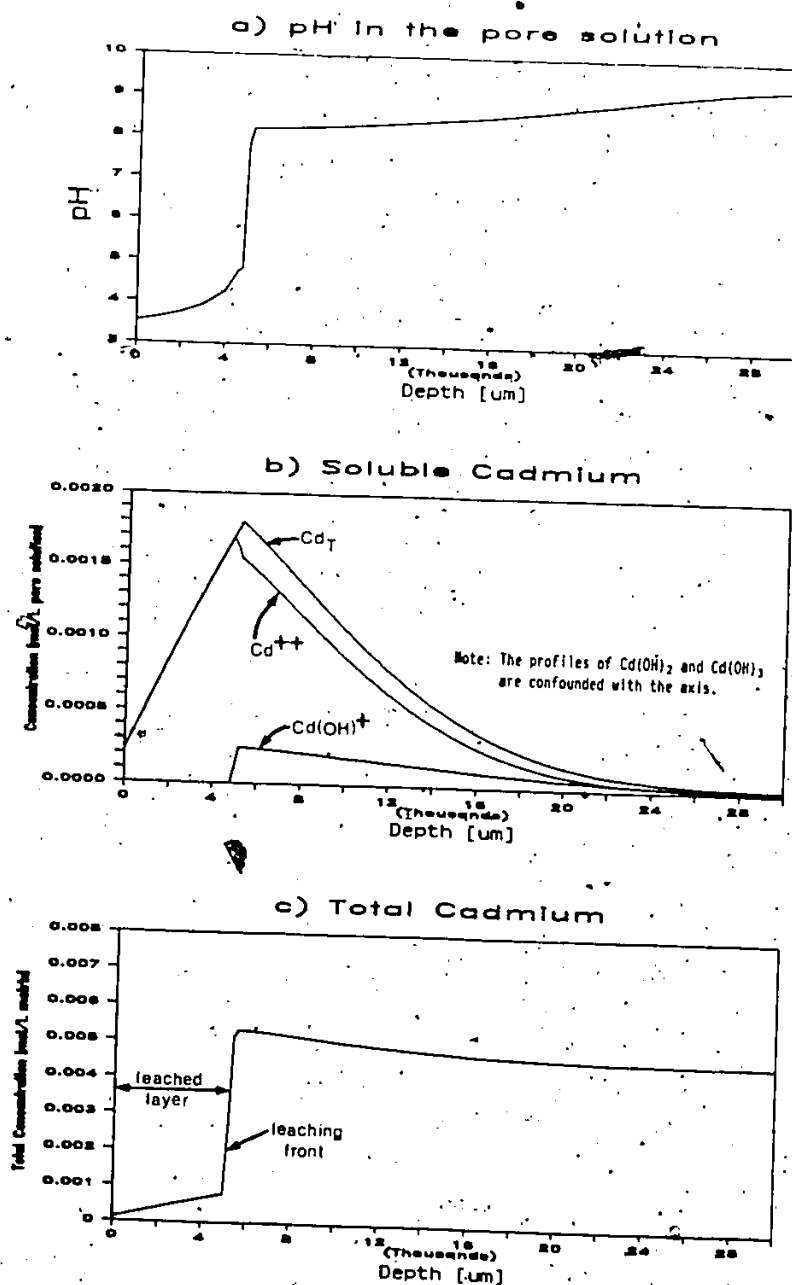


Figure 5.2 Profiles at 1 day for the dissolution of  $\text{Cd}(\text{OH})_2(\text{s})$  using equilibrium chemistry (Simulation 27).

the difference in concentration between  $10^{-3.52}$  mol/L (in the aqueous solution) at the interface and a concentration which is essentially zero ( $\sim 10^{-8}$  mol/L) at the reaction front (Figure 5.2a). The total soluble concentration of cadmium  $Cd_T$  ( $[Cd_T] = [Cd^{+2}] + [Cd(OH)^+] + [Cd(OH)_2] + [Cd(OH)_3]$ ) peaks at the leaching front (Figure 5.2b). This establishes gradients for cadmium to leach outward and inward. The outward gradient results from the fact that cadmium has been depleted from the leached layer and is still present in a relatively small concentration in the aqueous solution. The inward gradient is related to solubility considerations. As can be seen from the profile of the individual species included in  $Cd_T$ , only  $Cd^{+2}$  contributes to leaching out while both  $Cd^{+2}$  and  $Cd(OH)^+$  contribute to diffusing in. The cadmium which diffuses in remains soluble in the pores since there is no excess alkalinity in the initial composition to cause it to precipitate. A higher than background soluble cadmium concentration is the explanation for the pH depletion (from the initial value of 9.42) which can be observed in the region from 5000 to 25000  $\mu m$  (Figure 5.2a). Figure 5.2c presents the profile of total cadmium (e.g. the soluble and precipitated forms) expressed on the basis of the porous matrix total volume. In the leached layer, where all the cadmium is in solution, the relationship between "total concentration" and pore solution "total soluble concentration" given by Equation 4.7 is applicable.

The convergence of the numerical solution was evaluated by running several simulations with different time steps as presented in Table 5.3. The precision of a simulation can be evaluated by calculating

the error relative to the smallest time step used. Equation 5.8 was used to calculate the error reported in the last column of Table 5.3 replacing  $M_{T,n}$  and  $M_{T,a}$  respectively by  $M_{T,r}$ , the mass leached for a ratio  $r$  and  $M_{T,1}$ , the mass leached for a ratio 1. The results show that the relative error remains smaller than 1% when the time step is less than 3.44 minutes ( $r=32$ ) and that using a  $r$  value smaller than 4 does not result in increased precision.

Table 5.3 Evaluation of the relative precision of the numerical solution.

Simulation Run	Time Step [min]	Ratio $r$ (Eq. 4.11)	Cadmium Leached [M]	Change Relative to $r=1$ [%]
27	0.11	1	4.774E-04	0.00
31	0.22	2	4.774E-04	0.00
32	0.43	4	4.774E-04	0.00
33	0.86	8	4.770E-04	-0.08
34	1.72	16	4.764E-04	-0.21
37	3.44	32	4.746E-04	-0.59
38	6.88	64	4.700E-04	-1.55
39	13.75	128	4.566E-04	-4.36
40	27.50	256	4.220E-04	-11.60

NOTE: All simulations were done with a slice thickness of 200  $\mu\text{m}$ .

#### 5.5.2 Profiles Calculated Using Titration and Solubility Curves (LEEX)

In order to use the program LEEX, the equilibrium chemistry of the pore solution (see Table 5.2) must be expressed using titration and solubility curves. An acid titration curve can be obtained with MINEQL by repetitively solving the equilibrium problem, while incrementally adding  $\text{H}^+$ . The results, expressed on a matrix wet weight basis, are presented in Figure 5.3. It can be seen that the pH is maintained around

8.0 until all precipitated cadmium has been neutralized. The solubility curve for cadmium can be generated by summing up the concentrations of all soluble species (Table 3.4, Equation 6) after expressing them as a function of pH and the equilibrium constants. It has the familiar shape of the solubility curve shown in Figure 3.4.

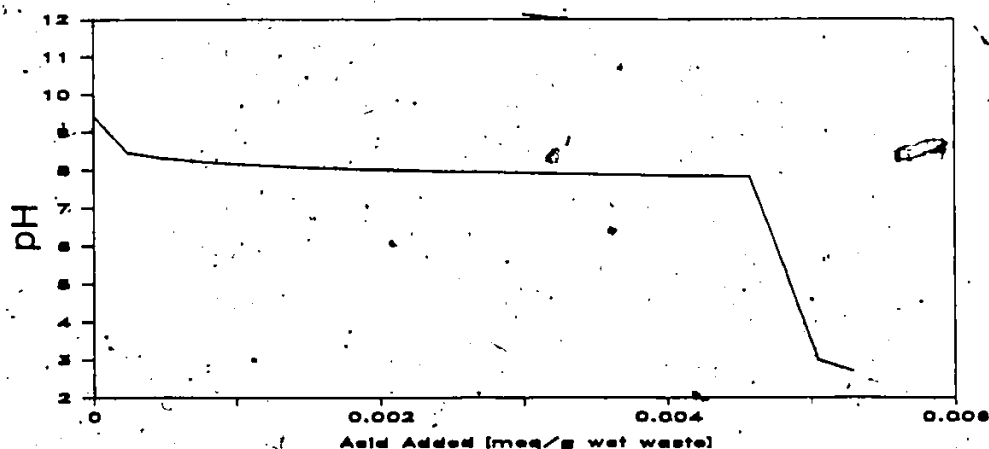


Figure 5.3 Titration curve of the waste form used in Simulation 28 prepared with MINEQL.

The profiles in the porous solid generated with LEEX are presented on Figure 5.4 along with those generated with LEEQ (extracted from Figure 5.2). The differences between the two sets of profiles illustrate well some of the limitations of the titration and solubility curve approach.

First consider the pH profiles (Figure 5.4a). The interface pH predicted by the two programs are identical and the pH profiles in the leached layer are superimposed. This results from the fact that  $H^+$  has a



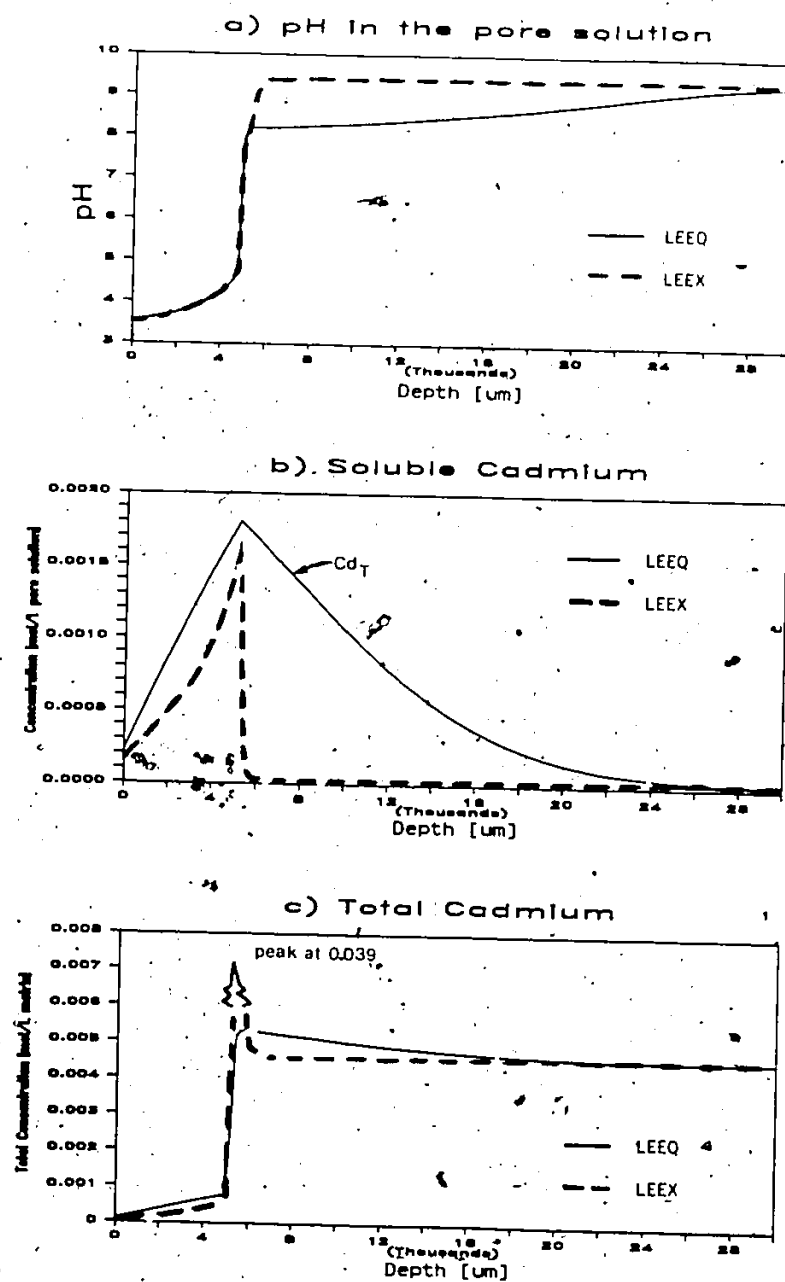
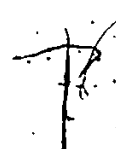


Figure 5.4 Comparison of the profiles at 1 day generated using titration and solubility curves (Simulation 28) to those generated using equilibrium chemistry (Simulation 27).

diffusion coefficient which is approximately one order of magnitude higher than the other species (Table 1-2); the concentration of  $H^+$  in the aqueous solution thus controls the penetration of the reaction front and can be considered an "Independent variable" for this leaching system.

The way by which solubilized cadmium diffuses in the matrix is, however, handled differently by the two programs. The pore solution contains no excess acid neutralization capacity (ANC) and LEEQ predicts that  $Cd^{+2}$  freely moves inward. In LEEEX, however, since little  $H^+$  has diffused past the reaction front, the cumulative amount of acid added to those layers is small (variable  $H_c(i)$ , Equation 4.18) and the titration and solubility curves indicate that the soluble concentration should remain equal to the initial concentration. As a result, the cadmium molecules which attempt to diffuse inward are precipitated just past the reaction front (see peak of total cadmium in Figure 5.4c).

The imprecision observed with the program LEEEX is due to the fact that the ANC for the case studied is entirely provided by the metal of interest for leaching. In practice, waste forms contain a large amount of excess ANC provided, for example, by lime or portland cement which make the contribution of the leaching metal to the overall ANC, essentially negligible. The soluble species would be, in that case, prevented from diffusing inward and the program LEEEX should more accurately describe the phenomenon. This will be discussed further in Chapter 7 in conjunction with the modelling of experimental results.



## 6. EXPERIMENTAL METHODS

Eight batches of solidified waste, referred to as Batches A to H, were prepared for experimentation. The composition of each batch is presented in Table 6.1.

The experimental program, consisting of seven experiments performed on the different batches, is also shown in Table 6.1. A more detailed chronological description of the testing program is presented in Table IV-1.

### 6.1 Preparation of Waste Form Specimens

#### 6.1.1 Materials

All the wastes used in the preparation of the waste form specimens were synthetic. These were prepared by adding reagent grade chemicals to distilled water in the concentrations listed in Table 6.1.

The solidification additives were commercially available products with the exception of the fly ash which was obtained from the Lakeview Power Generation Station, Mississauga, Ontario. The additives included hydrated lime ( $\text{Ca}(\text{OH})_2$ ), Type I portland cement, MIN-U-SIL, bentonite, soluble silicates and fly ash.

MIN-U-SIL is a high purity, inert, crystalline silica powder obtained from L.V. Lomas Chemical Company Ltd., Mississauga, Ontario. According to the supplier's specification, MIN-U-SIL is composed of

Table 6.1 Summary of the experimental testing programme.

Generic System	Powdered Silica without with cement cement		Fly Ash-Cement			Fly Ash-Lime	Clay-Cement	Soluble Silicates Cement
Batch Identification:	A	B	C	D	E	F	G	H
<u>Waste Composition (H)</u>								
As (as $\text{NaAsO}_2$ )			0.01	0.04	0.04	0.04	0.04	0.04
Cd (as $\text{Cd}(\text{NO}_3)_2 \cdot 2\text{H}_2\text{O}$ )	0.01	0.01	0.01	0.04	0.04	0.04	0.04	0.04
Cr (as $\text{CrCl}_3 \cdot 6\text{H}_2\text{O}$ )			0.01	0.04	0.04	0.04	0.04	0.04
Pb (as $\text{Pb}(\text{NO}_3)_2$ )			0.01	0.04	0.04	0.04	0.04	0.04
Li (as $\text{LiNO}_3$ )	0.01	0.1	0.01	0.1				
OH (as KOH)	0.02	0.02						
OH (as $\text{Ca}(\text{OH})_2$ )								
(—Lime was added to a pH of 9.5—)								
<u>Solidification Additives (w/w; wet-weight basis)</u>								
Bentonite							0.85	
Fly ash			2.00	1.85	2.10	1.85		
Lime						0.55		
NIR-U-SIL	3.88	3.88						
Portland cement		0.0154	0.015	0.30	0.45		0.55	0.65
Sodium Silicates								0.60
<u>Contaminant concentration (w/g; wet weight basis)</u>								
Arsenic			393	1051	2080	2260	3050	3230
Cadmium	275	215	373	1365	3580	3740	5290	5640
Chromium			215	680	1460	1520	2110	2250
Lead			687	2516	5640	5890	8350	8890
Lithium	17	170	23	220				
<u>(<math>\mu\text{mol/g}</math>; wet weight basis)</u>								
Arsenic			5.25	14.8	27.8	30.2	40.7	43.1
Cadmium	2.45	2.45	3.32	12.1	31.9	24.4	47.1	50.2
Chromium			4.13	13.1	28.1	29.2	40.6	43.3
Lead			3.32	12.1	27.2	28.4	40.3	42.9
Lithium	2.45	24.5	3.31	31.7				
<u>Experimental Programme</u>								
1. Porosity analysis					E1			
2. Equilibrium leaching					E2	F1	G1	H1
3. Tit. & sol. (low L/S)	A3	B3	C3	D3		F2	G2	H2
4. Tit. & sol. (high L/S)			C4	D4				
5. Static leaching test		B5	C5					
6. Dynamic leach (cont.)	A6	B6	C6	D6				
7. Dynamic leach (int.)					E7	F7	G7	H7

non-porous particles of a low specific surface area ( $0.54 \text{ m}^2/\text{g}$ ). It is composed of 99.7% silica, has a specific gravity equal to 2.65 and can absorb 0.325 gram of water per gram of dry weight.

The bentonite was a sodium montmorillonite clay obtained from the American Colloid Company, Skokie, Illinois. It is a fine powder of high specific surface area. It has a specific gravity of 2.7 and can absorb roughly five times its weight of water.

Type N soluble silicates were obtained from National Silicates, Toronto, Ontario. They come as a water solution of sodium silicate (37.6% solids) with a ratio of  $\text{SiO}_2$  to  $\text{Na}_2\text{O}$  of 3.22.

The acid neutralization capacity of hydrated portland cement was evaluated by titration with a strong acid. Cement was mixed with the inert silica powder (2 g of cement per 100 g of MIN-U-SIL) and water (W/C=17). The mixture was cured for 28 days, crushed to pass a 100 mesh sieve and titrated with  $\text{HNO}_3$  following the method described in Section 6.2.3 using a liquid-to-solid ratio of 10 to 1.

The particle size distributions of the three insoluble powdered additive, MIN-U-SIL, bentonite and fly ash, were determined with a Coulter-Counter.

The solidification additives were analyzed for the metals of interest for the leaching studies after digestion in aqua regia (3 parts of  $\text{HCl}$  for 1 part of  $\text{HNO}_3$ ). In addition, the fly ash was analyzed for several metals to determine its bulk composition. The results are presented in Table 6.2.

Table 6.2 Chemical analysis of the solidification additives.

Chemical Component	Concentration [ $\mu\text{g/g}$ ; wet weight basis]					
	Bentonite	Fly ash	Lime	MIN-U-SIL	Portland cement	Sodium Silicates
Arsenic	10	29	5.3	8.1	5.1	0.2
Cadmium	<2	<2	<2	<2	<2	0.2
Chromium	29	125	29	31	85	0.3
Lead	<2	<2	<2	<2	<2	0.5
Lithium	40	105	5.9	9.2	28	0.2

Note: All additives were commercially available except the fly ash (see text). Gross analysis of Lakeview fly ash: 46.1%  $\text{SiO}_2$ ; 20.4%  $\text{Al}_2\text{O}_3$ ; 15.6%  $\text{Fe}_2\text{O}_3$ ; 3.6%  $\text{CaO}$ ; 1.55%  $\text{K}_2\text{O}$  and 0.78%  $\text{Na}_2\text{O}$ .

#### 6.1.2 Mixing and Molding

All batches were prepared using a Hobart mixer by adding the ingredients in the following order and mixing between each addition: distilled water, waste chemicals, cement or lime and the bulking additive, MIN-U-SIL, fly ash, bentonite or soluble silicates. All dosages indicated in Table 6.1 are expressed by wet weight of additives as described in Section 6.1.1.

In the case of Batches E to H, an additional step was involved as the sludge obtained from liming to  $\text{pH} = 9.5$  was concentrated by discarding the supernatant. A volume of 0.4 L of sludge was obtained per litre of initial solution. The metals (As, Cd, Cr, Pb) were essentially completely segregated with the sludge.

The concentration data presented in Table 6.1 was calculated

based on the weight change of the waste resulting from mixing the solidification additives. The contribution of contaminants from the additives themselves was taken into account when appropriate.

Differently shaped specimens were prepared as described in Table 6.3. The specimens were cured in double plastic bags, normally for 28 days, prior to initiation of testing. Table IV-1 gives the duration of the curing period for any given test.

Table 6.3 Molds used to prepare specimens for leaching tests.

<u>Type</u>	<u>Dimension</u>	<u>Volume</u> [cm <sup>3</sup> ]	<u>Exposed Area</u> [cm <sup>2</sup> ]	<u>Used for</u> <u>Batches</u>
Extraction thimble (cellulose)	10. cm long 4.3 cm i.d. 0.2 cm thick	130.0	295.0	A
Straight wall jar (small)	4.50 cm i.d. 3.25 cm high	51.7	15.9	C
Straight wall jar (large)	9.40 cm i.d. 4.90 cm high	340.0	69.4	B, C, D
2 inch cube	5.08 cm side	131.1	154.8	E to H

## 6.2 Characterization of the Specimens

All specimens, molded in geometrical shapes, were weighed to calculate their bulk density. The water content was determined by drying triplicates of each batch at 60°C to constant weight. Drying at 60°C is a provision of the ASTM Standard Method for Laboratory Determination of Water (Moisture) Content of Soils, Rock and Soil-Aggregate Mixtures (D2216-80) for samples which might undergo

loss of water of crystallization. The specific gravity of the solids from Batches C to H were measured using the ASTM Test for Specific Gravity of Soils (D854-58).

The total metal concentration was determined by crushing a specimen of waste form to pass a 100 mesh sieve and digesting it in aqua regia. Samples of Batches E to H were also submitted to a Sequential Chemical Extraction test following a method described by Fraser and Lum (1983). The metal analyses in all leachates were done by atomic adsorption using a graphite furnace.

#### 6.2.1 Mercury Intrusion Porosimetry

Measurements of porosity and pore size distribution were performed on batches E to F using a 0-60,000 psi Micromeritics Autopore 9200 porosimeter. All samples were dried and outgassed for 45 minutes.

The cumulative volume of mercury was monitored as a function of pressure in intrusion and extrusion modes.

#### 6.2.2 Equilibrium Leaching

Equilibrium leaching tests were performed on Batches E to H as well as on the liquid sludge which was used for their preparation. Samples were crushed and sieved to pass 100 mesh size (149  $\mu\text{m}$ ). Ten grams were mixed with 300 mLs of distilled water and contacted for 28 days. The leaching containers were hand agitated every day. At the end of the test, the pH and conductivity were measured, the samples were filtered through a 0.45  $\mu\text{m}$  filter paper, acidified and analyzed for the parameters listed in Table VII-1.



### 6.2.3 Titration and Solubility (low liquid-to-solid ratio)

Titration of a cement paste and of waste form batches A to D was performed in a series of 20-40 mL centrifuge tubes. 500 grams of the sample were first crushed and sieved to pass 100 mesh. Subsamples of 20 g were precisely weighed and added to each tube. A precise amount of 2.02 N  $\text{HNO}_3$  and distilled water was added incrementally to the tubes in order to cover a wide pH range (preliminary tests were required to determine the maximum amount of acid required). The actual amount of acid added is listed in the Tables of Appendix VIII. The total of the volumes of acid and distilled water added was about 20 mL so that the liquid-to-solid ratio was approximately 1.

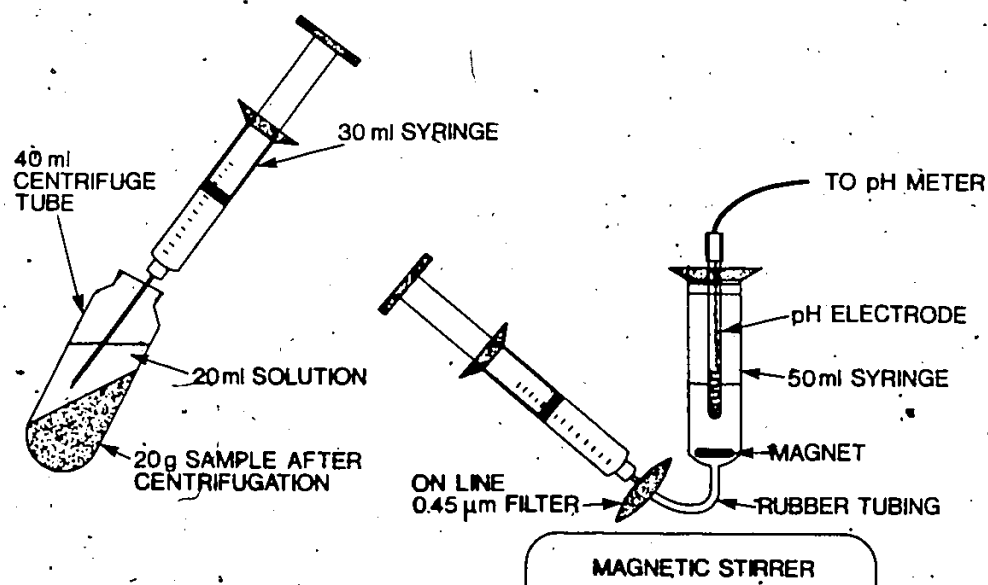
Nitric acid (2.02 N) was prepared by dilution from concentrated acid. Its precise normality was measured by titrating a standard solution of sodium carbonate. The end point of the titration was determined by Gran analysis (Table VIII-10). The acid was added to each tube using a high precision microburette (Gilmont Instrument Inc. 54200A).

The 20 centrifuge tubes were tumbled for 24 hours and then centrifuged at 10,000 rpm for 10 minutes. The pH of the supernatants were measured following the steps illustrated on Figure 6.1. This procedure was necessary to obtain stable pH readings.

The supernatant from a tube was withdrawn using a 30 mL luer-lok type syringe. The long needle was then replaced by an on-line 0.45  $\mu\text{m}$  filter assembly and the solution was introduced into a 50 mL syringe.

used to measure the pH. As shown in Figure 6.1b, the solution was isolated from atmospheric  $\text{CO}_2$  and was also agitated during the measurement. This set up provided stable readings throughout the pH range. The pH was measured with a Orion Ross electrode and a digital Fisher Accumet Model 750 meter.

After pH measurement, the solution was drained into a sampling bottle, acidified and saved for metal analysis by atomic adsorption. The pH measurement syringe was triple rinsed with distilled water before starting the next sample.



a) Separate the solution after centrifugation.

b) Filtration of the sample and measurement of pH.

Figure 6.1 Set-up for the titration and solubility experiments.

#### 6.2.4 Titration and Solubility (high liquid-to-solid ratio)

This experiment was conducted on Batches C and D in a manner similar to the low liquid-to-solid ratio test described in Section 6.2.3. However, a much larger quantity of water was used in order to avoid solubility limits. Samples of approximately 1 g were precisely weighed and mixed with 900 mL of distilled water in a series of 1 L bottles. Different amounts of  $\text{HNO}_3$  were added to each bottle to cover a wide range of pH. The bottles were tumbled for 24 hours, the pH was measured and liquid samples were filtered and analyzed for metals.

#### 6.2.5 Static Leaching

Static leaching tests were performed on Batches B and C. The experiments are described in general terms here as specific information is given in Appendix X.

A 4-litre beaker placed in a 25°C temperature bath was used as leaching reactor. The leachant was prepared from distilled water by the addition of potassium nitrate as the ionic medium and of nitric acid to lower the pH. A known volume of the leachant was poured into the reactor. The test was initiated by lowering the waste form specimen of known exposed surface area into the reactor. An Orion Ross pH electrode connected to a Fisher Accumet meter interfaced with a HP 1000 mini-computer was used to monitor the pH. The aqueous solution in the reactor was slowly stirred to ensure good mixing. The reactor was covered with a plastic sheet to prevent evaporation.

Aliquots of 20 mL of the aqueous solution were taken at frequent times during the experiment, acidified and saved for analysis.

#### 6.2.6 Dynamic Leaching (Continuous Flow)

Dynamic leaching tests, in a continuous flow mode, were performed on Batches A, B, C and D. The experiments are described on general terms here as specific details are given in Appendix XI.

The experimental set-up, illustrated in Figure 6.2, was composed of a feed system, a leaching reactor and an automatic sampler. The experiments were conducted in a way similar to the static leaching tests described in Section 6.2.5 with the difference that kinetic information was obtained in the dynamic test by sampling the effluent from the reactor.

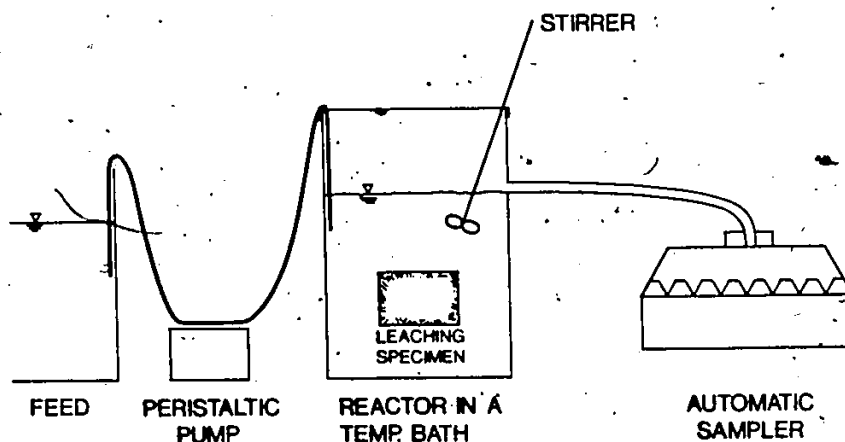


Figure 6.2 Experimental set-up to obtain kinetic leaching data.

### 6.2.7 Dynamic Leaching (Intermittent Flow)

Dynamic leaching tests were carried out for 665 days on Batches E to H. The tests were carried out in closed 2 litre plastic bottles using distilled water as a leachant. A test was conducted by immersing a waste form specimen (5.04 cm cube) in the leachant using a specimen surface area-to-leachant volume ratio of  $0.10 \text{ cm}^{-1}$ . The leachant was renewed at frequent intervals, and the concentrations of the species of interest leached during each interval were determined. The test bottles were not agitated because it was assumed that the dispersion rate of the contaminants in the leachate was much larger than their leaching rate, thus eliminating concentration gradients in the leachate.

The schedule for leachant renewal was established based on the fact that bulk diffusion is the controlling leaching mechanism. When this is the case, the leach rates decrease with time and it is necessary to gradually increase the contact time between renewals to ensure that the leached species can be analytically measured in the leachate. A leaching renewal schedule that ensures equal amounts leached per leaching period (for bulk diffusion controlled leaching) is expressed as (Côté and Isabel, 1984):

$$t_n = n^2 t_1 \quad 6.1$$

where:  $n$  = leaching period  
 $t_1$  = end of the first leaching period [T]  
 $t_n$  = end of the nth leaching period [T]

Different values of  $t_1$  can be used for contaminants of various mobilities to ensure that concentration buildup in the leachate does not limit leaching. Two frequencies were used,  $t_1 = 1$  hour for arsenic

(Experiments terminated by "I", Appendix XII) and  $t_1 = 4$  hours for cadmium, chromium and lead (Experiments terminated by "II"). The leachate renewal schedule calculated from Equation 6.1 was adjusted for compatibility with working hours. After approximately 5 months, constant renewal frequencies of 1 week (for arsenic) and two weeks (for cadmium, chromium and lead) were adopted. The actual leachant changes times are recorded in the tables of Appendix XII. Equation 4.6, which defines the leachant velocity  $v$  in terms of the specimen surface area-to-aqueous solution ratio and the leachant renewal frequency, can be combined with Equation 6.1 to express theoretically the leachant velocity used in the dynamic leaching test:

$$v = \frac{1}{B} \times \frac{1}{t_1(2n-1)} \quad (6.2)$$

The target leachant velocity calculated with Equation 6.2 is compared to the actual velocity in Figure 6.3.

At the end of each leaching period, the pH and conductivity of the leachates were measured and aliquots were taken for analysis.

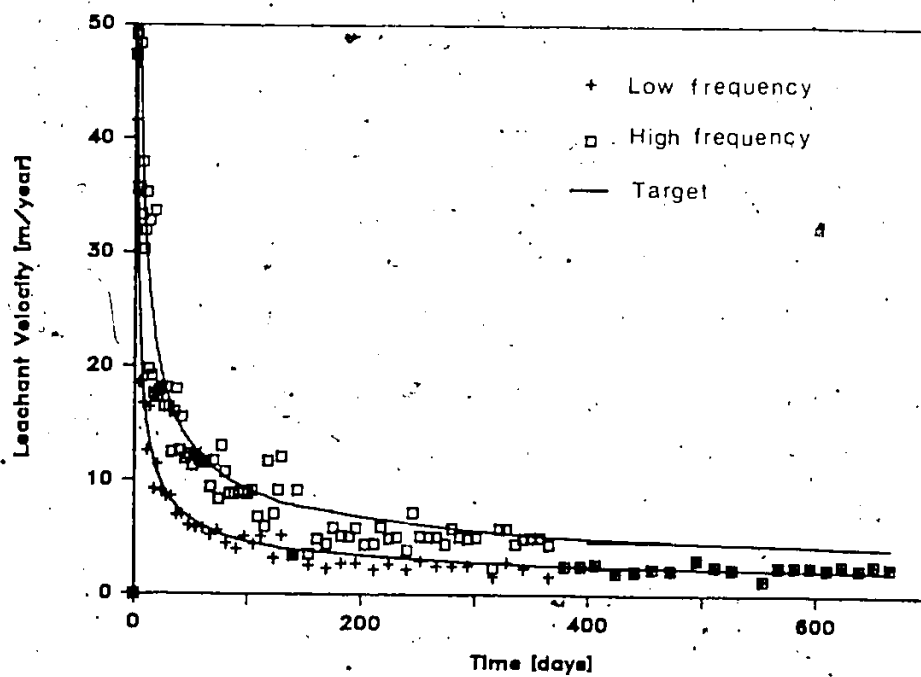


Figure 6.3 Target and actual leachant velocities for the intermittent flow dynamic leaching tests.

## 7. RESULTS AND DISCUSSION

Cement-based waste forms are complex from both a morphological and a chemical point of view. The approach taken in the experimental programme was to study several waste forms of increasing complexity, starting with a non-reactive matrix containing a soluble chemical species. Several chemical species were monitored: lithium as a tracer, cadmium, chromium and lead representing typical metal contaminants and arsenic as a complex anionic species.

This chapter is divided into four sections. The morphological properties of the waste forms is first examined in Section 7.1. In Section 7.2, the contaminant solubility and availability for leaching at equilibrium are determined using pH as a master variable. The kinetics of leaching are studied and modelled in Section 7.3. Severe experimental conditions (i.e. low pH and/or high leachant velocity) were used in order to speed up leaching and reduce the duration of the experiments. Finally, in Section 7.4, the results of long term dynamic leaching tests conducted under conditions more representative of field environments are analyzed and interpreted.

The leaching model presented in Chapter 4 is based on an idealized representation of the waste form matrix and on simple mechanisms of interaction between the leachant and the waste matrix. This model is used as a tool to study leaching mechanisms. In this context, the goodness of fit is not important since it is not intended



to use the model for predictive purposes.

### 7.1 Microstructure of the Waste Forms

In this section, the porosity, pore size distribution and degree of saturation of waste form matrices will be examined. These factors are important in view of the fact that leaching takes place via diffusive exchanges through a water path within the waste matrix.

#### 7.1.1 Particle Size Distribution of Insoluble Powdery Additives

The average particle diameters of the fly ash, the powdered silica (MIN-U-SIL) and the bentonite were 11.7, 11.7 and 7.5  $\mu\text{m}$  respectively. The fly ash and the MIN-U-SIL had similar particle size distributions (Figure III-1), while the bentonite was composed of smaller particles.

Fly ash and bentonite particles are porous materials which will absorb water and chemically interact with the waste components. The powdered silica is non-porous and should be relatively inert. Thus it was selected as a bulking agent to be used in simple waste forms to identify, by reference, interactions of the contaminants with the other matrices.

#### 7.1.2 Moisture-density Characteristics

Measurement of the waste form bulk density, water content and solids specific gravity allows calculation of the matrix porosity and degree of saturation (relationships presented in Table III-2). The

moisture-density properties of all the batches used in the experimental programme are presented in Table 7.1.

Table 7.1 Moisture-density relationships of the specimens prepared in the laboratory.

Batch ID	Solidification System	Bulk Density [g/cm <sup>3</sup> ]	Water Content [w/w]	Solids Specific Gravity	Porosity [%]	Degree of Saturation [%]
A	Powdered Silica	1.90	0.240	2.65	45.5	100.0
B	Powdered Silica-cement	1.76	0.240	2.65	49.5	85.3
C	Fly Ash-cement	1.62	0.310	2.81	60.2	83.4
D	Fly Ash-cement	1.69	0.240	2.81	54.3	74.7
E	Fly Ash-cement	1.72	0.143	2.90	49.2	50.0
F	Fly Ash-lime	1.63	0.179	2.25	40.5	72.0
G	Clay-cement	1.54	0.303	3.64 (2.33)	53.9	42.4
H	Soluble Silicate-cement	1.25	0.518	4.89 (1.57)	61.6	23.7

NOTE: The specific gravity values in bracket were back-calculated from the porosity measured by mercury intrusion.

The bulk density of the batches prepared ranged from 1.25 to 1.90 g/cm<sup>3</sup> while the water content varied from 0.143 to 0.518. The lower bulk densities are associated with high water contents.

The specific gravity of the solids was measured using a soil standard method (ASTM D854.58) except for Batches A and B where the published value for silica (2.65) was used. The soil method, which involves measuring the volume of water displaced by a known amount of

sample works well provided that the sample is not water soluble. If it is, the measured specific gravity is artificially higher because dissolved solids occupy a much smaller volume. The specific gravities of the batches based on fly ash (C to F), ranged between 2.25 and 2.90, and are comparable to published values, while the values for the clay-cement batch (3.64) and the soluble silicates-cement batch (4.89) are higher. It was noted in the equilibrium leaching tests that those waste forms based on bentonite and soluble silicates are much more soluble than those based on fly ash. Therefore, for the purpose of reporting porosity and degree of saturation, specific gravities derived from mercury intrusion data analysis (Section 7.1.3) were used for Batches G and H.

The porosity of the waste form specimens varied from 40.5% to 61.6% and the voids, except for Batch A, were only partially saturated with water.

### 7.1.3. Mercury Intrusion Porosity

The results of the mercury intrusion analyses are presented in Table V-1 as the amount of mercury intruded ( $\text{cm}^3/\text{g}$ ) as a function of the pressure of intrusion. The pore size distribution can be approximated by estimating the pore size intruded at a certain mercury pressure. The Washburn Equation (Orr, 1969) can be used for this purpose if it is assumed that the pores are straight cylindrical capillaries. The pore radius is given by:

$$r = \frac{-2 \sigma \cos \theta}{P} \quad (7.1)$$

where  $\theta$  = contact angle ( $130^\circ$ )  
 $\sigma$  = Hg surface tension (4585 dynes/cm)  
 $P$  = pressure of intrusion

The pore diameters calculated with this equation, presented in the second column of Table V-1, range from 0.003  $\mu\text{m}$  to 325  $\mu\text{m}$ .

The amount of mercury intruded at maximum pressure, as presented in Table V-1, can not be directly associated with the specimen total porosity for two reasons: first, the large pores are destroyed by drying the sample prior to processing and secondly, the initial sample volume (calculated as the difference between the chamber volume and the volume of mercury required to fill the chamber at the initial pressure) is underestimated since some pores are intruded at the low initial pressure. Therefore, this method underestimates total porosity.

A better estimation of the true specimen porosity can be obtained by adding to the volume of mercury intruded, a correction volume, which accounts for the volume of voids destroyed by drying the sample and the volume of voids initially intruded at the minimum pressure. The calculations are presented in Table V-2. The corrected cumulative porosity of 5 samples is shown in Figure 7.1. Replicates, run on Batch E, show good reproducibility. The bentonite and fly ash systems have pores in three distinct ranges:  $>100 \mu\text{m}$ ,  $\approx 1 \mu\text{m}$  and  $<0.1 \mu\text{m}$ . These are interpreted as follows. The volume in the pores larger than 100  $\mu\text{m}$  comprises voids between clumps of particles (macropores), while the volume in pores of approximately 1  $\mu\text{m}$  is interparticle space, within the clumps. Finally, for pore sizes smaller than 0.1  $\mu\text{m}$ , mercury

intruded the fly ash and clay particles as well as the cement gel pores. The soluble silicate-based porosity is almost entirely composed of macropores.

Plots of the cumulative porosity as a function of pore diameter in intrusion and extrusion mode, shows marked hysteresis (Figures V-1 to V-4). This is indicative of pores with narrow throats opening into large cavities (Orr, 1969). As a result, the volume of these large cavities are added to the cumulative porosity at a pore diameter which corresponds to the narrow throats. Therefore, although the total porosity might be considered exact, the pore volume distribution is not: the volume of large pores is underestimated, and the volume of small pores is overestimated.

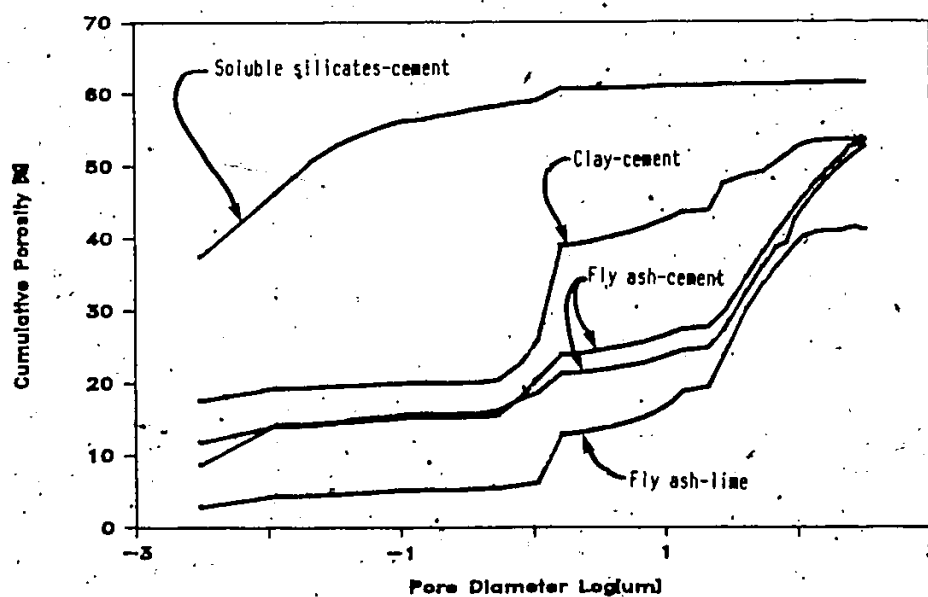


Figure 7.1 Corrected cumulative porosity from mercury intrusion.

## 7.2 Chemical Containment of Contaminants

The purpose of the experimental work reported in this section was to measure the solubility of chemical species in the waste form matrix, at equilibrium and as a function of pH. The distribution of chemical species among the different fractions described in Figure 4.1 is discussed in Section 7.2.1. Titration and solubility curves, which will be used in the model LEEX to simulate leaching under dynamic conditions, are presented in Section 7.2.2.

All the waste form samples were crushed to a powder ( $\sim 150 \mu\text{m}$ ) in order to speed up attainment of chemical equilibrium. As seen in the preceding section, this crushing exposes a larger surface of contact with the leachant without destroying the microstructure of the matrix (i.e., most of the pore openings are much smaller than  $150 \mu\text{m}$ , with the exception of the soluble silicate system).

### 7.2.1 Distribution of Chemical Species in the Matrix

The total concentrations of chemical species in the waste form matrices calculated from the amount originally present in the waste are presented in Table 6.1. These concentrations were verified by performing a total digestion and a chemical sequential extraction on Batches E to H. The results, presented in Tables VI-1 to VI-3, indicate complete recovery of Cd, Cr and Pb with respect to the calculated concentrations. It is worth noting that negligible amounts of the metals were recovered in fraction E of the Chemical Sequential Extraction tests, indicating that the metals were not present as silicates in the matrix (Fraser and Lum, 1983).

### Fraction in Solution in the Pores

The concentrations measured in the equilibrium leaching test (Experiment 2), where no acid was added, closely reflect the composition of the waste form pore solution. Dilution of the pore solution by the leachant is not a factor since the metals of interest, As, Cd, Cr and Pb, were present in sufficiently large concentrations in the matrix to saturate the leaching test solutions. The leachate pH from the solidified wastes ranged from 11.1 to 11.9 (Table 7.2). The pH of the fly ash based systems was slightly lower than the other systems, probably due to pozzolanic reactions immobilizing the free lime.

The calculated fractions of As, Cd, Cr and Pb in solution in the pores of each of the four matrices are presented in Table 7.2. The soluble fractions are small, ranging from  $10^{-2.52}$  for arsenic in the soluble silicate matrix to  $10^{-6.55}$  for cadmium in the fly ash-cement matrix (note that all contaminants were originally present in the waste in the same molar concentration).

### Fraction Available for Leaching

The availability for leaching was defined in Section 4.1 as that fraction soluble in a leaching medium when an equilibrium leaching test is conducted at infinite liquid-to-solid ratio. Specification of an infinite ratio implies that, i) a high concentration in the liquid phase does not drive an adsorption reaction on the solid surface and, ii) no solubility product is exceeded.

Table 7.2 Results of the equilibrium leaching experiments.

	Batch E Fly ash cement	Batch F Fly ash lime	Batch G Clay cement	Batch H Soluble Silicates cement
pH	11.15	11.50	11.75	11.85
Conductivity [ $\mu\text{S}/\text{cm}$ ]	1380	1755	3065	4550
Calculated fraction in solution in the pore				
Arsenic	$10^{-4.44}$	$10^{-4.83}$	$10^{-4.94}$	$10^{-2.52}$
Cadmium	$10^{-6.55}$	$10^{-6.42}$	$10^{-6.50}$	$10^{-6.74}$
Chromium	$10^{-4.48}$	$10^{-4.97}$	$10^{-5.20}$	$10^{-5.06}$
Lead	$10^{-5.58}$	$10^{-5.14}$	$10^{-4.67}$	$10^{-5.20}$

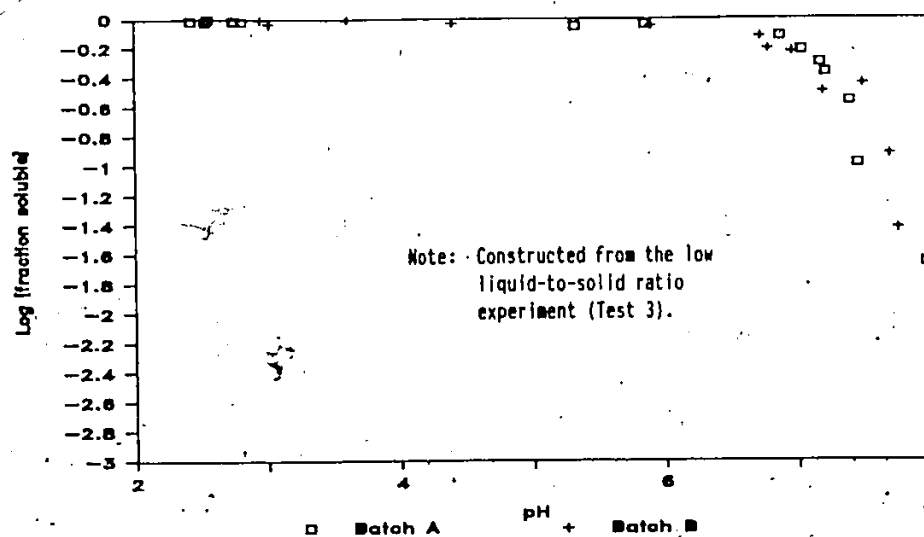
Note: Based on the results of Experiment 2 presented in Appendix VII

Titration and solubility experiments were conducted at low (1/1 in Experiment 3) and high (1200/1 in Experiment 4) liquid-to-solid ratios to measure the availability of metals for leaching under acidic conditions. The experiments were run on Batches A to D, which were also used in the validation of the models LEEQ and LEEEX (see Section 7.3). The soluble fractions, calculated from the concentration data of Appendix VIII and IX, are presented in Figure 7.2 for Batches A, B and C. The results for Batch D are similar to those of Batch C and will not be discussed in detail.

The soluble fractions are presented for the acidic pH range only since, at higher pH, the solubility is limited by hydroxide precipitation. At pH values smaller than 7, however, the hydroxide solubility products were not exceeded indicating that the portion of a



## a) Cadmium from Batches A and B



## b) Cadmium from Batch C

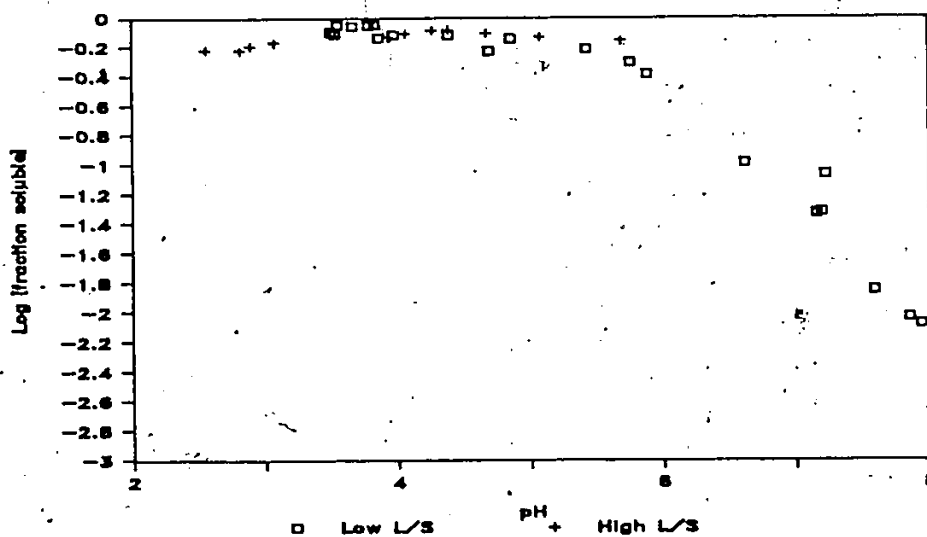
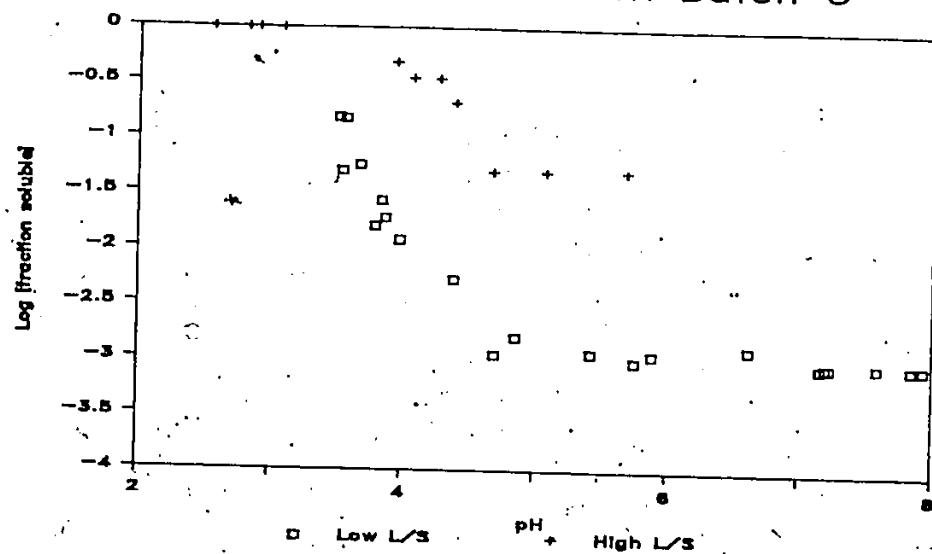


Figure 7.2 Fraction available for leaching under acidic conditions.

## c) Chromium from Batch C



## d) Lead from Batch C

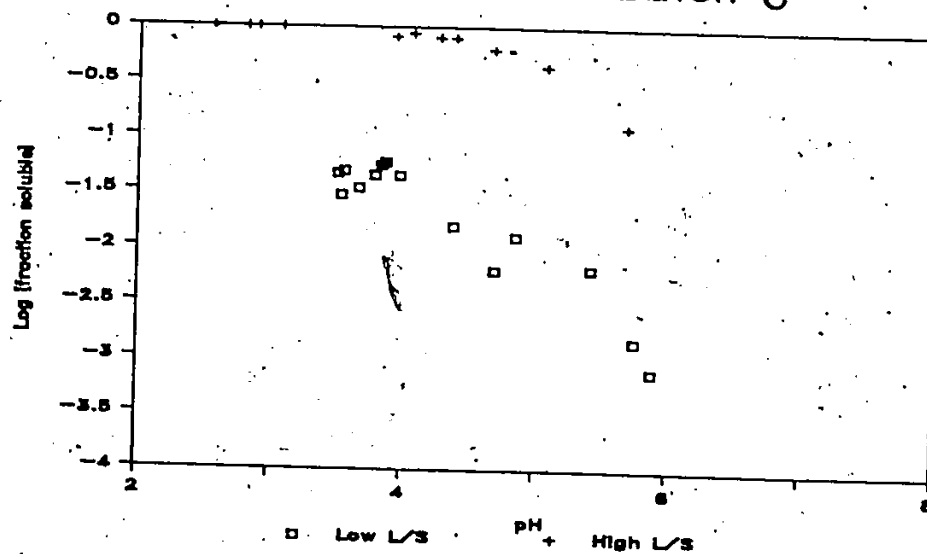


Figure 7.2 Continued ...

metal found insoluble was kept out of solution as a result of interactions with the matrix (unless other precipitates were formed at low pH which might be the case for cadmium, as discussed below).

The matrix of Batches A and B, composed of inert MIN-U-SIL, did not immobilize cadmium at low pH (Figure 7.2a). For pH values smaller than 6.5, all of the cadmium was solubilized.

In Batch C, however, the data collected between pH values ranging from 2 to 6 indicate that no more than approximately 60% of the total cadmium concentration was solubilized at the 1/1 or at the 1200/1 liquid-to-solid ratio (Figure 7.2b). Furthermore, for pH values smaller than 3, the amount of soluble cadmium decreased (drastically for Batch D). It is postulated that acid dissolved the fly ash and that insoluble calcium silicates were produced, incorporating cadmium. This mechanism is confirmed by the drop in calcium concentration observed as pH is reduced (Table IX-1).

Chromium was essentially unavailable for leaching at pH larger than 4 (Figure 7.2c). It became available for leaching at lower pH values. Lead availability is similar to that of chromium. In both cases there was a large difference between the 1/1 and the 1200/1 liquid-to-solid ratios, indicating that the mechanisms of immobilization might be adsorption, which is a function of the concentrations in the liquid phase.

Based on the concentration data, it was calculated that the matrices of Batches C and D could adsorb between 1 to 3  $\mu\text{g/g}$  of wet matrix of each of the three metals studied at pH values ranging between

3 and 7 (Figure IX-1). These represent a significant fraction of the metals present in the matrix.

The implications of these findings are important. Even if the pH in the pores drops to a value as low as 4, the amount of metal solubilized will be small (for Cd) or even negligible (for Cr and Pb) as long as the pore metal concentration does not decrease to small values. This will indeed eventually happen as the soluble metals leach out. However, the fraction available for leaching tends to maintain a relatively high concentration in the pores. Furthermore, if the transport mechanism is diffusion controlled, the concentration will decrease very slowly, as will be seen in the next sections. Overall, it appears that, for the fly ash-cement system, interaction with the matrix played an important role in the containment of metals.

#### 7.2.2 Titration and Solubility

##### Solubility

The results of Experiment 3 can be used to evaluate the solubility of toxic metals as a function of pH, in the waste environment. Since this experiment was conducted at a low liquid-to-solid ratio, the results can be interpreted as the concentration in the pores of the matrix as a function of pH.

Batches A and B are based on powdered silica; A does not contain cement while B does. Similarly, Batches C and D are both fly ash based, but contain a different dosage of cement. Although different amounts of acid were necessary to bring the pH in the titration test

tubes down to the same values, the solubility seems to be independent of the presence of cement. Indeed, the concentrations plotted as a function of pH in Figure 7.3 and 7.4 show no difference between Batches A and B, or between Batches C and D.

The measured solubility of cadmium, chromium and lead is compared to their hydroxide solubility in Figures 7.3 and 7.4. The hydroxide solubilities were calculated using Equation 6 of Table 3.4 and the stability constants listed on Figure 3.4.

For Batches A and B, the measured solubility of cadmium (Figure 7.3) corresponds to its hydroxide solubility. The solubility product ( $K_{SO}=11.28$ ) and stability constants ( $K_1=8.27$ ;  $\beta_2=21.0$ ;  $\beta_3=-33.3$ ), determined by non-linear least squares estimation fall well within the range of published values (Sillen and Martell, 1964). The details of the statistical analysis are given in Table VIII-5.

For Batches C and D, the measured solubilities of the three metals are comparable to their hydroxide solubility in the intermediate and high pH ranges while they are lower by several orders of magnitude for pH less than 7 (Figure 7.4). The effect for chromium is unique. Its solubility is reduced to a minimum which compares to the minimum hydroxide solubility throughout a pH range from 4 to 12 (Figure 7.4b). The fly ash matrix obviously interacted with the metals, most likely by adsorption, to limit their solubility.

The measured solubilities as a function of pH for Batches C and D were fitted with empirical models using non-linear least square estimation. The models, presented in Table VIII-5, are plotted in Figure

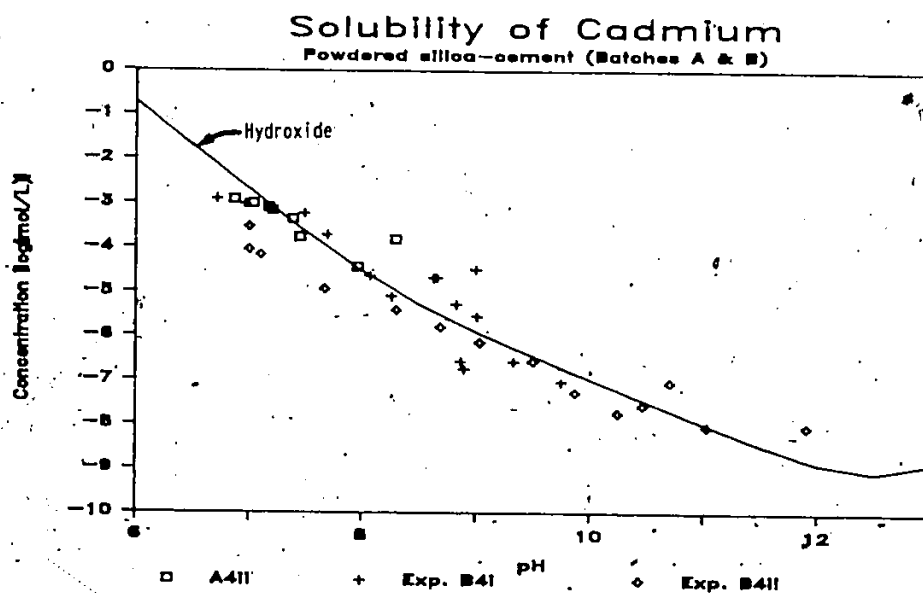


Figure 7.3 Comparison of measured solubility and hydroxide solubility for Batches A and B.

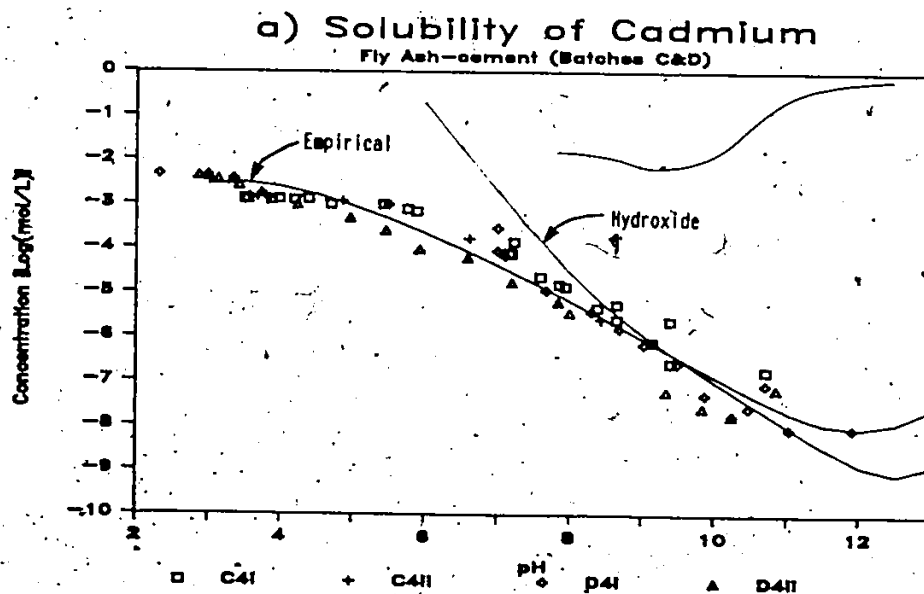
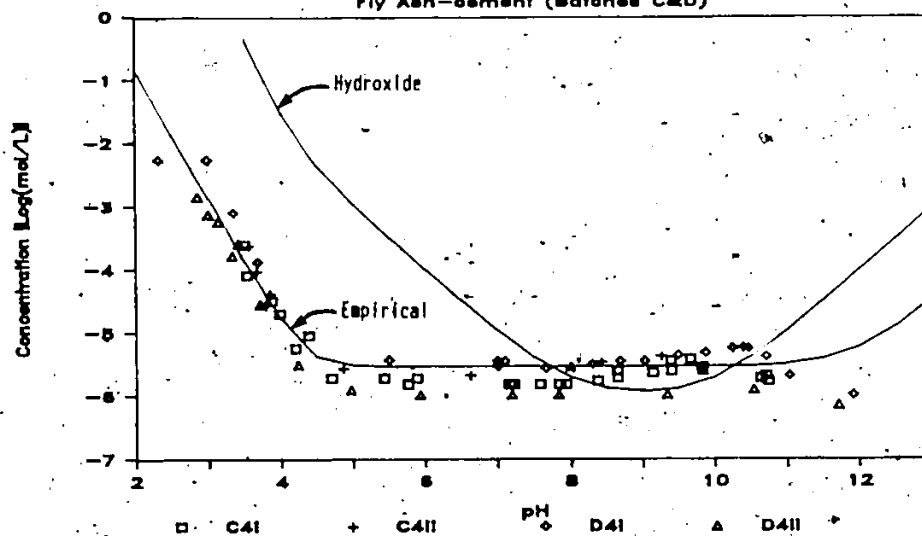


Figure 7.4 Comparison of measured solubility and hydroxide solubility for Batches C and D.

## b) Solubility of Chromium

Fly Ash-cement (Batches C&amp;D)



## c) Solubility of Lead

Fly Ash-cement (Batches C&amp;D)

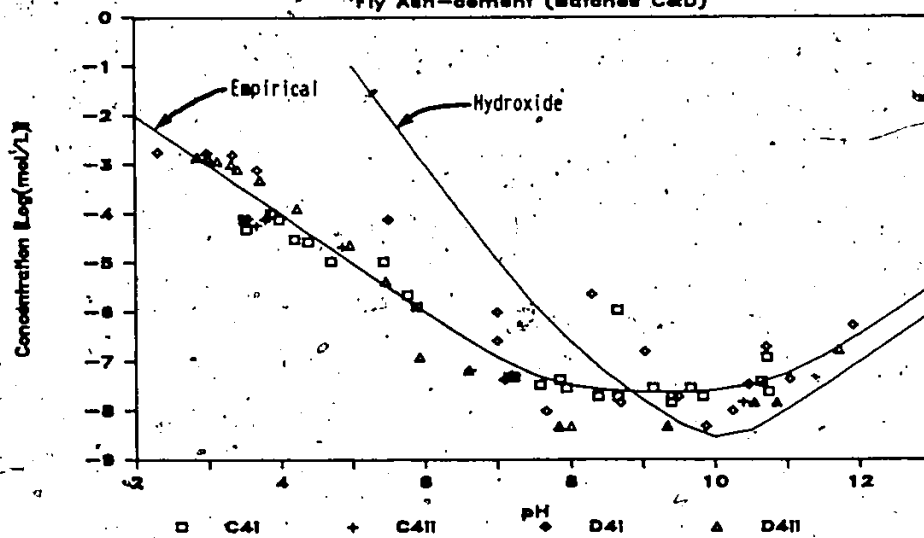


Figure 7.4 Continued ...

7.4. These empirical models will be used in Section 7.3 to simulate the kinetics of leaching with the model LEEX.

#### Acid Neutralization Capacity

The acid neutralization capacity (ANC) can be analyzed from the titration and solubility experiment (3) for Batches A, B, C and D. Acid neutralization capacity is defined as the amount of a strong acid required, in a titration, to reach an equivalence point (Stumm and Morgan, 1981). In our case, the titration end point is that beyond which the added acid stays as free hydrogen ion in solution. The end point can be determined using Gran analysis (Stumm and Morgan, 1981). The changes required to use this analysis when titrating solid samples are outlined in Table VIII-6. The total ANC of a waste form is contributed by the waste itself and by the matrix constituents.

One of the most important ANC contributing additives in waste forms is portland cement. Based on the lime content of the powder, 65% by weight as  $\text{CaO}$ , the ANC would be 23.0 milliequivalents (meq) per gram of dry portland cement. The theoretical amount of  $\text{Ca(OH)}_2$  produced from hydration is 8 meq/g dry cement, as calculated in Section 3.2.2. Table III-3 shows the results of an acid titration performed on a fully hydrated cement paste. The use of Gran analysis does not permit the identification of an end point even though the pH was brought down to a value as low as 2.53. There is, however, a sharp break on the curve at approximately 20 meq/g of dry cement where the pH drops from 8 to less than 4. pH measurements, done after 24 and 48 hours of mixing, indicated



that equilibrium had been reached after 24 hours. It is important to note that, when attacked by a strong acid, portland cement provides ANC in a pH range (i.e.  $> 8.5$ ) where toxic metals have minimum solubility and completely dissolves before the metals become soluble. These results agree with data reported by Poon et al (1985) who conducted sequential batch tests using a strong acid. They determined that a breakthrough of toxic metals occurred after approximately 66% of the hydrated cement paste had been neutralized (measured as the fraction of calcium solubilized). This is equivalent to 15 meq/g of dry cement paste.

The measured titration curves of Batches A to D are presented in Figure VIII-1 to VIII-4. They will be analyzed with reference to Table 7.3. Each titration experiment was conducted in replicate and showed good reproducibility. The measured ANCs cover a wide range, from 0.011 to 2.4 meq/g of wet waste. The titration end point could only be determined using Gran analysis for Batch A. For Batches B, C and D, a pH = 4 was arbitrarily selected as the end point since addition of acid beyond that pH continued dissolving the matrix. The contribution of the waste and portland cement to the overall ANC (Table 7.3) was calculated from their respective dosages (Table 8.1). These calculations left a residual which was associated with the matrix (i.e. the powdered silica or the fly ash).

Batch A did not contain cement and the measured ANC is approximately equally split between the waste and the matrix. Examination of the titration data (Table VIII-1) reveals that all cadmium had dissolved by the time the pH reached 7. The matrix ANC is

thus consumed in a lower pH range. Even if Batch B contained only a small dosage of cement (0.38% of the total matrix by weight), it increased the waste form ANC by a factor of nine.

Table 7.3 Acid neutralization capacity (ANC) of waste forms.

Batch	System	Total Measured [meq/g; w.w.b]	Contributed by		Residual Matrix	
			Waste [meq/g; w.w.b]	Cement [meq/g; w.w.b]	[meq/g] w.w.b	[meq/g] d.w.b.
A	Powdered Silica	0.011	0.006	-----	0.005	0.0066
B	Powdered Silica Cement	0.09	0.005	0.083 <sup>(2)</sup>	0.002	0.0026
C	Fly Ash-Cement	0.42	----- <sup>(1)</sup>	0.110 <sup>(2)</sup>	0.31	0.47
D	Fly Ash-Cement	2.4	----- <sup>(1)</sup>	2.10 <sup>(2)</sup>	0.30	0.45

(1) Cement was directly added to the waste solution.

(2) Based on cement ANC of 22 meq/g dry cement.

The calculated residual ANC of powdered silica (0.0066 meq/g from titration of Batch A and 0.0026 meq/g from titration of Batch B) can be compared to published values. Shindler (1981) reported that the concentration of hydroxyl groups on amorphous silica surfaces was approximately 5.0 OH/100 Å<sup>2</sup>. Based on a specific surface area for MIN-U-SIL of 0.54 m<sup>2</sup>/g (Section 6.1.1), this is equivalent to 0.0045 meq/g of silica powder.

Very little cement was added to Batch C and a large portion of it was consumed to neutralize the waste. A large fraction of the ANC

(=75%) was thus associated with the matrix (e.g. fly ash). For Batch D, the cement dosage (9.5% by weight of total waste form) is more typical of a commercial waste form (Cote and Hamilton, 1983). The ANC, in that case, is essentially associated with the cement. Based on the alkali content of the Lakeview fly ash (Table 6.2), a theoretical ANC can be calculated to be approximately 2 meq/gram of dry fly ash. This is much higher than the value derived from titration of Batches C and D (0.46 meq/g) indicating that the alkalis are not available to neutralize acid. Ness et al (1978) reported that the availability of alkalis from western coal fly ashes varied from 65% to as low as 10% as a function of pH.

### 7.3 Mechanisms of Leaching

Kinetic conditions were maintained in leaching experiments 5 and 6 to study the mechanisms of leaching. The samples used in these experiments had defined shapes of known geometrical surface area of contact with the leachant. Furthermore, the experimental conditions were adjusted to allow optimal use of the models LEEQ and LEEX, described in Chapter 4, while producing precise analytical results in a short period of time. The most important model limitations are related to the numerical solution of the diffusion equation. A relatively thick layer must be affected by leaching to obtain numerical precision (Section 5.4). At the same time, the semi-infinite geometry assumption must be respected. The first limitation applies to reacting species (e.g. dissolution of a metal) while the second applies to soluble species. For that reason, for any given experiment, the results might

be usable for model validation with only either the soluble or the insoluble species contained in the matrix. A number of factors, including sample geometrical shape, concentration of species in the matrix, leachant-volume-to-specimen-surface-area, leachant velocity and pH were used to adjust the experimental conditions.

Two types of contaminants will be studied in this section. For soluble contaminants (Section 7.3.1) which reside in the pores of the matrix, the important leaching mechanisms include diffusivity, matrix connected porosity and the effect of leachant flow. For insoluble contaminants (Section 7.3.2), in addition to the above mentioned factors, mobilization through reaction (with  $H^+$  in our case) must be considered. A low leachant pH of 3 was used to reduce the duration of the experiments.

The concentrations predicted by the models are instantaneous concentrations while those measured in the dynamic leaching tests are averages over the sampling period (4 or 6 hours, for most experiments). The measured concentrations will thus be compared to simulated concentrations corresponding to the middle of a sampling interval. In order for this comparison to be valid it is assumed that leach rates are linear over a period of time corresponding to the sampling period.

The results of the experiments, along with the details of the experimental conditions, are presented in Appendices X (Static Leaching Tests) and XI (Dynamic Leaching Tests - Continuous Flow). The input data for all simulations are presented in Table II-2.

### 7.3.1 Soluble contaminants

#### Powdered Silica (Batch B)

The powdered silica matrix (Batch A or B) is a simple matrix for which the connected porosity can easily be determined. Because MIN-U-SIL is a non-porous solid and since there was very little if any cement added, the water content determined by drying can be taken as the connected porosity.

The results of replicated Experiment B5 and of Experiment B6 are presented in Figure 7.5 along with three simulation runs for the leaching of lithium. The results are presented as normalized concentrations (concentration in the reactor/initial concentration in the pores). In the static experiments (B5I and B5II), the concentration of lithium in the reactor increased until the end of the experiment. If the experiment was run for a very long time, the concentration in the reactor would level off and become equal to the concentration in the pore solution (i.e. equilibrium would be reached). In the dynamic experiment (B6I), the concentration in the reactor went through a maximum as the "wash off" effect of renewing the leachant became more important than the diffusion controlled leach rate after about 20 hours. It is interesting to note that even though the concentrations in the dynamic experiment are lower than in the static experiment, the leaching rates (and to the same extent the cumulative amounts leached) are higher since a lower interface concentration maintained a higher driving force for leaching.

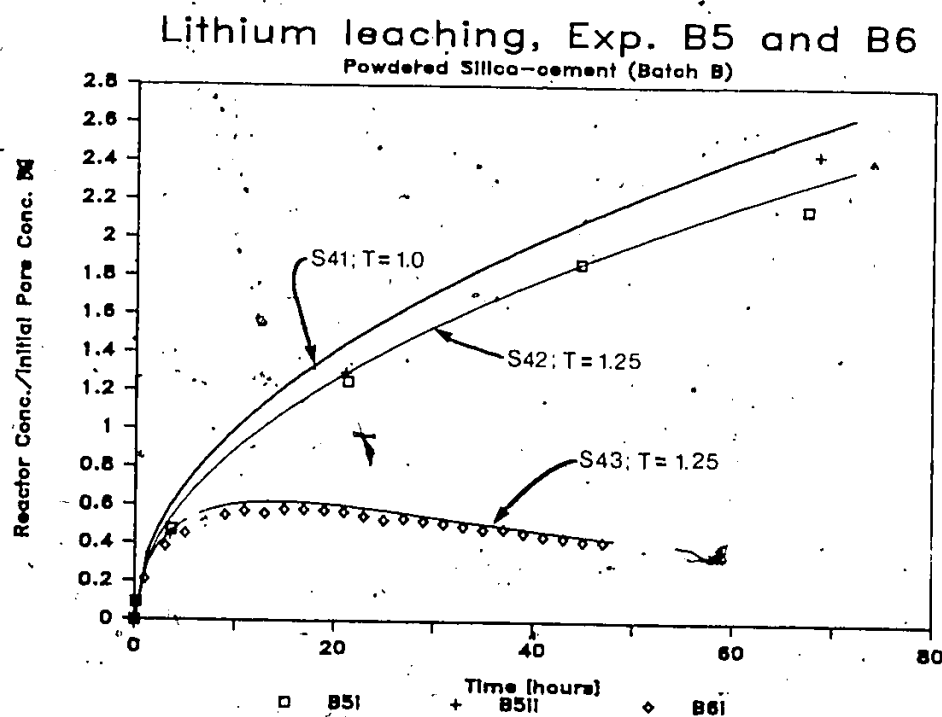


Figure 7.5 Simulation of lithium leaching from the powdered silica-cement matrix (Batch B).

Simulation 41 was run with the theoretical diffusion coefficient for lithium taken from Table I-2,  $D = 10.3 \times 10^{-6} \text{ cm}^2/\text{sec}$ . This simulation is thus totally independent of the experiment. The simulation slightly overestimates the measured concentrations. The difference might be attributed to several factors: tortuosity of the matrix (defined in Table I-1), ionic-assisted diffusion, etc. Since it is not possible to evaluate those factors independently, their effect

was lumped in a diffusion coefficient correction factor:

$$D_e = \frac{D}{T} \quad (7.2)$$

where  $D_e$  = effective diffusion coefficient [ $\text{cm}^2/\text{sec}$ ]  
 $D$  = molecular diffusion coefficient (taken from Table I-2)  
 $T$  = diffusion coefficient correction factor

The value of  $T$  was determined through non-linear regression analysis, by interfacing the leaching model LEEQ with a non-linear regression program. A value of  $T = 1.25$  was obtained and is represented by Simulation 42 in Figure 7.5. Simulation 43 was also run with  $T = 1.25$  to simulate the dynamic leaching experiment. This value of  $T$  is typical of tortuosity values of sediments and various soils reported by Berner (1980). Thus, for a soluble contaminant in a simple matrix, the release can be modelled using a molecular diffusion coefficient corrected for matrix tortuosity.

#### Fly Ash Cement, Low Cement Dosage (Batch C)

Batch C was prepared with fly ash and a minimum of cement, just enough to get the mass to set and prevent particles from being detached from the surface during handling. The results of lithium leaching in dynamic tests C6I and C6II are presented in Figure 7.6 along with five simulation runs. The two experiments, which were originally designed as replicates, are presented separately because they were run with different flow rates (pumping problems). Simulations 44 and 47 were done with a diffusion coefficient correction factor of  $T = 1.0$  and a value of

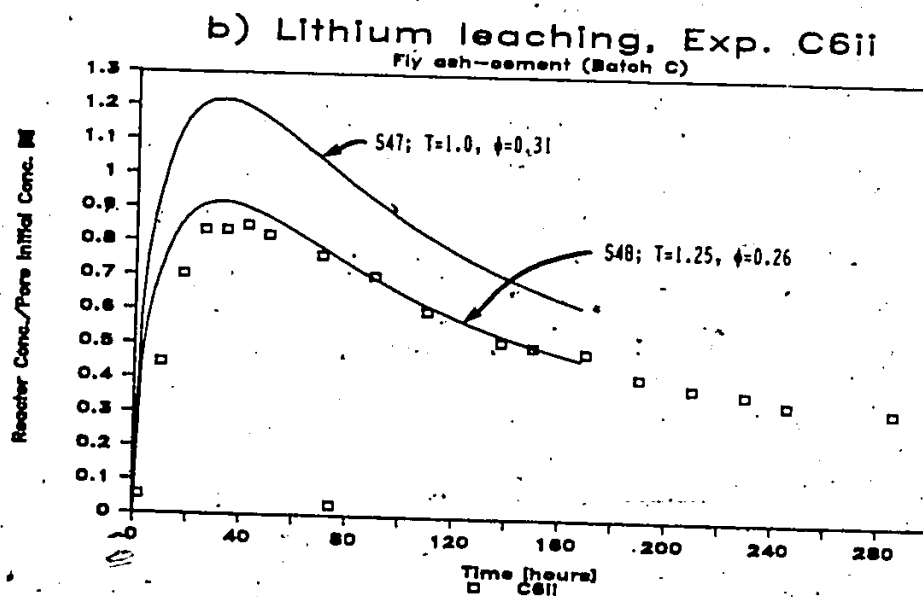
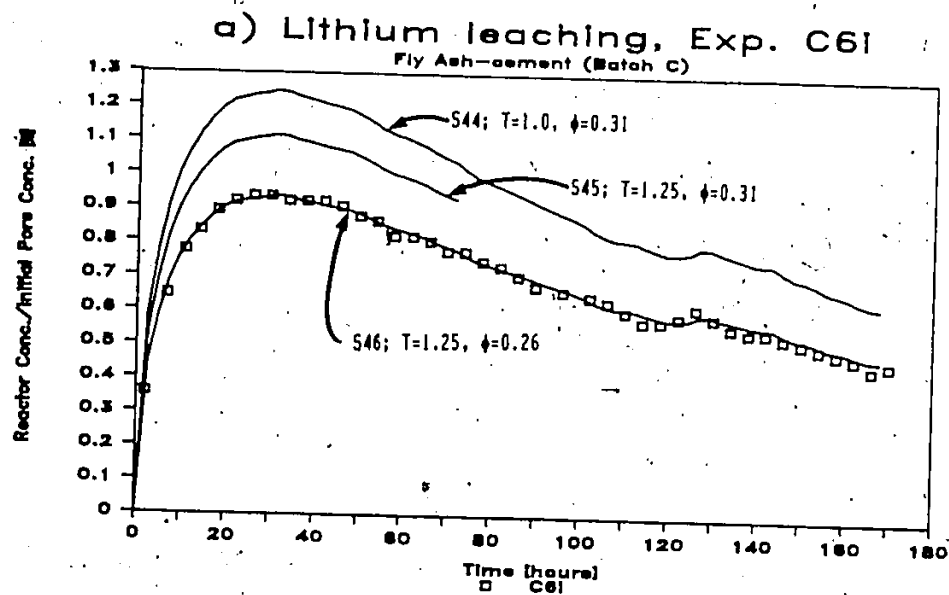


Figure 7.6 Simulation of lithium leaching from the fly ash-cement matrix (Batch C).



connected porosity equal to the water content  $\phi=0.31$  (as for Batch B). The simulated concentration values exceed the measured concentrations by about 30%. Using the tortuosity determined for Batch B ( $T=1.25$ ), in Simulation 45 (Figure 7.6a), resulted in the simulated concentrations still exceeding the measured concentrations by more than 20%.

Increasing  $T$  and/or reducing  $\phi$  would both result in the model predicting a lower concentration. There is no reason, based on physical considerations, to increase  $T$  over 1.25 since matrices of batches B and C have similar particle size distribution (Section 7.1.1) and thus should also have similar tortuosities. However, the connected porosity of Batch C could be lower than its water content determined by drying (0.31) since the fly ash particles are porous and thus have the potential for absorbing water. Examination of Figure 7.1, the cumulative porosity, indicates that there is a large volume of pores intruded in pore sizes ranging from approximately 0.003 to 0.05  $\mu\text{m}$ . This volume ( $\sim 0.175 \text{ cm}^3/\text{g}$ ) comprises cement gel and fly ash particles porosities and could, by absorbing interparticle pore water, decrease connected porosity. Simulations 46 and 48 which best fit the data were performed with a value of  $\phi=0.26$ . The difference between the water content (0.31) and the connected porosities (0.26) is equivalent to 0.10 gram of water absorbed per gram of fly ash particles. This value of  $\phi=0.26$  is close to the value used for Batch B,  $\phi=0.24$ , which is made of non-porous particles.

The initial concentration in the waste form matrix can be provided to the model in 2 different ways (Variable UGG, Table 1-3): 1)

per unit of wet matrix weight, or 2) per unit volume of water in the connected pores. In the simulations presented so far, Method 2 was used. Therefore, reducing the connected porosity effectively reduced the amount of lithium in the matrix to a fraction of the total equal to the ratio of connected porosity over the water content,  $0.26/0.31 = 0.84$ , for Batch C.

It is interesting to note that the initial lithium pore concentration was 0.1 mol/L in Batch B and 0.01 mol/L in Batch C. The fact that the model predicted the leaching behavior equally well without taking into account ionic assisted diffusion (i.e. respect electroneutrality at all point of the matrix) indicates that this might be negligible in the face of other factors such as matrix connected porosity or tortuosity.

#### Fly Ash Cement, High Cement Dosage (Batch D)

Simulation efforts for lithium leaching from Batch D are summarized in Figure 7.7. Simulation 57 was done using values of  $T=1.0$  and  $\phi=0.24$  for reference purposes. The value 0.24 used for connected porosity is the water content as determined by drying. Simulation 58 was done using the tortuosity and connected porosity information obtained for the simulation work done on Batch C. Value of  $T = 1.25$  and  $\phi = 0.19$  were thus selected. The connected porosity value of 0.19 is based on the assumption that the same amount of water absorbed in Batch C was absorbed by the fly ash. The reactor concentrations predicted in Simulation 58 are still much higher than the measured values. It is

postulated that the values selected for  $\phi$  and  $T$  do not adequately describe the morphology of the matrix.

Batch D was prepared using a relatively high dosage of cement. The amount of water used for hydration (which should roughly correspond to the difference in water content of Batch C and Batch D, i.e.  $0.31 - 0.24 = 0.07$  g/g of wet matrix), empties pores of their solution, creates dead ends or even isolates some pores from the connected porosity. Furthermore, cement hydration produces a tighter, more densely packed matrix. The combined effect of these factors is to both decrease connected porosity and increase tortuosity. Since it was not possible to independently determine the two factors the simulation efforts were terminated.

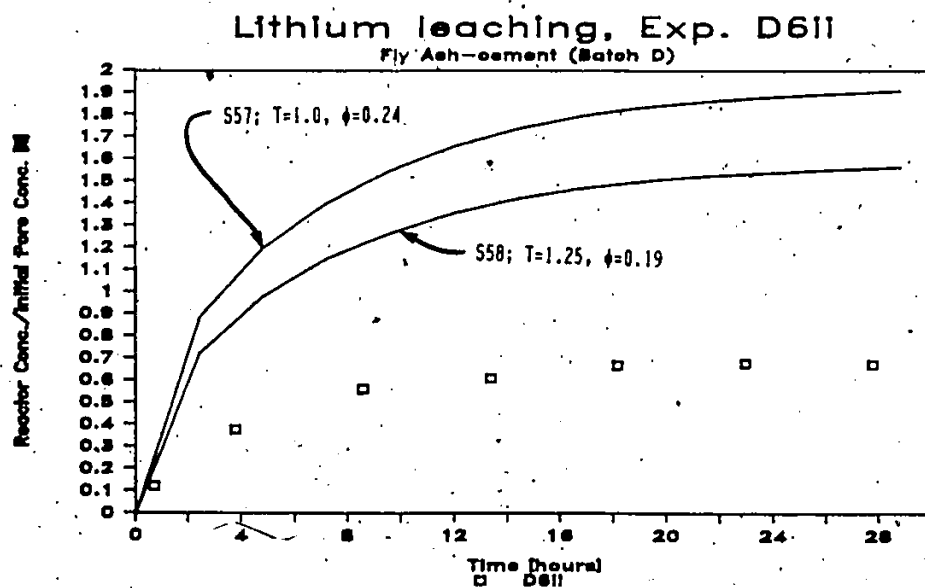


Figure 7.7 Simulation of lithium leaching from the fly ash-cement matrix (Batch D).

### 7.3.2 Insoluble Contaminants

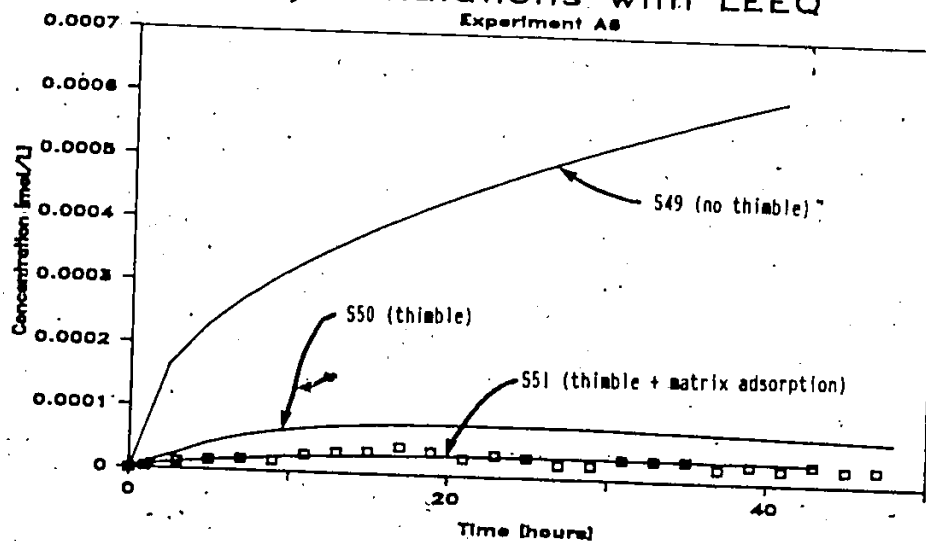
#### Powdered Silica (Batch A)

A wet powdered silica matrix containing cadmium hydroxide (0.01 M) in its pores is the simplest waste form that was prepared. Adding the minimum amount of cement to stabilize the mass, as was done in Batch B, increased the acid neutralization capacity of the system by almost one order of magnitude (compare ANC of Batches A and B in Table 7.3) and rendered the chemical system complex. Therefore Batch A was prepared in order to validate the computer program LEEQ which is based on a complete description of the chemical reactions, and to compare its results to the program LEEEX based on titration and solubility curves. A soxhlet thimble was used to mold a sample of Batch A into a regular shape and to prevent it from falling apart when immersed in the aqueous solution.

The simulations conducted with programs LEEQ and LEEEX are completely independent of the experiment. The connected porosity  $\phi=0.24$  and tortuosity  $T=1.25$  were selected based on the results described in Section 7.3.1. In LEEQ, the chemical system was described theoretically using MINEQL (Table 5.2). The titration and solubility curves of Batch A (Section 7.2.2) were used with LEEEX.

The results of the simulation runs done with LEEQ are presented in Figures 7.8 and 7.9. In Simulation 49, the retarding effect of the soxhlet thimble wall (20 mm) was not taken into account and the release of cadmium was grossly overestimated. This was corrected in Simulation

## a) Simulations with LEEQ



## b) Comparison of LEEQ and LEEEX

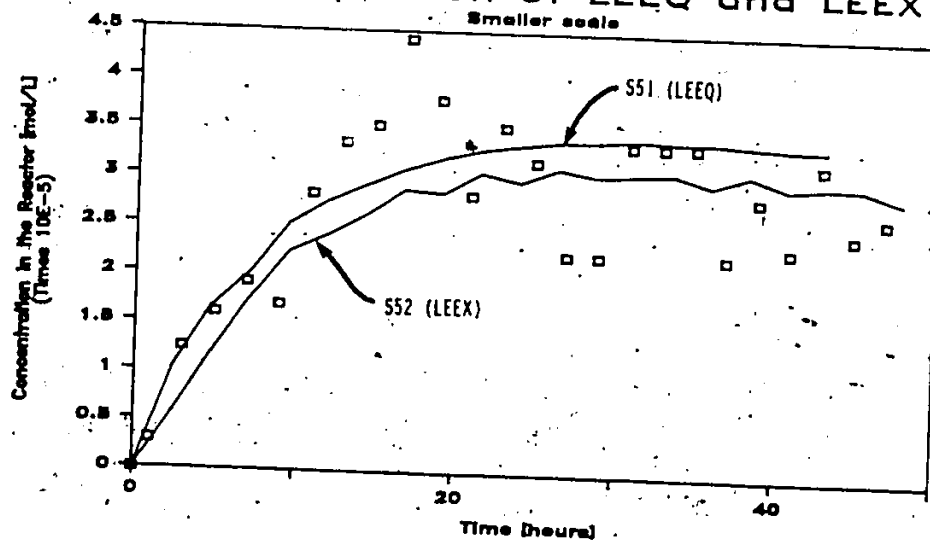


Figure 7.8 Simulation of cadmium leaching from the powdered-silica matrix (Batch A).

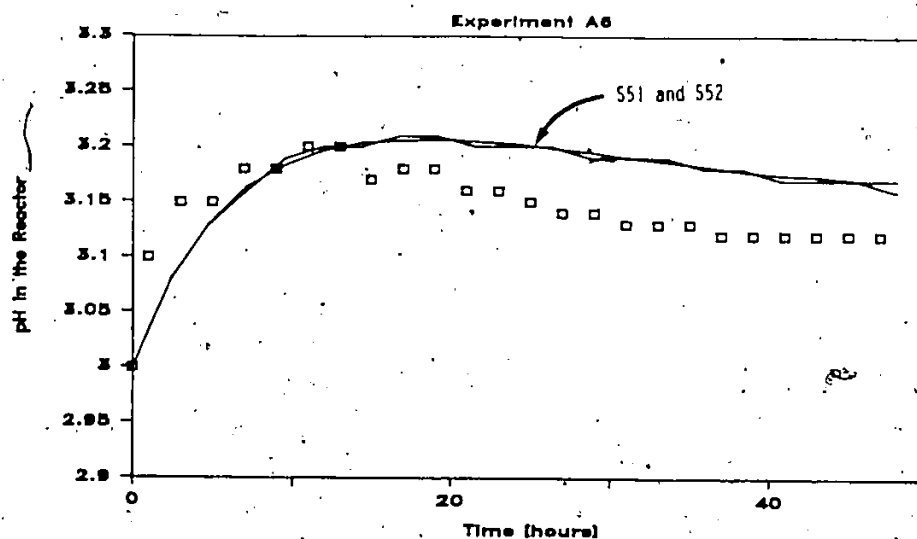


Figure 7.9 Simulation of the reactor's pH in the leaching of the powdered silica matrix (Batch A).

50 by considering in the model a diffusive layer of 20 mm, having the same porosity and tortuosity as the matrix, but depleted of chemicals initially. This modification corrected the concentration, as illustrated in Figure 7.8a, but still overestimated the release compared to the experimental data. The residual difference can be attributed to the acid neutralization capacity (ANC) of the powdered silica matrix as determined in Section 7.2.2. The inward diffusion of the hydrogen ion is retarded by its reaction with the hydroxyl groups present on the surface of amorphous silica. This results in less cadmium being solubilized. This effect was simulated in the model LEEQ by associating an acid neutralization capacity of 0.006 meq/g to the wet matrix. The

results (Simulation 51) , presented on Figure 7.8a (and on Figure 7.8b using a smaller scale), compare well with the measured cadmium concentration.

Figure 7.8b also shows the results of Simulation 52, done with LEEX, after modifying the program to account for the presence of the thimble. The effect of the matrix ANC was already included in the measured titration curve.

The pH histories in the reactor predicted by both programs are identical (Figure 7.9). Furthermore, the models predict the same pH history in the reactor whether or not the presence of the soxhlet thimble is simulated. This is due to the fact that the hydrogen ion has a diffusion coefficient about one order of magnitude larger than other ions (Table 1-2) and can thus be considered the "independent variable" in leaching processes taking place under acidic conditions.

#### Powdered Silica-cement (Batch B)

The results of the leaching experiments and simulations of cadmium leaching conducted on Batch B are presented in Figure 7.10. The experiments were conducted both in the static and dynamic modes. The simulations, done with the model LEEX, are based on titration and solubility curves presented earlier.

It is important to note that, in the static Experiment B5, the pH increased rapidly while, in the dynamic experiment, it stayed low as a result of renewing the pH 3 leachant. The decrease of cadmium concentration observed in Experiment B5 (Figure 7.10a) at the end of the

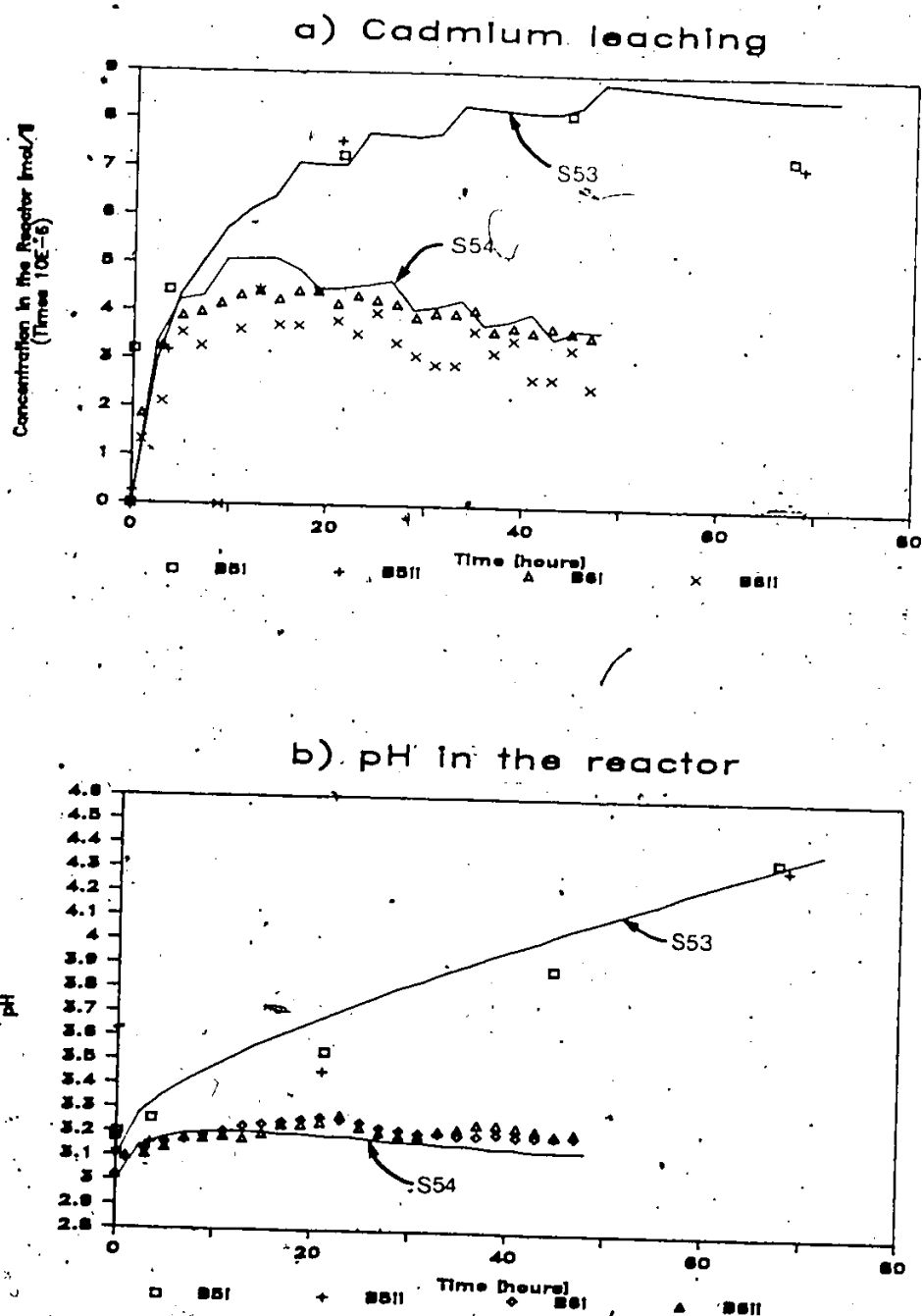


Figure 7.10 Simulation of cadmium leaching from a powdered silica-cement matrix (Batch B).



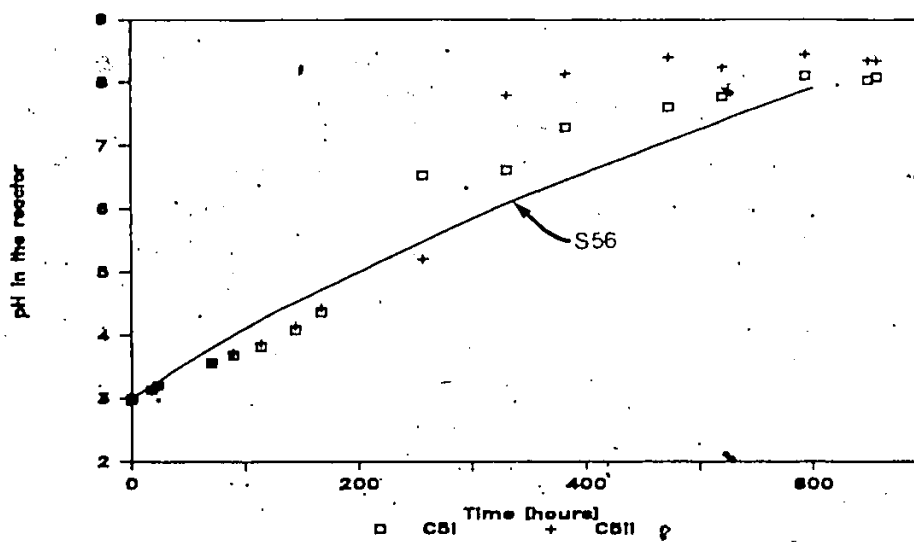
experiment ( $t = 60$  hours) is related to the increase in pH as the cadmium profile in the matrix is reversed and cadmium is starting to diffuse back into the matrix. This phenomenon will be analyzed using the results of Batch C below (The decrease in cadmium concentration observed in Experiment B6 was simply due to the washing off effect of the leachant renewal).

The oscillations in the simulated cadmium concentrations are related to the slice thickness used in the numerical solution. They occur because the slices are emptied of their cadmium content one at a time. In the model LEEX, each slice is considered a completely mixed reactor being titrated by diffusing  $H^+$  (Figure 4.4). The ANC (provided by cement or other compounds) has to be neutralized before the pH of the slice is reduced to a value corresponding to a sharp increase in cadmium solubility. At that point, the cadmium content of the slice is rapidly solubilized and starts leaching out. This effect becomes more important as the ANC of the matrix increases. The oscillations can, of course, be reduced by considering thinner slices (with the penalty on computational time as discussed in Section 5.4).

#### Fly Ash-Cement (Batch C) - Static Leaching

The results of the static leaching experiment on Batch C are presented on Figure 7.11. The initial pH in the reactor was 3.0. After 1 month, it had increased to over 8.0 (Figure 7.11a). The matrix of Batch C contained three contaminants, cadmium, chromium and lead, which had different concentration histories in the reactor. Chromium

## a) pH In the reactor



## b) Cadmium

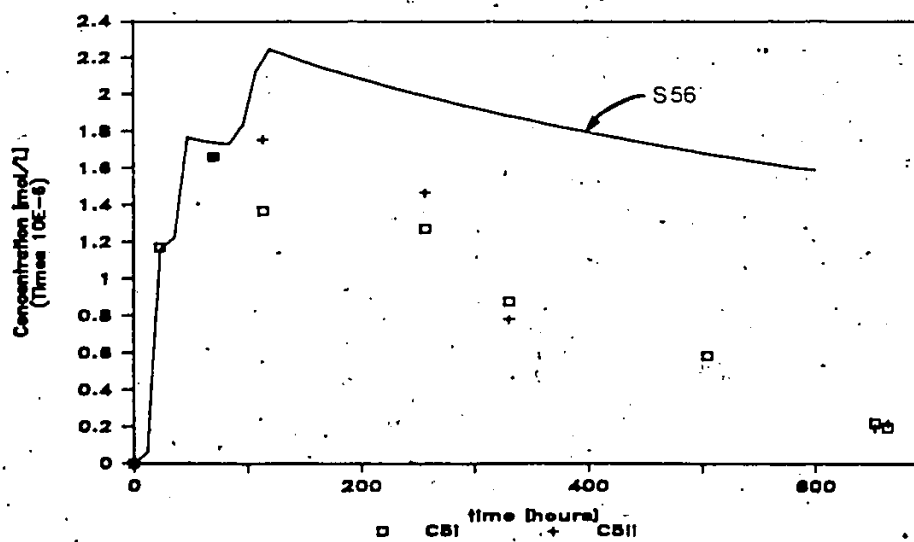
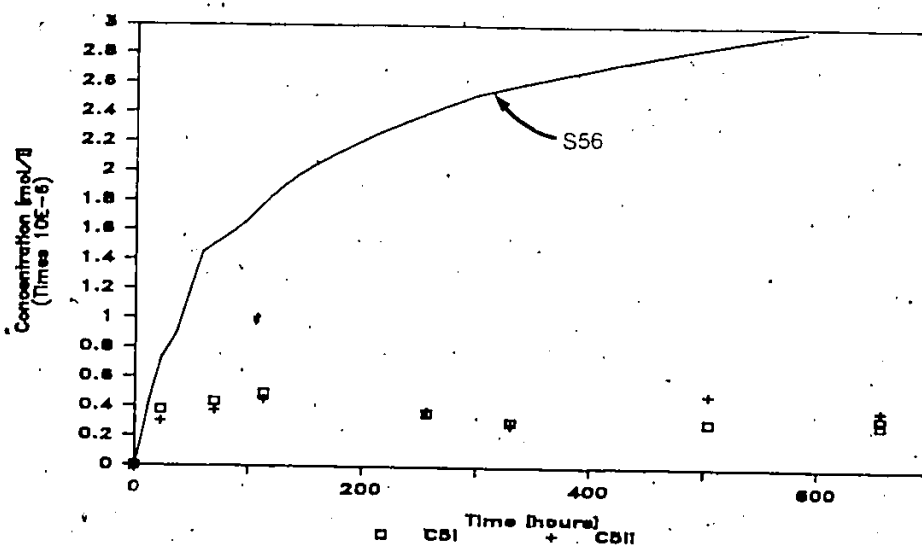


Figure 7.11 Simulation of static leaching from a fly ash-cement matrix (Batch C).

## c) Chromium



## d) Lead

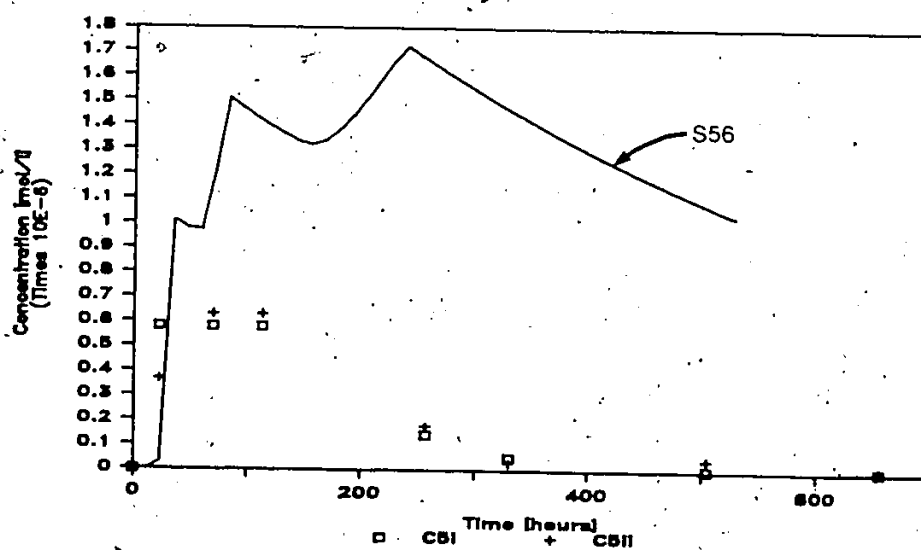


Figure 7.11 Continued ...

concentration rapidly increased to its final value (Figure 7.11c). Cadmium and lead (Figures 7.11b and 7.11d) concentrations went through a maximum at ~100 hours and slowly decreased afterwards to very low values (close to the analytical detection level in the case of lead). This phenomenon was observed but unexplained by Mahoney et al (1981). Since there was no leachant renewal, those concentration histories have to be explained in terms of diffusive transport and chemical reactions.

The results of Simulation 56 are also presented on Figure 7.11. The model was used assuming that the total concentration of a contaminant in the matrix was available for leaching, using the solubility relationships presented earlier. The model accurately predicts the increase in pH to a final value of 8 after 1 month. It overestimates the amount of the three metals leached during that period. However, for cadmium and lead, it correctly shows a decrease of concentration in the reactor after 100 hours. The discrepancies between the model and the experiments will be analyzed with reference to the results of the equilibrium tests on Batches C and D presented in Section 7.2.

The results of the titration experiments presented in Figure 7.2 suggest that the availability of contaminants for leaching varies with the loading (i.e., amount of contaminant per unit weight of matrix), the concentration in solution and with pH. It was demonstrated in Section 7.2.1 that, even at pH values where solubility is not limiting, there was a significant portion of the metals associated with the solid phase. It is postulated that this immobile portion interacted with the matrix

(fly ash and hydrated cement) following complex mechanisms of diffusion within the pores of the particles (i.e., outside of connected porosity) and sorption on to surface sites. The reversibility of these mechanisms was not addressed. Therefore, the model overestimates the amounts leached because it does not account for the fact that the contaminants are only partly available for leaching. A "fraction available for leaching" could be used in the model to correct the predicted releases. However the fraction available for leaching is specific to the matrix and is not a constant: it varies with pH and concentration, which are themselves variable as a function of depth in the matrix. Inclusion of these mechanisms in the model would be waste specific and would have to be based on intensive experimental work. Furthermore, it would not represent an improvement of the mechanistic description of leaching. It should be remembered, in addition, that the model LEEX lumps all the soluble forms into one mobile species. In complex situations, especially at high pH, several species of the same component can have different leaching behavior (see the example with cadmium hydroxide species in Section 5.5). The simulation effort was therefore terminated in the face of the complexity of the observed phenomena.

Solubility considerations are helpful in interpreting the experimental results of Experiment C5. Comparison of the reactor's concentration with the solubility data (Figure 7.4), indicates that, at any time during the experiment (i.e. at different pH values), the solubility limit was not approached. Therefore, precipitation did not take place in the reactor. The flatness of the chromium concentration

curve is associated with its low solubility throughout a pH range from 4 to 10 (Figure 7.4b). Therefore, chromium leaching in the static experiment was insensitive to  $H^+$  diffusing into the matrix; it rapidly leached until the concentration in the reactor approached that in the pores, reducing the driving force for leaching.

The significant decrease in cadmium and lead concentrations observed at time  $t > 100$  hours, is due to the reabsorption of the leached metals into the matrix. Consider the soluble metal profiles presented in Figure 7.12. The initial profile (1) shows a low concentration in the pores of the matrix (corresponding to solubility at the initial high pore pH) and, of course, no metal present in the aqueous solution. The profile at time (2) develops as a result of  $H^+$  diffusion into the matrix (as explained in Section 5.5.1). The profile at time (3) illustrates how the leaching front advances into the matrix as more  $H^+$  solubilize the metal. It should be noted that the metal concentration in the aqueous solution (i.e., reactor) increases from time (1) to time (3). Concurrently,  $H^+$  is depleted from the reactor and, by time (3), the pH has reached a high value.  $H^+$  thus stops diffusing to the leaching front and no more metal is solubilized. As a result, the metal concentration peak flattens out and eventually an inverse profile (4) develops. From then on, the metal starts diffusing back into the matrix and its concentration in the aqueous solution decreases (Profile 5).

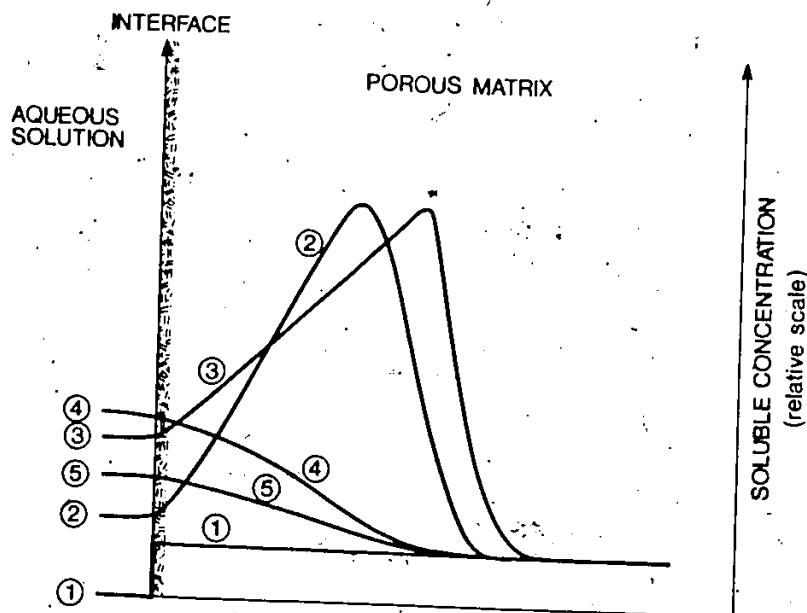


Figure 7.12 Soluble metal profile as a function of time.

Fly Ash-cement (Batches C & D) - Dynamic Experiments

The results of the dynamic leaching tests (continuous flow of an acidic leachant) performed on Batches C and D were not simulated with the model for the reasons explained above. These results will be analyzed by comparing the amount of a contaminant leached to the total amount contained in the calculated waste form weight neutralized by acid (called leaching efficiency).

Table 7.4 summarizes the steps involved in the calculation of the leaching efficiency. The acid consumed was calculated from a numerical

Integration of the  $H^+$  mass balance in the reactors over the duration of the experiment. The weight of waste form neutralized is obtained by dividing the acid consumed by the ANC (from Table 7.3). The depth of penetration was calculated based on the geometry of the specimen used in each experiment.

Table 7.4 Analysis of dynamic leaching tests.

Leaching Exp.	Duration [hours]	Final pH	Acid Consumed [meq]	Weight Neutralized [g]	Depth $H^+$ Penetration [ $\mu m$ ]	Leaching Efficiency [%]		
						Cd	Cr	Pb
A6	48	3.12	1.88	157	2800	61	--	--
B6I	48	3.20	2.11	23.4	1900	51	--	--
B6II	48	3.29	2.17	30.0	2500	41	--	--
C6I	172	3.67	7.69	20.6	1800	21.6	3.0	32.6
C6II	296	3.61	13.1	29.1	2600	21	3.1	14.9
D6I	310	4.87	29.8	14.9	600	0.54	2.4	6.5
D6II	312	4.73	32.8	16.4	600	0.37	1.6	3.6

Notes: Leachant pH was 3.0 in all experiments.  
Leaching efficiency is defined as the amount of a contaminant leached over that amount present in the weight of waste form neutralized.

Interpretation of the leaching efficiency for dynamic leaching situations can be done with reference to the following case. Consider a simple matrix (such as the powdered silica-cement matrix) containing a precipitated metal. Assume that the metal is completely available for leaching under acidic conditions. From a stoichiometric point of view,



the amount of the metal solubilized in an acid leaching test is equal to the total amount contained in the weight of waste form neutralized. This situation corresponds to a leaching efficiency of 100%. We will now examine the calculated leaching efficiencies which are reported in Table 7.4.

It was shown in Section 7.2.1 that Matrices A and B did not chemically immobilize cadmium. However, the calculated cadmium leaching efficiencies were 61% for Experiment A6 and an average of 46% for Experiments B6I and B6II. The reduced leaching efficiencies, as compared to those based on stoichiometry, are due to the fact that only a fraction of the metal solubilized leached out, as the complement diffused inward. Consider the matrix profile of a soluble metal presented in Figure 5.2b. This profile was calculated using a waste form and leaching conditions very close to those of Experiment A6. There is a slightly higher gradient for outward diffusion than for inward diffusion (i.e. slope of the concentration curve). As a result, a larger amount of cadmium solubilized leached out (61%) as compared to the amount that diffused in ( $100 - 61 = 39\%$ ). Batch B contained portland cement which provide ANC in the form of excess  $\text{OH}^-$ . This excess  $\text{OH}^-$  caused the inward diffusing metal to precipitate just past the leaching front. As a result, the gradient for inward diffusion became steeper than the gradient for outward diffusion and a larger fraction of the solubilized cadmium diffused in. This explains the lower leaching efficiencies calculated for Experiments B6I and B6II.

The same mechanism is partly responsible for the low leaching efficiencies calculated for the four metals monitored in Experiments C6I and C6II. In addition, the leaching efficiencies are further reduced due to the fact that the metals are only partially available for leaching (Section 7.2.1), (i.e., a fraction of the metal concentration stays associated with the solid phase, even in the low pH leached layer). In Experiments D6I and D6II, an additional mechanism contributed to the observed very low leaching efficiencies of cadmium (0.37%), chromium (1.6%) and lead (3.6%). Batch D had a high ANC and the experiments were conducted using a larger value of  $\beta$ , the ratio of the specimen geometrical surface area-to-aqueous solution volume. As a result, the rate of acid addition, through leachant renewal, was not sufficient to maintain a low pH in the reactor (Tables XI-6 and XI-7). Therefore, a leached layer did not develop in the matrix and leaching took place via diffusion of a low soluble fraction (at high pH), as opposed to dissolution from the surface.

Figure 7.13 was prepared to summarize the findings from the analysis of the dynamic leaching tests. It shows that the leaching efficiency of cadmium decreased from 61% for Batch A to less than 1% for Batch D. Batch D, a typical "real life" waste form, leached only a very small fraction of the metals contained in the weight of its matrix neutralized by a strong acid and is thus an effective waste form for metals under acidic leaching conditions.

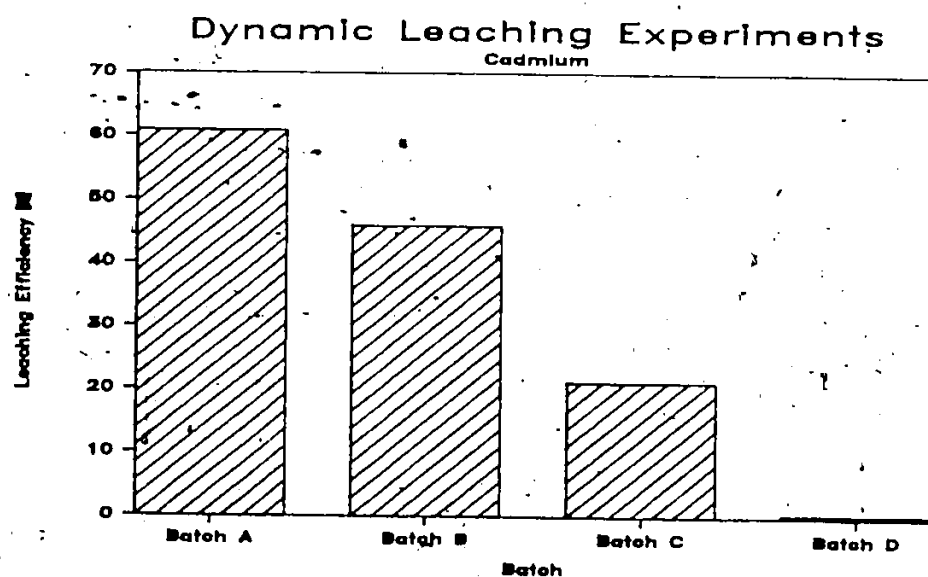


Figure 7.13. Leaching efficiency of cadmium under acidic conditions for various waste form matrices.

#### 7.4 Long Term Leaching Results

The data presented in this section were obtained from leaching tests conducted over a period of almost two years. The test protocol described in Section 6.2.7 involved renewing the distilled water leachant frequently in order to maintain high driving forces for leaching (Figure 6.3).

The long term leaching tests are a generalization of the experimental programme to four different solidification systems which represent the state-of-the-art technology (see Section 3.1). The testing

conditions were selected to represent a mild leaching environment.

The results of the long term tests cannot be simulated with the mechanistic models LEEQ or LEEEX because, as outlined in the last section, the morphology and chemical system of those waste forms are too complex. Furthermore, the use of a mild leachant resulted in small amounts of contaminants leached from a thin layer of the solidified sample surface; the numerical limitations outlined in Chapter 5 thus also rule out using the mechanistic models for these conditions. The results will therefore be analysed qualitatively and interpreted using the time-dependent expressions for the cumulative amount leached presented in Section 3.4.

The raw data generated in the long term tests are presented in Tables XII-1 to XII-8 for Batches E to H. Two leachant renewal frequencies ("I" and "II") were used for each batch. Each table contains the following information: leaching interval, cumulative time at the end of the interval, leachant weight, pH, conductivity and concentration of the contaminants.

#### 7.4.1 Data History

The total cumulative mass leached for each of the four systems is presented as a function of time in Figure 7.14. The total dissolved solids were not monitored in the leachates; the masses leached were calculated based on the measured ionic conductivity following the method outlined in Table VII-2. Figure 7.14 indicates that the fly ash-based systems were the less leachable systems with a total mass fraction lost

(after 665 days) of approximately 3%. The clay and soluble silicate-based systems lost respectively 7% and 13%. The release decreased over time in a way which is characteristic of diffusion-controlled leaching (i.e. plotting the fraction leached versus  $t^{1/2}$  would yield a straight line (Cote and Isabel, 1984)).

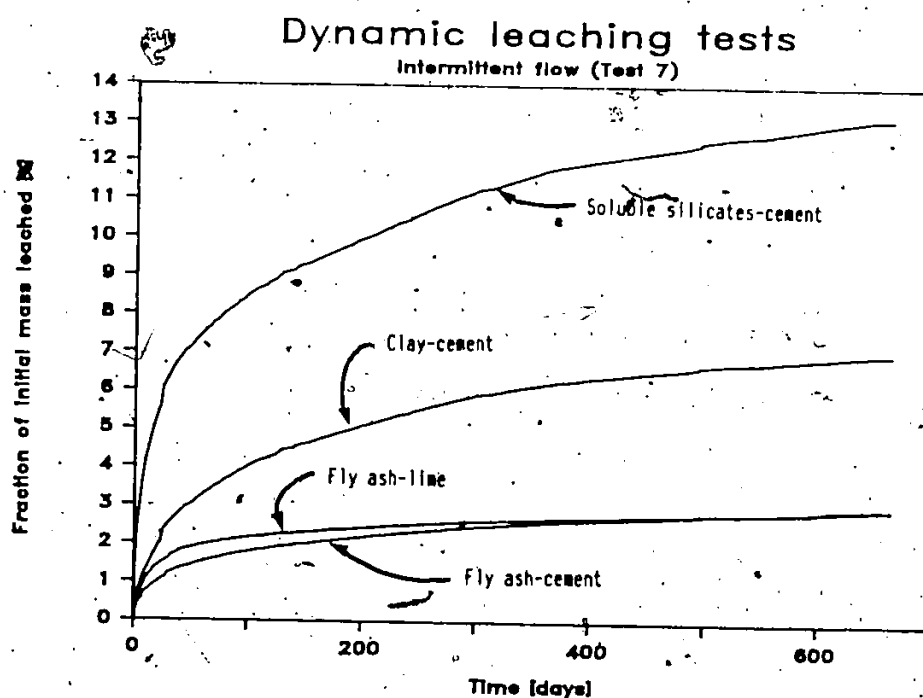


Figure 7.14 Fractions of the total masses leached in the long term dynamic leaching tests.

Despite the masses lost by leaching, all samples had gained weight after one year of testing. The mass balances presented in Table XII-9 are based on the sample masses at the beginning of the test and

after one year of leaching and on the calculated masses lost by leaching. The amounts of water absorbed by the samples roughly correspond to those required to saturate them (see porosity data Table 7.1). These results point out that the morphology changed with time as the pores filled with water, effectively increasing the potential for diffusion leaching.

The pH history for the high leaching frequency "I" is presented graphically in Figure 7.15. The leachate pH's were all initially in a range from 10.5 to 12.0 and decreased by approximately one unit over the duration of the tests. The pH of leachates from the fly ash-based systems were initially lower than those of the clay and soluble silicates systems and also tended to decrease faster with time. This is attributed to the pozzolanic reactions which immobilized the  $\text{Ca(OH)}_2$  produced from cement hydration (see Section 3.2).

The concentration data history for the leaching of arsenic, cadmium, chromium and lead (presented in Figures XII-1 to XII-4) outlines the importance of the choice of a proper leachant renewal frequency: it had to be low enough to ensure that the concentrations leached were above the analytical detection levels and high enough to avoid approaching equilibrium conditions between leachant changes. The frequencies selected, based on diffusion controlled leaching (Equation 6.1), generated constant concentrations of Cd, Cr and Pb over the duration of the tests; the concentration of arsenic gradually increased with time, which indicates that its release was not controlled by diffusion. Comparing the results to the concentrations measured in the

equilibrium leaching tests (Table VII-1), we can see that the leachant renewal frequency was sufficiently high to generate concentrations in the testing bottles low enough to justify models based on zero-surface concentration (with the exception of arsenic in the fly ash and clay-based systems). It is probable, however, that arsenic solubility increased over time as basic calcium arsenite was transformed into calcium arsenite through reaction with atmospheric  $\text{CO}_2$  (discussed below). This being the case, the zero surface concentration condition would also be valid for arsenic.

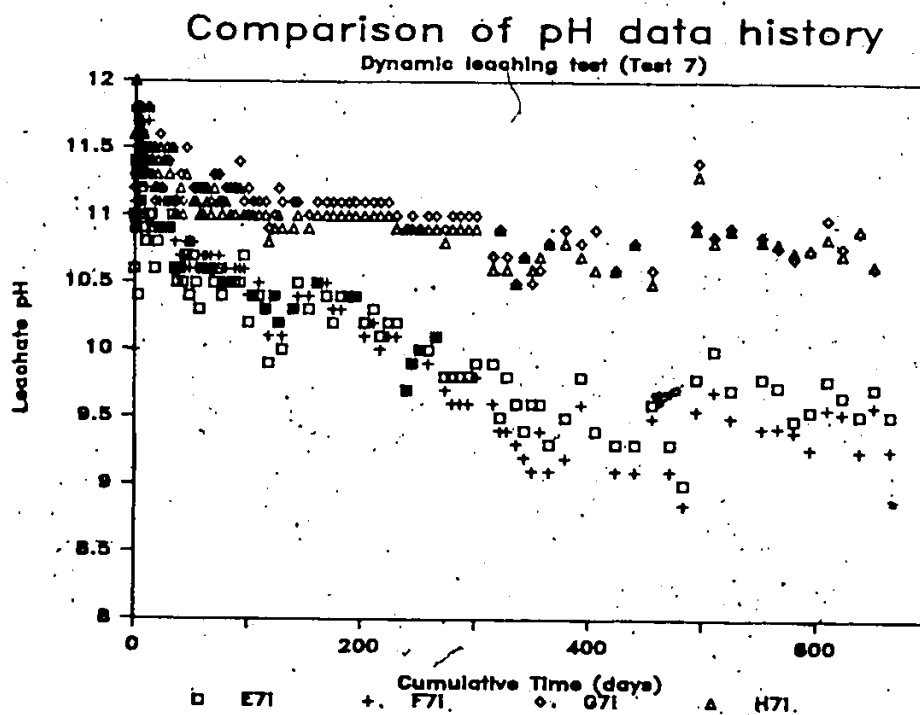


Figure 7.15 pH histories for the long term dynamic leaching tests.

The cumulative masses and cumulative fractions of contaminants leached after 665 days are presented in Table 7.5. Generally, for all solidification systems, the release increased in the following order: cadmium < chromium < lead < arsenic. The cumulative fraction of the heavy metals leached was smaller than 1% for all systems. Arsenic leached more readily; especially from the soluble silicates-based system, attaining 15% after 665 days.

Table 7.5 Masses of contaminants leached after 665 days in the dynamic leaching tests (Test 7).

Batch ID	Solidification System	Arsenic	Cadmium	Chromium	Lead
Cumulative amount leached [umol]					
E	Fly ash-cement	248.7	1.5	12.3	7.0
F	Fly ash-lime	311.0	1.5	11.2	51.8
G	Clay-cement	282.0	3.6	9.1	55.7
H	Soluble silicates-cement	1067.8	11.2	13.2	29.1
Cumulative fraction leached [%]					
E	Fly ash-cement	3.97	0.02	0.19	0.11
F	Fly ash-lime	4.82	0.03	0.18	0.85
G	Clay-cement	3.42	0.04	0.11	0.68
H	Soluble silicates-cement	15.16	0.14	0.19	0.42



#### 7.4.2 Semi-empirical Modelling

In Section 3.4, several expressions were presented to describe the variation of leaching as a function time. We retain the following time-dependent terms for the cumulative fraction or amount leached which describe several important rate-limiting leaching mechanisms (note that an expression for the leaching rate can be obtained by taking the derivative of the cumulative fraction leached expression, Equation 3.1):

$k_1(1 - e^{-k_2t})$  : Equation 3.15; describing the kinetics of exchanges between the surface and the aqueous solution. Rate-limiting for small values of time.

$k_3t^{1/2}$  : Equation 3.4; describing transport by diffusion in a porous matrix. Valid for intermediate values of time.

$k_4t$  : Equation 3.13; describing a slow, mobilizing chemical reaction. Rate-limiting for large values of time. Equation 3.21; describing leaching as a result of corrosion or matrix dissolution. This mechanism can be rate-controlling at any value of time.

The three terms can be combined to describe the cumulative amount leached (CAL) in a general expression:

$$CAL(t) = k_1(1 - e^{-k_2t}) + k_3t^{1/2} + k_4t \quad 7.3$$

This equation can lose its mechanistic meaning if it is used to obtain the best fit of experimental data. For example, in the case where the initial surface exchanges are fast relative to the time span of the data being analysed, the first term of Equation 7.3 can be reduced to the constant  $k_1$ . The resulting equation is an empirical formula which has been extensively used to describe the time variation of leaching of nuclear waste forms (Godbee and Joy, 1974; Stone, 1981; Richardson, 1981). However, in this work, Equation 7.3 was used in a semi-empirical

manner by retaining only the terms which significantly contributed to leaching in any given region of the time domain. These terms can thus be interpreted mechanistically, provided that the assumptions which led to their development were respected in the generation of the experimental data. We will examine the validity of these assumptions before presenting the results of regression analysis.

The main assumption used to derive the relationships of Section 3.4 is that leaching takes place in a time-invariant chemical environment. The models describe a single species, and do not consider the transport and reactions of other species which could drastically change the chemical environment. In the context of this work the most important environmental change would be a drop in pH which would change the solubility of metals. However, the pH history (Figure 7.15) indicates that, over the duration of the experiment, the pH remained in a range where the metal precipitates are stable.

The derivation of the models was also based on simple boundary conditions: 1) the solid is semi-infinite and 2) a zero surface concentration is maintained. Work done in support of the development of a standard leaching test by the American Nuclear Society (1984) indicated that a semi-infinite geometry is applicable to finite geometry specimens provided that the cumulative fraction leached is less than 20%. This is the case for all specimens and contaminants (Table 7.5). As noted in Section 7.4.1, the concentrations measured in the leachates (i.e. the surface concentration) were small compared to the equilibrium concentration, thus approximating the second boundary condition of zero surface concentration.

The results of regression analysis on the long term leaching data are presented in Table 7.6. The models are compared to the data in Figures 7.16 to 7.19 for each of the four contaminants and the four solidification systems. Note that the scale of arsenic is different from that of the other metals by a factor of 1000.

The surface phenomenon term, important for short values of time, is present in every model. A value of  $k_2 = \infty$  means that the surface phenomena were so rapid compared to the time span over which the data were collected that they can be considered to have taken place at time zero and be represented by the term  $k_1$  only; a negative value of  $k_1$  represents a delay in leaching.

The leaching of the three metals, Cd, Cr and Pb was a function of the square root of time, which is indicative of diffusion controlled leaching (with the exception of Cr in fly ash-based systems). However, calculated diffusion coefficients (Table 7.6, numbers in brackets) are several orders of magnitude lower than the molecular diffusion coefficients of the respective metals ( $\sim 10^{-5}$  cm<sup>2</sup>/sec). As discussed in Section 4.1.2, the calculated diffusion coefficients reflect physical properties of the matrix: partial saturation of the pore system and tortuosity. Both these factors were also changing with time as the specimens were saturating (Section 7.4.1). More importantly, a lower calculated coefficient also reflects a chemical property of the system: the fact that only a fraction of a contaminant is present in a mobile form. For the case where this fraction is controlled by a linear

Table 7.6 Coefficients for the leaching model represented by Equation 7.3.

		Controlling Mechanism			
		Surface Phenomena $k_1(1-e^{-k_2t})$	Diffusion $k_3t^{1/2}$	Chemical Reaction $k_4t$	
		$k_1$	$k_2$	$k_3$	$k_4$
<u>Arsenic</u>					
Fly ash-cement	(E71)	-0.892	-	-----	0.411
Fly ash-lime	(F71)	-6.189	-	-----	0.500
Clay-cement	(G71)	5.107	-	-----	0.433
Sol. sil.-cement	(H71)	-0.127	-	$0.207(10^{-14.3})$	0.807
<u>Cadmium</u>					
Fly ash-cement	(E71)	0.035	-	$0.054(10^{-15.4})$	-----
Fly ash-lime	(F71)	0.380	-	$0.044(10^{-15.3})$	-----
Clay-cement	(G71)	0.177	-	$0.144(10^{-14.8})$	-----
Sol. sil.-cement	(H71)	-0.843	-	$0.477(10^{-13.7})$	-----
<u>Chromium</u>					
Fly ash-cement	(E71)	0.037	-	$0.168(10^{-14.4})$	0.177
Fly ash-lime	(F71)	0.703	-	-----	0.015
Clay-cement	(G71)	-0.041	-	$0.384(10^{-13.9})$	-----
Sol. sil.-cement	(H71)	0.759	-	$0.461(10^{-13.6})$	-----
<u>Lead</u>					
Fly ash-cement	(E71)	1.922	0.092	$0.149(10^{-14.4})$	-----
Fly ash-lime	(F71)	45.55	0.178	$0.235(10^{-14.0})$	-----
Clay-cement	(G71)	29.39	0.012	$1.091(10^{-12.9})$	-----
Sol. sil.-cement	(H71)	1.666	-	$1.122(10^{-12.8})$	-----

Notes: - Values of  $k_1$  calculated for CAL expressed in  $\mu\text{mol}$  and  $t$  in days.  
 - The numbers in bracket are effective diffusion coefficient [ $\text{cm}^2/\text{d}$ ] calculated with Eq. 3.4.

### Leaching of Arsenic

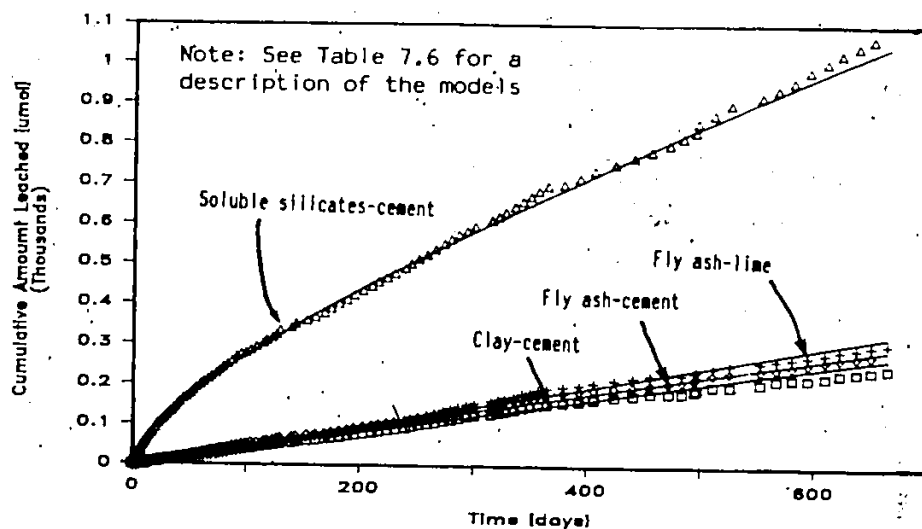


Figure 7.16 Modelling the leaching of arsenic from the dynamic leaching tests.

### Leaching of Cadmium

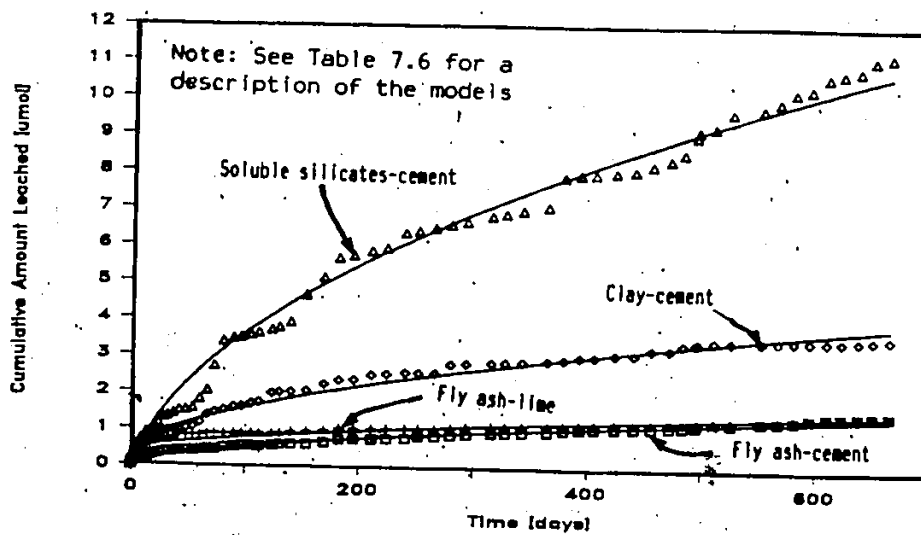


Figure 7.17 Modelling the leaching of cadmium from the dynamic leaching tests.

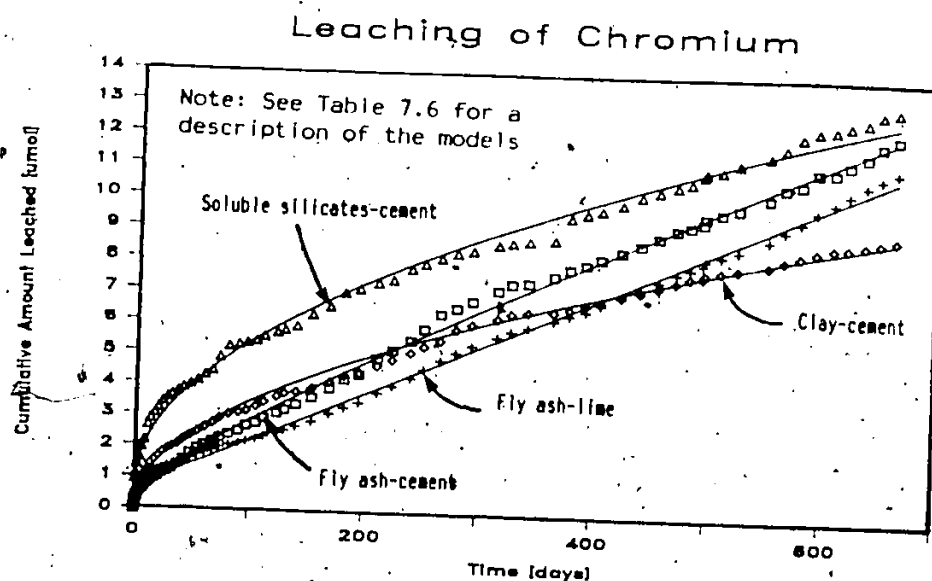


Figure 7.18 Modelling the leaching of chromium from the dynamic leaching tests.

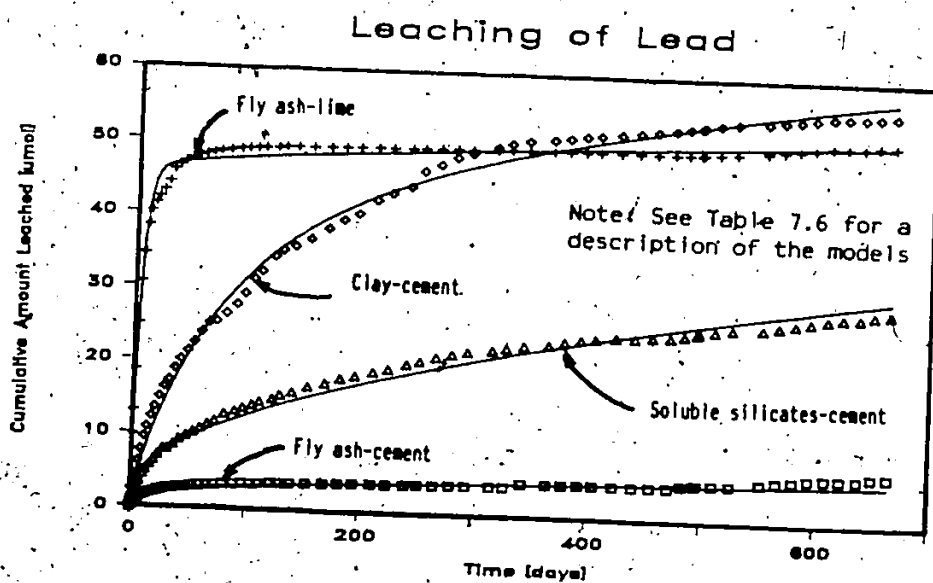


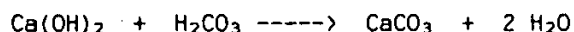
Figure 7.19 Modelling the leaching of lead from the dynamic leaching tests.

adsorption isotherm, Equation 3.5 expresses that the effective diffusion coefficient is reduced by a factor of  $(1/(1+K_d))$  where  $K_d$  represents the ratio of the immobile ( $C_{im}$ ) to the mobile ( $C_{mo}$ ) forms of the species. Of course, Cd, Cr and Pb were precipitated as hydroxides and their mobilization was not controlled by adsorption but Equation 3.5 still seems applicable if interpreted as follows:  $C_{im}$  is the precipitated metal concentration in the matrix and  $C_{mo}$  is the soluble pore concentration in equilibrium with the precipitated form.  $C_{mo}$  is thus constant in a fixed pH environment (e.g. controlled by solubility). Furthermore, since the total initial metal concentration was large and the leaching rates were low,  $C_{im}$  only decreased very slightly over the duration of the tests and can be approximated as a constant. This shows the importance of achieving the minimum solubility of a contaminant in the chemical environment established by the solidification system since a high value of  $K_d$  controls the rate of leaching by diffusion in a mild leachant.

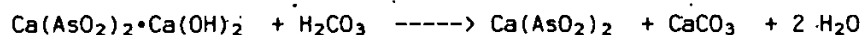
The leaching of arsenic is function of a linear term for the four solidification systems (Table 7.6). This behaviour is also evident from Figure 7.16. For the soluble silicate system, diffusion ( $t^{1/2}$ ) seems to be controlling leaching in the first 6 months as evidenced by the curvature of the data and the model in this area. The models of Section 3.4 offer two mechanisms to explain a linear time term leaching pattern. The first, surface dissolution or corrosion, can be ruled out on the basis that it should equally affect all contaminants. The second, a slow chemical reaction of mobilization, could involve electron

transfer (Stumm and Morgan, 1981). However, as pointed out by Robins (1985), air and oxygen at ambient temperature do not oxidize  $\text{As}^{+3}$  to  $\text{As}^{+5}$ . Arsenic was precipitated as basic calcium arsenite  $[\text{Ca}(\text{AsO}_2)_2 \cdot \text{Ca}(\text{OH})_2]$ . Nishimura et al (1985) reported that this precipitate is converted to the more soluble calcium arsenite  $[\text{Ca}(\text{AsO}_2)_2]$  and to arsenite ion by reaction with carbon dioxide in the following way:

-conversion of excess lime into calcium carbonate



-conversion of basic calcium arsenite into calcium arsenite



-mobilization of the arsenite ion



Even though these reactions are probably rapid, the rate of conversion is limited by the availability of the carbonates which are introduced with the fresh leachant. It is thus postulated that the rate of arsenic leaching was controlled by the rate of leachant renewal. This can be confirmed by comparing the amount of arsenic leached to the amount of carbonates added with the leachant. For the fly ash and clay based systems, approximately 300  $\mu\text{mol}$  of arsenic (Table 7.5) were leached over a period of 665 days with 162 liters of  $\text{CO}_2$  saturated distilled water. Based on a partial  $\text{CO}_2$  pressure of  $10^{-3.5}$ , the  $\text{H}_2\text{CO}_3$  concentration in the distilled water is approximately  $10^{-5.65}$  M which is equivalent to 360  $\mu\text{mol}$  of  $\text{H}_2\text{CO}_3$  over the duration of the experiments. The estimated amount of carbonates which reacted with the specimen is thus of the same



order of magnitude as the amount of arsenic mobilized. Given the stoichiometry of the reactions presented above, this is in agreement with the postulate that leachant renewal rate limited the release of arsenic.

## 8. INFERENCE OF LONG TERM LEACHABILITY

Waste forms, prepared for the purpose of containing contaminants, are normally disposed of by shallow burial and may therefore be contacted with natural waters. Leaching rates are a function of the waste form, the contaminant properties and the characteristics and hydraulic regime of the leachant. In Section 8.1, the knowledge gained in reviewing the literature and doing the experimental work was combined with simplified leaching conditions to develop eight (8) long term leaching scenarios. The assumptions and models that allow prediction of leaching rates for a period of up to 100 years will be presented for each scenario. In Section 8.2, a simple dilution model allowing interpretation of leaching rates in terms of concentration is presented. In the light of the predicted long term leachability, factors that affect the preparation of better waste forms and the design better landfill will be discussed.

### 8.1. Long Term Inference of Leaching Rates

A waste form is a primary containment system. Proper landfilling operations often provide secondary barriers between the natural waters and the wastes such as impervious liners and covers. Leaching will start when the secondary barriers fail and natural waters come into contact with the waste form. Therefore, for modelling purposes, time zero corresponds to the failure of the secondary barriers.

### 8.1.1 Assumptions about Landfilling Conditions.

The general landfill layout is presented in Figure 8.1. A slab of waste form is disposed of in the ground and is surrounded by up to three materials of various thicknesses and properties. It is assumed that the waste form is continuously surrounded by either a moving groundwater body or infiltrating rainwater. Depending on the relative permeability of the waste form with respect to the surrounding materials, we distinguish three groundwater hydraulic regimes.

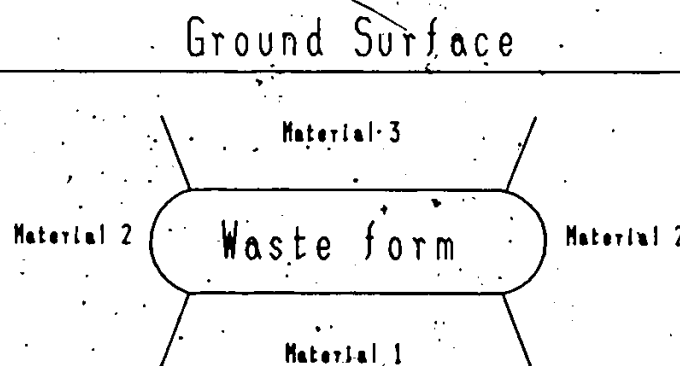


Figure 8.1 Layout of a waste form in a landfill.

Case 1: Static Groundwater. The waste form will be in contact with a finite volume of static groundwater for the case where the permeability of Materials 1 and 2 is much smaller than the permeability of the waste form and/or Material 3. This would occur, for example, if

- the waste form was sitting in a bed of impervious clay with no cover or
- a failed cover.

Case 2: Water Flowing around the Waste. Water would flow around the waste for the case where the permeability of the waste form is much lower than the permeability of any of the surrounding materials (e.g. the waste form is disposed of in sandy soil). In this case, water would follow the path of least resistance and flow around the waste. Based on rainfall of 0.5 m/year and a concentration factor of 100 (i.e. each square meter of waste form is contacted with the rain falling on 100 m<sup>2</sup>) we calculate an equivalent groundwater velocity of 50 m<sup>3</sup>/m<sup>2</sup>-year. The groundwater velocity will be used in some of the scenarios described in Section 8.1.3.

Case 3: Water Flowing through the Waste. Two situations can be identified where a hydraulic gradient would develop to force water to flow through the waste. First, the permeability of Material 1 is much smaller than the permeability of the waste form or Materials 2 and 3; for example, the waste form is sitting on an inclined bed of impervious rock or clay. Secondly, the permeability of Material 2 is much smaller than the permeability of the waste form or Materials 1 or 3; for example, a clay liner or geomembrane failure occurs at the bottom of the landfill. We will develop convective transport models based on a hydraulic gradient ranging from 1 to 5 (the hydraulic gradient is the ratio of the height of the column of water over the thickness of waste form).

In addition to developing groundwater hydraulic regime models, assumptions have to be made about the composition of the groundwater. We will distinguish two cases. First, a non-reactive

leachant, defined as one which does not mobilize contaminants through reaction with the waste form, will be used. This non-reactive leachant acts only as a transport medium. Secondly, a reactive leachant, one containing any chemical which can mobilize contaminants or destroy the matrix, will be considered. This chemical could be, for example, the hydrogen ion, a metal complexing agent or the carbonate ion (e.g. arsenic mobilization, Section 7.4). Because of its significance for metal mobilization, we will use in our calculations a  $10^{-3}$  mol/L acidic leachant (i.e. pH = 3 for a strong acid).

#### 8.1.2 Assumptions about the Waste Form.

The waste form is regarded as a cement-based porous matrix containing a high concentration of a contaminant. The matrix has a bulk density of  $1.6 \text{ g/cm}^3$  and is composed of 76% solids and 24% interconnected pore solution (on a weight basis). The typical porosity of such a matrix would be 50%, with the pores saturated with water. We will assume that the matrix may have two permeabilities:  $10^{-8}$  m/sec for an integral waste form (see Section 3.4.1) and  $10^{-6}$  m/sec in the case of a failure (e.g. the matrix is reduced to a powder by weathering).

For the leaching scenarios where the waste form is contacted with an acidic leachant, we will assume that the matrix was prepared by adding cement to an aqueous waste at a dosage varying between 0.2 to 0.6 parts of cement per part of waste (weight by weight basis) and that solidification resulted in a volume increase of 20% to 100% (Cote and Hamilton, 1983). Based on a hydrated cement acid neutralization capacity

(ANC) of 15 meq/g (see Section 7.2.2). It can be calculated that the ANC of the waste form ranges between  $2 \times 10^6$  and  $3 \times 10^6$  meq/m<sup>3</sup>.

It is assumed that the waste form contains 0.1 mole of a contaminant per litre of pore solution. Based on the physical characteristics of the matrix described above it can be calculated, using Equation 4.7, that this is equivalent to 0.0384 mole per litre of total matrix. To give a familiar point of reference, if the contaminant in question had a molecular weight of 100 (typical of a heavy metal), this would translate into a concentration of 2400 ppm, on a wet weight basis. The contaminant is distributed in the matrix following the fractions described in Figure 4.1. We will distinguish two cases. In the first case, the contaminant is completely soluble; i.e. it is initially present in solution in the pores of the matrix. In the second case, the contaminant is largely insoluble. It is assumed that the largest part, precipitated or immobilized with the matrix, is in chemical equilibrium with a pore concentration of  $10^{-5}$  mol/L (typical of a metal hydroxide solubility in an alkaline environment, see Table 7.2). It will further be assumed that the insoluble fraction is available for leaching in a proportion ranging from 50% to 100%.

### 8.1.3 Long Term Leaching Scenarios

From the description of the waste form and landfilling environment above, four master variables are retained to develop long term leaching scenarios: hydraulic regime of the groundwater, chemical characteristics of the groundwater, permeability of the waste form and chemical speciation of the contaminant. These variables have been laid

out in a matrix form in the legend of Figure 8.2, groundwater variables horizontally and waste form variables vertically. Different settings of these variables were combined to develop eight leaching scenarios, identified by the letters A to H. For each scenario, expressions were developed to predict the leaching rate as a function of time for a period of up to one hundred years. The detailed calculations are presented in Appendix XIII and summarized in Figure 8.2. The leaching rates for each scenario are presented as a range where important variables (other than the four master variables) have been set at two typical values. Full lines are used for calculated rates while broken lines are used to indicate trends. The direction of the arrow across a leaching rate area indicates how the rate varies with the contaminant concentration in the matrix (i.e. a vertical arrow means that a change in concentration should result in a change in leaching rate while an horizontal arrow means that a change in concentration does not affect the leaching rate but rather results in a change of the duration of the leaching period). Each of the eight leaching scenarios will now be discussed.

Scenario A: Static groundwater. In the case of a static groundwater, the setting of the other master variables, chemical composition of the groundwater, permeability of the matrix and mobility of the contaminant are not important. Indeed, if the waste form is surrounded by a finite, unrenewed volume of groundwater, the leaching rates will rapidly decrease with time as a result of accumulation of the contaminant in the groundwater. Leaching will take place via surface

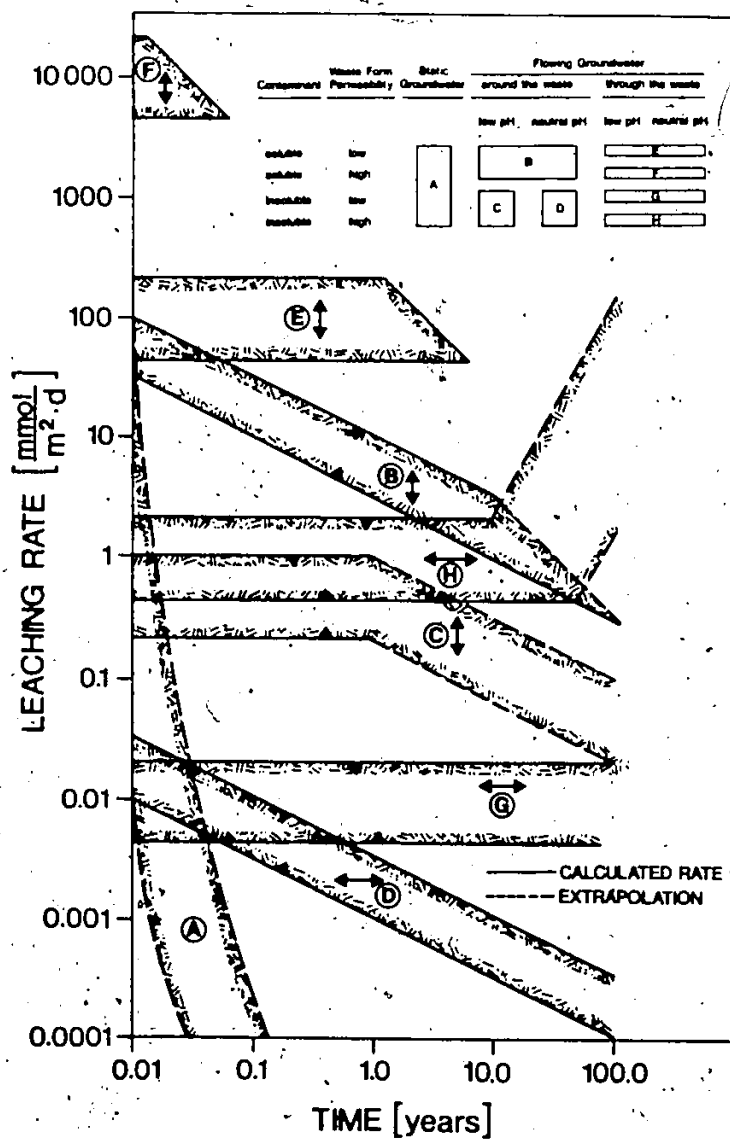


Figure 8.2 Inference of leaching rates following different disposal scenarios.



exchanges and the initial rates can be taken from Scenarios B, C and D. The rates should rapidly decrease to negligible values as the system approaches equilibrium. There is, therefore, no long term leaching in this scenario.

Scenario B: Groundwater flowing around the waste; soluble contaminant. The rate of leaching in this scenario is limited by diffusion of the soluble contaminant in the pore system of the matrix and thus decreases with time. The rate is independent of the composition of the groundwater since the contaminant is already mobile. Furthermore, the rate is considered independent of the waste permeability because it is assumed that water does not flow through the matrix. The range of leaching rates showed in Figure 8.2 was obtained by using two effective diffusion coefficients ( $10^{-5}$  and  $10^{-6}$  cm<sup>2</sup>/sec) in Equation 3.3. These values cover the range of contaminant molecular diffusion coefficients (Table 1-2) and also account for the tortuosity of the matrix. The calculated leaching rates represent maximum values since derivation of Equation 3.3 was based on maintaining zero surface concentration. The leaching rates are directly proportional to the initial contaminant concentration (i.e. Equation 3.3); the range would therefore be shifted vertically for other concentrations. Calculated leaching rates (Figure 8.2) extend to 10 years at which point the concentration at the centre of the 2 metre thick slab would start decreasing as a result of the leaching process (for the higher  $D_e$  value). For times larger than 10 years, the rate should therefore be smaller than these predicted for a semi-infinite slab.

Scenario C: Groundwater flowing around the waste; Insoluble contaminant under acidic leaching conditions. The leaching rate is initially controlled by the amount of acid available to neutralize the waste form matrix. It is assumed that 1) cement ANC is consumed before the contaminant is solubilized (see Section 7.2.2), 2) the leaching efficiency varies between 10 and 50% (Table 7.4) and 3) the matrix does not entirely dissolve. Assumption 2) was formulated based on the compounded effects that only a fraction of the total concentration of a contaminant can be solubilized under acidic conditions (Section 7.2.1) and that only part of the solubilized concentration leaches (Section 7.3.2). Because of Assumption 3), diffusion of species between the leaching front and the waste form-groundwater interface eventually becomes rate limiting. The leaching rate (Figure 8.2) is thus constant, a function of the rate of acid contacted with the matrix, until diffusion becomes rate limiting.

Scenario D: Groundwater flowing around the waste; Insoluble contaminant under neutral leaching conditions. This situation corresponds to the long term leaching experiments (Experiment 7) for which nearly two years of data were analyzed in Section 7.4. It was demonstrated that leaching rates were controlled by the rate of diffusion in the waste matrix and that chemical equilibrium between the soluble and insoluble forms of the contaminants was maintained at all times. The leaching rate area defined on Figure 8.2 is based on Equation 3.3, using effective diffusion coefficients of  $10^{-12}$  and  $10^{-13}$   $\text{cm}^2/\text{sec}$ , as reported in Table 7.6. These values can also be obtained

theoretically by considering a molecular diffusion coefficient equal to  $10^{-6}$  cm<sup>2</sup>/sec and  $K_d$  values of  $10^6$  to  $10^7$ ; as defined in Equation 3.5,  $K_d$  is the ratio of the insoluble to the soluble concentration in the matrix. Calculations indicate that the centre of the 2 m thick slab is not affected by leaching, even after 100 years. The leaching rates are independent of total concentration (they are a function of the soluble concentration).

Scenario E: Groundwater flowing through the waste; soluble contaminant, low matrix permeability. Leaching takes place via convective transport. The groundwater flows through the waste form following Darcy's Law. A hydraulic gradient varying from 1.0 to 5.0 defines the range showed in Figure 8.2. The contaminant is completely washed from the matrix as the front of groundwater progresses through the matrix. Leaching stops when the matrix has been emptied of its content, after approximately 5 years.

Scenario F: Groundwater flowing through the waste; soluble contaminant, high matrix permeability. This scenario is similar to scenario E with the exception that, as a result of a failure of the matrix, the matrix permeability is 100 times higher. The leaching rate and duration are directly proportional to permeability as reflected in the area defined on Figure 8.2.

Scenario G: Groundwater flowing through the waste; insoluble contaminant, low matrix permeability. The soluble portion of the contaminant is transported by convection. Chemical equilibrium between the insoluble and soluble parts ensures a constant pore concentration

and leach rate. The leaching rate range shown in Figure 8.2 is based on a soluble concentration of  $10^{-5}$  mol/L and a hydraulic gradient varying between 1 and 5. Acidic groundwater is neutralized by the matrix ANC. Contaminants might be solubilized but reprecipitate downstream. A breakthrough would occur when the full 2 m slab has been neutralized. In this scenario however, because of low permeability, this does not occur within a period of 100 years even with the low pH groundwater. It is doubtful whether this scenario would ever control leaching since surface dissolution under low pH conditions (Scenario C) results in much higher leaching rates.

Scenario H: Groundwater flowing through the waste; insoluble contaminant, high matrix permeability. This scenario is similar to Scenario G with the exception that, as a result of a failure of the matrix, the matrix permeability is 100 times higher. In this case, the amount of acid contacted with the waste is sufficient to neutralize the entire waste form ANC in a relatively short period of time and produce a leaching breakthrough (Figure 8.2).

## 8.2 From Leaching Rates to Concentrations

The environmental impact of contaminants is normally evaluated based on concentration. Figures 8.3 and 8.4 were prepared to help interpret leaching rates by examining groundwater concentrations resulting from a simple dilution model (Figure 8.3). The model assumes that a stream of leachate is completely mixed with a stream of groundwater; the groundwater stream is then diluted as it flows away.

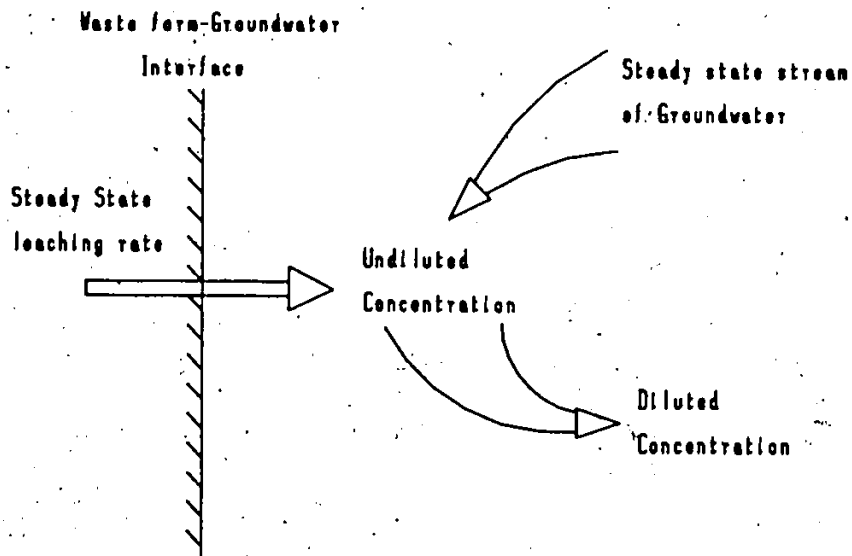


Figure 8.3 Simplified groundwater mixing model.

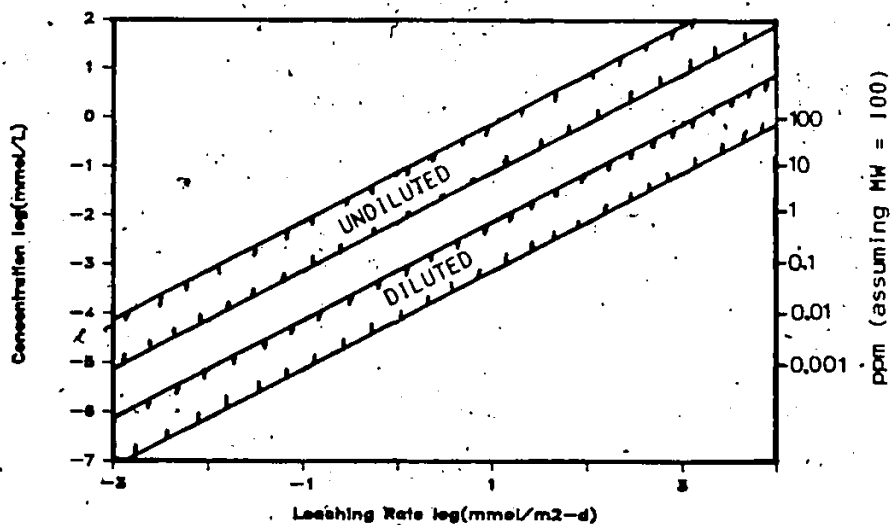


Figure 8.4 Groundwater contaminant concentration based on the simple mixing model represented by Figure 8.3.

from the waste form. The resulting concentrations before and after dilution (100 fold) are presented in Figure 8.4. Each range was constructed based on a groundwater flow rate varying between 5 and 50  $\text{m}^3/\text{m}^2\text{-year}$ . It was furthermore assumed that the leaching rate is independent of the groundwater hydraulic regime. A higher groundwater flow rate thus simply represents a higher dilution factor.

Groundwater quality criteria for toxic contaminants are typically lower than 1 mg/L (Ontario Ministry of the Environment, 1978). It can be read from Figure 8.4 that such a concentration at the waste form-groundwater interface (undiluted range) can result from a leaching rate varying between 0.1 and 1.0  $\text{mmol}/\text{m}^2\text{-d}$ . This concentration will be reduced by dilution as the groundwater flows away from the waste form.

### 8.3 Practical Implications

Preparation of waste forms to dispose of concentrated hazardous wastes proceeds from the philosophy that containment represents a better management practice than dilution into the environment. Figure 8.2 indicates that, after the secondary barriers fail, leaching will occur in all of the studied scenarios at a rate which can vary over some eight orders of magnitude.

#### 8.3.1 Preparation of Better Waste Forms

From examination of Figure 8.2 it appears that the most important factor to reduce leaching is to ensure that the contaminants are present in the matrix in an insoluble form. The scenarios where the contaminants

are in solution in the pore system (B,E,F) result in the highest leaching rates. Properties related to the waste form matrix, such as permeability and factors affecting diffusivity (connected porosity, tortuosity) also affect leaching rates, but to a lesser extent. Finally, in the case where the waste form is subjected to an aggressive leachant, the neutralizing capacity (in our case acid) of the matrix is important.

Preparing a waste form therefore requires a fundamental knowledge of the waste chemistry. Specification of a solidification system (even a patented one!) offers no guaranty of pollutant containment.

Insolubilization in a waste form matrix can be done in two ways, i) by pretreatment of the waste to speciate contaminants as insoluble salts or ii) by promoting reactions of immobilization with the solid additives (i.e. the waste form matrix). For the solidification systems studied in this work, hydroxide solubility controlled pore solubility in the alkaline environment established by cement while the interactions with the matrix controlled at lower pH.

It is desirable to obtain a waste form matrix of low permeability as convective leaching can be more important than interface exchanges. The same operational variables which can be manipulated to reduce matrix permeability, waste dewatering, use of dry powdery additives, high dosage of cement, should also improve the properties which affect diffusivity of species in the pore system: connected porosity, water content, tortuosity. It is worth noting that efforts should be directed toward reducing the total porosity rather than the water content since it appears that solidified waste matrices surrounded by water rapidly

become saturated, even if they are not subjected to a hydraulic gradient (Section 7.4.1).

The matrix will keep its initial beneficial properties only if it is protected from destruction by weathering (i.e., wetting/drying or freezing/thawing cycles). It is important, for that purpose, that the cement added to the waste be allowed to solidify properly. Cement should only be added to neutral or alkaline wastes (lime is a cheaper neutralizing agent than portland cement). Quick setting, which often happens in high sulphate environment, should be avoided since it does not result in good bonding (sulphates can first be precipitated as  $\text{CaSO}_4$  with lime). Finally, a proper curing environment (temperature, humidity) should be provided.

The waste form matrix should have buffering capacity to maintain the chemical environment in which the contaminants are insolubilized. For example, 1) for metal sulfides, a low redox environment can be maintained using an insoluble sulfide salt (such as  $\text{FeS}$ ), less stable than the toxic metal sulfides (Section 3.3.3) and 2) for metal hydroxides or carbonates, excess alkalinity should be provided. It is also important to provide the buffering capacity in an insoluble form. From this point of view, pozzolanic systems are superior to other portland cement systems since their excess lime is immobilized in compounds which will not leach in a neutral pH environment but still provide acid neutralization capacity in a low pH environment.



### 8.3.2 The Design of Better Landfills

Based on the leaching scenarios presented in Figure 8.2, it appears that landfilling situations where the groundwater flows around the waste are superior to those where it flows through the waste. Indeed, for a soluble contaminant, Scenarios E and F, for convective leaching at low and high permeability, result in much higher rates than Scenario B, describing diffusive transport. Similarly for an insoluble contaminant, Scenarios C and D, based on surface exchanges, predict lower leaching rates than the convective transport Scenario H (high matrix permeability). (Scenario G, convective transport for a low permeability matrix, initially predicts a lower leach rate than Scenarios C or D but, as pointed out in Section 8.1.3, it is unlikely that this scenario would ever control the leaching rate.)

In all the leaching scenarios involving interface exchanges (A,B,C,D), the leaching rates decrease with time as a result of diffusion being rate limiting. On the other hand, in the scenarios involving convective transport (E,F,G,H), the rates are steady or, as shown in Figure 8.2 for Scenario H, might even increase if a breakthrough occurs. A breakthrough will occur whenever a species (often non-hazardous), responsible for the insolubilization of a contaminant, is washed from the matrix pore system. This phenomenon was illustrated in Scenario H for pH, but it can occur with any chemical insolubilization system.

It is interesting to note that diffusion controlled Scenarios B and D represent "worst case conditions" since they were based on the assumption of zero surface concentration. Any accumulation of leached species near the groundwater-waste form interface resulting from a slow moving groundwater would reduce the driving force for leaching. The limiting case is illustrated by Scenario A in which the absence of groundwater renewal causes a rapid decrease of the leaching rates as the system tends toward equilibrium.

Factors which can be controlled to favor interface exchanges rather than convective transport in designing a landfill include 1) avoiding potential build-up of hydraulic gradients, and 2) protecting the waste mass from weathering. Factors which can be controlled to minimize leaching resulting from surface exchange include 1) minimizing the waste surface area-to-volume ratio, 2) reducing the rate of groundwater flow around the waste, and 3) preventing contact with aggressive waters.

## 9.0. CONCLUSIONS

Conclusive statements have been grouped into 4 sections. The first three are derived directly from the experimental work and are thus somewhat specific to the systems studied. Observations on the morphology of the matrix of cement-based waste forms are presented in Section 9.1 and findings about mechanisms of containment and leaching are presented in Sections 9.2 and 9.3, respectively. Finally, the long term leachability of cement-based waste forms is discussed in Section 9.4.

### 9.1 Microstructure

Since a waste form is prepared by adding a bulking agent (when required) and the minimum amount of cement to an aqueous waste, the matrix does not normally resemble the intimately interlocked network of hydrated products observed in cement paste.

The matrices of the cement-based waste forms tested were largely insoluble in neutral water, losing between 3 and 13% of their initial mass after 665 days of leaching in water. The observed mass losses can be accounted for by the leaching of major ions (e.g. sodium from the bentonite clay and the soluble silicates, and lime from hydrated cement). Fly ash-based systems exhibited lower mass losses as a result of the lime in these systems being immobilized through pozzolanic reactions with the fly ash particles. For all the systems studied, the total masses of contaminants leached (i.e. As, Cd, Cr and Pb)

represented a negligible fraction of the total mass loss.

The porosity of the matrices studied varied between 40 and 60%. The pore volume was distributed among three ranges comprising voids between clumps of particles, inter-particle space and intra-particle space. Large pores were interconnected through small openings.

The water content of the matrices studied varied from 0.14 to 0.52 (weight basis). The connected porosity of a matrix made from non-porous silica particles was found equal to its water content. However, the connected porosities of fly ash matrices were lower than their water content since pore solution was absorbed by the fly ash particles.

The samples used in the long term leaching tests (5.04 cm cubes) gained weight as they became saturated with water over a one year period (even though they were not exposed to a hydraulic gradient).

## 9.2 Mechanisms of Containment

Containment of contaminants in cement-based waste forms is effected by both physical and chemical mechanisms. An obvious physical mechanism is the formation of a large mass of low permeability and reduced surface area of contact with leaching waters. The importance of this will be outlined in Section 9.4 below. Conclusions on the chemical mechanisms of containment follow.

Lithium was not immobilized in the waste form matrix. As it stayed in solution in the pores, it was completely recovered in equilibrium leaching tests, throughout the pH range.

Cement establishes an alkaline environment where toxic metals can be precipitated. The concentrations of soluble cadmium, chromium and lead were limited by their hydroxide solubility at high pH. For pH values between 7 and 3, interactions with a fly ash matrix reduced metal solubility by several orders of magnitude compared to hydroxide solubility. The interactions with the matrix were dependent on both the concentration and pH in the liquid phase. Complete resolubilization of chromium and lead could only be achieved at very low pH (2 to 3) and small liquid phase concentrations (i.e. in a high liquid-to-solid ratio leaching test). Only approximately 60% of cadmium was solubilized at low pH.

Arsenic was precipitated as basic calcium arsenite. Its rate of mobilization was a function of the rate of leachant renewal since it depended on the availability of carbonates to drive a carbonation reaction. Once mobilized, the arsenite ion did not seem to interact with the matrix as it leached readily.

Portland cement provides acid neutralization capacity to maintain the high pH environment where the waste form is stable. The free lime, produced from hydration of portland cement (8 meq/g of dry portland cement), can establish a high pH when neutral water is contacted with the waste form. When acidic waters are contacted with the waste form, hydrated cement will dissolve, providing a neutralizing capacity of approximately 20 meq/g of dry cement. Based on the typical amount of cement added, it was calculated that a typical waste form can neutralize between 2000 to 3000 times its volume of pH 3 groundwater. It is

Important to stress that the products of cement hydration dissolve in acidic water before most toxic metals are solubilized.

### 9.3 Mechanisms of Leaching

For the general case of a contaminant immobilized in the matrix, leaching takes place via solubilization and transport through the pore system.

For cement-based waste forms in contact with a neutral leachant, leaching rates were limited by molecular diffusion after correction for matrix tortuosity. The rate of solubilization of toxic contaminants (As, Cd, Cr and Pb) was very fast as it was successfully described using equilibrium chemistry. The cumulative fraction of metals (Cd, Cr and Pb) leached after 665 days was less than 1% for the four systems studied. Arsenic leached more readily, the cumulative fraction leached attaining 15% for the soluble silicate-cement system.

For leaching under acidic conditions, the rate was initially limited by the supply of  $H^+$  (its availability as opposed to its rate of diffusion). Modelling indicated that  $H^+$  diffused inside the waste form, thus neutralizing the matrix and mobilizing contaminants. There was no stoichiometric relationship between the amount of  $H^+$  absorbed in the matrix and the amount of contaminant leached, for three reasons. First, contaminants mobilized at the leaching front diffused both outward and inward. The relative amount diffusing in each direction depended on the respective concentration gradients. The gradient for outward diffusion was a function of the thickness of the leached layer and the

concentration at the interface, whereas the gradient for inward diffusion varied with the matrix acid neutralization capacity. Second,  $H^+$  reacted with the matrix. Third, only a fraction of a contaminant was available for leaching, depending on both the pH and the pore soluble concentration.

The leaching efficiency under acidic leaching conditions was defined as the amount of a contaminant leached over the amount contained in the weight of matrix neutralized. For the inert silica matrix, only the first mechanism of the three listed above was effective and the leaching efficiency of cadmium was approximately 50%. For a fly ash matrix containing a normal amount of cement, the three mechanisms reduced the leaching efficiency of chromium and lead to less than 10% and that of cadmium to less than 1%.

Since the matrix of a cement-based waste form does not entirely dissolve when leached under low pH conditions, a leached layer develops, through which  $H^+$  and the contaminants must diffuse. Thus, diffusion of the contaminants through this layer should eventually become rate limiting (rather than the availability of  $H^+$ ). It is unlikely that  $H^+$  diffusion would ever be rate-limiting since  $H^+$  diffuses about 10 times faster than any other chemical species.

#### 9.4 Long Term Leachability

The following statements are based on the assumptions and modelling of Chapter 8. Leaching rates are the best way of expressing long term leachability. However, since toxicity is normally a function

of concentration, concentrations calculated based on the simple groundwater mixing model described in Section 8.2 will also be presented (concentrations in ppm are based on a molecular weight of 100).

Contaminants which are not immobilized in the waste form matrix and thus remain in the pore solution will leach readily, at a rate larger than  $10 \text{ mmol/m}^2 \cdot \text{d}$ . This is equivalent to concentrations at the interface larger than  $0.1 \text{ mmol/L}$  (10 ppm). Landfilling scenarios which avoid convective transport, forcing interface exchanges, should be favored as the leaching rates will decrease with time.

For contaminants immobilized in the matrix, either through precipitation as insoluble salts or interaction with the matrix, the rate of leaching is dependent on the characteristics of the groundwater. We distinguish two extreme cases: a pH 3 groundwater and a neutral, non-aggressive groundwater.

An acidic groundwater will result in an initially constant leaching rate of approximately  $1 \text{ mmol/m}^2 \cdot \text{d}$ , equivalent to  $0.01 \text{ mmol/L}$  (1.0 ppm), which is a function of the relative amount of acid contacted and the acid neutralization capacity of the waste form. As in the previous case, flow of groundwater through the waste form should be avoided as it may result in a leaching breakthrough. In this case, however, interface exchanges should eventually lead to diffusion becoming rate limiting and result in decreased leach rates.

Finally, for immobile contaminants and a mild groundwater, initial leaching rates of  $0.1 \text{ mmol/m}^2 \cdot \text{d}$  should rapidly decrease below  $0.01 \text{ mmol/m}^2 \cdot \text{d}$  if convection transport is avoided (equivalent to 0.0001



mmol/L or 0.01 ppm). The rates for this scenario are independent of the contaminant concentrations in the matrix.

The above mentioned leaching rates should be taken as rough guidelines only. They are based on realistic waste forms properties but represent worst case leaching condition since they were calculated assuming steady-state groundwater flows and zero surface concentration (for diffusion-controlled rates). Furthermore, any attenuation or dilution resulting from groundwater transport was not taken into account.

## 10. RECOMMENDATIONS

Based on the work done in this thesis, recommendations will be formulated to, 1) continue the development of predictive models of the leaching phenomena, 2) evaluate waste form environmental stability in the laboratory, and 3) minimize leach rates under field leaching conditions.

### 10.1 Modelling

The following recommendations are derived from the development of the models LEEQ and LEEX based on a mechanistic description of the chemical reactions and transport phenomena that control leaching.

Modelling based on a numerical solution of interrelated transport and chemical reaction equation systems should be limited to the interpretation of laboratory experiments for the purpose of studying mechanisms of leaching and containment. The computational burden of such a solution is too extensive to apply to long term prediction.

The numerical method consisting of alternately solving between transport and chemical reactions should be preferred over that consisting of combining the two sets of equations. The former method proved to be precise and flexible in describing various chemical systems using equilibrium chemical equations or experimental data.

There are three main areas where future modelling efforts should be directed: morphology of the matrix, chemical reactions and transport mechanisms.

Morphology. Efforts should be expended to better characterize the connected porosity and its changes with time by 1) determining the distribution of water among the various phases of the matrix, 2) studying the conditions and rates at which the matrix immersed into water will saturate and, 3) characterizing the structure and chemical composition of the leached layer under various pH conditions.

Chemical reactions. The interactions between contaminants and the matrix should be investigated with particular focus on the following aspects: reversibility and speed of reaction (an equilibrium approach may not be always applicable).

Transport. For diffusive transport, an attempt should be made to measure the connected porosity and tortuosity independently. For convective transport, the applicability of Darcy's law to describing flow through the matrix should be evaluated in the light of the morphological changes that take place as a result of leaching.

#### 10.2 Laboratory Evaluation

Modeling indicated that the chemical properties of a contaminant are more important than the physical properties of the matrix for predicting long term leachability. Laboratory evaluation of chemical properties can be done by conducting leaching tests which can be classified on the basis of whether they provide kinetic or equilibrium information.

Leaching tests where changes are measured as a function of time

(i.e. kinetic tests) are best suited for mechanistic studies. Their results can be used for modelling and extrapolation to evaluate long term leachability. They are, however, expensive and time consuming since initial wash off phenomena often cloud the longer term rate controlling mechanisms.

Equilibrium leaching tests can be used to measure the concentrations of contaminants which can be solubilized in different chemical environments. The concentrations measured do not normally relate to field concentrations where transport factors prevent attainment of equilibrium. Equilibrium leaching tests, however, are well suited for the comparison of waste forms or for quality control in a solidification plant. Waste form samples should be crushed to accelerate attainment of equilibrium. Equilibrium leaching tests which can be used to evaluate cement-based waste forms include:

Mild Leachant Equilibrium Leaching Test: This test aims at measuring the soluble fraction of a contaminant in the waste environment. It is a measure of the effectiveness of immobilization. To achieve this goal, the test should be conducted using a low liquid-to-solid ratio to avoid dilution and a mild leachant to allow the waste to control the chemical environment.

Aggressive Leachant Equilibrium Leaching Test: This test aims at measuring the fraction of a contaminant available for leaching in an environment established by an aggressive leachant. A high liquid-to-solid ratio should be used to minimize the contaminant concentration in solution (which represents the driving force for

interactions with the matrix) and to allow the leachant to establish the chemical environment.

Acid Neutralization Capacity. This test aims at measuring the capacity of the matrix to neutralize acid, thus preventing contaminants from being solubilized. If the test is conducted in a series of batch reactors, with an increasing amount of acid added to each reactor, the liquid fraction of each reactor can be analyzed for contaminants of interest to measure the effectiveness of immobilization throughout the pH range.

### 10.3 Minimization of Field Leaching Rates

Recommendations for the minimization of leaching rates must take into account the chemical properties of the contaminants in the waste form matrix as well as the flow and chemical characteristics of the groundwater.

The most important factor is to ensure that, when the waste form is prepared, the contaminants are chemically immobilized in the matrix. Immobilization can be carried out in two ways: 1) by pretreatment of the waste to speciate contaminants as insoluble salts, or 2) by promoting reactions with the solid additives (i.e. the waste form matrix).

The waste form matrix should have buffering capacity to maintain the chemical environment in which the contaminants are immobilized (e.g. low redox or high pH). It is also important to provide this buffering capacity in an insoluble (i.e. non-leachable) form.

Acidic wastes should be neutralized before cement is added in

order to provide an optimal environment for the solidification reaction to occur. Under these conditions, the typical cement dosages required to solidify aqueous wastes also provide ample acid neutralization capacity.

Efforts should be directed toward minimizing the total porosity of the matrix rather than the water content, as the matrices of cement-based waste forms rapidly become saturated when immersed in water, even if they are not subjected to a hydraulic gradient.

Landfilling conditions should be provided to prevent hydraulic gradient buildup and flow of groundwater through the waste. This can be achieved by avoiding placement of the waste form in a material of similar permeability. If the waste form is placed in a material of much lower permeability, groundwater flow through the surrounding material should be minimized and leaching will decrease as the system approaches chemical equilibrium. If the waste form is placed in a material of much higher permeability, groundwater will tend to flow around the waste rather than through it. These conditions will result in leaching taking place through interface exchanges, with the following desirable properties: 1) the leaching rates will be controlled by molecular diffusion, and thus decrease with time (rate  $\sim 1/t^{1/2}$ ), and 2) a leached layer will rapidly develop at the surface of the waste form which will isolate it from direct contact with the groundwater.

## REFERENCES

Alford, M.N. et al., "The Effect of Lead Nitrate on the Physical Properties of Cement Paste", Cem. and Concr. Res., 11, p 235-245, 1981.

American Nuclear Society, "Measurement of the Leachability of Solidified Low-Level Radioactive Wastes", Draft of a standard, working group ANS-16.1, June 20, 1984.

Anderson, M.A. and Rubin, A.J., Eds., Adsorption of Inorganics at Solid-Liquid Interfaces, Ann Arbor Science, 1981.

Arliguie, G., Ollivier, J.P. and Grandet, J., "Etude de l'effet retardateur du zinc sur l'hydratation de la pate de ciment portland", Cement and Concrete Research, 12(79-86), 1982.

Bartos, M.J. and Palermo, M.R., "Physical and Engineering Properties of Hazardous Wastes and Sludges", U.S. EPA-600/2-77-139, 1977.

Benson, R.E., "Natural Fixing Materials for the Containment of Heavy Metals on Landfills", 12th Mid-Atlantic Industrial Waste Conference, 1980.

Berner, R.A., "Early Diagenesis - A Theoretical Approach", Princeton University Press, Princeton, N.J., 1980.

Bishop, P.L., Ransom, S.B., Gress, D.L., "Fixation Mechanisms in Solidification/Stabilization of Inorganic Hazardous Wastes", Proceedings of the 38th Industrial Waste Conference, Purdue University, 1984.

Bishop, P.L., Ransom, S.B., Gress, D.L., "Fixation Mechanisms in Solidification/Stabilization of Inorganic Hazardous Wastes", Proceedings of the 38th Industrial Waste Conference, Purdue University, 1984.

Bruce, R.B. et al., "Physical and Chemical Properties of Chemically Fixated Uranium Mine-Mill Tailings", Ontario Research Foundation, May 1981.

Calleja, J., "Durability", Proceedings of the 7th International Congress on the Chemistry of Cement, Editions Septima, Paris, 1980.

Chan, P.C., Listowitz, J.W., Perna, A. and Trattner, P., "Evaluation of Sorbents for Industrial Sludge Leachate Treatment", U.S. Environmental Protection Agency, Cincinnati, EPA-600/2-80-052, 1980.

Cheremisinoff, P.N. and Ellerbusch, F., Carbon Adsorption Handbook, Ann Arbor Science, Ann Arbor, Michigan, 1980.

Conner, J.R., "Method of Making Wastes Non-Polluting and Disposable" U.S. Patent 3,837,872, January 4, 1972.

Conner, J.R., "Considerations on Selecting Chemical Fixation and Solidification Alternatives - The Engineered Approach, Second Annual Conference of Applied Research and Practice on Municipal and Industrial Waste, Madison, Wisconsin, September 9, 1979.

Côté, P.L. and Hamilton, D.P., "Leachability Comparison of Four Hazardous Waste Solidification Processes", Presented at the 38th Annual Purdue Industrial Waste Conference, May 10-12, 1983.

Côté, P.L. and Isabel, D., "Application of a Dynamic Leaching Test to Solidified Hazardous Wastes", Hazardous and Industrial Waste Management and Industrial Waste Management and Testing: Third Symposium, ASTM STP 851, Larry P. Jackson, Alan R. Rohlik, and Richard A. Conway, Eds., American Society for Testing and Materials, Philadelphia, 1984, p 48-60.

Côté, P.L., "Evaluation of the Long Term Stability of Solidified Wastes", presented at a Workshop on Environmental Assessment of Waste Stabilization/Solidification, Organized by the Alberta Environmental Centre and Environment Canada, Vegreville, Alberta, November 21 and 22, 1983.

Côté, P.L. and Constable, T.W., "Evaluation of Experimental Conditions in Batch Leaching Procedures", Resources and Conservation, 9:59-73, 1982.

Crank, J., The Mathematics of Diffusion, Oxford University Press, London, 1956.

Cussler, E.L., "Dissolution and Reprecipitation in Porous Solids", AIChE Journal, 28(3):500-508, 1982.

Daimon, M., "Mechanisms and Kinetics of Slag Cement Hydration", Proceedings of the 7th Congress on the Chemistry of Cement, Editions Septima, Paris, 1980.

Demoulian, E., Vernet, C., Hawthorn, F. and Gourdin, P., "Détermination de la teneur en laitier dans les ciments par dissolution sélective", Proceedings of the 7th International Congress on the Chemistry of Cement, Editions Septima, Paris, 1980.

Double, D.D. and Hellewell, A., "The Solidification of Cement", Scientific American, 237(1):82-91, 1977.

Double, D.D., Thomas, N.L. and Jameson, D.A., "The Hydration of Portland Cement. Evidence for an Osmotic Mechanism", Proceedings of the 7th International Congress on the Chemistry of Cement, Editions Septima, Paris, 1980.



Environmental Laboratory (Waterways Experiment Station), "Guide to the Disposal of Chemically Stabilized and Solidified Waste", Publication SW-872, U.S. Environmental Protection Agency, 1980.

Falcone, J.S., Spencer, R.W., Reisnyder, R.H. and Katsanis, E.P.L., "Chemical Interaction of Soluble Silicates in the Management of Hazardous Wastes" in Hazardous and Industrial Waste Management and Testing, Third Symposium, ASTM, STP 851, L.P.  
Franklin, A.J., Cement and Mortar Additives, Noyes Data Corporation, Park Ridge, NJ., 1976.

Fraser, J.L. and Lum, K.R., "The Availability of Elements of Environmental Importance in Incinerated Sludge Ash", Environmental Science and Technology, 17(1):52-54, 1983.

Gatcho, M.H. Ed., "Cement and Mortar Technology and Additives, Developments since 1977", Noyes Data Corporation, Park Ridge, NJ, 1980.

Gerald, C.F., Applied Numerical Analysis, Addison-Wesley Publishing Company, 2nd Edition, 1980.

Godbee, H.W. and Joy, D.S., Assessment of the Loss of Radioactive Isotopes from Waste Solids to the Environment. Part 1: Background and Theory, ORNL, TM-4333, 1974.

Godbee, H.W., Compere, E.L., Joy, D.S., Kibbey, A.H., Moore, J.G., Nestor, Jr., C.W., Anders, O.U., Neilson, R.M. Jr., "Application of Mass Transport Theory to the Leaching of Radionuclides from Waste Solids", Nuclear and Chemical Waste Management 1 (29-35), 1980.

Huang, C.P., "Chemical Interaction Between Inorganics and Activated Carbon", in Carbon Adsorption Handbook, Cheremisinoff and Ellerbusch, Eds., Ann Arbor Science, Ann Arbor, 1978.

Iler, R.K., The Chemistry of Silica, Solubility, Polymerization, Colloid and Surface Properties, and Biochemistry, Wiley Interscience, 1979.

Jackson, A.R. Rohlih and R.A. Conway, Eds. American Society for Testing and Materials, Philadelphia, 1984.

Jennings, A.A., Kirkner, D.J. and Theis, T.L., "Multicomponent Equilibrium Chemistry in Groundwater Quality Models", Water Resources Research, 18(4):1089-1096, 1982.

Kinniburgh, D.G. and Jackson, M.L., "Cation Adsorption by Hydrous Metal Oxides and Clay" in Adsorption of Inorganics of Solid-Liquid Interface, Anderson and Rubin, Eds., Ann Arbor Science Publishers Inc., Ann Arbor, Michigan, 1981.

Kirkner, D.J., Theis, T.L. and Jennings, A.A., "Multicomponent Solute Transport with Sorption and Soluble Complexation", Adv. Water Resources, 7:120-125, 1984.

Kondo, R., Daimon, M., Sakai, E. and Ushiyama, H., "Influence of Inorganic Salts on the Hydration of Tricalcium Silicate", J. Appl. Chem. Biotechnol. 27(191), 1977.

Lasaga, A.C., "The Treatment of Multi-Component Diffusion and Ion Pairs in Diagenetic Fluxes", American Journal of Science, 279:(324-346), 1979.

Lea, F.M., The Chemistry of Cement and Concrete, Edward Arnold (Publishers) Ltd., 1970.

Li, Y.H. and Gregory, S., "Diffusion of Ions in Sea Water and in Deep-Sea Sediments", Geochimica and Cosmochimica Acta, 38:(703-714), 1974.

Lindstrom, F.T., and L. Boersma, "Theory of Chemical Transport with Simultaneous Sorption in a Water Saturated Porous Medium", Soil Science, 110(1):1-9, 1970.

Locher, F.U., "Hydration of Pure Portland Cement", Proceedings of the 7th International Congress on the Chemistry of Cement, Editions Septima, Paris, 1980.

Longuet, P. and Bellina, G., "Chimie des ciments et traitement des boues minerales", Seminaire B, in the Proceedings of the 7th International Congress on the Chemistry of Cement, Editions Septima, Paris, 1980.

Machiels, A.J. and Pescatore, C., "Modeling of Waste Form Leaching: Part 1 Status of Leach Modeling", University of Illinois Report UILU-ENG-82-5319, 1982.

Mahloch, J.L., Averett, D.E. and Bartos, M.J., "Pollutant Potential of Raw and Chemically Fixed Hazardous Industrial Wastes and Flue Gas Desulfurization Sludge - Interim Report, EPA-600/2-76-182, 1976.

Mahoney, J.D., Dwyer, E.A., Saukin, W.P. and Spinna, R.J., "Radiochemical Studies of the Leaching of Metal Ions from Sludge Bearing Concrete", Third Conference in Advanced Pollution Control for the Metal Finishing Industry, Kissimmee, Florida, April 14-16, 1980, EPA-600/2-81-028, 1981.

Malone, P.G. and Larson, R.V., "Scientific Basis of Hazardous Waste Immobilization", Presented at the Second Annual ASTM Symposium on Testing of Hazardous and Industrial Solid Wastes, Orlando, Jan. 28-29, 1982.

Malone, P.G., Mercer, R.B. and Thompson, D.W., "The Effectiveness of Fixation Techniques in Preventing the Loss of Contaminants from Electroplating Wastes", First Annual EPA/AES Conference on Advanced Pollution Control for the Metal Finishing Industry, Lake Buena Vista, Florida, January 17-19, 1978.

McCarthy, G.J., Ed., Scientific Basis for Nuclear Waste Management, Plenum Press, New York, 1979.

Mendel, J.E. et al, "A State-of-the-art Review of Materials Properties of Nuclear Waste Forms", PNL-3802 Pacific Northwest Laboratory, 1981.

Meredith, J.W., "Electrolating Wastewater Sludge Characterization", Cooperative Study, US EPA and American Electroplaters' Society, Cincinnati, 1980.

Meric, J.P., "La solidification des boues", Ciments, Betons, Chaux, 718:133-6, 1979.

Miller, C.W. and Benson, L.V., "Simulation of Solute Transport in a Chemically Reactive Heterogeneous System: Model Development and Application", Water Resources Research, 19(2):381-391, 1983.

Minnick, L.J., "Reactions of Hydrated Lime with Pulverized Coal Fly Ash", Proc. Fly Ash Utilization Conference, Bureau of Mines Information Circular 8348, 1967.

Moore, J.G., Godbee, H.W., Lebbey, A.H. and Joy, D.S., "Development of Cementitious Grouts for the Incorporation of Radioactive Wastes, Part 1 Leach Studies, ORNL-4962, 1975.

Morel, F.M.M., Westall, J.C. and Yeasted, J.G., Adsorption Models: A Mathematical Analysis in the Framework of General Equilibrium Calculations", in Adsorption of Inorganics at Solid-Liquid Interfaces, Anderson and Rubin, Eds., Ann Arbor Science, 1981.

Nathwanji, J.S. and Phillips, C.R., "Leachability of Ra-226 from Uranium Mill Tailing Consolidated with Naturally Occurring Materials and/or Cement. II Analysis Based on Mass Transport Equation", Water, Air, and Soil Pollution, 14:389-402, 1980.

Ness, H.M., Volesky, A.F. and Johnson, S.Y., "Physical and Chemical Characteristics of Fly Ash and Scrubber Sludge from some Low-Rank Western Coals, Presented at Ash Management Conference, Texas A&M University, Sept. 25-27, 1978.

Nishimura, T., Ito C.T., Tozawa, K. and Robins, R.G., "The Calcium-Arsenic-Water-Air System", Proceedings of the 15th Annual Meeting on Impurity Control & Disposal, Vancouver, August 18-22, 1985.

Nordstrom, D.D., Plummer, L.N., Wigley, T.M.L., Wolery, T.J., Ball, J.W., Jenne, E.A., Bassett, R.L., Crerar, D.A., Florence, T.M., Fritz, B., Hoffman, M., Hodren, G.R., Jr., Lafon, G.M., Mattigod, S.V., McDuff, R.E., Morel, F., Reddy, M.M., Sposito and Thraillkill, J., in Chemical Modeling in Aqueous Systems, E.A. Jenne, ed., ACS Symposium series No. 93, ACS, Washington, D.C., 1979, pp. 857-897.

Oak Ridge National Laboratory, "ORNL Conference on the Leachability of Radioactive Solids", Gatlinburg, Tennessee, December 9-12, 1980.

Ontario Ministry of the Environment, "Water Management Goals, Policies, Objectives and Implementation Procedures", November, 1978.

Orr, C. Jr., "Application of Mercury Penetration to Materials Analysis", Powder Technol 3:(117-123), 1969.

Patterson, J.M., Wastewater Treatment Technology, Ann Arbor Science, Ann Arbor, Michigan, 1975.

Patterson, J.W., Allen, H.E. and Scala, J.J., "Carbonate Precipitation from Heavy Metals Pollutants" Journal Water Pollution Control Federation 49(12):2397-2410, 1977.

Peck, R.B., Hanson, W.E., Thornburn, T.H., Foundation Engineering, John Wiley and Sons, Inc., 1974.

Perrich, J.R., Ed., Activated Carbon Adsorption for Wastewater Treatment CRC Press, Inc., Boca Raton, Florida, 1981.

Petit, L. and Rouxhet, P.G., "Incorporation d'ions métalliques dans la silice", Séminaire B in the Proceedings of the 7th International Congress on the Chemistry of Cement, Editions Septima, Paris, 1980.

Pojasek, R., Ed., "Toxic and Hazardous Waste Disposal", Vol. 1, 2, 3 and 4, Ann Arbor Science Publishers Inc., Ann Arbor, Mich., 1979a.

Pojasek, R.B., "Solid-Waste Disposal: Solidification", Chemical Engineering, August 13, 1979b.

Poon, C.S., Peters, C.J. and Perry, R., "Use of Stabilization Processes in the Control of Toxic Wastes", Effluent and Water Treatment Journal, p 451-459, November 1983.

Poon, C.S., Clark, A.I., Peters C.J. and Perry, R., Mechanisms of Metal Fixation and Leaching by Cement Based Fixation Processes, Water Management & Research (1985) 3, 127-142.

Popovics, S., Concrete Making Materials, McGraw-Hill Book Company, 1979.

Ramachandran, J.S., Calcium Chloride in Concrete, Applied Science Publishers Ltd., London, 1976.

Regourd, M., "Structure and Behaviour of Slag Portland Cement Hydrates", Proceedings of the 7th Congress on the Chemistry of Cement, Editions Septima, Paris, 1980.

Richardson, G.L., "The Phantom Dissolution Leach Model", Nuclear and Chemical Waste Management, 2(3):237-241, 1981.

Robins, R.G., "The Aqueous Chemistry of Arsenic in Relation to Hydrometallurgical Processes", Proceeding of Annual Meeting on Impurity Control & Disposal, Vancouver, August 18-22, 1985.

Rousseaux, J.M. and Craig, Jr., A.B., "Stabilization of Heavy Metal Wastes by the SOLIROC Process", Third Conference in Advanced Pollution Control for the Metal Finishing Industry, Kissimmee, Florida, April 14-16, 1980, EPA/600-2-81-028, 1981.

Sawyer, C.N. and McCarty, P.L., Chemistry for Environmental Engineering, McGraw-Hill Book Company, 1978.

Schindler, P.W., "Surface Complexes of Oxide-Water Interfaces", in Adsorption of Inorganics at a Solid-Liquid Interface, Anderson and Rubin, Eds., Ann Arbor Science, 1981.

Scott, M.C., "SULFEX™ - A New Process Technology for Removal of Heavy Metals from Waste Streams", Proceedings of the 32nd Industrial Waste Conference, Ann Arbor, MI., Ann Arbor Science Publishers, Inc., 1977.

Sillen, L.G. and Martell, A.E., "Stability Constants of Metal-ion Complexes", Special Publ. No. 17, The Chemical Society, London, 1964.

Skalny, J. and Young, J.F., "Mechanisms of Portland Cement Hydration", Proceeding of the 7th International Congress on the Chemistry of Cement, Editions Septima, Paris, 1980.

Smolczyk, H.G., "Slag Structure and Identification of Slags", Proceedings of the 7th Congress on the Chemistry of Cement, Editions Septima, Paris, 1980.

Société Internationale de Publicité et d'Agences Commerciales, "Improvements in and relating to the Treatment of Waste", Belgium Patent 1,518,024, July 16, 1975.

Stone, J.D., "An Overview of Factors Affecting the Leachability of Nuclear Waste Forms", Nuclear and Chemical Waste Management (2):113-118, 1981.

Stumm, W. and Morgan, J.J., Aquatic Chemistry, 2nd ed., John Wiley and Sons, 1981.

Suffet, I.H. and McGuire, M.J., "Activated Carbon Adsorption of Organics from the Aqueous Phase, Volumes 1 and 2, Ann Arbor Science Publishers Inc., Ann Arbor, Michigan, 1981.

Sugi, T., Kataoka, K., Yamada, S. and Ando, Y., "Solidification of Sludges with Cement-Slag- $\text{CaSO}_4$ ", Seminaire A in the Proceedings of the 7th International Congress on the Chemistry of Cement, Edition Septima, Paris, 1980.

Theis, T.L., Wirth, J.E., Richter, R.O. and Marley, J.J., "Sorptive Characteristics of Heavy Metals in Fly-Ash-Soil Environments", Proceedings of the 31st Industrial Waste Conference, Purdue University, 1976.

Thomas, G.B. Jr., "Calculus and Analytic Geometry", Addison-Wesley Publishing Company, Reading, Massachusetts, 1969.

Thomas, N.L., Jameson, D.A. and Double, D.D., "The Effect of Lead Nitrate on the Early Hydration of Portland Cement", Cement and Concrete Research 11:143-153, 1981.

Travis, C.C. and Etnier, E.L., "A Survey of Sorption Relationships for Reactive Solutes in Soils", J. Environ. Qual., 10(1):8-17, 1981.

Treybal, Robert E., Mass Transfer Operations, McGraw-Hill Book Company, second edition, 1968.

U.S. EPA, "Test Methods for Evaluating Solid Waste", Office of Water and Waste Management, U.S. Environmental Protection Agency, Report SW-846, August, 1980.

Van der Sloot, H.A. and Wijkstra, J., "Short and Long Term Effects in the Leaching of Trace Elements from Stabilized Waste Products", presented at the Fifth International Ocean Disposal Symposium, Corvallis, Oregon, September 10-14, 1984.

Van Genuchten, M. Th., Davidson, J.M. and Wierenga, P.J., "An Evaluation of Kinetic and Equilibrium Equations for the Prediction of Pesticide Movement through Porous Media", Soil Sci. Soc. Amer. Proc., 38:(29-35), 1974.

Wagner, N.J. and Julia, R.J., "Activated Carbon Adsorption", in Activated Carbon for Wastewater Treatment, J.R. Perrich Ed., CRC Press, Inc., Boca Raton, Florida, 1981.

Westall, J., Zachary, J.L. and Morel, F., "MINEQL, A Computer Program for the Calculation of Chemical Equilibrium Composition of Aqueous Systems" Technical Note No. 18, Ralph M Parsons Laboratory, Massachusetts Institute of Technology, Cambridge, MA, 1976.

## Appendix I

## MATHEMATICAL MODEL

- Table I-1 Derivation of the diffusion equation for a porous solid.
- Table I-2 Tracer and self-diffusion coefficients of ions at infinite dilution and at 25°C.
- Table I-3 Source code of the program LEEQ.
- Table I-4 Definition of input data requirement for the program LEEQ.
- Table I-5 Source code of the program LEEEX.
- Table I-6 Definition of input data requirement for the program LEEEX.

Note: Tables I-3 to I-6 are provided as ASCII files on a 5 1/4 inch diskette that can be read in the DOS environment.

Table I-1 Derivation of the Diffusion Equation for a Porous Solid

Diffusion of uncharged species in aqueous solution can be described with Fick's laws of diffusion (Crank, 1956):

$$\text{First Law: } J = -D \frac{\delta C}{\delta z} \quad (1)$$

$$\text{Second Law: } \frac{\delta C}{\delta t} = - \frac{\delta J}{\delta z} \quad (2)$$

where,

C = concentration [mass / unit volume of solution],  
 D = diffusion coefficient [area of solution / time],  
 J = flux [mass / area of solution • time],  
 t = time [T],  
 z = distance [L].

In a porous solid, transport takes place only in the pores filled with solution. Since the "area of porous solution" is not known, the flux is normally expressed on an "area of porous solid" basis. Defining  $J_s$  as the flux in terms of mass per unit area of solid per unit time and assuming that the pore solution is evenly distributed, we establish that:

$$J_s = J \times \phi \quad (3)$$

where  $\phi$ , the connected porosity, is defined as the volume of connected pore solution per unit volume of total waste form. Another modification has to be made to Fick's Law in order to apply it to a porous solid.

Equation 1 implies that there is a direct diffusion path along the axis



z. However, in a porous solid, diffusion takes place in a tortuous path of fluid between and around the solid particles. One way of accounting for this phenomena is to correct the diffusion coefficient for tortuosity (Berner, 1980):

$$D_s = \frac{D}{T} \quad (4)$$

where:  $D_s$  = molecular coefficient of diffusion corrected for the tortuosity of the matrix [ $L^2/T$ ],

$T$  = tortuosity, defined as the ratio of the length of the actual sinuous path over a depth interval [ $]$ .

Replacing Equation 3 into the mass balance (Equation 2) and assuming that the porosity  $\phi$  is independent of position (i.e.  $\delta\phi/\delta x = 0$ ), we obtain

$$\frac{\delta C}{\delta t} = -\frac{1}{\phi} \frac{\delta J_s}{\delta z} \quad (5)$$

Combining Equations 1, 3 and 4, we can adapt Fick's Law to porous solids:

$$J_s = -\phi D_s \frac{\delta C}{\delta z} \quad (6)$$

Replacing the expression for the flux  $J_s$  from Equation 6 into Equation 5:

$$\frac{\delta C}{\delta t} = -\frac{1}{\phi} \frac{\delta(-\phi D_s \delta C / \delta z)}{\delta z} \quad (7)$$

Expanding, and stating that  $\delta D_s / \delta z = 0$  (the diffusion coefficient is independent of position along the axis) and that  $\delta p / \delta z = 0$  leads to:

$$\frac{\delta C}{\delta t} = -D_s \frac{\delta^2 C}{\delta z^2} \quad (8)$$

Table 1-2 Tracer and self-diffusion coefficients of ions at infinite dilution and at 25 °C  
(Adapted from Li and Gregory, 1974).

Cation	$D_J^0$ ( $10^{-6}$ cm <sup>2</sup> /sec)	Anion	$D_J^0$ ( $10^{-6}$ cm <sup>2</sup> /sec)
H <sup>+</sup>	93.1	OH <sup>-</sup>	52.7
Li <sup>+</sup>	10.3	F <sup>-</sup>	14.6
Na <sup>+</sup>	13.3	Cl <sup>-</sup>	20.3
K <sup>+</sup>	19.6	Br <sup>-</sup>	20.1
Rb <sup>+</sup>	20.6	I <sup>-</sup>	20.0
Cs <sup>+</sup>	20.7	IO <sub>3</sub> <sup>-</sup>	10.6
NH <sub>4</sub> <sup>+</sup>	19.8	HS <sup>-</sup>	17.3
Ag <sup>+</sup>	16.6	S <sub>2</sub> <sup>-</sup> (20°C)	6.95
Tl <sup>+</sup>	20.1	HSO <sub>4</sub> <sup>-</sup>	13.3
Cu(OH) <sup>+</sup>	8.30	SO <sub>4</sub> <sup>2-</sup>	10.7
Zn(OH) <sup>+</sup>	8.54	SeO <sub>4</sub> <sup>2-</sup>	9.46
Be <sup>2+</sup>	5.85	NO <sub>2</sub> <sup>-</sup>	19.1
Mg <sup>2+</sup>	7.05	NO <sub>3</sub> <sup>-</sup>	19.0
Ca <sup>2+</sup>	7.93	HCO <sub>3</sub> <sup>-</sup>	11.8
Sr <sup>2+</sup>	7.94	CO <sub>3</sub> <sup>2-</sup>	9.55
Ba <sup>2+</sup>	8.48	H <sub>2</sub> PO <sub>4</sub> <sup>-</sup>	8.46
Ra <sup>2+</sup>	8.89	HPO <sub>4</sub> <sup>2-</sup>	7.34
Mn <sup>2+</sup>	6.88	HP <sub>4</sub> <sup>3-</sup>	6.12
Fe <sup>2+</sup>	7.19	H <sub>2</sub> AsO <sub>4</sub> <sup>-</sup>	9.05
Co <sup>2+</sup>	6.99	H <sub>2</sub> SbO <sub>4</sub> <sup>-</sup>	8.25
Ni <sup>2+</sup>	6.79	CrO <sub>4</sub> <sup>2-</sup>	11.2
Cu <sup>2+</sup>	7.33	MoO <sub>4</sub> <sup>2-</sup>	9.91
Zn <sup>2+</sup>	7.15	WO <sub>4</sub> <sup>2-</sup>	9.23
Cd <sup>2+</sup>	7.17		
Pb <sup>2+</sup>	9.45		
UO <sub>2</sub> <sup>2+</sup>	4.26		
Se <sup>3+</sup>	5.74		
Y <sup>3+</sup>	5.50		
La <sup>3+</sup>	6.17		
Yb <sup>3+</sup>	5.82		
Cr <sup>3+</sup>	5.94		
Fe <sup>3+</sup>	6.07		
Al <sup>3+</sup>	5.59		

## Appendix II

## SIMULATION RUNS

- Table II-1 Input data for simulations used in validation of the numerical solution.
- Table II-2 Input data for simulations used for comparison with leaching experiments.
- Table II-3 Sample input data file: S27.
- Table II-4 Sample output data file: S27.
- Table II-5 Sample input data file: S28.
- Table II-6 Sample output data file: S28.

Note: Table II-3 to II-6 are provided as ASCII files on a 5<sup>1/4</sup> inch diskette that can be read in the DOS environment.

Table II-1 Input data for simulations used in validation of the numerical solution.

Run Program	Simulation	Specimen Characteristics										Leachant	Chemical System				Solubility Source	Simulation Purpose	
		TF (d)	DX (mm)	RATIO (l)	SW (g)	SV (l)	AG (cm2)	MC (l)	TDR	CHAR1/2 (l)	VE (l)	Q (l/d)	Id	UGG (ug/g)	CAPO (M)	CL (M)	B (cm2/g)		
1	LEEX*	1.0	500	1.0	607	0.340	69	0.23	1	1.0/1.0	2	2.05	H+	N/A	1.00E-03	1.00E-03	N/A	non-reactive	Validate the numerical solution of Equation 4.15 (Section 4.5.2).
2	LEEX	1.0	500	1.0	607	0.340	69	0.23	1	1.0/1.0	2	100	H+	2.99E+02	0.00E+00	0.00E+00	1.00E-05	non-reactive	Validate the numerical solution of Equation 4.15 (Section 4.5.3).
3	LEEX	1.0	500	1.0	607	0.340	69	0.23	1	1.0/1.0	2	100	H+	0.00E+00	1.00E+00	1.00E+00	1.00E-05	non-reactive	Validate the numerical solution of Equation 4.18 (Section 4.5.3).
4	LEEX*	1.0	100	60.0	607	0.340	69	0.23	1	1.0/1.0	2	100	H+	2.99E+02	0.00E+00	0.00E+00	1.00E-05		
5	LEEX*	1.0	100	6.0	607	0.340	69	0.23	1	1.0/1.0	2	100	H+	2.99E+02	0.00E+00	0.00E+00	1.00E-05		
6	LEEX*	1.0	100	0.6	607	0.340	69	0.23	1	1.0/1.0	2	100	H+	2.99E+02	0.00E+00	0.00E+00	1.00E-05		
7	LEEX*	1.0	100	50.0	607	0.340	69	0.23	1	1.0/1.0	2	100	H+	2.99E+02	0.00E+00	0.00E+00	1.00E-05		
8	LEEX*	1.0	100	120.0	607	0.340	69	0.23	1	1.0/1.0	2	100	H+	2.99E+02	0.00E+00	0.00E+00	1.00E-05	linear	Validate the iteration technique for handling chemical reactions
9	LEEX*	1.0	400	1.0	607	0.340	69	0.23	1	1.0/1.0	2	100	H+	2.99E+02	0.00E+00	0.00E+00	1.00E-05	adsorption	(Section 5.4).
10	LEEX*	1.0	400	3.0	607	0.340	69	0.23	1	1.0/1.0	2	100	H+	2.99E+02	0.00E+00	0.00E+00	1.00E-05	isotherm	
11	LEEX*	1.0	400	7.5	607	0.340	69	0.23	1	1.0/1.0	2	100	H+	2.99E+02	0.00E+00	0.00E+00	1.00E-05	Eq-9	
12	LEEX*	1.0	400	15.0	607	0.340	69	0.23	1	1.0/1.0	2	100	H+	2.99E+02	0.00E+00	0.00E+00	1.00E-05		
13	LEEX*	1.0	400	22.5	607	0.340	69	0.23	1	1.0/1.0	2	100	H+	2.99E+02	0.00E+00	0.00E+00	1.00E-05		
14	LEEX*	1.0	400	30.0	607	0.340	69	0.23	1	1.0/1.0	2	100	H+	2.99E+02	0.00E+00	0.00E+00	1.00E-05		
15	LEEX*	1.0	400	45.0	607	0.340	69	0.23	1	1.0/1.0	2	100	H+	2.99E+02	0.00E+00	0.00E+00	1.00E-05		
16	LEEX	1.0	400	0.4	607	0.340	69	0.23	1	1.0/1.0	2	100	H+	2.99E+02	0.00E+00	0.00E+00	1.00E-06	non-reactive	L.A.S. with corrected coefficient
17	LEEX*	1.0	100	120.0	607	0.340	69	0.23	1	1.0/1.0	2	100	H+	2.99E+02	0.00E+00	0.00E+00	1.00E-05		
18	LEEX*	1.0	100	30.0	607	0.340	69	0.23	1	1.0/1.0	2	100	H+	2.99E+02	0.00E+00	0.00E+00	1.00E-05		
19	LEEX*	1.0	100	6.0	607	0.340	69	0.23	1	1.0/1.0	2	100	H+	2.99E+02	0.00E+00	0.00E+00	1.00E-05	linear	Validate the iteration technique for handling chemical reactions
20	LEEX*	1.0	100	1.0	607	0.340	69	0.23	1	1.0/1.0	2	100	H+	2.99E+02	0.00E+00	0.00E+00	1.00E-05	adsorption	(Section 5.4).
21	LEEX*	1.0	100	0.5	607	0.340	69	0.23	1	1.0/1.0	2	100	H+	2.99E+02	0.00E+00	0.00E+00	1.00E-05	isotherm	
22	LEEX*	1.0	25	1920	607	0.340	69	0.23	1	1.0/1.0	2	100	H+	2.99E+02	0.00E+00	0.00E+00	1.00E-05	Eq-999	
23	LEEX*	1.0	25	400.0	607	0.340	69	0.23	1	1.0/1.0	2	100	H+	2.99E+02	0.00E+00	0.00E+00	1.00E-05		
24	LEEX*	1.0	25	96.0	607	0.340	69	0.23	1	1.0/1.0	2	100	H+	2.99E+02	0.00E+00	0.00E+00	1.00E-05		
25	LEEX*	1.0	25	9.6	607	0.340	69	0.23	1	1.0/1.0	2	100	H+	2.99E+02	0.00E+00	0.00E+00	1.00E-05		
26	LEEX*	1.0	25	1.0	607	0.340	69	0.23	1	1.0/1.0	2	100	H+	2.99E+02	0.00E+00	0.00E+00	1.00E-05		
27	LEEX	1.0	200	1.0	247	0.130	295	0.24	1.5	1.0/1.0	2	0		Ca= 3.56E+02	0.00E+00	N/A	7.17E-06		Dissolution of cadmium hydroxide.
														N= 0.00E+00	1.00E-03	N/A	9.31E-05		Compare programs LEEX and LEEQ.
														Ca(OH) 0.00E+00	0.00E+00	N/A	7.17E-06	BIHEQ	Stoichiometric amount of Cd and OH added. See Section 5.5.
														Ca(OH)2 0.00E+00	0.00E+00	N/A	7.17E-06		
														OH 1.00E+02	0.00E+00	N/A	5.27E-05		Paired to Simulation 27
														Ca(T) 3.56E+02	0.00E+00	N/A	5.27E-05		
														N= 0.00E+00	1.00E-03	N/A	9.31E-05		
31	LEEX	1.0	200	2.0	247	0.130	295	0.24	1.5	1.0/1.0	2	0							
32	LEEX	1.0	200	4.0	247	0.130	295	0.24	1.5	1.0/1.0	2	0							
33	LEEX	1.0	200	8.0	247	0.130	295	0.24	1.5	1.0/1.0	2	0							
34	LEEX	1.0	200	16.0	247	0.130	295	0.24	1.5	1.0/1.0	2	0							
37	LEEX	1.0	200	32.0	247	0.130	295	0.24	1.5	1.0/1.0	2	0							
38	LEEX	1.0	200	64.0	247	0.130	295	0.24	1.5	1.0/1.0	2	0							
39	LEEX	1.0	200	128.0	247	0.130	295	0.24	1.5	1.0/1.0	2	0							
40	LEEX	1.0	200	256.0	247	0.130	295	0.24	1.5	1.0/1.0	2	0							

Notes: - Variables are defined in Tables I-4 and I-6.  
 - A \* besides the program name refers to specific changes made to the program for that simulation, as listed below.

Table II-1 Continued

Modifications to the Programs

<u>Simulation</u>	<u>Description of the Change</u>
S1	<p>Commented out "100 CALL CRANK" from the MAIN  added below "100 RL(1) = -1.0E-4"  Commented out "CALL LEACH" from the MAIN  Commented out "CALL SMEQLB" from the MAIN</p>
S4 to S15	<p>Subroutine SMEQ  replace "210 CTOT(I,J) = CPOR(I,J)*CONV  by  "CTOT(I,J)=CTOT(I,J)+CINV*CPOR(I,J)-CPOR0(I,J)"  "210 CPOR(I,J)=CTOT(I,J)/CONV/(1+KD)"  where KD=9.</p>
S17 to S26	<p>Subroutine SMEQ  replace "210 CTOT(I,J) = CPOR(I,J)*CONV  by  "CTOT(I,J)=CTOT(I,J)+CINV*CPOR(I,J)-CPOR0(I,J)"  "210 CPOR(I,J)=CTOT(I,J)/CONV/(1+KD)"  where KD=999</p>

Table 11-2 Input data for simulations used for comparison with leaching experiments.

Run Program	Simulation	Specimen Characteristics										Leachant	Chemical System					Solubility Data Source		Simulation Purpose
		TI	IX	RATIO	SM	SV	AG	NC	TORT	CHAR1/2	VR	0	Id	WCC	CAQ0	CL	0			
		(t)	(m)		(g)	(t)	(cm2)	(t)					(t)	(mg/g-mb)	(M)	(M)	(cm2/s)			
41	LEEX	3.0	500	1.0	597	0.340	69	0.24	1.00	1.0/1.0	2.0	0.0	Li	170	0.00E+00	0.00E+00	1.03E-05	N/A		Compare to Experiment B5i & B5ii
42	LEEX	3.0	500	1.0	597	0.340	69	0.24	1.25	1.0/1.0	2.0	0.0	Li	170	0.00E+00	0.00E+00	1.03E-05	N/A		Compare to Experiment B5i & B5ii
43	LEEX	3.0	500	1.0	597	0.340	69	0.24	1.25	1.0/1.0	2.0	2.0	Li	170	0.00E+00	0.00E+00	1.03E-05	N/A		Compare to Experiment B6i
44	LEEX*	7.0	500	1.0	551	0.340	69	0.31	1.00	1.0/1.0	1.9	1.3	Li	23	0.00E+00	0.00E+00	1.03E-05	N/A		Compare to Experiment C6i
45	LEEX*	7.0	500	1.0	551	0.340	69	0.31	1.25	1.0/1.0	1.9	1.3	Li	23	0.00E+00	0.00E+00	1.03E-05	N/A		Compare to Experiment C6i
46	LEEX*	7.0	500	1.0	551	0.340	69	0.26	1.25	1.0/1.0	1.9	1.3	Li	23	0.00E+00	0.00E+00	1.03E-05	N/A		Compare to Experiment C6i
47	LEEX*	7.0	500	1.0	551	0.340	69	0.31	1.00	1.0/1.0	1.9	1.3	Li	23	0.00E+00	0.00E+00	1.03E-05	N/A		Compare to Experiment C6i
48	LEEX*	7.0	500	1.0	551	0.340	69	0.26	1.25	1.0/1.0	1.9	1.3	Li	23	0.00E+00	0.00E+00	1.03E-05	N/A		Compare to Experiment C6ii
49	LEEX	2.0	400	1.0	247	0.130	295	0.24	1.25	1.0/1.0	2.0	3.3	Ca	275	0.00E+00	0.00E+00	7.17E-06	N/A		Compare to Experiment A6
													Matrix	N/A	1.00E-03	1.00E-03	9.30E-05	N/A		Compare to Experiment A6
50	LEEX*	2.0	400	1.0	247	0.130	295	0.24	1.25	1.0/1.0	2.0	3.3	Ca	275	0.00E+00	0.00E+00	5.27E-05	N/A		Compare to Experiment A6
													Matrix	N/A	1.00E-03	1.00E-03	9.30E-05	N/A		Compare to Experiment A6
51	LEEX*	2.0	400	1.0	247	0.130	295	0.24	1.25	1.0/1.0	2.0	3.3	Ca	275	0.00E+00	0.00E+00	7.17E-06	N/A		Compare to Experiment A6
													Matrix	N/A	1.00E-03	1.00E-03	9.30E-05	N/A		Compare to Experiment A6
52	LEEX	2.0	400	1.0	247	0.130	295	0.24	1.25	1.0/1.0	2.0	3.3	Ca	275	0.00E+00	0.00E+00	7.17E-06	Exp. A4ii		Compare to Experiment A6
53	LEEX	3.0	100	1.0	597	0.340	69	0.24	1.25	1.0/1.0	2.0	0.0	Ca	275	0.00E+00	0.00E+00	7.17E-06	Exp. B4ii		Compare to Experiment B5i & B5ii
54	LEEX	3.0	100	1.0	597	0.340	69	0.24	1.25	1.0/1.0	2.0	2.0	Ca	275	0.00E+00	0.00E+00	7.17E-06	Exp. B4ii		Compare to Experiment B6i & B6ii
55	LEEX	7.0	100	5.0	550.0	0.340	69	0.26	1.25	1.0/1.0	1.9	1.3	Ca	393	0.00E+00	0.00E+00	9.05E-06	Exp. C4ii		Compare to Experiment C6i & C6ii
													Cr	373	0.00E+00	0.00E+00	7.17E-06			
													Cr	215	0.00E+00	0.00E+00	5.94E-06			
													Pb	607	0.00E+00	0.00E+00	9.45E-06			
56	LEEX	27.0	200	5.0	83	0.052	16	0.26	1.25	1.0/1.0	7.1	0.0	Ca	393	0.00E+00	0.00E+00	9.05E-06	Exp. C4ii		Compare to Experiment C5i & C5ii
													Cr	373	0.00E+00	0.00E+00	7.17E-06			
													Cr	215	0.00E+00	0.00E+00	5.94E-06			
													Pb	607	0.00E+00	0.00E+00	9.45E-06			
57	LEEX	1.3	500	1.0	221	0.131	155	0.24	1.00	1.0/1.0	2.3	1.5	Li	220	0.00E+00	0.00E+00	1.03E-05	N/A		Compare to Experiment B6i
58	LEEX	1.3	500	1.0	221	0.131	155	0.19	1.25	1.0/1.0	2.3	1.5	Li	220	0.00E+00	0.00E+00	1.03E-05	N/A		Compare to Experiment B6ii

Notes: - Variables are defined in Tables I-4 and I-6.  
 - A \* besides the program name refers to specific changes made to the program for that simulation, as listed below.

Table 11-2, Continued

Modifications to the Programs

<u>Simulation</u>	<u>Description of the Change</u>
S42	LEEQ was interfaced with UWHAUS with the diffusion coefficient correction factor T being used as the optimization parameter
S44 to S48	The flow rates used in the simulations were variable to reflect the actual flow rates measured during the experiments. Added subroutine FLOW to read flow rate as a function of time.
S51 to S52	Initialize the first 5 slices (400um each) to 0.0 to account for the thickness of the soxhlet thimble. In INIT, after solving initial equilibrium: "DO 998 J=1,NJ" "DO 998 I=1,5" "998 CTO(I,J)=CPOR(I,J)/CONV In EQSM, MINEQL is not called for these slices.



## Appendix III

## SOLIDIFICATION ADDITIVES

Table III-1 Particle size distribution of solidification additives.

Table III-2 Moisture-density relationships of porous materials.

Table III-3 Titration of a cement paste.

Figure III-1 Particle size distribution of solidification additives.

Figure III-2 Titration of a portland cement paste after 28 days of curing.

Table III-1 Particle size distribution of solidification additives.

Particle Size [microns]	Relative Number of Particles of Stated Size [percent]		
	MIN-U-SIL	Fly Ash	Bentonite
2.00	3.87	NA	7.06
2.52	3.47	NA	7.56
3.17	4.46	NA	9.07
3.00	5.16	7.15	9.68
5.04	6.55	9.02	9.78
6.35	7.84	11.50	9.48
8.00	10.32	13.37	9.58
10.08	13.49	14.30	10.08
12.70	14.78	15.70	9.68
16.00	15.28	11.83	8.67
20.20	8.63	9.19	6.45
25.40	4.37	5.29	2.92
32.00	0.99	2.64	0.00
40.30	0.79	0.00	0.00

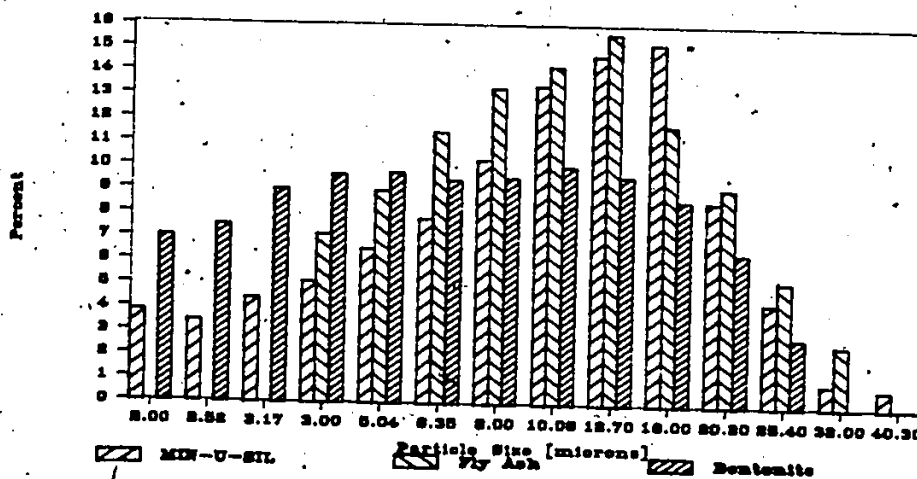


Figure III-1 Particle size distribution of solidification additives.

Table III-2 Moisture-density relationships of porous materials.

A number of relationships can be derived for the properties of porous solids based on the measurement of their bulk density, water content and solid specific gravity (Peck et al., 1974):

Water content

$$sw = \frac{w}{(1-w)} \quad (1)$$

Dry bulk density

$$\gamma_d = \gamma_b (1 - w) \quad (2)$$

Void Ratio

$$e = \frac{G_s \gamma_w}{\gamma_b (1-w)} - 1 \quad (3)$$

Porosity

$$n = 1 - \frac{\gamma_b (1-w)}{G_s \gamma_w} \quad (4)$$

Degree of Saturation

$$S_r = \frac{w G_s}{(1-w) e} \quad (5)$$

Where:

- e : void ratio (volume of voids / volume of solids)
- G<sub>s</sub> : specific gravity of the solids
- n : porosity (volume of voids / total volume)
- sw : water content (w/w, dry weight basis)
- w : water content (w/w, wet weight basis)
- γ<sub>b</sub> : bulk density [g/cm<sup>3</sup>]
- γ<sub>d</sub> : dry bulk density [g/cm<sup>3</sup>]
- γ<sub>w</sub> : water density [g/cm<sup>3</sup>]
- S<sub>r</sub> : degree of saturation

Table III-3 Titration of Portland Cement Paste

Cumulative acid added [meq/g] dry cement	pH	
	after 24 hrs	after 48 hrs
0.00	10.36	10.41
1.69	9.99	10.05
3.38	9.73	9.80
5.07	9.55	9.63
6.77	9.34	9.44
8.46	9.24	9.35
10.15	9.20	9.26
11.84	9.09	9.17
13.53	8.98	9.08
15.22	8.86	8.97
16.91	8.71	8.83
18.60	8.57	8.68
20.30	8.25	8.36
21.99	6.81	7.22
23.68	3.81	3.92
25.37	3.38	3.41
27.06	3.13	3.14
28.75	2.77	2.79
30.44	2.55	2.54

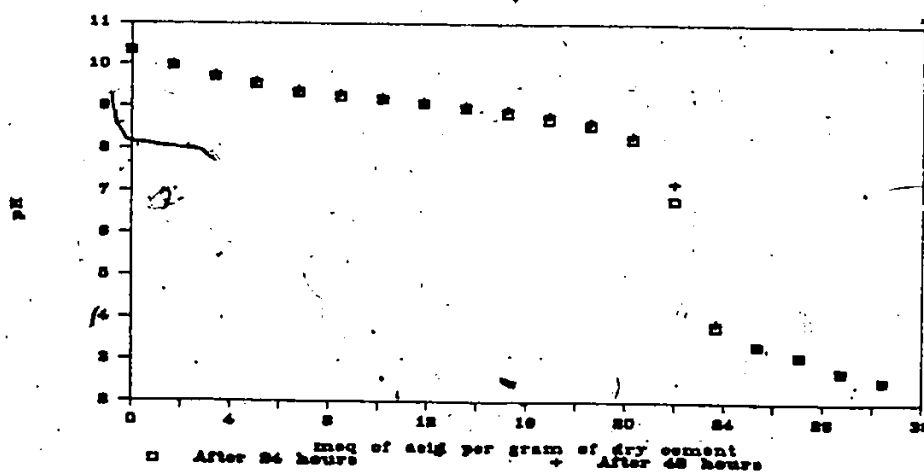


Figure III-2 Titration of a portland cement paste after 28 days of curing.

## Appendix IV

## EXPERIMENTAL PROGRAMME

Table IV-1 Chronology of the experimental programme.

Table IV-1 Chronology of the Experimental Programme

EXPERIMENT	Started	Completed	Duration [hours]	Lab. Ref. #
Batch A: powdered silica				
A Preparation of the batch	18.06.84			B14
A31 Titration and Solubility	26.06.84	27.06.84	24	ML202
A311	03.07.84	04.07.84	24	ML213
A6 Dynamic Leaching Test	20.06.84	22.06.84	48	PC337
Batch B: powdered silica-cement				
B Preparation of the batch	13.06.84			B13
B31 Titration and solubility	16.07.84	17.07.84	24	ML222
B311	24.07.84	25.07.84	24	ML226
B51 Static Leaching Test	13.07.84	16.07.84	72	PC340
B511	20.07.84	23.07.84	68	PC342
B61 Dynamic leaching test	18.07.84	20.07.84	48	PC341
B611 (done with B11)	10.04.84	12.04.84	48	DC331
Batch C: fly ash-cement				
C Preparation of the batch	14.11.84			B16
C31 Titration and solubility	03.12.84	04.12.84	24	PC358
C311	03.01.85	04.01.85	24	PC362
C4 Solubility (high L/S)	09.10.85	10.01.85	24	PC364
C51 Static Leaching Test	13.12.84	10.01.85	672	PC360
C511	13.12.84	10.01.85	672	PC361
C61 Dynamic leaching test	04.12.84	11.12.84	172	PC357
C611	08.01.85	20.01.85	296	PC363
Batch D: fly ash-cement				
D Preparation of the batch	04.07.84			B15
D31 Titration and solubility	01.08.84	02.08.84	24	ML236
D311	15.08.84	16.08.84	24	ML256
D4 Solubility (high L/S)	12.11.84	13.11.84	24	PC354
D61 Dynamic Leaching Test	03.08.84	16.08.84	310	PC344
D611	17.08.84	30.08.84	312	PC345
Batch E: fly ash-cement				
E Preparation of the batch	08.11.82			B159
E1 Porosity Analysis	08.02.83			
E2 Equilibrium leaching test	10.08.83	07.09.83	672	
E71 Dynamic leaching test	06.12.82	22.10.84	2 years	Spec38
E711	06.12.82	22.10.84	2 years	Spec39
Batch F: Fly ash-lime				
F Preparation of the batch	08.11.82			B158
F1 Porosity analysis	08.02.83			
F2 Equilibrium leaching test	10.08.83	07.09.83	672	
F71 Dynamic leaching test	06.12.82	22.10.84	2 years	Spec36
F711	06.12.82	22.10.84	2 years	Spec37
Batch G: clay-cement				
G Preparation of the batch	09.11.82			B161
G1 Porosity analysis	08.02.83			
G2 Equilibrium leaching test	10.08.83	07.09.83	672	
G71 Dynamic leaching test	07.12.82	22.10.84	2 years	Spec42
G711	07.12.82	22.10.84	2 years	Spec43
Batch H: soluble silicates-cement				
H Preparation of the batch	09.11.82			B160
H1 Porosity analysis	08.02.83			
H2 Equilibrium leaching test	10.08.83	07.09.83	672	
H71 Dynamic leaching test	07.12.82	22.10.84	2 years	Spec40
H711	07.12.82	22.10.84	2 years	Spec41

## Appendix V

## RESULT OF MERCURY INTRUSION

- Table V-1 Porosity analysis of waste forms by mercury intrusion.  
Table V-2 Correction of the mercury intrusion data.  
Table V-3 Correction of mercury intrusion data to obtain the total porosity.

- Figure V-1 Hysteresis effect for the fly ash-cement system.  
Figure V-2 Hysteresis effect for the fly ash-lime system.  
Figure V-3 Hysteresis effect for the clay-cement system.  
Figure V-4 Hysteresis effect for the soluble silicates-cement system.

Table V-1 Porosity Analysis of Waste forms by Mercury Intrusion.

Pressure [psia]	Pore Diameter [um]	Intrusion volume measured [cm <sup>3</sup> /g]				
		EI-1	EI-2	F1	G1	H1
0.6	324.830	0.0015	0	0	0	0.0024
2.1	86.827	0.0394	0.0156	0.0116	0.0167	0.1484
4.1	44.112	0.0411	0.0172	0.0129	0.0187	0.2262
6.0	30.143	0.0419	0.0188	0.0137	0.02	0.258
8.0	22.608	0.0424	0.0225	0.0149	0.0209	0.2756
10.0	18.086	0.0431	0.0238	0.0156	0.0214	0.2874
12.0	15.072	0.0441	0.0245	0.0162	0.0222	0.2965
15.0	12.057	0.0448	0.0254	0.017	0.0229	0.3062
16.9	10.702	0.0453	0.0259	0.0176	0.0234	0.3117
19.9	9.088	0.0463	0.0271	0.0183	0.0239	0.3177
28.5	6.346	0.0463	0.0271	0.0183	0.0239	0.3206
38.9	4.649	0.0463	0.0271	0.0183	0.0239	0.3291
49.4	3.661	0.0463	0.0271	0.0183	0.0239	0.3348
73.4	2.464	0.0463	0.0277	0.0193	0.0246	0.3442
99.5	1.818	0.0485	0.0302	0.0203	0.0276	0.3506
149.3	1.211	0.0656	0.0413	0.0229	0.0495	0.3585
196.2	0.922	0.0816	0.0468	0.0252	0.0774	0.3637
296.3	0.610	0.1048	0.0652	0.0754	0.2016	0.3911
398.8	0.454	0.1061	0.0662	0.0771	0.2036	0.3915
499.4	0.362	0.1076	0.0676	0.0793	0.2066	0.3918
745.5	0.243	0.1115	0.0702	0.0839	0.2134	0.3932
994.6	0.182	0.1143	0.0729	0.0886	0.2187	0.3942
1253.4	0.144	0.1168	0.075	0.093	0.2237	0.395
1498.5	0.121	0.1194	0.0776	0.0975	0.2285	0.396
1749.5	0.103	0.1219	0.08	0.1023	0.233	0.3967
1996.8	0.091	0.1245	0.0826	0.1076	0.2367	0.3974
2486.9	0.073	0.129	0.087	0.1195	0.2447	0.3984
2882.5	0.047	0.1312	0.0898	0.1247	0.2472	0.399
3996.6	0.045	0.1327	0.0916	0.1282	0.2487	0.3991
5024.7	0.036	0.1442	0.1057	0.1563	0.2811	0.3998
7483.1	0.024	0.1774	0.1416	0.2048	0.292	0.4007
9986.4	0.018	0.2011	0.1653	0.23	0.2961	0.4007
12474.8	0.014	0.2187	0.1833	0.2477	0.3075	0.4009
14933.5	0.012	0.2315	0.1878	0.2602	0.3179	0.4012
17481.6	0.010	0.2426	0.2099	0.2706	0.3259	0.4022
19940.3	0.009	0.2518	0.2203	0.2785	0.3315	0.4025
24947.2	0.007	0.2666	0.2361	0.2839	0.3363	0.4032
29924.5	0.006	0.2772	0.2474	0.2852	0.3377	0.4038
34991.0	0.005	0.2856	0.2561	0.2856	0.338	0.4038
39953.3	0.005	0.2915	0.262	0.2858	0.338	0.4038
44945.4	0.004	0.2999	0.2677	0.288	0.3382	0.4038
49907.9	0.004	0.3016	0.2723	0.2894	0.339	0.4038
54840.3	0.003	0.3055	0.2764	0.2868	0.3392	0.4038
58802.9	0.003	0.3062	0.2789	0.287	0.3394	0.4038
54856.1	0.003	0.3092	0.2789	0.287	0.3394	0.4038
49803.1	0.004	0.3092	0.2789	0.287	0.3394	0.4038
45064.4	0.004	0.3092	0.2789	0.287	0.3394	0.4038
40116.9	0.005	0.3092	0.2789	0.287	0.3394	0.4038
35035.3	0.005	0.3092	0.2789	0.287	0.3394	0.4038
30013.3	0.006	0.3092	0.2789	0.287	0.3392	0.4026
25036.1	0.007	0.3092	0.2789	0.2864	0.3372	0.4017
20073.7	0.009	0.3087	0.2782	0.286	0.3365	0.4004
15051.8	0.012	0.3027	0.2725	0.2851	0.3354	0.3976
12533.4	0.014	0.2982	0.269	0.2842	0.3344	0.3857
10029.9	0.018	0.2917	0.2643	0.2833	0.3338	0.3923
7511.6	0.024	0.2842	0.2571	0.2833	0.3338	0.3879
4993.3	0.036	0.2693	0.2427	0.2833	0.333	0.3829
4009.9	0.045	0.2578	0.2305	0.283	0.3312	0.3785
2481.4	0.073	0.2526	0.225	0.2617	0.3294	0.3763



Table V-1 Continued

Pressure [psia]	Pore Diameter [ $\mu$ m]	Intrusion volume measured [cm <sup>3</sup> /g]				
		EI-1	EI-2	F1	G1	H1
2001.9	0.090	0.2446	0.2166	0.2796	0.3266	0.3741
977.0	0.185	0.2256	0.195	0.267	0.3169	0.3712
749.0	0.241	0.2201	0.1878	0.262	0.3139	0.3699
494.2	0.366	0.213	0.1815	0.258	0.3105	0.3688
393.3	0.460	0.2103	0.1784	0.2529	0.3105	0.3678
295.9	0.611	0.2075	0.1754	0.2497	0.3089	0.3674
198.3	0.912	0.2045	0.1719	0.2458	0.3066	0.3665
89.9	2.012	0.2014	0.1693	0.2423	0.3051	0.3661
61.6	2.936	0.1999	0.1679	0.2405	0.3043	0.3657
48.9	3.699	0.1994	0.1672	0.2394	0.3036	0.3654
34.3	5.273	0.1969	0.1665	0.2386	0.3033	0.3651
19.6	9.228	0.1982	0.1661	0.2377	0.3028	0.3648
5.0	36.172	0.1979	0.1661	0.2367	0.3023	0.3648
8.9	20.321	0.1979	0.1849	0.2367	0.3023	0.3648

Sample ID	Sample Description	Dry density [g/cm <sup>3</sup> ]	
		Bulk	Skeletal
EI-1	fly ash - cement (rep 1)	1.61	3.19
EI-2	fly ash - cement (rep 2)	1.67	3.13
F1	fly ash - lime	1.38	2.3
G1	bentonite - cement	1.29	2.32
H1	soluble silicates-cement	0.96	1.57

Table V-2 Correction of the Mercury Intrusion Data.

For reasons discussed in Section 7.1.3, the total amount of mercury intruded is less than the total matrix porosity. A correction volume can be obtained by assuming that the bulk density (obtained by weighing a sample molded in a 2 inch cube) and the water content (obtained by drying to a constant weight) listed in Table 7.1 are the true values. Consider columns 3 and 4 of Table V-3. The dry bulk density of column 3 was obtained from the bulk density and water content of Table 7.1, using Equation 2 of Table III-2. The dry bulk density of column 4, obtained from the mercury intrusion data (table V-1) is significantly lower. The correction volume of column 5 was calculated as follows:

$$V_c = \frac{1}{\gamma_d(MD)} - \frac{1}{\gamma_d(MI)} \quad (1)$$

where  $V_c$  = correction volume [ $\text{cm}^3/\text{g}$ ]  
 $\gamma_d(MD)$  = dry bulk density from moisture-density data [ $\text{g}/\text{cm}^3$ ]  
 $\gamma_d(MI)$  = dry bulk density from mercury intrusion data [ $\text{g}/\text{cm}^3$ ]

The total porosity, in the last column of Table V-3 was thus obtained by adding this correction volume to the volume of mercury intruded:

$$P = 100 (V_I + V_c) \times \gamma_d(MD) \quad (2)$$

where  $P$  = porosity [%]  
 $V_I$  = volume of mercury intruded [ $\text{cm}^3/\text{g}$ ]

The total porosity figures estimated from mercury intrusion compared

well to those obtained for moisture-density relationships for the fly ash based systems (within 7%) while they are significantly different for the bentonite and soluble silicate-based system. As explained above, the porosities derived from mercury intrusion are considered more precise. The specific gravity of solids in batches G and H was therefore back calculated using Equation 4 of Table III-2 and are presented in Table 7.1.

Table V-3 Correction of Mercury Intrusion Data to Obtain the Total Porosity.

Batch ID	Solidification System	Dry Bulk Density [g/cm <sup>3</sup> ]		Correction Volume [cm <sup>3</sup> /g]	Mercury Intruded [cm <sup>3</sup> /g]	Total Porosity [%]
		from mercury intrusion data (Table V-1)	from moisture-density data (Table 7.1)			
E rep 1	Fly Ash-cement	1.61	1.47	0.057	0.309	54.0
E rep 2	Fly Ash-cement	1.67	1.47	0.080	0.279	52.8
F	Fly Ash-lime	1.38	1.34	0.023	0.287	41.4
G	Clay-cement	1.30	1.07	0.162	0.339	53.9
H	Sol. Sil.-cement	0.96	0.60	0.618	0.404	61.6

Figure V-1 Hysteresis Effect (E1-1)

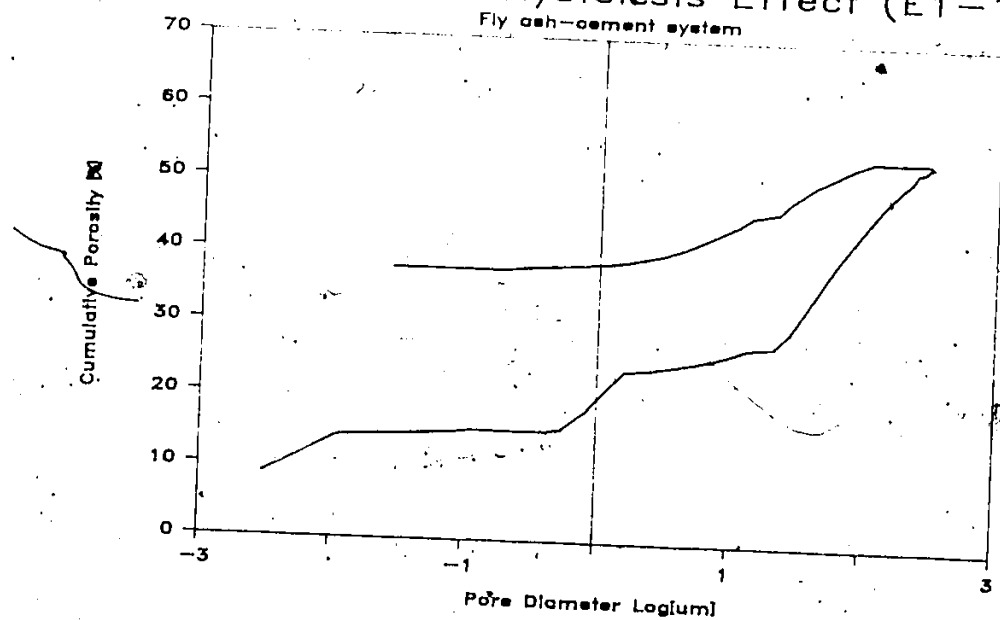


Figure V-2 Hysteresis Effect (F1)

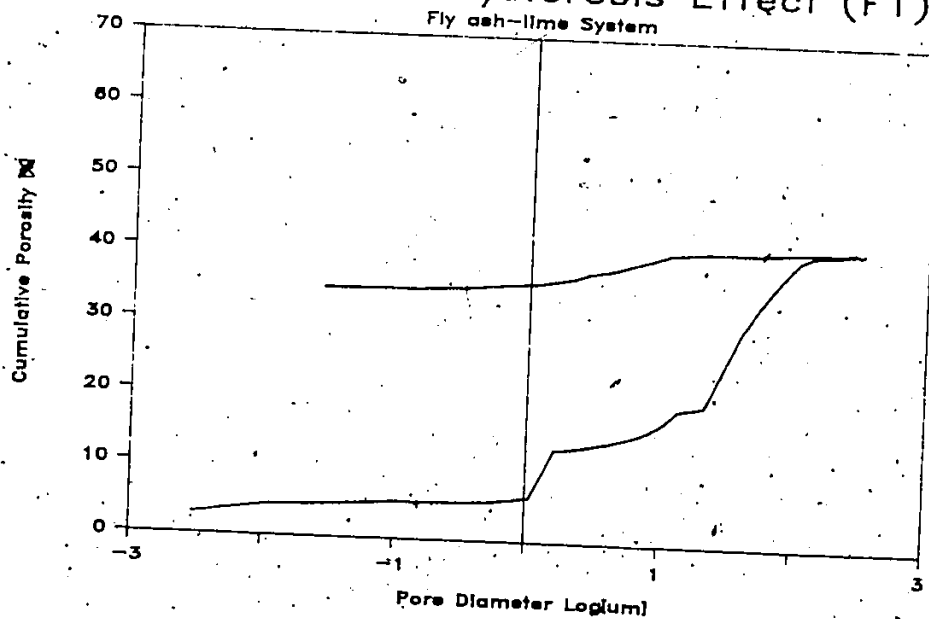


Figure V-3 Hysteresis Effect (G1)

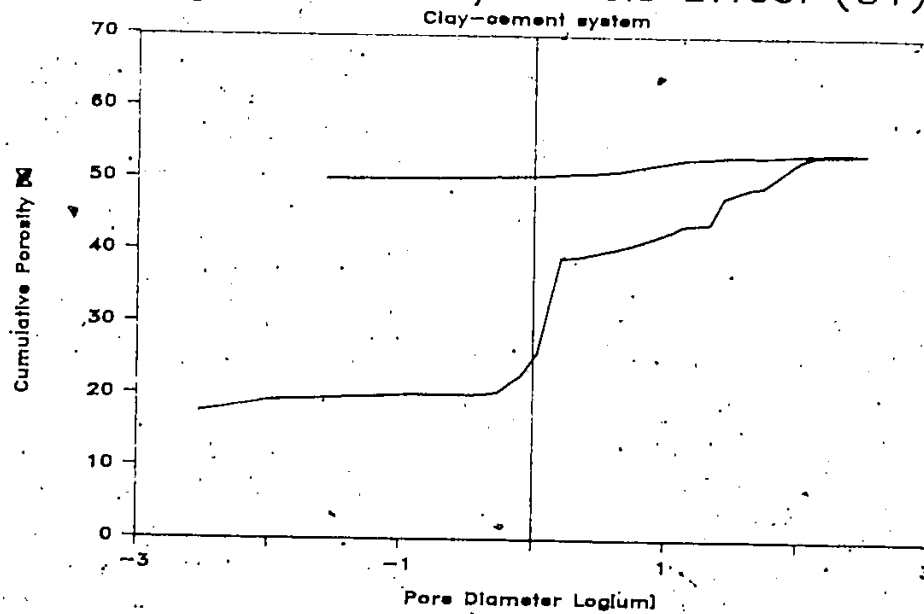
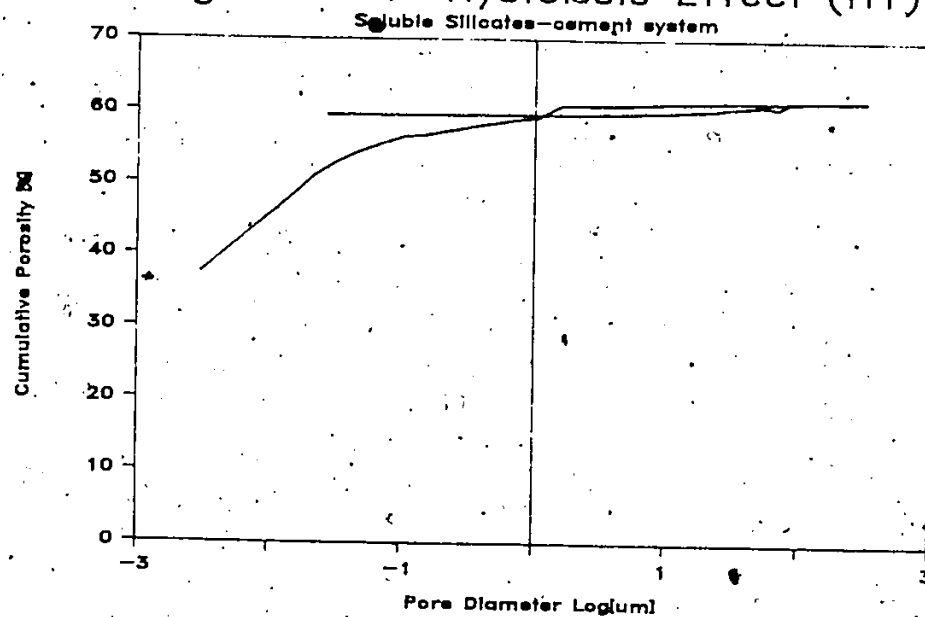


Figure V-4 Hysteresis Effect (H1)



## Appendix VI

## RESULTS OF TOTAL METAL ANALYSIS

Table VI-1. Total cadmium concentration.

Table VI-2. Total chromium concentration.

Table VI-3. Total lead concentration.

Table VI-1 Total cadmium concentration.

	Fly ash-cement		Fly ash-lime		Clay-cement		Sol. sil.-cement	
	rep 1	rep 2	rep 1	rep 2	rep 1	rep 2	rep 1	rep 2
Water Content [W/W;w.w.b]	0.143	0.093	0.179	0.156	0.303	0.319	0.518	0.440
Concentration [ug/g; wet weight basis]								
Calculated (Table 6.1)	3580	3580	3740	3740	5290	5290	5640	5640
Total Extraction	3437	3771	3448	3899	4537	4433	4822	4822
Sequential Extraction								
total	3226	3643	2904	3194	4535	4081	5523	4528
fraction A	444	94	461	162	166	141	93	66
fraction B	2413	1517	1226	1249	323	1558	81	121
fraction C	357	1960	1182	1722	3820	2230	5113	4158
fraction D	-12	67	34	61	215	142	227	178
fraction E	0	5	0	0	10	10	10	6
Concentration [ug/g; dry weight basis]								
Calculated (Table 6.1)	4177	3947	4555	4431	7590	7768	11701	10071
Total Extraction	4011	4158	4200	4620	6510	6510	10004	8610
Sequential Extraction								
total	3764	4016	3537	3784	6506	5992	11458	8086
fraction A	518	104	562	192	238	207	192	118
fraction B	2816	1672	1493	1480	464	2288	168	216
fraction C	416	2161	1440	2040	5481	3274	10607	7425
fraction D	14	74	42	72	308	208	471	317
fraction E	0	5	0	0	15	15	20	10

Table VI-2 Total chromium concentration.

	Fly ash-cement		Fly ash-lime		Clay-cement		Sol. sil.-cement	
	rep 1	rep 2	rep 1	rep 2	rep 1	rep 2	rep 1	rep 2
Water Content [W/W;w.w.b]	0.143	0.093	0.179	0.156	0.303	0.319	0.518	0.440
Concentration [ug/g; wet weight basis]								
Calculated (Table 6.1)	1460	1460	1520	1520	2110	2110	2250	2250
Total Extraction	1226	1197	1264	1207	1533	1423	1781	1848
Sequential Extraction								
total	1423	1601	1289	1523	1878	1773	2282	1859
fraction A	6	0	0	0	0	0	0	0
fraction B	322	239	0	0	0	0	0	0
fraction C	926	1156	1127	1247	1581	1510	2058	1693
fraction D	66	92	83	98	245	219	160	118
fraction E	103	113	79	177	52	44	65	48
Concentration [ug/g; dry weight basis]								
Calculated (Table 6.1)	1704	1610	1851	1801	3027	3098	4668	4018
Total Extraction	1430	1320	1540	1430	2200	2090	3696	3300
Sequential Extraction								
total	1660	1765	1570	1804	2695	2604	4735	3320
fraction A	7	0	0	0	0	0	0	0
fraction B	376	264	0	0	0	0	0	0
fraction C	1080	1275	1373	1478	2268	2218	4269	3024
fraction D	77	101	101	116	352	321	331	211
fraction E	120	125	96	210	75	65	135	85



Table VI-3 Total lead concentration

	Fly ash-cement		Fly ash-lime		Clay-cement		Sol. sil.-cement	
	rep 1	rep 2	rep 1	rep 2	rep 1	rep 2	rep 1	rep 2
Water Content [W/W;w.w.b]	0.143	0.093	0.179	0.156	0.303	0.319	0.518	0.440
Concentration [ug/g; wet weight basis]								
Calculated (Table 6.1)	5460	5460	5890	5890	8350	8350	8890	8890
Total Extraction	4319	4762	4827	4431	6001	5863	6923	7174
Sequential Extraction								
total	4746	5345	5129	5224	6482	6467	8492	7489
fraction A	6	0	6	0	0	0	28	0
fraction B	2160	1117	631	243	67	278	4	31
fraction C	2059	3497	3972	4254	5915	5629	7669	6819
fraction D	418	626	442	636	423	482	740	591
fraction E	103	104	79	91	77	78	51	48
Concentration [ug/g; dry weight basis]								
Calculated (Table 6.1)	6371	6020	7174	6979	11980	12261	18444	15875
Total Extraction	5040	5250	5880	5250	8610	8610	14364	12810
Sequential Extraction								
total	5538	5893	6247	6189	9300	9497	17618	13374
fraction A	7	0	7	0	0	0	59	0
fraction B	2520	1232	768	288	96	408	8	56
fraction C	2403	3856	4838	5040	8487	8266	15911	12177
fraction D	488	690	538	753	607	708	1535	1056
fraction E	120	115	96	108	110	115	105	85

## Appendix VII

### RESULTS OF EQUILIBRIUM LEACHING

- Table VII-1 Results of the equilibrium leaching test.
- Table VII-2 Calculation of ionic conductance from wet chemistry analysis.
- Table VII-3 Conductivity and dissolved solids in the equilibrium leaching test.

Table VII-1 Results of the Equilibrium Leaching Test

	Fly ash-cement		Fly ash-lime		Clay-cement		Sol. sil.-cement	
	rep 1	rep 2	rep 1	rep 2	rep 1	rep 2	rep 1	rep 2
pH	11.4	10.9	11.6	11.4	11.8	11.7	11.9	11.8
Conductivity [ $\mu\text{S}/\text{cm}$ ]	1700	1060	2200	1310	3280	2850	5100	4000
Concentration [M]								
Aluminum	1.19E-04	4.45E-05	2.04E-04	1.26E-04	1.04E-04	1.48E-04	5.19E-05	9.27E-05
Arsenic	2.80E-06	1.12E-05	1.33E-06	3.67E-06	1.55E-06	1.55E-06	4.23E-04	7.47E-05
Calcium	4.34E-03	2.02E-03	3.64E-03	2.42E-03	3.64E-03	2.99E-03	2.74E-04	9.23E-04
Cadmium	8.90E-08	3.56E-08	4.45E-08	9.79E-08	8.90E-09	8.90E-08	2.67E-08	8.90E-09
Chromium	7.31E-06	5.67E-06	2.56E-06	9.62E-07	7.50E-07	9.23E-07	8.46E-07	5.96E-07
Lead	9.41E-07	6.76E-08	1.93E-06	3.81E-07	3.54E-06	2.17E-06	4.92E-07	5.55E-07
Silicon	2.21E-04	3.92E-04	1.21E-04	9.97E-05	8.90E-05	9.97E-05	4.31E-03	8.19E-04
Sodium	8.70E-04	9.57E-04	9.13E-04	9.13E-04	5.79E-03	5.57E-03	2.82E-02	1.95E-02
Chloride	1.04E-03	1.33E-03	1.22E-03	1.20E-03	2.16E-03	1.78E-03	4.48E-03	2.81E-03
Nitrate	4.84E-05	3.23E-05	3.06E-05	1.39E-04	8.06E-05	1.39E-04	1.24E-04	1.16E-04
Sulfate	3.83E-04	4.90E-04	4.52E-04	4.43E-04	7.97E-04	6.57E-04	1.66E-03	1.04E-03
Concentration [mg/L]								
Aluminum	3.200	1.200	5.500	3.400	2.800	4.000	1.400	2.500
Arsenic	0.210	0.840	0.100	0.275	0.116	0.116	31.700	5.600
Calcium	174.000	81.000	146.000	97.000	146.000	120.000	11.000	37.000
Cadmium	0.010	0.004	0.005	0.011	0.001	0.010	0.003	0.001
Chromium	0.380	0.295	0.133	0.050	0.039	0.048	0.044	0.031
Lead	0.195	0.014	0.400	0.079	0.733	0.450	0.102	0.115
Silicon	6.200	11.000	3.400	2.800	2.500	2.800	121.000	23.000
Sodium	20.000	22.000	21.000	21.000	133.000	128.000	648.000	449.000
Chloride	36.800	47.000	43.400	42.500	76.500	63.100	159.000	99.800
Nitrate	3.000	2.000	1.900	8.600	5.000	8.600	7.700	7.200
Sulfate	36.800	47.000	43.400	42.500	76.500	63.100	159.000	99.800
Fraction solubilized [%]								
Arsenic	0.30	1.21	0.13	0.37	0.11	0.11	29.44	5.20
Cadmium	0.01	.00	.00	0.01	.00	0.01	.00	.00
Chromium	0.78	0.61	0.26	0.10	0.06	0.07	0.06	0.04
Lead	0.10	0.01	0.20	0.04	0.26	0.16	0.03	0.04

Table VII-2 Calculation of ionic conductance from wet chemical analysis.

The theoretical ionic conductance of a solution can be estimated from the equivalent ionic conductance of individual ions under the hypothesis of infinite dilution (Sawyer and McCarthy, 1978).

$$K = \sum_{i=1}^n \frac{N_i}{1000} G_i \quad (1)$$

where

$G_i$  = equivalent ionic conductance [ $\text{mho} \cdot \text{cm}^2/\text{eq}$ ]

$N_i$  = normality of ion "i" [ $\text{eq/L}$ ]

$K$  = conductivity of the solution [ $\text{mho/cm}$ ]

The average theoretical conductivity and corresponding dissolved solids for each of the four solidification systems are presented in columns 2 and 3 of Table VII-3. The measured leachate conductivities, in column 4 of Table VII-3 are higher than those based on wet chemistry, indicating that not all ions present were included in the calculations. The ratio of measured to calculated conductivity was thus used to multiply the calculated dissolved solids and obtain the extrapolated values of column 5.

Table VII-3 Conductivity and dissolved solids in the equilibrium test leachates.

System	Theoretical (based on wet chemistry)		Measured Conductivity	Extrapolated Dissolved Solids
	Conductivity [ $\mu\text{S/cm}$ ]	Dissolved Solids [ $\text{mg/L}$ ]		
Fly ash-cement	1844	247	1380	403
Fly ash-lime	1222	242	1755	347
Clay-cement	1994	417	3065	641
Sol sil-cement	3127	932	4550	1355

## Appendix VIII

## RESULTS OF TITRATION AND SOLUBILITY (LOW L/S)

- Table VIII-1 Titration and solubility data for Batch A.  
Table VIII-2 Titration and solubility data for Batch B.  
Table VIII-3 Titration and solubility data for Batch C.  
Table VIII-4 Titration and solubility data for Batch D.  
Table VIII-5 Empirical relationships for the solubility of metals from Batches C and D.  
Table VIII-6 Gran analysis in the titration of a solid's sample.
- Figure VIII-1 Titration curve of Batch A.  
Figure VIII-2 Titration curve of Batch B.  
Figure VIII-3 Titration curve of Batch C.  
Figure VIII-4 Titration curve of Batch D.

Table VIII-1 Titration and Solubility data for Batch A  
(low liquid-to-solid ratio)

Cumulative acid added [meq/g] w.w.b	pH	Species concentration [M]
		Cadmium
Experiment A4I		
0.000	8.04	N/A
0.001	7.51	N/A
0.002	7.20	N/A
0.002	7.12	N/A
0.003	6.89	N/A
0.004	6.98	N/A
0.005	6.87	N/A
0.006	6.80	N/A
0.007	6.52	N/A
0.007	6.47	N/A
0.008	6.17	N/A
0.009	6.21	N/A
0.010	4.96	N/A
0.011	4.23	N/A
0.011	3.92	N/A
0.012	3.67	N/A
0.013	3.55	N/A
0.015	3.28	N/A
Experiment A4II		
0.000	8.30	1.51E-04
0.001	7.96	3.59E-05
0.002	7.45	1.69E-04
0.003	7.39	4.45E-04
0.004	7.21	6.94E-04
0.005	7.17	8.10E-04
0.006	7.03	9.88E-04
0.007	6.87	1.23E-03
0.008	5.85	1.49E-03
0.009	5.32	1.43E-03
0.010	4.25	1.63E-03
0.011	3.48	1.64E-03
0.012	3.25	1.65E-03
0.013	2.97	1.67E-03
0.014	2.81	1.56E-03
0.015	2.75	1.57E-03
0.016	2.56	1.61E-03
0.017	2.54	1.55E-03
0.018	2.43	1.57E-03
0.019	2.37	1.73E-03

Table VIII-2 Titration and Solubility data for Batch B  
(low liquid-to-solid ratio)

Cumulative acid added [meq/g] $\phi$ w.w.b	pH	Species concentration [M]	
		Cadmium	
Experiment B41			
0.000	9.75	8.90E-08	
0.006	8.90	1.78E-07	
0.011	9.33	2.67E-07	
0.017		sample lost	
0.023	8.87	2.67E-07	
0.028	9.00	3.23E-05	
0.033	9.01	2.76E-06	
0.039	8.83	5.34E-06	
0.044	8.63	2.11E-05	
0.050	8.66	2.13E-05	
0.056	8.26	7.83E-06	
0.061	8.07	2.30E-05	
0.067	7.69	1.96E-04	
0.072	7.49	5.96E-04	
0.078	6.96	9.79E-04	
0.083	6.72	1.25E-03	
0.089	4.40	1.53E-03	
0.094	3.61	1.63E-03	
0.100	3.02	1.51E-03	
0.106	2.95	1.63E-03	
Experiment B411			
0.000	9.71	b.d.l	
0.006	9.58	b.d.l	
0.011	9.40	b.d.l	
0.017	9.28	b.d.l	
0.022	9.16	b.d.l	
0.028	9.07	b.d.l	
0.033	8.97	b.d.l	
0.039	8.85	b.d.l	
0.044	8.76	3.56E-07	
0.050	8.58	7.12E-07	
0.055	8.40	2.49E-06	
0.061	8.15	9.52E-06	
0.066	7.75	6.17E-05	
0.072	7.19	5.25E-04	
0.077	6.78	1.02E-03	
0.083	5.90	1.48E-03	
0.088	5.20	1.71E-03	
0.094	3.29	1.73E-03	
0.099	2.99	1.73E-03	
0.105	2.75	NA	

Note: b.l.d. = below detection level

Table VIII-3. Titration and Solubility data for Batch C  
(low liquid-to-solid ratio)

Cumulative acid added [meq/g] w.w.b	pH	Species concentration [M]			
		Cadmium	Chromium	Lead	Lithium
Experiment C4I					
0.00	10.64	b.d.l.	1.92E-06	3.86E-08	1.30E-03
0.00	10.74	b.d.l.	1.73E-06	2.41E-08	1.30E-03
0.04	10.71	1.78E-07	2.12E-06	1.21E-07	1.36E-03
0.09	9.83	b.d.l.	2.88E-06	1.93E-08	1.38E-03
0.08	9.66	b.d.l.	3.85E-06	2.90E-08	1.41E-03
0.12	9.4	2.67E-07	2.50E-06	1.93E-08	1.58E-03
0.12	9.39	2.40E-06	3.65E-06	1.45E-08	1.58E-03
0.16	9.14	8.01E-07	2.31E-06	2.90E-08	1.58E-03
0.20	8.65	5.60E-06	1.92E-06	1.93E-08	1.58E-03
0.20	8.65	2.58E-06	2.50E-06	1.11E-06	1.58E-03
0.24	8.38	4.71E-06	1.73E-06	1.93E-08	1.73E-03
0.26	7.85	1.55E-05	1.54E-06	4.34E-08	1.73E-03
0.26	7.94	1.40E-05	1.54E-06	2.90E-08	1.73E-03
0.28	7.59	2.33E-05	1.54E-06	3.38E-08	1.87E-03
0.30	7.2	7.83E-05	1.54E-06	4.83E-08	1.87E-03
0.30	7.23	1.42E-04	1.54E-06	4.83E-08	1.87E-03
0.32	7.16	7.93E-05	1.54E-06	4.83E-08	2.02E-03
0.34	5.76	7.74E-04	1.54E-06	2.28E-06	1.87E-03
0.36	5.89	6.94E-04	1.92E-06	1.32E-06	2.02E-03
0.36	5.43	1.01E-03	1.92E-06	1.08E-05	2.02E-03
0.40	4.7	1.01E-03	1.92E-06	1.08E-05	2.02E-03
0.40	4.39	1.26E-03	5.77E-06	3.10E-05	2.31E-03
0.48	3.98	1.32E-03	9.23E-06	2.72E-05	2.16E-03
0.52	3.87	1.31E-03	2.08E-05	7.72E-05	2.31E-03
0.56	3.54	1.25E-03	3.27E-05	1.01E-04	2.31E-03
0.60	3.51	1.27E-03	8.25E-05	4.83E-05	2.16E-03
		1.33E-03	2.54E-04	7.72E-05	2.31E-03
Experiment C4II					
0.00	10.4	b.d.l.	5.92E-06	1.45E-08	1.33E-03
0.00	10.4	b.d.l.	5.71E-06	b.d.l.	1.31E-03
0.10	9.26	b.d.l.	4.23E-06	b.d.l.	1.40E-03
0.20	8.43	2.49E-06	3.38E-06	b.d.l.	1.58E-03
0.30	6.62	1.69E-04	2.12E-06	6.76E-08	1.73E-03
0.40	4.86	1.22E-03	2.75E-06	2.14E-05	2.02E-03
0.53	3.84	1.41E-03	4.27E-05	8.69E-05	2.16E-03
0.60	3.67	1.48E-03	9.66E-05	5.79E-05	2.16E-03
0.68	3.79	1.53E-03	2.75E-05	7.72E-05	2.16E-03
0.70	3.56	1.49E-03	2.50E-04	8.20E-05	2.31E-03

Note: b.l.d. = below detection level



Table VIII-4 Titration and Solubility data for Batch D  
(low liquid-to-solid ratio)

Cumulative acid added [meq/g] w.w.b	pH	Species concentration [M]			
		Cadmium	Chromium	Lead	Lithium
		Experiment D4I			
0.00	11.91	8.90E-09	1.04E-06	5.31E-07	1.12E-02
0.20	11.04	8.90E-09	2.12E-06	4.34E-08	1.20E-02
0.40	10.71	8.90E-08	4.23E-06	1.98E-07	1.22E-02
0.60	10.47	2.67E-08	5.71E-06	3.38E-08	1.21E-02
0.80	10.25	1.78E-08	5.71E-06	9.65E-09	1.22E-02
1.00	9.87	5.34E-08	4.87E-06	4.83E-09	1.21E-02
1.20	9.50	2.67E-07	4.44E-06	1.93E-08	1.21E-02
1.30	9.03	7.12E-07	3.60E-06	1.59E-07	1.22E-02
1.40	8.69	1.60E-06	3.60E-06	1.45E-08	1.24E-02
1.50	8.30	3.83E-06	3.17E-06	2.34E-06	1.21E-02
1.60	7.67	1.16E-05	2.75E-06	9.65E-09	1.24E-02
1.70	7.10	6.85E-05	3.60E-06	4.34E-08	1.27E-02
1.80	7.00	8.90E-05	2.96E-06	2.65E-07	1.28E-02
1.90	7.00	2.94E-04	3.60E-06	1.01E-06	1.27E-02
2.00	5.50	9.88E-04	3.81E-06	7.72E-05	1.37E-02
2.40	3.69	ERR	1.36E-04	7.87E-04	1.27E-02
2.80	3.35	3.73E-03	8.27E-04	1.57E-03	1.30E-02
3.20	2.99	4.40E-03	5.69E-03	1.72E-03	1.30E-02
3.60	2.32	4.66E-03	5.69E-03	1.82E-03	1.21E-02
Experiment D4II					
0.00	11.71	b.l.d.	7.12E-07	1.69E-07	1.07E-02
0.20	10.85	7.12E-08	2.50E-04	1.45E-08	1.25E-02
0.40	10.54	b.l.d.	1.27E-06	1.45E-08	1.27E-02
0.60	10.24	1.78E-08	8.54E-05	b.l.d.	1.27E-02
0.80	9.84	2.67E-08	2.54E-06	b.l.d.	1.34E-02
1.00	9.34	6.23E-08	1.06E-06	4.83E-09	1.35E-02
1.20	8.00	3.65E-06	2.96E-06	4.83E-09	1.28E-02
1.40	7.84	6.41E-06	1.06E-06	4.83E-09	1.35E-02
1.50	7.20	1.77E-05	1.06E-06	5.31E-08	1.40E-02
1.60	6.60	6.22E-05	1.92E-04	6.76E-08	1.35E-02
1.70	5.93	9.79E-05	1.06E-06	1.25E-07	1.33E-02
1.80	5.46	2.58E-04	ERR	4.30E-06	1.38E-02
1.90	4.97	4.89E-04	1.27E-06	2.35E-05	1.37E-02
2.00	4.24	9.70E-04	3.17E-06	1.30E-04	1.31E-02
2.20	3.72	1.82E-03	2.91E-05	4.87E-04	1.41E-02
2.40	3.42	2.65E-03	2.69E-04	8.16E-04	1.37E-02
2.60	3.33	3.42E-03	1.71E-04	1.03E-03	1.43E-02
2.80	3.13	3.68E-03	5.96E-04	1.20E-03	1.38E-02
3.00	3.00	4.23E-03	7.69E-04	1.39E-03	1.40E-02
3.20	2.86	4.41E-03	1.48E-03	1.45E-03	1.41E-02

Note: b.l.d. = below detection level.

Table VIII-5 Empirical relationships for the solubility of metals from Batches C and D (mol/L).  
(plotted on Figure 7.4)

Cadmium  $[Cd_T] = 10^{(3.808 - pH - 9.52/pH)}$   
 $+10^{(-8.06)}$   
 $+10^{(-20.0 + pH)}$

Chromium  $[Cr_T] = 10^{(3.081 - 2 \cdot pH)}$   
 $+10^{(-5.425)}$

Lead  $[Pb_T] = 10^{(0.1795 - pH)}$   
 $+10^{(-7.187)}$   
 $+10^{(-18.44 + pH)}$

Table VIII-6 Gran analysis in the titration of a solid's sample.

The purpose of this analysis is to determine the end point in the titration of a solid's sample. When the acid added remains as free  $H^+$ , the following relationship holds (Stumm and Morgan, 1981):

$$(V + v) \cdot 10^{-PH} = (v - v_e) \cdot C_a \quad (1)$$

where

- $V$  : Initial volume of sample [L]
- $v$  : volume of strong acid added [L]
- $v_e$  : volume of strong acid corresponding to the end point of titration [L]
- $C_a$  : molarity of strong acid

The left hand term of Equation 1 is referred to as  $F_1$  and plotted as a function of  $v$ . When  $F_1 = 0$ , the titration end point  $v_e$  can be determined. In order to use the method to determine the end point of the titrations performed in batch mode (Section 6.2.3), the following changes are required.

- define  $V_L$ , the total volume of liquid present per gram of wet waste present in each titration bottle (i.e., water from the solid's pores and water added to perform the test).  $V_L$  is constant since the amount of distilled water added was adjusted to provide a constant liquid-to-solid ratio.
- define  $a$ , the amount of acid added per gram of wet solid, expressed in meq/g.

Equation 1 can be rewritten as:

$$1000 V_L \cdot 10^{-PH} = (a - a_e) \quad (2)$$

The factor of 1000 transform [eq] into [meq].

$$V_L = \frac{\text{water from sample}}{\text{solid}} + \frac{\text{water from solution added}}{\text{solid}}$$

For 1 gram of wet solid sample,

$$V_L = \frac{W}{Y_W} + \frac{R}{1000} \quad (3)$$

where  $w$  : water content [w/w, w.w.b]  
 $\gamma_w$  : water density [g/l]  
 $R$  : liquid-to-solid ratio [w/w, w.w.b]

Replacing Equation 3 into Equation 2 and simplifying leads to

$$(w + R) 10^{-\text{pH}} = (a - a_e) \quad (4)$$

where  $a$  : acid added [meq/g]  
 $a_e$  : titration end point

Figure VIII-1 Titration Curves

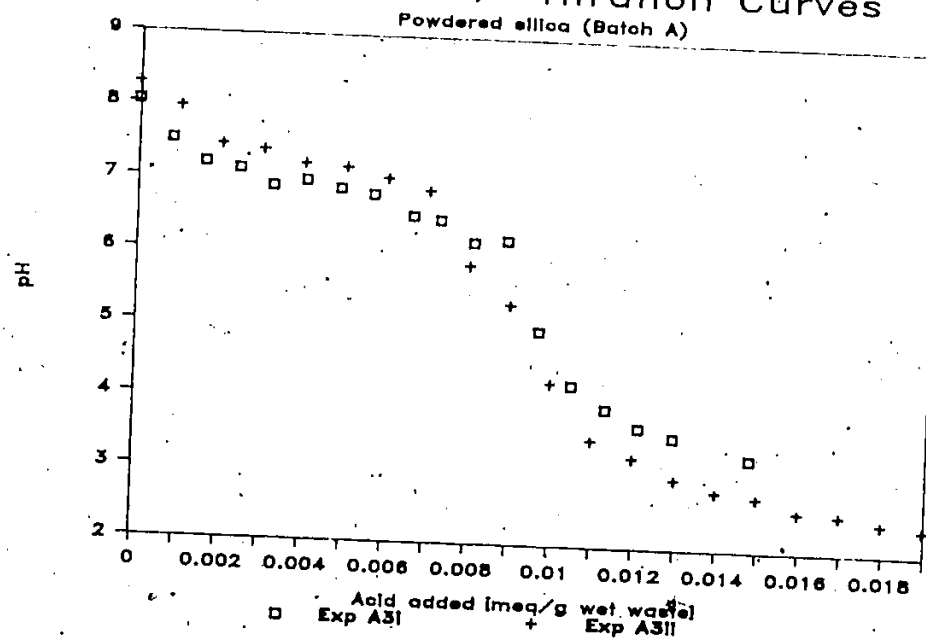


Figure VIII-2 Titration Curves

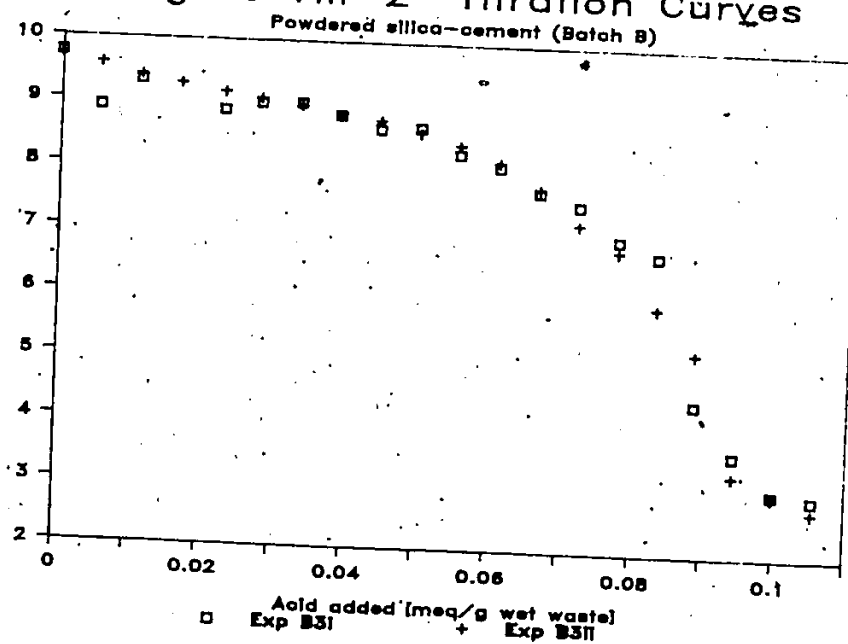


Figure VIII-3 Titration Curves

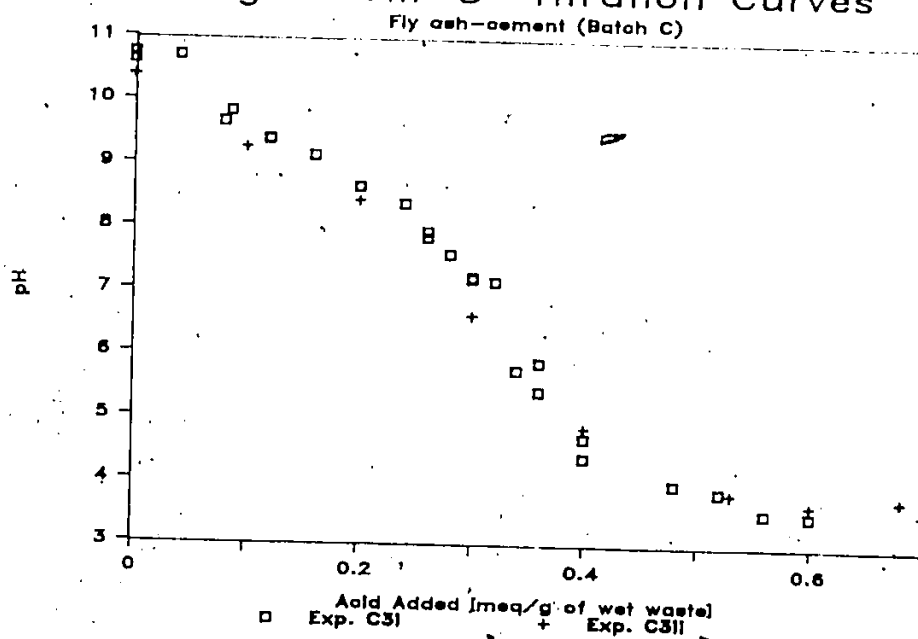
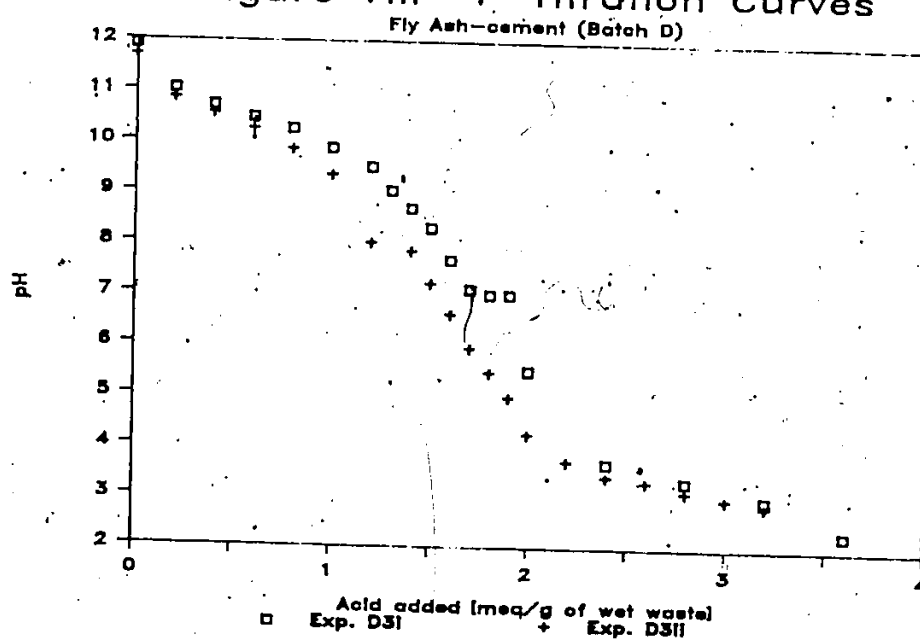


Figure VIII-4 Titration Curves



## Appendix IX

## RESULTS OF TITRATION AND SOLUBILITY (HIGH L/S)

Table IX-1 Titration and solubility data for Batch C.

Table IX-2 Titration and solubility data for Batch D.

Figure IX-1 Titration at high L/S (cadmium).

Figure IX-2 Titration at high L/S (chromium).

Figure IX-3 Titration at high L/S (lead).

Table IX-1 Titration and Solubility Data for Batch C  
(High liquid-to-solid ratio)

Sample Weight (g/d.w.b.)	Acid 2.02N (ml)	Distilled Water (L)	pH	Species Concentration [m]							
				Aluminum	Arsenic	Calcium	Cadmium	Chromium	Lead	Lithium	Silica
0.704	0.15	0.9	5.69	1.85E-06	1.15E-06	2.00E-04	2.62E-06	1.92E-07	4.03E-07	4.32E-06	3.56E-05
0.704	0.2	0.9	5.08	1.11E-05	1.17E-06	6.00E-05	2.80E-06	1.92E-07	1.69E-06	4.32E-06	4.27E-05
0.711	0.25	0.9	4.68	3.71E-05	1.20E-06	6.75E-05	2.99E-06	1.92E-07	2.41E-06	4.32E-06	4.98E-05
0.675	0.3	0.9	4.39	6.67E-05	1.49E-06	2.00E-04	2.99E-06	7.69E-07	2.90E-06	4.32E-06	6.41E-05
0.725	0.35	0.9	4.27	9.27E-05	1.52E-06	2.93E-04	3.18E-06	1.35E-06	3.14E-06	4.32E-06	8.19E-05
0.715	0.4	0.9	4.07	1.07E-04	2.50E-06	3.00E-04	2.99E-06	1.35E-06	3.38E-06	5.76E-06	8.90E-05
0.667	0.4	0.9	3.94	1.33E-04	2.35E-06	2.93E-04	2.62E-06	1.73E-06	2.90E-06	4.32E-06	1.14E-04
0.726	1.2	0.9	3.08	2.34E-04	3.08E-06	3.53E-04	2.62E-06	4.04E-06	4.10E-06	5.76E-06	1.67E-04
0.704	1.5	0.9	2.90	2.34E-04	3.38E-06	1.00E-04	2.43E-06	4.04E-06	3.86E-06	5.76E-06	1.71E-04
0.760	1.5	0.9	2.82	2.34E-04	3.52E-06	8.00E-05	2.43E-06	4.23E-06	4.20E-06	5.76E-06	1.85E-04
0.748	2	0.9	2.56	2.56E-04	3.96E-06	7.50E-05	2.43E-06	4.62E-06	4.10E-06	5.76E-06	1.92E-04



Table IX-2 Titration and Solubility data for Batch D  
(high liquid-to-solid ratio)

Sample Weight [g(d.w.b)]	Acid 2.02N [ml]	Distilled Water [L]	pH	Species Concentration [M]											
				Arsenic			Cadmium			Chromium			Lead		
				rep 1	rep 2	b.i.d.	rep 1	rep 2	b.i.d.	rep 1	rep 2	b.i.d.	rep 1	rep 2	b.i.d.
0.020	0.00	0.9	10.64	4.99E-06	4.55E-06	b.i.d.	4.99E-06	4.55E-06	b.i.d.	5.38E-07	4.81E-07	5.38E-07	9.65E-09	1.45E-08	1.45E-08
0.796	0.00	0.9	10.60	4.26E-06	4.99E-06	b.i.d.	4.26E-06	4.99E-06	b.i.d.	9.79E-07	2.69E-07	9.79E-07	1.09E-05	1.93E-08	1.22E-06
0.801	0.50	0.9	9.63	6.17E-06	6.46E-06	b.i.d.	6.17E-06	6.46E-06	b.i.d.	3.56E-08	4.42E-07	4.42E-07	1.45E-08	3.86E-08	3.86E-08
0.777	0.50	0.9	9.56	5.87E-06	5.87E-06	0.90E-09	5.87E-06	5.87E-06	0.90E-09	2.69E-07	4.81E-07	4.81E-07	2.41E-08	1.45E-09	1.45E-09
0.769	0.75	0.9	8.47	1.91E-06	1.47E-06	3.91E-06	1.91E-06	1.47E-06	3.91E-06	9.29E-06	6.06E-06	9.29E-06	3.38E-08	1.45E-08	1.45E-08
0.783	0.75	0.9	8.31	4.11E-06	3.96E-06	1.51E-07	4.11E-06	3.96E-06	1.51E-07	4.81E-07	5.96E-07	4.81E-07	9.65E-09	1.45E-08	1.45E-08
0.780	1.00	0.9	7.27	2.20E-06	2.35E-06	4.08E-06	2.20E-06	2.35E-06	4.08E-06	4.11E-06	4.23E-07	4.11E-06	9.65E-09	3.38E-08	3.38E-08
0.781	1.00	0.9	6.86	1.76E-06	1.62E-06	4.11E-06	1.76E-06	1.62E-06	4.11E-06	3.62E-06	7.27E-06	3.62E-06	1.45E-08	3.38E-08	3.38E-08
0.827	1.25	0.9	6.25	6.41E-07	1.17E-06	1.36E-05	6.41E-07	1.17E-06	1.36E-05	1.36E-05	4.23E-07	2.88E-07	1.01E-07	6.69E-08	6.69E-08
0.786	1.25	0.9	5.45	5.87E-07	5.34E-07	1.91E-05	5.87E-07	5.34E-07	1.91E-05	1.27E-05	1.73E-07	6.86E-06	1.54E-06	1.33E-06	1.33E-06
0.774	1.50	0.9	4.56	6.14E-07	5.47E-07	1.59E-05	6.14E-07	5.47E-07	1.59E-05	1.68E-05	1.38E-06	2.96E-06	7.88E-06	7.38E-06	7.38E-06
0.806	1.50	0.9	4.56	1.32E-06	1.32E-06	1.68E-05	1.32E-06	1.32E-06	1.68E-05	1.45E-05	1.23E-06	1.08E-06	3.24E-06	3.40E-06	3.40E-06
0.807	2.00	0.9	4.02	1.76E-06	1.76E-06	1.04E-05	1.76E-06	1.76E-06	1.04E-05	5.92E-06	6.13E-06	5.92E-06	7.20E-06	1.43E-05	1.43E-05
0.804	2.00	0.9	4.01	1.76E-06	1.76E-06	5.89E-06	1.76E-06	1.76E-06	5.89E-06	4.11E-06	1.25E-05	1.09E-05	1.06E-05	1.13E-05	1.13E-05
0.761	2.00	0.9	3.76	1.62E-06	1.47E-06	3.72E-06	1.62E-06	1.47E-06	3.72E-06	4.01E-06	8.48E-06	1.05E-05	1.11E-05	1.23E-05	1.23E-05
0.831	2.25	0.9	3.20	2.20E-06	1.97E-05	9.98E-06	2.20E-06	1.97E-05	9.98E-06	4.63E-07	1.41E-05	1.49E-05	8.11E-06	1.71E-05	1.71E-05
0.778	2.50	0.9	3.06	2.79E-06	2.20E-06	4.68E-06	2.79E-06	2.20E-06	4.68E-06	5.58E-06	1.47E-05	1.37E-05	1.55E-05	1.21E-05	1.21E-05
0.782	2.50	0.9	3.00	2.50E-06	2.50E-06	4.70E-06	2.50E-06	2.50E-06	4.70E-06	4.60E-06	1.45E-05	1.40E-05	1.33E-05	1.21E-05	1.21E-05

Figure IX-1 Titration-high L/S

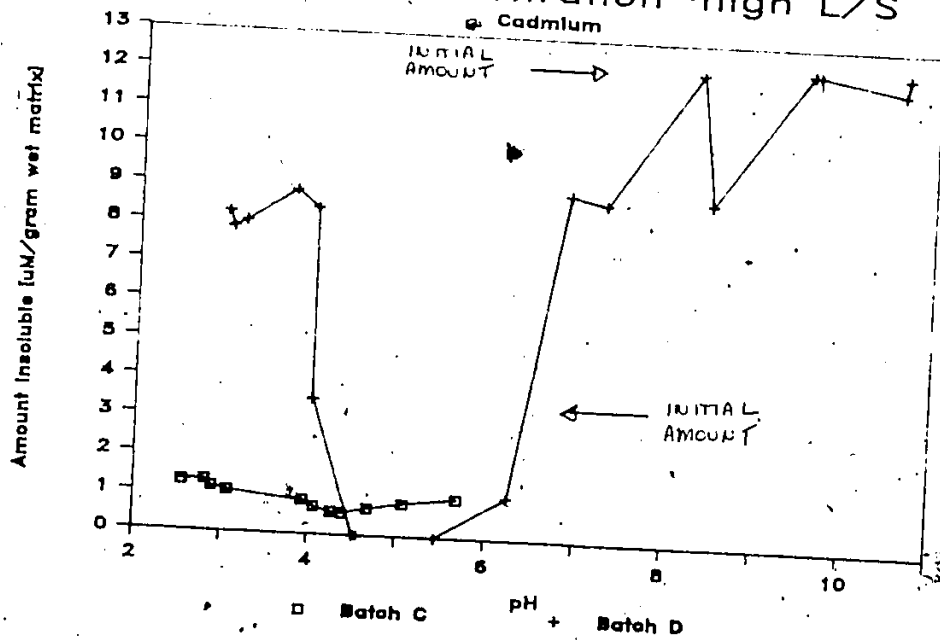


Figure IX-2 Titration-high L/S

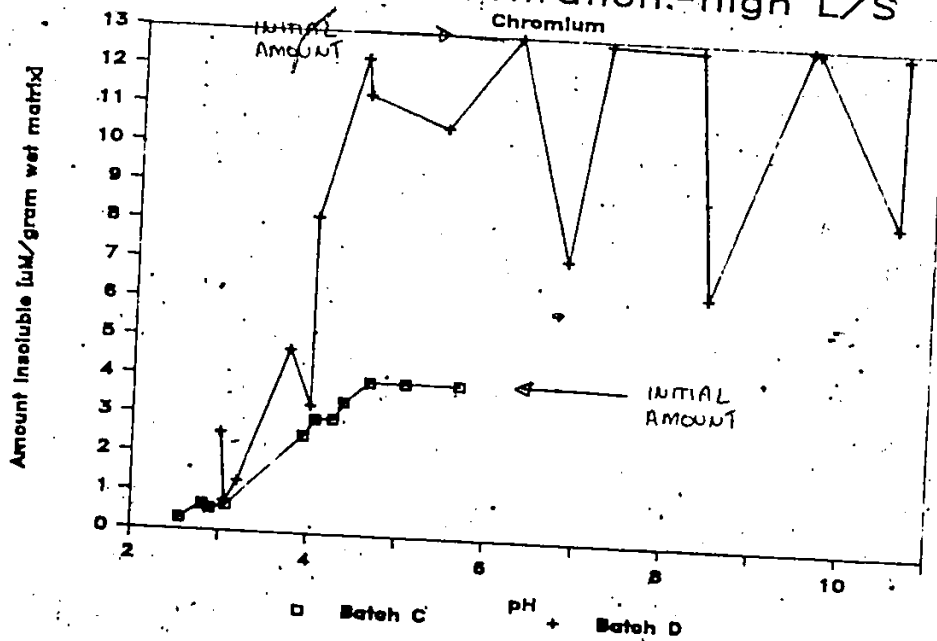
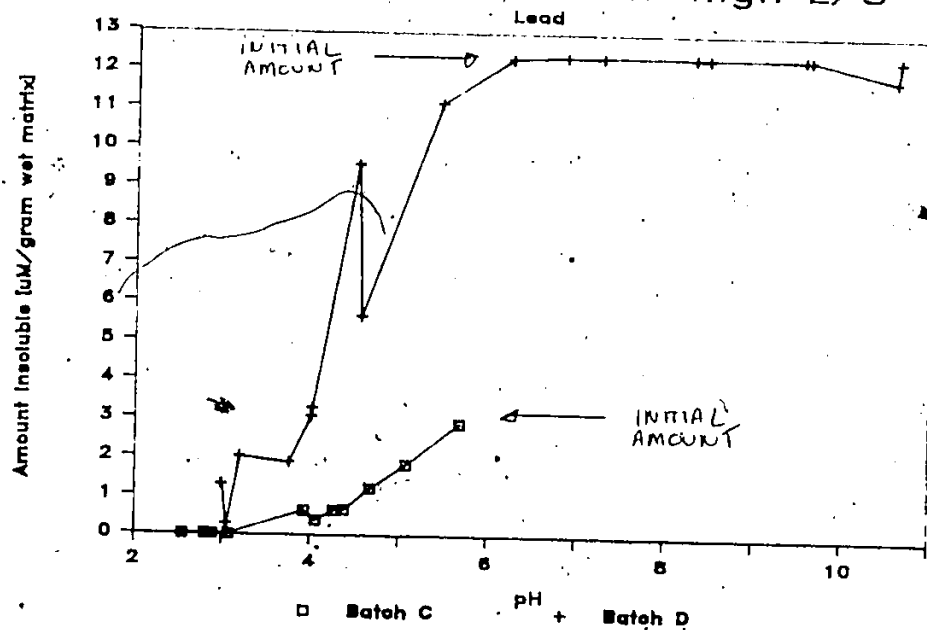


Figure IX-3 Titration-high L/S



## Appendix X

## RESULTS OF STATIC LEACHING

Table X-1	Leaching experiment B5i results.
Table X-2	Leaching experiment B5ii results.
Table X-3	Leaching experiment C5i results.
Table X-4	Leaching experiment C5ii results.

Table X-1 Leaching Experiment B51 Results.

Experiment: B51  
duration: 72 hours

#### Specimen Characteristics

Batch: Powdered Silica-cement (B)  
Shape: straight wall jar  
Volume: 0.340 liter  
Weight: 597.0 grams  
Surface: 69.4 cm<sup>2</sup>  
Water Content (w.w.b): 0.24

#### Leaching Characteristics

Reactor's volume: 2.0 liters  
Flow Conditions: static  
Leachant Composition: 0.001 M HNO<sub>3</sub>  
Ionic Medium: 0.02 M KNO<sub>3</sub>

NOTE: The reactor's volume decreased by 20 mls each time  
a sample was taken for metal analysis.

Time [hours]	pH	Concentration [M]	
		Cadmium	Lithium
0.0	3.18	0.00E+00	0.00E+00
0.2	3.20	3.20E-06	9.51E-05
3.6	3.26	4.45E-06	4.78E-04
21.3	3.94	7.26E-06	1.25E-03
44.7	3.89	8.17E-06	1.87E-03
67.4	4.35	7.26E-06	2.16E-03

Table X-2 Leaching Experiment B511 Results.

Experiment: B511  
duration: 72 hours

#### Specimen Characteristics

Batch: Powdered Silica-cement (B)  
Shape: straight wall jar  
Volume: 0.340 liter  
Weight: 597.0 grams  
Surface: 69.4 cm<sup>2</sup>  
Water Content (w.w.b): 0.24

#### Leaching Characteristics

Reactor's volume: 2.0 liters  
Flow Conditions: static  
Leachant Composition: 0.001 M HNO<sub>3</sub>  
Ionic Medium: 0.02 M KNO<sub>3</sub>

NOTE: The reactor's volume decreased by 20 mls each time a sample was taken for metal analysis.

Time [hours]	pH	Concentration [M]	
		Cadmium	Lithium
0.0	3.10	0.00E+00	0.00E+00
0.1	3.12	2.67E-07	8.93E-05
3.5	3.16	3.20E-06	4.47E-04
21.1	3.46	7.56E-06	1.30E-03
68.5	4.32	7.12E-06	2.45E-03

Table X-3 Leaching Experiment C51 Results

Experiment: C51  
Duration: 672 hours

## Specimen Characteristics

Batch: Fly Ash-cement (C)  
Shape: straight wall Jar  
Volume: 0.0517 liter  
Weight: 83.0 grams  
Surface: 15.9 cm<sup>2</sup>  
Water Content (w.w.b): 0.31

## Leaching Characteristics

Reactor's volume: 1.1 liters  
Flow Conditions: static  
Leachant Composition: 0.001 M HNO<sub>3</sub>  
Ionic Medium: 0.02 M KNO<sub>3</sub>

NOTE: The reactor's volume decreased by 20 mls each time  
a sample was taken for metal analysis.

Time [hours]	pH	Concentration [M]				
		Arsenic	Cadmium	Chromium	Lead	Lithium
0.0		0.00E+00	0.00E+00	0.00E+00	0.00E+00	0.00E+00
23.4		8.01E-07	1.17E-06	3.85E-07	5.84E-07	4.76E-05
70.9		1.12E-06	1.66E-06	4.42E-07	5.84E-07	9.65E-05
113.9		1.12E-06	1.37E-06	5.00E-07	5.84E-07	1.25E-04
256.8		1.12E-06	1.27E-06	3.65E-07	1.45E-07	1.87E-04
330.8		7.61E-07	8.81E-07	3.08E-07	5.31E-08	2.03E-04
504.4		8.81E-07	5.87E-07	3.08E-07	4.83E-09	2.33E-04
652.0		1.28E-06	2.22E-07	3.08E-07	4.83E-09	2.48E-04
663.0		1.28E-06	1.96E-07	3.46E-07	4.83E-09	2.45E-04
0.0	2.98					
0.9	3.01					
17.9	3.15					
23.4	3.21					
70.9	3.57					
89.6	3.69					
113.9	3.83					
143.9	4.09					
167.0	4.37					
256.8	6.54					
330.8	6.62					
382.4	7.30					
472.5	7.62					
520.3	7.78					
593.3	8.11					
648.8	8.04					
656.7	8.09					

Table X-4 Leaching Experiment C511 Results.

Experiment: C511  
duration: 672 hours

## Specimen Characteristics

Batch: Fly Ash-cement (C)  
Shape: straight wall jar  
Volume: 0.0517 liter  
Weight: 83.0 grams  
Surface: 15.9 cm<sup>2</sup>  
Water Content (w.w.b): 0.31

## Leaching Characteristics

Reactor's volume: 1.1 liters  
Flow Conditions: static  
Leachant Composition: 0.001 M HNO<sub>3</sub>  
Ionic Medium: 0.02 M KNO<sub>3</sub>

NOTE: The reactor's volume decreased by 20 mls each time  
a sample was taken for metal analysis.

Time [hours]	pH	Concentration [M]				
		Arsenic	Cadmium	Chromium	Lead	Lithium
0.0		0.00E+00	0.00E+00	0.00E+00	0.00E+00	0.00E+00
23.4		8.41E-07	5.77E-06	3.08E-07	3.72E-07	4.47E-05
70.9		1.04E-06	1.66E-06	3.85E-07	6.37E-07	9.51E-05
113.9		1.04E-06	1.76E-06	4.62E-07	6.37E-07	1.24E-04
256.8		1.12E-06	1.47E-06	3.85E-07	1.79E-07	1.84E-04
330.8		1.00E-06	7.83E-07	2.88E-07	3.38E-08	2.02E-04
504.4		1.15E-06	8.41E-06	5.00E-07	4.83E-08	2.29E-04
652.0		1.44E-06	1.96E-07	4.04E-07	1.45E-08	2.44E-04
663.0		1.68E-06	2.22E-07	4.04E-07	4.83E-09	2.45E-04
0.0	2.98					
0.9	2.99					
17.9	3.14					
23.4	3.21					
70.9	3.58					
89.6	3.73					
113.9	3.89					
143.9	4.16					
167.0	4.45					
256.8	5.22					
330.8	7.81					
382.4	8.15					
472.5	8.41					
520.3	8.24					
593.3	8.45					
648.8	8.35					
656.7	8.35					



## Appendix XI

## RESULTS OF DYNAMIC LEACHING (CONTINUOUS FLOW)

Table XI-1	Leaching experiment A6 results.
Table XI-2	Leaching experiment B6I results.
Table XI-3	Leaching experiment B6II results.
Table XI-4	Leaching experiment C6I results.
Table XI-5	Leaching experiment C6II results.
Table XI-6	Leaching experiment D6I results.
Table XI-7	Leaching experiment D6II results.

Table XI-1 Leaching Experiment A6 Results.

Experiment: A6  
Duration: 48 hours

#### Specimen Characteristics

Batch: Powdered Silica (A)  
Shape: soxhlet thimble  
Volume: 0.130 liter  
Weight: 247.0 grams  
Surface: 295.0 cm<sup>2</sup>  
Water Content (w.w.b): 0.24

#### Leaching Characteristics

Reactor's volume: 2.0 liters  
Flow Conditions: 3.28 L/day  
Leachant Composition: 0.001 M HNO<sub>3</sub>  
Ionic Medium: 0.02 M KNO<sub>3</sub>

Time <sup>a</sup> [hours]	pH	Concentration [M]	
		Cadmium	Lithium
0.00	3.00	0.00E+00	0.00E+00
1.00	3.10	2.95E-06	5.30E-04
3.00	3.15	1.25E-05	7.91E-04
5.00	3.15	1.60E-05	9.51E-04
7.00	3.18	1.92E-05	8.94E-04
9.00	3.18	1.69E-05	9.01E-04
11.00	3.20	2.82E-05	9.35E-04
13.00	3.20	3.35E-05	9.19E-04
15.00	3.17	3.53E-05	8.26E-04
17.00	3.18	4.41E-05	8.24E-04
19.00	3.18	3.79E-05	7.70E-04
21.00	3.16	2.82E-05	7.23E-04
23.00	3.16	3.53E-05	6.90E-04
25.00	3.15	3.18E-05	6.46E-04
27.00	3.14	2.23E-05	6.23E-04
29.00	3.14	2.23E-05	5.89E-04
31.00	3.13	3.35E-05	5.55E-04
33.00	3.13	3.35E-05	5.29E-04
35.00	3.13	3.35E-05	5.00E-04
37.00	3.12	2.23E-05	4.78E-04
39.00	3.12	2.82E-05	4.51E-04
41.00	3.12	2.32E-05	4.28E-04
43.00	3.12	3.18E-05	4.02E-04
45.00	3.12	2.47E-05	3.88E-04
47.00	3.12	2.65E-05	3.67E-04

Table XI-2 Leaching Experiment B61 Results

Experiment: B61  
duration: 48 hours

Specimen Characteristics

Batch: Powdered Silica-cement (B)  
Shape: straight wall jar  
Volume: 0.340 liter  
Weight: 597.0 grams  
Surface: 69.4 cm<sup>2</sup>  
Water Content (w.w.b): 0.24

Leaching Characteristics

Reactor's volume: 2.0 liters  
Flow Conditions: 2.80 L/day  
Leachant Composition: 0.001 M HNO<sub>3</sub>  
Ionic Medium: 0.02 M KNO<sub>3</sub>

Time [hours]	pH	Concentration [M] Cadmium
0.0	3.02	0.00E+00
1.0	3.09	1.33E-06
3.0	3.13	2.14E-06
5.0	3.16	3.56E-06
7.0	3.17	3.29E-06
9.0	3.19	4.09E-06
11.0	3.21	3.65E-06
13.0	3.23	4.45E-06
15.0	3.24	3.74E-06
17.0	3.25	3.74E-06
19.0	3.26	4.45E-06
21.0	3.27	3.83E-06
23.0	3.26	3.56E-06
25.0	3.25	4.00E-06
27.0	3.23	3.38E-06
29.0	3.22	3.11E-06
31.0	3.21	2.94E-06
33.0	3.21	2.94E-06
35.0	3.20	3.65E-06
37.0	0.32	3.20E-06
39.0	3.21	3.47E-06
41.0	3.20	2.67E-06
43.0	3.20	2.67E-06
45.0	3.20	3.29E-06
47.0	3.20	2.49E-06

Table XI-3 Leaching Experiment B611 Results.

Experiment: B611  
duration: 48 hours

#### Specimen Characteristics

Batch: Powdered Silica-cement (B)  
Shape: straight wall jar  
Volume: 0.340 liter  
Weight: 597.0 grams  
Surface: 69.4 cm<sup>2</sup>  
Water Content (w.w.b): 0.24

#### Leaching Characteristics

Reactor's volume: 2.0 liters  
Flow Conditions: 2.89 L/day  
Leachant Composition: 0.001 M HNO<sub>3</sub>  
Ionic Medium: 0.02 M KNO<sub>3</sub>

Time [hours]	pH	Concentration (M)	
		Cadmium	Lithium
0.0	3.02	0.00E+00	0.00E+00
1.0	3.10	1.87E-06	2.13E-04
3.0	3.11	3.29E-06	3.88E-04
5.0	3.14	3.91E-06	4.55E-04
7.0	3.18	4.00E-06	5.13E-04
9.0	3.18	4.18E-06	5.50E-04
11.0	3.19	4.36E-06	5.72E-04
13.0	3.18	4.45E-06	5.61E-04
15.0	3.20	4.27E-06	5.82E-04
17.0	3.24	4.45E-06	5.82E-04
19.0	3.24	4.45E-06	5.78E-04
21.0	3.25	4.18E-06	5.69E-04
23.0	3.28	4.36E-06	5.48E-04
25.0	3.23	4.27E-06	5.29E-04
27.0	3.21	4.18E-06	5.36E-04
29.0	3.20	3.91E-06	5.23E-04
31.0	3.20	4.00E-06	5.12E-04
33.0	3.22	4.00E-06	4.97E-04
35.0	3.23	4.09E-06	4.80E-04
37.0	3.25	3.65E-06	4.83E-04
39.0	3.25	3.74E-06	4.63E-04
41.0	3.24	3.65E-06	4.45E-04
43.0	3.23	3.74E-06	4.38E-04
45.0	3.21	3.65E-06	4.21E-04
47.0	3.22	3.56E-06	4.18E-04

Table XI-4 Leaching Experiment C61 Results.

Experiment: C61  
Duration: 172 hours

#### Specimen Characteristics

Batch: Fly Ash-cement (C)  
Shape: straight wall jar  
Volume: 0.340 liter  
Weight: 550.8 grams  
Surface: 69.4 cm<sup>2</sup>  
Water Content (w.w.b): 0.31

#### Leaching Characteristics

Reactor's volume: 1.94 liters  
Flow Conditions: 1.3 L/day  
Leachant Composition: 0.001 M HNO<sub>3</sub>  
Ionic Medium: 0.02 M KNO<sub>3</sub>

Time [hours]	pH	Time [hours]	pH	Time [hours]	pH
0.00	3.02	5.37	3.52	69.92	3.80
0.03	3.06	5.62	3.55	71.20	3.80
0.18	3.08	6.03	3.57	72.07	3.79
0.33	3.10	6.28	3.58	72.83	3.79
0.43	3.15	9.47	3.73	73.78	3.78
0.68	3.19	24.23	4.05	74.68	3.78
0.87	3.21	25.22	4.06	75.10	3.78
1.12	3.23	26.40	4.06	75.93	3.77
1.45	3.26	27.12	4.06	77.57	3.77
1.62	3.28	28.25	4.06	97.97	3.74
1.87	3.30	29.47	4.05	99.37	3.73
2.03	3.31	30.22	4.05	101.10	3.73
2.20	3.33	30.83	4.05	124.47	3.79
2.37	3.34	31.45	4.03	142.53	3.72
2.77	3.37	46.28	3.92	145.62	3.72
2.95	3.39	46.78	3.92	147.12	3.72
3.20	3.41	47.77	3.91	149.50	3.71
3.53	3.42	48.28	3.91	150.32	3.70
3.70	3.44	48.85	3.90	166.25	3.68
3.87	3.45	50.03	3.88	168.93	3.68
4.12	3.46	51.37	3.87	171.37	3.67
4.45	3.48	52.33	3.86	172.42	3.67
4.70	3.49	53.53	3.85	final	
5.12	3.52	54.30	3.85	calibration	3.59

Table XI-4 Leaching Experiment C61 Results (cont'd).

Time [hours]	Leachate Weight [g]	Concentration [M]				
		Arsenic	Cadmium	Chromium	Lead	Lithium
2	207.3	6.14E-07	5.34E-07	0.00E+00	2.12E-07	3.60E-05
6.75	298.1	7.21E-07	8.90E-07	3.85E-07	2.36E-07	6.48E-05
10.8	153.0	6.94E-07	9.79E-07	1.92E-07	2.08E-07	7.78E-05
14.1	221.8	7.61E-07	8.01E-07	3.85E-07	2.17E-07	8.36E-05
18.1	209.1	7.07E-07	8.01E-07	3.85E-07	2.17E-07	8.93E-05
22.1	230.2	6.41E-07	8.01E-07	3.85E-07	2.08E-07	9.22E-05
26.1	222.9	4.80E-07	7.12E-07	2.69E-07	1.32E-06	9.36E-05
30.1	201.7	8.54E-07	7.12E-07	2.69E-07	1.52E-06	9.36E-05
34.1	237.2	3.87E-07	6.23E-07	2.50E-07	1.33E-06	9.22E-05
38.1	218.8	4.14E-07	7.12E-07	2.31E-07	1.42E-06	9.22E-05
42.1	211.7	1.12E-06	8.01E-07	2.31E-07	1.52E-06	9.22E-05
46.1	203.4	6.41E-07	8.01E-07	2.50E-07	1.52E-06	9.08E-05
50.1	227.7	5.34E-07	8.90E-07	2.31E-07	1.52E-06	8.79E-05
54.1	232.4	8.01E-07	1.07E-06	1.73E-07	1.42E-06	8.64E-05
58.1	205.2	6.54E-07	1.25E-06	1.92E-07	1.52E-06	8.21E-05
62.1	209.2	5.47E-07	1.25E-06	1.54E-07	1.62E-06	8.21E-05
66.1	223.8	6.27E-07	1.42E-06	1.73E-07	1.82E-06	8.07E-05
70.1	211.3	5.07E-07	1.33E-06	2.12E-07	1.82E-06	7.78E-05
74.1	246.9	5.87E-07	1.60E-06	1.92E-07	1.93E-06	7.78E-05
78.1	211.9	7.47E-07	1.60E-06	1.73E-07	1.82E-06	7.49E-05
82.1	214.2	7.21E-07	1.60E-06	1.92E-07	2.13E-06	7.35E-05
86.1	216.8	1.49E-06	1.69E-06	7.89E-07	2.84E-06	7.06E-05
90.1	220.1	4.54E-07	1.51E-06	2.12E-07	2.13E-06	6.77E-05
96.2	444.5	6.41E-07	1.60E-06	2.12E-07	2.23E-06	6.63E-05
102.3	259.4	5.34E-07	2.14E-06	3.85E-07	2.33E-06	6.48E-05
106.3	215.2	5.07E-07	1.78E-06	2.12E-07	2.03E-06	6.34E-05
110.3	182.4	5.87E-07	1.78E-06	2.31E-07	2.43E-06	6.05E-05
114.3	227.8	4.80E-07	1.51E-06	1.92E-07	2.33E-06	5.76E-05
118.3	213.7	7.21E-07	1.60E-06	1.92E-07	2.13E-06	5.76E-05
122.3	166.5	5.47E-07	1.60E-06	1.92E-07	2.03E-06	5.91E-05
126.3	108.3	5.34E-07	1.78E-06	2.69E-07	2.43E-06	6.20E-05
130.3	215.0	6.67E-07	1.60E-06	2.31E-07	2.43E-06	5.91E-05
134.3	207.4	7.47E-07	1.60E-06	1.92E-07	2.33E-06	5.62E-05
138.3	211.4	3.87E-07	1.51E-06	1.92E-07	2.33E-06	5.47E-05
142.3	174.4	4.80E-07	1.60E-06	1.73E-07	2.43E-06	5.47E-05
146.3	263.9	4.94E-07	1.51E-06	1.92E-07	2.43E-06	5.33E-05
150.3	199.2	4.27E-07	1.42E-06	2.12E-07	2.53E-06	5.19E-05
154.3	256.8	4.40E-07	1.42E-06	1.92E-07	2.23E-06	5.04E-05
158.3	214.4	4.40E-07	1.51E-06	1.92E-07	2.74E-06	4.90E-05
162.3	257.2	4.00E-07	1.42E-06	1.92E-07	2.64E-06	4.75E-05
166.3	207.4	3.60E-07	1.42E-06	1.92E-07	2.84E-06	4.47E-05
170.3	209.2	3.87E-07	1.42E-06	1.92E-07	2.84E-06	4.61E-05

Table XI-5. Leaching Experiment C611 Results.

Experiment: C611  
Duration: 296 hours

#### Specimen Characteristics

Batch: Fly Ash-cement (C)  
Shape: straight-wall Jar  
Volume: 0.340 liter  
Weight: 550.8 grams  
Surface: 69.4 cm<sup>2</sup>  
Water Content (w.w.b): 0.31

#### Leaching Characteristics

Reactor's volume: 1.94 liters  
Flow Conditions: 1.3 L/day  
Leachant Composition: 0.001 M HNO<sub>3</sub>  
Ionic Medium: 0.02 M KNO<sub>3</sub>

Time [hours]	pH
0.0	3
2.0	3.19
6.0	3.47
10.0	3.67
14.0	3.79
18.0	3.96
22.0	3.87
26.0	3.82
30.0	3.78
34.0	3.76
38.0	3.75
42.0	3.75
46.0	3.74
50.0	3.73
54.0	3.72

Time [hours]	pH
58.0	3.72
62.0	3.7
66.0	3.69
70.0	3.72
74.0	3.69
78.0	3.68
82.0	3.69
86.0	3.69
90.0	3.67
94.0	3.66
98.0	3.63
102.0	3.61
106.0	3.61
110.0	3.61

pH data missing to the  
end of experiment.

Table XI-5 Leaching Experiment C611 Results (cont'd).

Time [hours]	Leachate Weight [g]	Concentration [M]				
		Arsenic	Cadmium	Chromium	Lead	Lithium
2.0	285.2	4.27E-07	5.34E-07	1.54E-07	7.96E-07	5.76E-06
6.0	254.9	NA	NA	NA	NA	NA
10.0	106.9	1.28E-06	1.25E-06	2.69E-07	1.70E-06	4.47E-05
14.0	113.0	NA	NA	NA	NA	NA
18.0	123.2	1.07E-06	1.25E-06	2.88E-07	1.54E-06	7.06E-05
22.0	212.5	NA	NA	NA	NA	NA
26.0	229.2	1.12E-06	1.33E-06	2.69E-07	1.75E-06	8.36E-05
30.0	230.0	NA	NA	NA	NA	NA
34.0	228.6	1.04E-06	1.07E-06	2.69E-07	1.06E-06	8.36E-05
38.0	223.3	NA	NA	NA	NA	NA
42.0	230.5	1.01E-06	1.25E-06	2.12E-07	7.96E-07	8.50E-05
46.0	237.7	NA	NA	NA	NA	NA
50.0	215.3	6.54E-07	1.25E-06	3.27E-07	7.96E-07	8.21E-05
54.0	230.0	NA	NA	NA	NA	NA
58.0	231.1	NA	NA	NA	NA	NA
62.0	299.9	NA	NA	NA	NA	NA
66.0	230.7	NA	NA	NA	NA	NA
70.0	230.7	6.14E-07	1.42E-06	2.12E-07	9.56E-07	7.64E-05
74.0	131.7	3.07E-06	1.07E-06	1.54E-07	9.03E-07	3.17E-06
78.0	163.8	NA	NA	NA	NA	NA
82.0	100.2	NA	NA	NA	NA	NA
86.0	153.9	NA	NA	NA	NA	NA
90.0	121.0	7.21E-07	1.51E-06	2.12E-07	6.90E-07	7.06E-05
94.0	167.7	NA	NA	NA	NA	NA
98.0	173.7	NA	NA	NA	NA	NA
102.0	107.8	NA	NA	NA	NA	NA
106.0	88.9	NA	NA	NA	NA	NA
110.0	163.2	6.67E-07	1.51E-06	1.92E-07	6.90E-07	6.05E-05
114.0	11.6	NA	NA	NA	NA	NA
118.0	0.0	NA	NA	NA	NA	NA
122.0	0.0	NA	NA	NA	NA	NA
126.0	0.0	NA	NA	NA	NA	NA
130.0	0.0	NA	NA	NA	NA	NA
134.0	0.0	NA	NA	NA	NA	NA
138.0	176.2	6.41E-07	1.33E-06	1.73E-07	7.43E-07	5.19E-05
142.0	230.7	NA	NA	NA	NA	NA
146.0	227.6	NA	NA	NA	NA	NA
150.0	249.4	5.61E-07	1.25E-06	1.73E-07	7.43E-07	5.04E-05
154.0	203.0	NA	NA	NA	NA	NA
158.0	234.2	NA	NA	NA	NA	NA
162.0	226.3	NA	NA	NA	NA	NA



Table XI-5 Leaching Experiment C611 Results (cont'd).

Time [hours]	Leachate Weight [g]	Concentration [M]				
		Arsenic	Cadmium	Chromium	Lead	Lithium
166.0	425.9	NA	NA	NA	NA	NA
170.0	29.2	6.14E-07	1.25E-06	2.31E-07	9.03E-07	4.90E-05
174.0	227.6	NA	NA	NA	NA	NA
178.0	230.6	NA	NA	NA	NA	NA
182.0	214.8	NA	NA	NA	NA	NA
186.0	241.6	NA	NA	NA	NA	NA
190.0	226.6	4.40E-07	1.16E-06	1.73E-07	7.43E-07	4.18E-05
194.0	0.0	NA	NA	NA	NA	NA
198.0	0.0	NA	NA	NA	NA	NA
202.0	0.0	NA	NA	NA	NA	NA
206.0	0.0	NA	NA	NA	NA	NA
210.0	227.7	6.41E-07	1.25E-06	1.73E-07	6.37E-07	3.89E-05
214.0	227.8	NA	NA	NA	NA	NA
218.0	228.5	NA	NA	NA	NA	NA
222.0	229.1	NA	NA	NA	NA	NA
226.0	229.9	NA	NA	NA	NA	NA
230.0	229.6	4.81E-07	1.25E-06	1.92E-07	6.37E-07	3.75E-05
234.0	231.8	NA	NA	NA	NA	NA
238.0	221.8	NA	NA	NA	NA	NA
242.0	229.8	NA	NA	NA	NA	NA
246.0	231.1	3.74E-07	1.07E-06	1.73E-07	6.37E-07	3.46E-05
250.0	231.2	NA	NA	NA	NA	NA
254.0	228.6	NA	NA	NA	NA	NA
258.0	231.5	NA	NA	NA	NA	NA
262.0	221.0	NA	NA	NA	NA	NA
266.0	250.7	NA	NA	NA	NA	NA
270.0	231.0	NA	NA	NA	NA	NA
274.0	237.9	NA	NA	NA	NA	NA
278.0	230.7	NA	NA	NA	NA	NA
282.0	226.7	NA	NA	NA	NA	NA
286.0	228.6	2.80E-07	8.01E-07	2.88E-07	8.49E-07	3.31E-05
290.0	226.2	NA	NA	NA	NA	NA
294.0	119.2	NA	NA	NA	NA	NA

Table XI-6 Leaching Experiment D61 Results.

Experiment: D61  
Duration: 310 hours

#### Specimen Characteristics

Batch: Fly Ash-cement (D)  
Shape: 2-inch cube  
Volume: 0.1311 liter  
Weight: 221.0 grams  
Surface: 154.8 cm<sup>2</sup>  
Water Content (w.w.b): 0.24

#### Leaching Characteristics

Reactor's volume: 2.25 liters  
Flow Conditions: 1.0 L/day  
Leachant Composition: 0.002 M HNO<sub>3</sub>  
Ionic Medium: 0.02 M KNO<sub>3</sub>

Time [hours]	Leachate Weight [g]	pH	Time [hours]	Leachate Weight [g]	pH
0.0		2.7	153.0	272.9	8.41
3.0	368.5	3.5	159.0	228.5	8.24
9.0	368.5	9.4	165.0	245.5	8.00
15.0	368.5	10.1	171.0	269.6	7.80
21.0	368.5	10.2	177.0	260.9	7.31
27.0	267.2	10.5	183.0	271.5	7.24
33.0	289.0	10.6	189.0	264.5	7.19
39.0	281.7	10.6	195.0	261.6	7.12
45.0	312.4	10.5	201.0	255.0	7.09
51.0	293.2	10.4	207.0	278.2	7.03
57.0	288.8	10.3	213.0	153.0	6.93
63.0	284.5	10.23	219.0	0.0	6.89
69.0	297.8	10.14	225.0	0.0	8.84
75.0	292.2	10.04	231.0	245.8	9.36
81.0	288.8	9.94	237.0	223.7	9.52
87.0	260.4	9.86	243.0	277.0	8.94
93.0	258.2	9.78	249.0	281.4	8.05
99.0	274.7	9.73	255.0	240.2	7.36
105.0	275.1	9.66	261.0	267.2	7.08
111.0	252.9	9.62	267.0	278.7	6.68
117.0	264.2	9.58	273.0	283.5	6.36
123.0	264.7	9.51	279.0	248.7	6.14
129.0	260.1	9.42	285.0	255.2	5.7
135.0	258.2	9.3	291.0	263.6	5.32
141.0	247.3	9.17	297.0	281.6	4.87
147.0	269.3	8.77			

Table XI-6 Leaching Experiment D61 Results (cont'd).

Time [hours]	Concentration [M]					
	Arsenic	Calcium	Cadmium	Chromium	Lead	Lithium
3.0	6.94E-07	4.99E-04	1.69E-07	3.27E-07	2.65E-07	3.56E-04
9.0	1.91E-06	5.99E-04	7.12E-08	2.69E-07	8.69E-08	6.48E-04
15.0	1.47E-06	8.73E-04	1.78E-08	4.42E-07	1.35E-07	7.46E-04
21.0	2.64E-06	9.73E-04	b.d.l.	2.50E-07	1.06E-07	7.93E-04
27.0	2.50E-06	9.98E-04	b.d.l.	2.89E-07	1.06E-07	8.00E-04
33.0	2.20E-06	1.07E-03	2.67E-08	1.21E-06	1.11E-07	7.93E-04
39.0	2.64E-06	1.37E-03	3.56E-08	4.23E-07	4.25E-07	7.55E-04
45.0	2.20E-06	1.10E-03	8.90E-09	4.04E-07	1.06E-07	7.49E-04
51.0	2.35E-06	1.05E-03	b.d.l.	3.27E-07	1.21E-07	7.20E-04
57.0	7.34E-07	1.07E-03	b.d.l.	3.65E-07	4.15E-07	6.89E-04
63.0	2.64E-06	1.10E-03	b.d.l.	3.65E-07	1.11E-07	6.48E-04
69.0	1.62E-06	1.05E-03	b.d.l.	2.89E-07	1.54E-07	6.14E-04
75.0	7.34E-07	1.05E-03	b.d.l.	3.08E-07	1.40E-07	6.01E-04
81.0	6.54E-07	1.05E-03	b.d.l.	4.42E-07	1.25E-07	5.68E-04
87.0	4.94E-07	1.05E-03	b.d.l.	1.92E-07	7.72E-08	5.45E-04
93.0	4.40E-07	9.98E-04	b.d.l.	7.50E-07	1.11E-07	5.17E-04
99.0	5.87E-07	1.02E-03	b.d.l.	2.89E-07	7.24E-08	4.90E-04
105.0	6.01E-07	9.98E-04	8.90E-09	3.27E-07	9.17E-08	4.70E-04
111.0	4.27E-07	1.07E-03	1.78E-08	3.27E-07	7.24E-08	4.65E-04
117.0	5.21E-07	1.20E-03	2.67E-08	3.65E-07	6.37E-07	4.29E-04
123.0	3.87E-07	1.10E-03	8.90E-09	3.46E-07	1.11E-07	4.18E-04
129.0	3.60E-07	1.02E-03	2.67E-08	3.46E-07	1.11E-07	4.01E-04
135.0	3.20E-07	1.07E-03	3.56E-08	3.46E-07	1.06E-07	3.79E-04
141.0	3.34E-07	1.12E-03	1.78E-08	3.46E-07	2.56E-07	3.67E-04
147.0	2.80E-07	9.98E-04	7.12E-08	2.69E-07	1.21E-07	3.46E-04
153.0	3.74E-07	9.98E-04	2.67E-08	2.89E-07	3.19E-07	3.39E-04
159.0	5.87E-06	1.05E-03	1.16E-07	5.39E-07	4.83E-06	3.29E-04
165.0	7.34E-06	9.48E-04	8.90E-08	5.58E-07	5.79E-06	3.17E-04
171.0	4.99E-06	9.98E-04	1.07E-07	4.23E-07	3.55E-06	2.97E-04
177.0	4.55E-06	1.07E-03	6.23E-08	4.23E-07	4.83E-08	2.87E-04
183.0	3.08E-06	9.98E-04	8.01E-08	3.46E-07	1.38E-06	2.74E-04
189.0	2.35E-06	1.02E-03	3.11E-07	3.46E-07	9.56E-07	2.64E-04
195.0	6.14E-07	1.02E-03	5.34E-08	3.08E-07	9.03E-07	2.48E-04
201.0	4.67E-07	8.98E-04	2.67E-08	3.08E-07	4.83E-08	2.44E-04
207.0	3.74E-07	9.98E-04	6.23E-08	2.89E-07	7.43E-07	2.28E-04
213.0	2.27E-07	1.02E-03	2.67E-08	2.69E-07	3.38E-07	2.22E-04
219.0	0.00E+00	0.00E+00	0.00E+00	0.00E+00	0.00E+00	0.00E+00
225.0	0.00E+00	0.00E+00	0.00E+00	0.00E+00	0.00E+00	0.00E+00
231.0	2.64E-06	9.23E-04	2.67E-08	2.69E-07	2.90E-07	2.67E-04
237.0	4.26E-06	9.48E-04	5.34E-08	2.89E-07	1.74E-06	2.54E-04
243.0	4.26E-06	8.23E-04	8.01E-08	2.89E-07	1.98E-06	2.35E-04
249.0	3.82E-06	7.73E-04	5.34E-08	2.50E-07	1.45E-06	2.18E-04
255.0	2.50E-06	9.48E-04	4.45E-08	1.92E-07	1.11E-06	2.12E-04
261.0	1.91E-06	8.23E-04	4.45E-08	1.73E-07	8.69E-07	1.99E-04
267.0	1.91E-06	6.99E-04	5.34E-08	1.92E-07	4.83E-07	1.86E-04
273.0	4.54E-07	8.73E-04	3.56E-08	1.54E-07	1.21E-06	1.80E-04
279.0	1.17E-06	7.49E-04	8.90E-08	1.15E-07	7.24E-07	1.70E-04
285.0	1.47E-06	6.99E-04	1.07E-07	1.15E-07	1.30E-06	1.63E-04
291.0	1.32E-06	7.98E-04	5.34E-08	1.35E-07	1.45E-06	1.56E-04
297.0	1.47E-06	7.98E-04	1.42E-07	1.15E-07	1.01E-06	1.51E-04

Table XI-7 Leaching Experiment D611 Results.

Experiment: D611  
Duration: 312 hours

## Specimen Characteristics

Batch: Fly Ash-cement (D)  
Shape: 2 Inch cube  
Volume: 0.1311 liter  
Weight: 221.0 grams  
Surface: 154.8 cm<sup>2</sup>  
Water Content (w.w.b): 0.24

## Leaching Characteristics

Reactor's volume: 2.25 liters  
Flow Conditions: 1.5 L/day  
Leachant Composition: 0.001 M HNO<sub>3</sub>  
Ionic Medium: 0.02 M KNO<sub>3</sub>

Time [hours]	Leachate Weight [g]	pH
0.0	0.0	2.82
0.7	131.4	2.98
3.8	301.1	3.66
8.6	297.5	7.28
13.4	307.3	9.58
18.2	312.5	9.94
23.0	311.0	10.09
27.8	285.6	10.14
99.0	286.5	10.12
104.4	253.2	10.00
109.2	243.6	9.91
114.0	254.6	9.82
118.8	259.0	9.80
123.6	248.3	9.66
128.4	274.2	9.54
133.2	277.3	9.40
138.0	265.7	9.36
142.8	269.0	9.25
147.6	270.3	8.96
152.4	271.1	9.66
157.2	267.6	8.40
164.4	514.9	8.11
171.6	297.3	7.84
176.4	277.5	7.64
181.2	296.2	7.45
186.0	300.8	7.23

Time [hours]	Leachate Weight [g]	pH
190.8	299.2	7.08
195.6	300.9	6.98
200.4	298.8	6.95
205.2	305.9	6.94
210.0	306.7	6.92
214.8	303.8	6.79
219.6	311.4	6.48
224.4	312.0	6.43
229.2	320.3	6.28
234.0	273.6	6.26
238.8	315.6	6.20
243.6	328.6	5.90
248.4	314.7	5.66
253.2	316.4	5.59
258.0	329.4	5.51
262.8	321.1	5.44
267.6	301.8	5.45
272.4	309.0	5.38
277.2	321.4	5.19
282.0	303.5	5.15
286.8	317.6	5.10
291.6	308.0	5.03
296.4	305.3	4.93
301.2	310.3	4.86
306.0	306.0	4.77
310.8	300.8	4.73

Table XI-7 Leaching Experiment D611 Results (cont'd).

Time [hours]	Concentration [M]					
	Arsenic	Calcium	Cadmium	Chromium	Lead	Lithium
0.7	1.32E-06	1.37E-04	2.22E-07	9.62E-08	ERR	1.24E-04
3.8	1.17E-06	4.24E-04	2.49E-07	2.69E-07	ERR	3.79E-04
8.6	1.76E-06	4.99E-04	1.42E-07	2.69E-07	ERR	5.62E-04
13.4	1.47E-06	5.24E-04	6.23E-08	1.92E-07	1.64E-07	6.10E-04
18.2	2.06E-06	5.24E-04	2.67E-08	1.92E-07	7.24E-08	6.70E-04
23.0	1.91E-06	5.24E-04	1.78E-08	1.92E-07	6.76E-08	6.79E-04
27.8	2.06E-06	5.49E-04	1.78E-08	2.12E-07	4.83E-08	6.74E-04
99.0	Pump failure					
104.4	3.82E-06	8.73E-04	2.67E-08	3.85E-07	1.11E-07	1.27E-03
109.2	3.52E-06	7.98E-04	5.34E-08	3.46E-07	1.59E-07	1.13E-03
114.0	3.52E-06	7.24E-04	3.56E-08	3.08E-07	1.83E-07	1.01E-03
118.8	3.38E-06	6.49E-04	2.67E-08	3.08E-07	7.72E-08	9.51E-04
123.6	2.94E-06	6.74E-04	4.45E-08	2.88E-07	2.41E-07	8.72E-04
128.4	3.52E-06	6.24E-04	5.34E-08	3.27E-07	b.l.d.	8.24E-04
133.2	2.79E-06	5.99E-04	3.56E-08	2.69E-07	1.11E-07	7.23E-04
138.0	3.87E-07	5.74E-04	2.67E-08	3.46E-07	6.76E-08	6.57E-04
142.8	2.50E-06	5.74E-04	2.67E-08	2.50E-07	1.25E-07	6.20E-04
147.6	2.64E-06	5.49E-04	2.67E-08	2.88E-07	6.27E-08	5.39E-04
152.4	2.50E-06	5.49E-04	2.67E-08	2.88E-07	5.31E-08	5.10E-04
157.2	2.94E-06	5.24E-04	2.67E-08	2.69E-07	4.83E-08	4.70E-04
164.4	7.34E-07	4.99E-04	2.67E-08	2.50E-07	4.34E-08	4.41E-04
171.6	6.81E-07	4.99E-04	2.67E-08	2.12E-07	6.76E-08	3.96E-04
176.4	6.27E-07	4.99E-04	3.56E-08	2.31E-07	5.31E-08	3.49E-04
181.2	6.27E-07	4.99E-04	2.67E-08	2.69E-07	6.90E-07	3.21E-04
186.0	5.74E-07	4.99E-04	1.78E-08	2.31E-07	5.31E-08	3.08E-04
190.8	5.74E-07	4.49E-04	1.25E-07	2.12E-07	5.31E-08	2.78E-04
195.6	3.52E-06	1.05E-03	5.34E-08	2.50E-07	5.31E-07	2.49E-04
200.4	4.94E-07	4.99E-04	4.45E-08	2.50E-07	8.69E-08	2.44E-04
205.2	4.27E-07	4.49E-04	5.34E-08	1.92E-07	b.d.l.	2.22E-04
210.0	3.47E-07	5.24E-04	2.67E-08	2.12E-07	1.06E-07	2.10E-04
214.8	3.20E-07	4.74E-04	1.96E-07	2.12E-07	6.76E-08	1.95E-04
219.6	3.34E-07	4.24E-04	3.56E-08	2.69E-07	7.72E-08	1.82E-04
224.4	4.67E-07	4.49E-04	1.78E-08	2.31E-07	1.93E-08	1.74E-04
229.2	4.27E-07	4.24E-04	2.67E-08	2.50E-07	3.38E-08	1.63E-04
234.0	5.07E-07	4.49E-04	1.78E-08	1.92E-07	3.38E-08	1.54E-04
238.8	4.67E-07	3.24E-04	2.67E-08	1.73E-07	2.90E-08	1.50E-04
243.6	2.64E-06	4.24E-04	2.67E-08	1.35E-07	8.20E-08	1.44E-04
248.4	2.94E-06	4.24E-04	2.67E-08	1.35E-07	1.11E-07	1.31E-04
253.2	1.76E-06	3.74E-04	1.78E-08	9.62E-08	1.83E-07	1.31E-04
258.0	1.91E-06	4.24E-04	1.78E-08	9.62E-08	3.86E-08	1.24E-04
262.8	1.47E-06	3.99E-04	1.78E-08	1.15E-07	7.24E-08	1.21E-04
267.6	1.91E-06	4.49E-04	1.78E-08	7.69E-08	6.27E-08	1.12E-04
272.4	1.91E-06	4.24E-04	2.67E-08	7.69E-08	9.65E-08	1.11E-04
277.2	1.62E-06	4.24E-04	1.78E-08	9.62E-08	4.83E-08	1.07E-04
282.0	1.76E-06	4.24E-04	1.78E-08	7.69E-08	3.86E-08	1.01E-04
286.8	2.20E-06	4.49E-04	1.25E-07	1.15E-07	3.86E-08	1.04E-04
291.6	1.47E-06	4.24E-04	1.78E-08	9.62E-08	3.38E-08	9.94E-05
296.4	1.17E-06	3.74E-04	3.56E-08	1.15E-07	6.27E-08	9.51E-05
301.2	1.62E-06	4.24E-04	1.78E-08	9.62E-08	4.34E-08	8.98E-05
306.0	1.47E-06	4.24E-04	2.67E-08	1.15E-07	1.06E-07	8.50E-05
310.8	1.17E-06	4.24E-04	1.78E-08	1.15E-07	1.59E-07	8.65E-05
	1.32E-06	4.24E-04	1.78E-08	1.15E-07	3.86E-08	8.50E-05

## Appendix XII

## RESULTS OF DYNAMIC LEACHING (INTERMITTENT FLOW)

- Table XII-1 Long term leaching data for sample E7i.  
Table XII-2 Long term leaching data for sample E7ii.  
Table XII-3 Long term leaching data for sample F7i.  
Table XII-4 Long term leaching data for sample F7ii.  
Table XII-5 Long term leaching data for sample G7i.  
Table XII-6 Long term leaching data for sample G7ii.  
Table XII-7 Long term leaching data for sample H7i.  
Table XII-8 Long term leaching data for sample H7ii.  
Table XII-9 Weight changes for the specimens in the dynamic leaching test after 1 year of leaching.  
Figure XII-1 Arsenic concentration history.  
Figure XII-2 Cadmium concentration history.  
Figure XII-3 Chromium concentration history.  
Figure XII-4 Lead concentration history.

TABLE XII-1 Long Term Leaching Data for the Fly Ash/Cement Solidification System (E7f).

Leaching Interval	Cumulative Time [d]	Leachate Weight [g]	Conductivity [ $\mu\text{S}/\text{cm}$ ]	pH	Concentration of As [ $\text{mg}/\text{L}$ ]
0	0.00	1500.0	0	7.0	<0.002
1	0.04	1499.9	91	10.6	0.008
2	0.15	1505.5	228	11.0	0.003
3	0.26	1500.5	221	11.0	0.005
4	1.01	1500.6	610	11.4	0.004
5	1.29	1494.4	195	10.9	0.006
6	2.01	1500.7	392	11.3	0.005
7	3.00	1496.1	385	11.3	0.006
8	3.29	1494.2	93	10.4	0.007
9	4.28	1502.1	280	11.1	0.008
10	5.02	1508.4	139	11.1	0.015
11	6.08	1502.1	188	11.2	0.024
12	7.02	1499.4	181	10.9	0.020
13	8.18	1496.8	630	11.0	0.024
14	9.29	1500.4	178	10.8	0.022
15	10.29	1501.2	164	10.8	0.019
16	12.08	1501.0	170	11.3	0.027
17	13.16	1501.8	130	11.0	0.024
18	15.01	1499.5	248	11.0	0.036
19	17.01	1500.5	230	10.9	0.045
20	18.06	1498.4	123	10.6	0.033
21	20.10	1501.3	188	10.8	0.040
22	22.08	1501.8	194	10.9	0.045
23	24.03	1500.6	188	10.9	0.042
24	26.18	1501.4	205	10.9	0.052
25	28.14	1507.1	173	10.9	0.040
26	30.30	1506.3	500	10.9	0.048
27	33.13	1497.0	205	11.0	0.050
28	35.33	1503.2	143	10.6	0.044
29	37.30	1506.7	125	10.5	0.049
30	40.09	1493.2	155	10.6	0.060
31	42.37	1502.8	131	10.5	0.056
32	45.34	1502.8	152	10.7	0.063
33	48.22	1498.2	108	10.4	0.056
34	51.32	1490.8	144	10.7	0.050
35	54.21	1504.2	165	10.5	0.070
36	57.19	1496.3	107	10.3	0.055
37	60.25	1503.7	144	10.6	0.062
38	63.30	1500.4	143	10.6	0.062
39	67.04	1497.6	165	10.6	0.048

Table XII-1 Continued

Leaching Interval	Cumulative Time [d]	Leachate Weight [g]	Conductivity [uS/cm]	pH	Concentration of As [mg/L]
40	70.04	1495.2	122	10.5	0.051
41	74.30	1512.7	140	10.6	0.096
42	77.00	1500.6	111	10.4	0.070
43	80.30	1506.3	132	10.5	0.060
44	84.30	1502.3	147	10.5	0.078
45	88.30	1501.5	135	10.5	0.075
46	92.26	1501.6	130	10.5	0.090
47	96.19	1510.7	95	10.7	0.088
48	100.22	1508.0	97	10.2	0.080
49	104.11	1503.4	123	10.4	0.088
50	109.31	1500.4	131	10.4	0.120
51	115.23	1494.7	132	10.3	0.116
52	118.24	1500.2	80	9.9	0.072
53	123.25	1501.1	130	10.4	0.090
54	127.12	1509.0	106	10.2	0.088
55	130.04	1500.6	85	10.0	0.070
56	140.22	1508.8	167	10.3	0.110
57	144.07	1500.2	135	10.5	0.115
58	154.03	1502.6	130	10.3	0.116
59	161.27	1502.0	140	10.5	0.120
60	169.24	1500.0	150	10.4	0.136
61	175.31	1508.6	133	10.2	0.116
62	182.22	1516.6	126	10.4	0.145
63	189.14	1500.5	120	10.4	0.145
64	195.20	1505.5	123	10.4	0.120
65	203.24	1508.1	129	10.2	0.150
66	211.15	1498.5	135	10.3	0.150
67	217.10	1500.2	109	10.1	0.136
68	224.24	1501.3	114	10.2	0.150
69	231.22	1502.4	107	10.2	0.150
70	240.31	1507.0	118	9.7	0.156
71	245.22	1501.9	103	9.9	0.165
72	252.11	1500.2	111	10.0	0.165
73	259.15	1521.2	87	10.0	0.150
74	266.15	1509.9	106	10.1	0.172
75	274.14	1500.5	105	9.8	0.176
76	280.19	1501.3	85	9.8	0.200



Table XII-1, Continued

Leaching Interval	Cumulative Time [d]	Leachate Weight [g]	Conductivity [uS/cm]	pH	Concentration of As [mg/L]
77	287.13	1501.9	90	9.8	0.155
78	294.28	1500.5	87	9.8	0.190
79	301.30	1503.1	85	9.9	0.155
80	316.11	1500.0	122	9.9	0.230
81	322.17	1502.1	77	9.5	0.150
82	328.26	1504.7	80	9.8	0.180
83	336.15	1504.9	78	9.6	0.165
84	343.26	1503.6	84	9.4	0.320
85	350.25	1501.7	75	9.6	0.190
86	357.25	1507.4	76	9.6	0.150
87	365.26	1501.5	83	9.3	0.120
88	379.31	1502.7	109	9.5	0.180
89	393.23	1513.8	106	9.8	0.190
90	406.31	1505.5	97	9.4	0.294
91	424.27	1500.5	116	9.3	0.275
92	441.07	1502.6	105	9.3	0.253
93	456.25	1502.1	103	9.6	0.253
94	472.13	1501.7	102	9.3	NA
95	484.02	NA	81	9.0	0.190
96	497.10	1504.3	79	NA	0.230
97	511.00	1501.9	84	10.0	0.400
98	495.23	1501.4	82	9.8	0.270
99	526.08	1500.3	80	9.7	NA
100	553.04	1502.9	92	9.8	0.370
101	567.02	1500.0	78	9.7	0.440
102	581.03	1506.2	83	9.5	0.200
103	595.06	1501.2	79	9.6	NA
104	610.03	1501.4	93	9.8	0.220
105	623.06	1500.8	95	9.7	0.420
106	638.02	1500.9	82	9.5	0.210
107	651.04	1501.4	70	9.7	0.230
108	665.31	1501.0	66	9.5	0.250

TABLE XII-2 Long Term Leaching Data for the Fly Ash/Cement  
Solidification System (E711).

Leaching Interval	Cumulative Time [d]	Leachate Weight [g]	Conductivity [uS/cm]	pH	Concentration of Species		
					Cd [mg/L]	Cr [mg/L]	Pb [mg/L]
0	0.00	1500.0	0	7.0	<0.002	<0.002	<0.002
1	0.16	1492.1	418	11.3	0.003	0.002	0.020
2	1.01	1504.3	875	11.6	0.004	0.008	0.055
3	1.30	1499.9	211	11.0	0.002	<0.002	0.009
4	2.30	1498.7	510	11.4	0.003	0.004	0.025
5	4.20	1497.3	630	11.4	0.002	0.005	0.036
6	6.08	1496.5	390	11.6	0.002	0.003	0.031
7	8.19	1493.1	435	11.3	<0.002	0.002	0.020
8	11.01	1509.9	450	11.4	0.002	0.004	0.033
9	13.16	1502.1	270	11.4	<0.002	0.003	0.022
10	17.01	1509.4	470	11.3	0.002	0.003	0.030
11	20.10	1501.5	350	11.2	0.003	0.002	0.019
12	24.03	1501.7	409	11.2	0.002	0.003	0.025
13	28.14	1501.9	380	11.2	0.003	0.003	0.024
14	32.25	1501.0	348	11.2	0.001	0.003	0.022
15	37.30	1493.7	332	11.1	0.001	0.005	0.015
16	42.37	1502.5	315	10.9	0.002	0.005	0.014
17	48.22	1500.0	260	10.9	0.001	0.007	0.015
18	54.21	1494.1	1075	11.0	<0.001	0.006	0.020
19	60.25	1507.4	265	10.8	0.001	0.004	0.010
20	67.04	1508.9	311	11.0	0.002	0.004	0.010
21	73.29	1498.8	259	10.9	<0.001	0.004	0.007
22	81.30	1519.4	282	10.9	0.004	0.004	0.012
23	90.16	1501.5	298	10.9	0.001	0.004	0.010
24	97.13	1507.8	172	11.0	0.002	0.006	0.007
25	105.15	1501.5	250	11.0	<0.001	0.003	0.006
26	112.01	1491.4	218	10.8	<0.001	0.005	0.004
27	123.25	1513.5	262	10.8	0.002	0.006	0.013
28	130.04	1503.9	181	10.6	0.001	0.004	0.005
29	140.22	1507.7	212	10.7	0.001	0.006	0.003
30	154.03	1500.5	210	10.7	<0.001	0.008	0.003
31	169.30	1500.8	240	10.6	0.004	0.010	0.012
32	182.22	1502.8	230	10.7	0.006	0.010	0.012
33	195.20	1511.6	208	10.7	0.001	0.006	0.003
34	211.15	1505.8	230	10.7	<0.001	0.018	0.005
35	224.24	1500.1	185	10.7	0.001	0.009	0.003
36	240.31	1508.4	212	10.6	0.001	0.011	0.005
37	252.11	1515.6	183	10.7	0.005	0.013	0.005
38	266.15	1511.5	180	10.5	<0.001	0.017	0.004

Table XII-2 Continued

Leaching Interval	Cumulative Time [d]	Leachate Weight [g]	Conductivity [uS/cm]	pH	Concentration of Species		
					Cd [mg/L]	Cr [mg/L]	Pb [mg/L]
39	280.19	1501.1	165	10.5	0.002	0.007	0.005
40	294.13	1510.1	148	10.4	0.002	0.008	0.002
41	316.11	1502.4	163	10.4	0.003	0.012	0.004
42	328.26	1500.0	122	10.4	0.001	0.008	0.002
43	343.26	1504.8	122	10.2	0.001	0.002	0.063
44	365.26	1510.5	134	10.3	0.001	0.008	0.001
45	379.31	1503.1	114	10.0	0.004	0.008	0.006
46	393.23	1503.3	130	10.2	0.002	0.005	0.001
47	406.31	1506.8	107	10.1	0.001	0.007	0.002
48	424.27	1503.6	116	9.8	0.001	0.008	0.001
49	441.07	1500.2	114	9.8	NA	0.008	0.001
50	456.25	1503.2	114	10.0	0.001	0.009	0.001
51	472.13	1503.2	110	9.8	NA	NA	NA
52	484.02	NA	92	9.5	0.013	0.004	0.045
53	497.10	1500.2	88	8.9	0.002	0.004	0.015
54	511.00	1500.8	92	10.4	0.002	0.006	0.009
55	495.23	1500.3	94	10.1	0.002	0.005	0.009
56	526.08	1501.0	89	10.2	0.001	0.005	0.003
57	553.04	1504.1	102	10.1	0.005	0.012	0.044
58	567.02	1500.2	88	10.1	NA	NA	NA
59	581.03	1503.5	83	9.9	0.003	0.004	0.021
60	595.06	1500.1	79	10.0	0.005	0.014	0.037
61	610.03	1502.3	104	9.9	0.003	<0.01	0.016
62	623.06	1501.2	102	10.0	0.001	0.009	<0.001
63	638.02	1500.0	86	9.1	0.001	0.009	0.001
64	651.04	1501.5	73	10.0	0.039	0.013	0.050
65	665.31	1506.9	70	9.9	0.001	0.008	0.009

TABLE XII-3 Long Term Leaching Data for the Fly Ash/Lime Solidification System (F71).

Leaching Interval	Cumulative Time [Days]	Leachate Weight [gm]	Conductivity [S/cm]	pH	Concentration of As [mg/L]
0	0.00	1500.0	0	7.0	<0.002
1	0.04	1497.9	42	10.0	0.010
2	0.15	1509.2	230	10.9	0.005
3	0.26	1507.1	355	11.1	0.002
4	1.01	1497.9	1180	11.6	0.004
5	1.29	1502.9	440	11.3	0.005
6	2.01	1497.2	870	11.6	0.004
7	3.00	1501.7	980	11.7	0.005
8	3.29	1496.1	280	11.0	0.007
9	4.28	1497.3	780	11.5	0.005
10	5.02	1496.8	430	11.6	0.008
11	6.08	1492.3	503	11.7	0.011
12	7.02	1506.2	530	11.4	0.009
13	8.18	1504.0	575	11.4	0.008
14	9.29	1503.4	500	11.3	0.007
15	10.29	1501.4	439	11.2	0.010
16	12.08	1503.1	429	11.7	0.010
17	13.16	1502.9	290	11.4	0.010
18	15.01	1506.3	480	11.3	0.014
19	17.01	1499.0	450	11.2	0.018
20	18.06	1501.5	215	10.9	0.015
21	20.10	1504.1	380	11.2	0.025
22	22.08	1497.8	320	11.1	0.023
23	24.03	1500.6	305	11.2	0.025
24	26.18	1500.2	305	11.1	0.031
25	28.14	1506.9	247	11.1	0.024
26	30.30	1511.4	650	11.1	0.032
27	33.13	1501.0	252	11.1	0.032
28	35.33	1496.8	198	10.8	0.030
29	37.30	1506.2	450	10.6	0.028
30	40.09	1504.7	192	10.7	0.042
31	42.37	1502.9	163	10.6	0.045
32	45.34	1500.8	183	10.8	0.046
33	48.22	1498.2	125	10.6	0.055
34	51.32	1504.9	152	10.8	0.050
35	54.21	1492.9	183	10.6	0.058
36	57.19	1499.7	138	10.6	0.050
37	60.25	1498.3	151	10.7	0.055
38	63.30	1503.5	155	10.7	0.056

Table XII-3 Continued

Leaching Interval	Cumulative Time [d]	Leachate Weight [g]	Conductivity [uS/cm]	pH	Concentration of As. [mg/L]
39	67.04	1503.1	172	10.7	0.040
40	70.04	1492.7	131	10.6	0.053
41	74.30	1498.0	142	10.7	0.100
42	77.00	1504.6	113	10.5	0.080
43	80.30	1500.3	133	10.6	0.100
44	84.30	1500.9	147	10.5	0.090
45	88.30	1501.1	139	10.6	0.110
46	92.26	1501.7	125	10.6	0.110
47	96.19	1509.3	78	10.6	0.100
48	100.22	1514.8	113	10.4	0.116
49	104.11	1500.1	129	10.4	0.125
50	109.31	1500.0	133	10.5	0.150
51	115.23	1491.1	124	10.3	0.200
52	118.24	1502.1	85	10.1	0.105
53	123.25	1501.0	123	10.4	0.136
54	127.12	1506.2	100	10.2	0.145
55	130.04	1501.6	80	10.1	0.140
56	140.22	1503.9	150	10.3	0.210
57	144.07	1500.0	132	10.4	0.145
58	154.03	1495.2	128	10.4	0.160
59	161.27	1501.1	130	10.5	0.160
60	169.24	1501.6	150	10.5	0.180
61	175.31	1502.0	124	10.3	0.200
62	182.22	1503.2	118	10.3	0.200
63	189.14	1503.2	107	10.4	0.216
64	195.20	1505.0	107	10.4	0.210
65	203.24	1508.7	122	10.1	0.230
66	211.15	1497.7	130	10.2	0.216
67	217.10	1507.0	94	10.0	0.192
68	224.24	1501.1	104	10.1	0.210
69	231.22	1509.5	96	10.1	0.200
70	240.31	1493.8	107	9.7	0.240
71	245.22	1510.4	89	9.9	0.200
72	252.11	1500.4	97	10.0	0.253
73	259.15	1492.0	74	9.9	0.220
74	266.15	1501.1	106	10.1	0.260
75	274.14	1501.9	88	9.7	0.300
76	280.19	1508.0	70	9.6	0.255
77	287.13	1500.1	74	9.6	0.220
78	294.28	1501.9	72	9.6	0.230

Table XII-3 Continued

Leaching Interval	Cumulative Time (d)	Leachate Weight (g)	Conductivity (uS/cm)	pH	Concentration of As (mg/L)
79	301.30	1501.2	70	9.8	0.220
80	316.11	1501.0	98	9.6	0.285
81	322.17	1501.9	65	9.4	0.200
82	328.26	1506.8	65	9.4	0.210
83	336.15	1501.9	65	9.3	0.200
84	343.26	1500.2	70	9.2	0.320
85	350.25	1512.9	64	9.1	0.230
86	357.25	1507.4	64	9.4	0.230
87	365.26	1502.9	68	9.1	0.165
88	379.31	1503.9	92	9.2	0.253
89	393.23	1502.8	90	9.6	0.190
90	406.31	1500.9	82	8.3	0.310
91	424.27	1501.4	104	9.1	0.330
92	441.07	1508.7	94	9.1	0.319
93	456.25	1501.4	85	9.5	0.330
94	472.13	1500.7	85	9.1	NA
95	484.02	NA	72	8.9	0.210
96	497.10	1501.1	66	8.1	0.357
97	518.00	1500.5	70	9.7	0.264
98	495.23	1502.2	69	9.6	0.326
99	526.08	1504.3	66	9.5	0.357
100	553.04	1503.8	76	9.4	0.319
101	567.02	1501.0	66	9.4	0.275
102	581.03	1501.0	64	9.4	0.253
103	595.06	1500.6	621	9.3	0.275
104	610.83	1504.1	78	9.6	0.341
105	623.06	1502.0	81	9.5	0.420
106	638.02	1500.4	68	9.3	0.286
107	651.04	1501.6	58	9.6	0.308
108	665.31	1503.5	56	9.3	0.253

TABLE XII-4

Long Term Leaching Data for the Fly Ash/Lime  
Solidification System (F711).

Leaching Interval	Cumulative Time [d]	Leachate Weight (g)	Conductivity (uS/cm)	pH	Concentration of Species		
					Cd (mg/L)	Cr (mg/L)	Pb (mg/L)
0	0.00	1500.0	0	7.0	<0.002	<0.002	<0.002
1	0.15	1498.0	353	11.1	0.004	0.002	0.360
2	1.01	1494.6	1410	11.8	0.006	0.009	1.020
3	1.30	1495.9	490	11.4	0.006	0.003	0.450
4	2.30	1499.6	1215	11.7	0.005	0.005	0.770
5	4.19	1494.4	1500	11.8	0.005	0.006	0.870
6	6.08	1503.0	1040	12.0	0.006	0.005	0.777
7	8.18	1491.8	1200	11.7	0.005	0.004	0.546
8	11.01	1500.6	1080	11.7	0.002	0.004	0.525
9	13.16	1500.7	560	11.7	0.003	0.003	0.264
10	17.01	1506.0	940	11.5	0.004	0.002	0.154
11	20.10	1506.4	599	11.4	0.003	0.001	0.120
12	24.03	1498.8	600	11.4	0.003	0.002	0.120
13	28.14	1503.8	520	11.4	0.002	0.002	0.165
14	32.25	1504.6	0	11.3	0.001	<0.001	0.220
15	37.30	1491.3	420	11.0	0.002	0.002	0.090
16	42.37	1497.3	375	11.0	0.007	0.003	0.075
17	48.22	1500.7	320	11.1	<0.001	0.004	0.055
18	54.21	1492.6	1140	11.0	<0.001	0.004	0.055
19	60.25	1497.8	280	10.9	0.001	0.003	0.035
20	67.04	1497.7	321	11.0	0.003	0.003	0.038
21	73.29	1501.9	267	10.9	<0.001	0.003	0.020
22	81.30	1501.4	282	10.9	<0.001	0.003	0.025
23	90.16	1501.1	275	11.1	<0.001	0.002	0.024
24	97.13	1501.9	445	10.9	0.001	0.002	0.013
25	105.15	1502.2	210	10.7	<0.001	0.003	0.010
26	112.01	1518.0	185	10.7	<0.001	0.003	0.010
27	123.25	1492.5	230	10.8	<0.001	0.004	0.011
28	130.04	1503.0	155	10.5	<0.001	0.003	0.010
29	140.22	1511.2	175	10.7	0.003	0.004	0.005
30	154.03	1498.5	188	10.7	0.002	0.006	<0.001
31	169.30	1500.0	160	10.5	0.002	0.009	0.011
32	182.22	1502.3	190	10.6	0.004	0.007	0.010
33	195.20	1501.8	160	10.5	<0.001	0.006	0.003
34	211.15	1504.1	175	10.6	<0.001	0.011	0.003
35	224.24	1501.6	160	10.7	<0.001	0.008	0.003
36	240.31	1500.1	172	10.4	0.001	0.009	0.004
37	252.11	1501.7	140	10.5	<0.001	0.010	0.004

Table XII-4 Continued

Leaching Interval	Duration (d)	Leachate Weight (g)	Conductivity (uS/cm)	pH	Concentration of Species		
					Cd (mg/L)	Cr (mg/L)	Pb (mg/L)
38	266.15	1518.0	140	10.3	<0.001	0.010	0.003
39	280.19	1500.8	125	10.8	0.002	0.009	0.007
40	294.13	1500.3	120	10.2	0.002	0.008	0.002
41	316.11	1502.7	120	10.1	0.002	0.010	0.004
42	328.26	1503.5	96	10.1	<0.001	0.007	0.003
43	343.26	1503.9	97	9.9	0.001	0.005	0.002
44	365.26	1503.2	103	9.8	0.001	0.008	0.001
45	379.31	1509.7	90	9.5	0.001	0.006	0.001
46	393.23	1510.3	95	9.8	0.002	0.005	0.001
47	406.31	1502.5	83	9.3	<0.001	0.008	0.002
48	424.27	1500.8	98	9.5	0.001	0.009	0.001
49	441.07	1500.6	94	9.4	NA	0.009	0.001
50	456.25	1500.3	92	9.7	0.001	0.009	0.001
51	472.13	1501.1	92	9.4	NA	NA	NA
52	484.02	NA	77	9.0	0.001	0.005	0.004
53	497.10	1500.6	72	8.7	0.001	0.005	0.006
54	511.00	1505.3	77	10.0	0.002	0.005	0.008
55	495.23	1500.1	75	9.7	0.002	0.005	0.013
56	526.08	1506.6	72	9.7	0.001	0.006	0.007
57	553.04	1505.9	86	9.7	<0.005	0.012	0.042
58	567.02	1500.1	71	9.6	0.003	0.011	0.032
59	581.03	1500.6	70	9.5	0.003	0.010	0.026
60	595.06	1501.5	72	9.4	0.002	0.012	0.032
61	610.03	1500.3	86	9.5	0.007	0.010	0.047
62	623.06	1500.2	85	9.7	0.013	0.010	0.002
63	638.02	1500.3	73	9.4	0.002	0.010	0.003
64	651.04	1502.1	61	9.5	0.002	0.008	0.030
65	665.31	1500.2	58	9.3	0.001	0.007	0.004



TABLE XII-5 Long Term Leaching Data for the Clay/Cement  
Solidification System (G71).

Leaching Interval	Cumulative Time [d]	Leachate Weight [g]	Conductivity [uS/cm]	pH	Concentration of As [mg/L]
0	0.00	1500.0	0	7.0	<0.002
1	0.05	1503.5	328	11.2	0.005
2	0.16	1500.6	435	11.3	0.008
3	0.29	1496.5	370	11.2	0.004
4	1.01	1509.1	1160	11.8	0.007
5	1.30	1495.8	409	11.3	0.004
6	2.00	1507.1	720	11.6	0.006
7	3.00	1506.6	830	11.5	0.008
8	3.29	1493.3	255	11.1	0.003
9	4.02	1500.1	440	11.6	0.021
10	5.08	1506.7	570	11.8	0.028
11	6.02	1501.7	540	11.4	0.021
12	7.01	1501.2	610	11.5	0.026
13	8.16	1492.2	620	11.5	0.026
14	9.29	1501.6	610	11.4	0.033
15	10.21	1501.8	460	11.3	0.026
16	12.16	1486.7	540	11.8	0.033
17	13.29	1501.9	540	11.5	0.032
18	15.02	1500.7	680	11.4	0.042
19	17.06	1500.5	670	11.5	0.075
20	18.05	1501.0	420	11.1	0.040
21	20.09	1501.0	640	11.4	0.055
22	23.06	1493.0	875	11.6	0.058
23	24.04	1500.2	350	11.2	0.032
24	26.16	1507.2	2050	11.4	0.070
25	28.22	1497.7	570	11.5	0.039
26	30.25	1500.0	490	11.4	0.065
27	33.13	1502.4	570	11.5	0.040
28	36.33	1504.5	460	11.1	0.053
29	37.32	1503.9	435	11.1	0.065
30	40.13	1500.5	500	11.3	0.100
31	42.24	1502.9	430	11.1	0.088
32	47.22	1500.6	580	11.5	0.060
33	48.33	1499.9	211	10.8	0.066
34	51.04	1498.0	422	11.2	0.075
35	55.25	1497.5	470	11.2	0.110
36	57.06	1500.4	435	11.2	0.075
37	60.11	1503.4	460	11.2	0.085
38	63.30	1496.2	470	11.2	0.085
39	66.15	1500.5	412	11.1	0.130

Table XII-5 Continued

Leaching Interval	Cumulative Time [d]	Leachate Weight [g]	Conductivity [ $\mu\text{S}/\text{cm}$ ]	pH	Concentration of As [ $\text{mg}/\text{L}$ ]
40	70.05	1498.5	470	11.3	0.121
41	74.11	1492.6	480	11.3	0.075
42	77.01	1510.6	370	11.1	0.100
43	80.30	1503.6	412	11.2	0.085
44	84.17	1509.0	430	11.2	0.110
45	88.03	1501.6	445	11.2	0.110
46	94.31	1500.6	550	11.4	0.140
47	97.31	1500.2	311	11.1	0.070
48	104.14	1507.3	520	11.2	0.145
49	108.31	1512.5	408	11.1	0.104
51	114.23	1498.2	425	11.1	0.000
52	117.24	1503.2	420	11.1	0.112
53	122.25	1502.5	268	10.9	0.140
54	126.12	1514.1	325	11.0	0.085
55	133.21	1501.0	430	11.2	0.120
56	139.22	1500.1	445	11.1	0.130
57	143.07	1510.6	425	11.1	0.110
58	153.03	1496.3	380	11.1	0.120
59	160.27	1511.1	460	11.0	0.130
60	168.25	1509.1	510	11.1	0.110
61	174.31	1500.5	440	11.1	0.125
62	181.22	1500.9	415	11.1	0.160
63	188.14	1511.2	405	11.1	0.150
64	194.20	1507.3	410	11.1	0.160
65	202.24	1504.9	420	11.1	0.180
66	210.15	1503.3	450	11.1	0.172
67	216.10	1500.7	365	11.1	0.172
68	223.24	1500.8	398	11.1	0.150
69	230.22	1509.1	400	11.1	0.150
70	239.31	1508.4	435	11.0	0.156
71	244.22	1500.8	362	10.9	0.172
72	251.11	1501.7	395	11.0	0.152
73	258.15	1508.6	332	10.9	0.195
74	265.15	1501.9	430	11.0	0.170
75	273.14	1500.8	395	11.0	0.216
76	279.19	1503.7	332	10.9	0.200
77	286.13	1500.4	308	11.0	0.180
78	293.13	1500.5	295	11.0	0.175
79	300.30	1503.9	298	11.0	0.180
80	315.11	1502.3	434	11.0	0.220

Table XII-5 Continued

Leaching Interval	Cumulative Time [d]	Leachate Weight [g]	Conductivity (uS/cm)	pH	Concentration of As [mg/L]
81	321.17	1501.2	275	10.7	0.250
82	327.26	1500.7	270	10.9	0.150
83	335.15	1500.1	245	10.7	0.300
84	342.26	1502.4	285	10.5	0.156
85	349.25	1502.8	225	10.7	0.242
86	356.25	1501.0	208	10.5	0.210
87	364.14	1502.7	NA	10.6	0.165
88	378.31	1508.5	265	10.8	0.155
89	392.23	1505.3	357	10.9	0.165
90	405.31	1509.0	285	10.8	0.210
91	423.27	1502.0	374	10.9	0.231
92	440.07	1507.3	295	10.6	0.187
93	455.25	1500.2	320	10.8	0.210
94	471.13	1505.7	305	10.6	NA
95	483.02	NA	242	10.2	NA
96	496.10	1506.0	247	9.8	0.189
97	510.00	1509.4	243	11.4	0.372
98	494.23	1501.0	236	10.9	0.210
99	525.08	1509.4	223	10.9	0.315
100	552.04	1507.8	248	10.9	0.275
101	566.02	1500.4	222	10.9	0.273
102	580.03	1501.9	192	10.8	0.231
103	594.06	1505.2	177	10.7	0.264
104	609.03	1500.3	253	10.8	0.399
105	622.06	1502.1	218	11.0	0.336
106	637.02	1500.6	201	10.8	0.315
107	650.84	1502.2	185	10.9	0.253
108	664.31	1502.3	153	10.6	0.220

TABLE XII-6 Long Term Leaching Data for the Clay/Cement  
Solidification System (G7ii).

Leaching Interval	Cumulative Time [d]	Leachate Weight [g]	Conductivity [ $\mu\text{S}/\text{cm}$ ]	pH	Concentration of Species		
					Cd [ $\text{mg}/\text{L}$ ]	Cr [ $\text{mg}/\text{L}$ ]	Pb [ $\text{mg}/\text{L}$ ]
0	0.00	1500.0	0	7.0	<0.002	<0.002	<0.002
1	0.16	1507.6	780	11.6	0.006	0.005	0.027
2	1.02	1496.0	1480	11.9	0.006	0.008	0.150
3	1.30	1496.7	450	11.3	0.004	0.002	0.030
4	2.29	1494.1	1030	11.7	0.002	0.004	0.125
5	4.02	1494.1	1050	12.0	0.009	0.006	0.264
6	6.02	1498.7	1320	11.8	0.007	0.007	0.264
7	8.16	1505.1	1100	11.7	0.003	0.005	0.220
8	11.08	1506.5	980	12.1	0.005	0.006	0.242
9	13.30	1500.1	1040	11.7	0.010	0.007	0.187
10	17.06	1501.0	1220	11.6	0.001	0.004	0.198
11	20.09	1501.0	1000	11.7	0.005	0.004	0.176
12	24.04	1510.0	1175	11.6	0.006	0.005	0.198
13	28.22	1500.9	1160	11.8	0.004	0.003	0.185
14	32.13	1501.4	960	11.7	0.003	0.003	0.130
15	37.32	1503.0	1090	11.6	0.001	0.003	0.220
16	42.24	1502.4	950	11.4	<0.001	0.005	0.170
17	48.33	1502.0	820	11.5	0.005	0.005	0.165
18	55.25	1510.0	940	11.6	0.003	0.004	0.165
19	60.11	1498.2	925	11.5	0.009	0.005	0.190
20	66.15	1497.1	900	11.5	0.015	0.006	0.180
21	67.19	1495.1	234	10.9	0.006	0.005	0.033
22	73.30	1498.3	710	11.4	0.005	0.006	0.145
23	81.06	1504.1	850	11.5	0.006	0.002	0.172
24	90.23	1503.5	950	11.5	0.001	0.002	0.210
25	97.31	1503.5	750	11.5	0.007	0.005	0.273
26	105.06	1504.7	770	11.5	0.003	0.005	0.152
27	114.23	1502.4	700	11.3	0.018	0.006	0.280
28	133.21	1500.0	800	11.4	0.002	0.004	0.126
29	139.22	1500.3	550	11.2	0.001	0.002	0.075
30	153.04	1504.3	750	11.3	0.002	0.004	0.150
31	168.26	1500.0	850	11.2	0.014	0.007	0.210
32	181.22	1501.0	810	11.3	0.008	0.007	0.165
33	194.20	1502.4	750	11.4	0.001	0.004	0.125
34	210.15	1501.0	750	11.5	0.010	0.008	0.265
35	223.24	1500.4	740	11.3	0.002	0.007	0.132
36	239.31	1519.4	780	11.3	0.003	0.008	0.132
37	251.11	1500.5	680	11.4	<0.001	0.007	0.300
38	265.15	1506.7	775	11.2	<0.001	0.007	0.125
39	279.19	1500.0	660	11.3	0.018	0.013	0.144

Table XII-6 Continued

Leaching Interval	Cumulative Time [d]	Leachate Weight [g]	Conductivity [uS/cm]	pH	Concentration of Species		
					Cd [mg/L]	Cr [mg/L]	Pb [mg/L]
40	293.13	1500.9	590	11.2	0.002	0.006	0.090
41	315.11	1502.3	670	11.1	0.002	0.007	0.125
42	327.26	1502.2	510	11.2	0.001	0.006	0.072
43	342.26	1500.5	500	11.0	0.001	0.002	0.063
44	364.27	1507.5	560	11.2	0.002	0.001	0.042
45	378.31	1500.6	420	11.0	0.003	0.003	0.030
46	392.23	1508.5	450	11.0	0.005	0.005	0.045
47	405.31	1501.1	349	11.0	0.001	0.004	0.020
48	423.27	1508.8	438	10.9	0.004	0.007	0.038
49	440.07	1501.4	400	10.8	NA	0.005	0.039
50	455.25	1507.7	362	10.9	0.011	0.006	0.031
51	471.13	1500.6	358	10.7	NA	NA	NA
52	483.02	NA	275	10.3	0.011	0.005	0.038
53	496.10	1501.5	302	9.8	0.002	0.004	0.015
54	510.00	1501.4	302	11.5	0.003	0.002	0.042
55	494.23	1500.2	306	11.0	0.002	0.001	0.030
56	525.08	1501.7	275	11.1	<0.001	0.003	0.029
57	552.04	1500.3	291	11.0	<0.005	0.005	0.165
58	566.02	1500.1	258	10.9	0.005	0.006	0.032
59	580.03	1500.7	213	10.8	0.002	0.005	0.023
60	594.06	1501.0	208	10.8	<0.001	0.005	0.034
61	609.03	1505.6	276	10.8	<0.004	0.040	0.040
62	622.06	1501.3	279	11.1	<0.001	0.001	0.013
63	637.02	1500.0	221	10.8	0.002	0.003	0.008
64	650.04	1501.4	212	10.8	0.002	0.003	0.013
65	664.31	1500.5	179	10.7	0.002	0.004	0.013

TABLE XII-7 Long Term Leaching Data for the Soluble Silicates/Cement Solidification System (H71).

Leaching Interval	Cumulative Time [d]	Leachate Weight [g]	Conductivity [uS/cm]	pH	Concentration of As [mg/L]
0	0.00	1500.0	0	7.0	<0.002
1	0.05	1497.0	1060	11.6	0.028
2	0.16	1493.2	1100	11.6	0.028
3	0.29	1493.8	880	11.6	0.028
4	1.01	1503.1	2460	12.0	0.070
5	1.30	1500.8	870	11.6	0.024
6	2.00	1498.5	1400	11.8	0.039
7	3.00	1505.9	1490	11.8	0.040
8	3.29	1496.3	460	11.3	0.016
9	4.02	1493.7	720	11.7	0.255
10	5.08	1498.8	900	11.8	0.485
11	6.02	1496.8	880	11.5	0.294
12	7.01	1507.2	860	11.6	0.315
13	8.16	1499.5	890	11.6	0.336
14	9.29	1506.5	805	11.5	0.360
15	10.31	1508.9	580	11.4	0.252
16	12.16	1500.3	675	11.8	0.630
17	13.29	1506.7	600	11.5	0.294
18	15.02	1501.3	730	11.4	0.336
19	17.06	1501.1	750	11.5	0.420
20	18.05	1501.0	430	11.2	0.220
21	20.09	1503.9	660	11.3	0.380
22	23.06	1500.4	798	11.5	0.484
23	24.04	1500.4	370	11.2	0.190
24	26.16	1500.3	1830	11.4	0.332
25	28.22	1504.5	490	11.4	0.300
26	30.25	1504.5	460	11.3	0.330
27	33.13	1500.3	550	11.5	0.375
28	35.33	1505.0	421	11.0	0.255
29	37.32	1498.2	380	11.0	0.330
30	40.13	1500.6	440	11.2	0.400
31	42.24	1503.2	352	11.0	0.330
32	47.22	1502.0	440	11.3	0.475
33	48.33	1502.6	210	10.8	0.220
34	51.04	1499.6	329	11.1	0.365
35	55.25	1509.3	388	11.1	0.410
36	57.06	1505.3	330	11.0	0.350
37	60.11	1502.6	373	11.0	0.400
38	63.30	1491.6	378	11.1	0.330
39	66.15	1502.9	330	11.0	0.320

Table XII-7 Continued

Leaching Interval	Cumulative Time [d]	Leachate Weight [g]	Conductivity [uS/cm]	pH	Concentration of As [mg/L]
40	70.05	1498.0	362	11.2	0.380
41	74.11	1493.8	357	11.1	0.360
42	77.01	1502.1	310	11.0	0.380
43	80.30	1501.0	305	11.1	0.380
44	84.17	1500.0	330	11.0	0.400
45	88.03	1502.4	322	11.0	0.440
46	94.31	1501.2	375	11.2	0.500
47	97.31	1507.8	257	11.0	0.315
48	104.14	1501.9	408	11.0	0.130
50	108.31	1501.4	299	11.0	0.375
51	114.23	1498.2	320	11.0	0.000
52	117.24	1506.0	300	11.0	0.420
53	122.25	1501.1	240	10.8	0.360
54	126.12	1503.5	280	10.9	0.315
55	133.21	1500.9	344	11.0	0.380
56	139.22	1500.1	310	10.9	0.510
57	143.07	1500.5	345	10.9	0.385
58	153.04	1523.6	292	11.0	0.430
59	160.27	1500.7	360	10.9	0.400
60	168.24	1508.3	380	11.0	0.420
61	174.31	1500.8	350	11.0	0.500
62	181.22	1500.5	332	11.0	0.570
63	188.14	1500.3	327	11.0	0.590
64	194.20	1502.1	335	11.0	0.525
65	202.24	1506.7	365	11.0	0.545
66	210.15	1492.8	330	11.0	0.560
67	216.10	1500.5	338	11.0	0.580
68	223.24	1504.8	342	11.0	0.506
69	230.22	1502.4	335	11.0	0.530
70	239.31	1504.5	350	10.9	0.546
71	244.22	1501.4	342	10.9	0.690
72	251.11	1502.5	330	10.9	0.570
73	258.15	1499.6	303	10.9	0.610
74	265.15	1509.7	400	10.9	0.546
75	273.14	1500.8	335	10.9	0.650
76	279.19	1503.8	300	10.8	0.690
77	286.13	1501.5	280	10.9	0.610
78	293.13	1501.6	285	10.9	0.585
79	300.30	1502.7	280	10.9	0.480
80	315.11	1509.0	345	10.9	0.530

Table XII-7 Continued

Leaching Interval	Cumulative Time [d]	Leachate Weight [g]	Conductivity [uS/cm]	pH	Concentration of As [mg/L]
81	321.17	1500.6	270	10.6	0.780
82	327.26	1503.9	260	10.9	0.480
83	335.15	1506.8	248	10.6	0.545
84	342.28	1500.7	250	10.5	0.756
85	349.25	1511.6	240	10.7	0.610
86	356.25	1501.5	240	10.6	0.610
87	364.26	1500.0	NA	10.7	0.680
88	378.31	1500.5	261	10.8	0.650
89	392.23	1504.1	305	10.8	0.253
90	405.31	1500.8	240	10.7	0.756
91	423.27	1501.4	268	10.6	0.925
92	440.07	1500.1	275	10.6	0.820
93	455.25	1507.5	295	10.8	0.800
94	471.13	1505.6	275	10.5	NA
95	483.02	NA	232	10.1	1.785
96	496.10	1500.6	239	9.6	0.189
97	510.00	1510.6	239	11.3	1.116
98	494.23	1500.3	254	10.8	0.819
99	525.08	1502.0	233	10.9	1.050
100	552.04	1501.4	254	10.9	1.224
101	566.02	1500.6	218	10.8	0.987
102	580.03	1500.9	220	10.8	0.945
103	594.06	1500.2	223	10.7	0.987
104	609.03	1500.2	272	10.8	1.275
105	622.06	1502.6	266	10.8	1.071
106	637.02	1501.1	205	10.7	1.071
107	650.04	1500.2	203	10.9	0.945
108	664.31	1501.9	194	10.6	0.924



TABLE XII-8 Long Term Leaching Data for the Soluble Silicate  
Solidification System (H711).

Leaching Interval	Cumulative Time [d]	Leachate Weight [g]	Conductivity [uS/cm]	pH	Concentration Cd [mg/L]
0	0.00	1500.0	0	7.0	<0.002
1	0.16	1500.7	2000	11.9	0.005
2	1.02	1500.3	3400	12.1	0.005
3	1.30	1492.1	910	11.6	0.002
4	2.29	1503.9	1830	11.9	0.004
5	4.02	1505.5	1710	12.1	0.012
6	6.02	1498.5	1998	11.9	0.014
7	8.16	1497.2	1610	11.8	0.010
8	11.08	1505.1	1210	12.1	0.004
9	13.30	1504.2	1200	11.7	0.011
10	17.06	1501.0	1300	11.7	0.003
11	20.09	1509.5	1060	11.6	0.008
12	24.04	1499.5	1075	11.6	0.009
13	28.22	1501.8	970	11.7	0.012
14	33.13	1504.8	730	11.6	0.003
15	37.32	1501.7	420	11.5	0.005
16	42.24	1499.6	720	11.5	0.007
17	48.33	1500.7	600	11.4	0.001
18	55.25	1497.1	650	11.4	0.004
19	60.11	1502.8	600	11.3	0.018
20	66.15	1505.5	575	11.3	0.018
21	67.19	1499.7	235	10.9	0.050
22	73.30	1500.6	440	11.2	0.050
23	81.06	1505.1	500	11.3	0.006
24	90.23	1500.1	540	11.4	0.003
25	97.31	1500.7	465	11.3	0.004
26	105.06	1504.9	470	11.3	0.005
27	114.23	1500.4	430	11.1	0.006
28	133.21	1496.0	455	11.2	0.005
29	139.22	1500.3	405	11.0	0.011
30	153.04	1500.1	406	11.2	0.055
31	168.30	1502.0	466	11.0	0.035
32	181.22	1500.3	470	11.1	0.040
33	194.20	1501.8	450	11.2	0.005
34	210.15	1505.3	515	11.2	0.009
35	223.24	1500.1	480	11.2	0.006
36	239.31	1502.7	500	11.1	0.032
37	251.11	1501.7	460	11.2	0.004
38	265.15	1505.1	640	11.1	0.006
39	279.19	1500.4	450	11.1	0.007

Table XII-8 Continued

Leaching Interval	Cumulative Time [d]	Leachate Weight [g]	Conductivity [uS/cm]	pH	Concentration Cd [mg/L]
40	293.13	1500.8	430	11.1	0.006
41	315.11	1510.0	460	11.1	0.012
42	327.26	1502.1	425	11.1	0.005
43	342.26	1500.7	420	10.9	0.007
44	364.14	1501.8	435	11.0	0.008
45	378.31	1504.1	378	10.9	0.060
46	392.23	1509.5	420	11.0	0.005
47	405.31	1510.5	353	10.9	0.001
48	423.27	1501.0	375	10.8	0.004
49	440.07	1508.4	400	10.8	NA
50	455.25	1504.6	375	10.9	0.011
51	471.13	1503.6	353	10.7	NA
52	483.02	NA	295	10.3	0.013
53	496.10	1500.1	281	9.7	0.035
54	510.00	1515.0	276	11.4	0.011
55	494.23	1500.5	296	11.0	0.008
56	525.08	1504.2	272	11.0	0.030
57	552.04	1502.1	316	11.0	0.007
58	566.02	1500.4	278	11.0	0.015
59	580.03	1500.1	257	10.9	0.020
60	594.06	1502.5	267	10.9	0.007
61	609.03	1506.4	300	10.8	0.024
62	622.06	1501.0	298	10.9	0.007
63	637.02	1500.2	247	10.9	0.007
64	650.04	1501.2	240	11.0	0.022
65	664.31	1500.2	212	10.7	0.007

Table XII-9 Weight changes of the specimens in the dynamic test (Test 7) after 1 year of leaching.

Batch	Solidification System	Measured sample weight [g]		Calculated weight lost by leaching [g]	Net water absorbed [g]
		Initial	Final		
EI	Fly ash-cement	225.5	238.4	6.0	18.9
EII	Fly ash-cement	213.5	238.6	6.0	31.1
FI	Fly ash-lime	213.7	227.2	5.7	19.2
FII	Fly ash-lime	206.3	227.0	6.2	26.9
GI	Clay-cement	202.5	204.0	12.1	13.6
GII	Clay-cement	206.4	206.9	12.1	12.6
HI	Sol sil-cement	163.4	164.9	17.5	19.0
HII	Sol sil-cement	174.0	184.2	19.6	29.8

Note: All numbers are average of replicates.

Figure XII-1 Concentration history

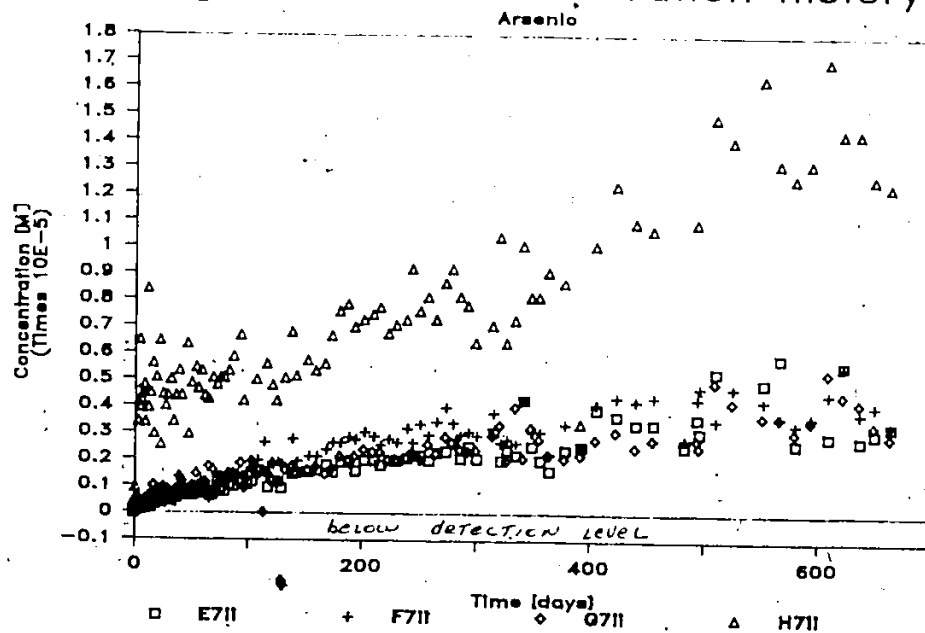


Figure XII-2 Concentration history

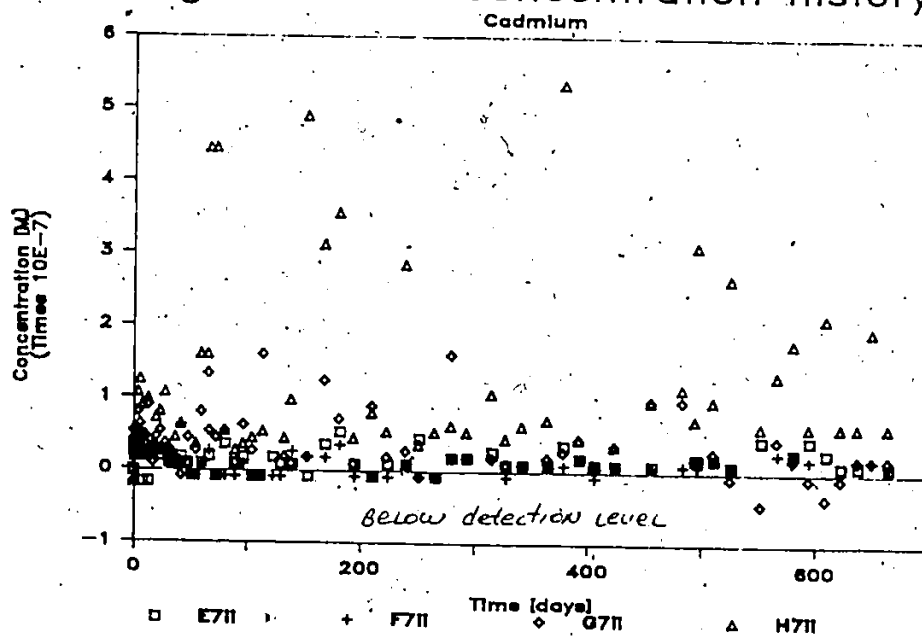


Figure XII-3 Concentration history

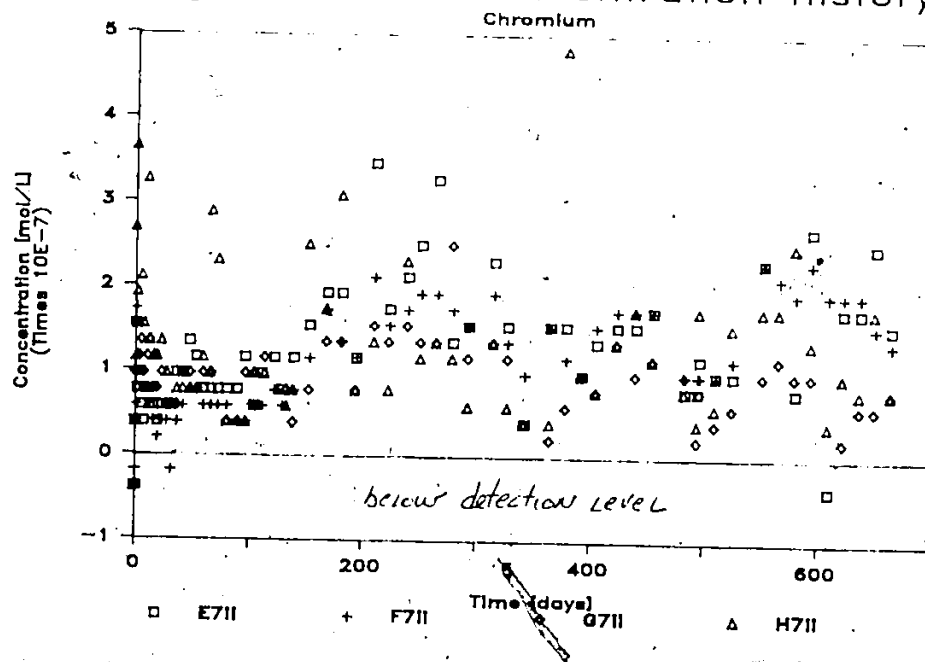
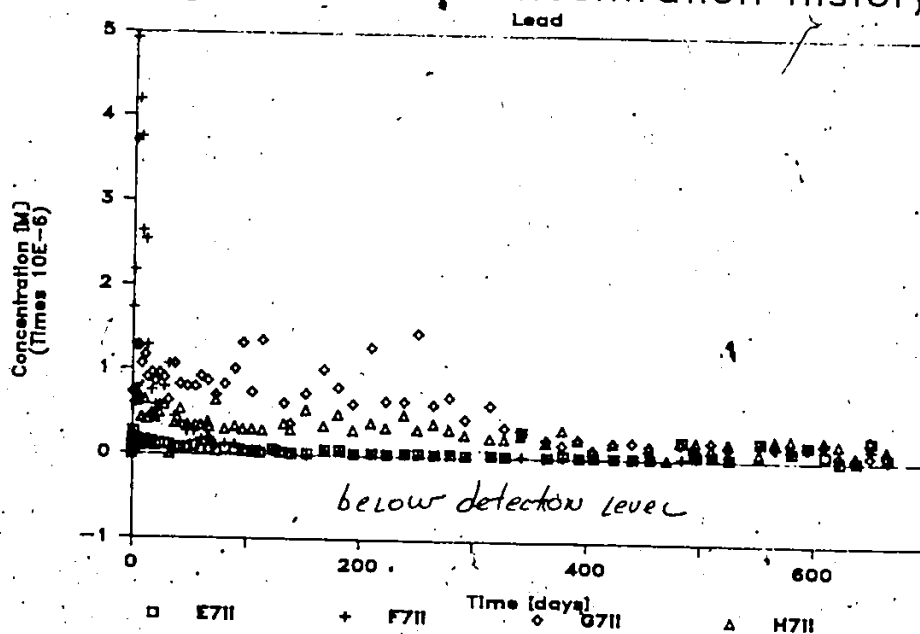


Figure XII-4 Concentration history



## APPENDIX XIII

## LONG TERM LEACHING SCENARIOS

Table XIII-1	Long Term Leaching Scenario A
Table XIII-2	Long Term Leaching Scenario B
Table XIII-3	Long Term Leaching Scenario C
Table XIII-4	Long Term Leaching Scenario D
Table XIII-5	Long Term Leaching Scenario E
Table XIII-6	Long Term Leaching Scenario F
Table XIII-7	Long Term Leaching Scenario H
Table XIII-8	Long Term Leaching Scenario I

SETTING OF MASTER VARIABLES

- Static groundwater
- Any composition of groundwater
- Any type of matrix
- Any mobility of contaminant

CONTROLLING LEACHING MECHANISMS

A finite volume of groundwater surrounds the waste form and it is not renewed in time. Leaching is initially controlled by surface exchanges and diffusion. The leaching rates rapidly decrease with time as a result of accumulation of the contaminant in the groundwater.

SETTING OF SECONDARY VARIABLES

N/A

CALCULATED LEACHING RATES

Initially identical to the leaching rates calculated for scenarios B, C or D.

EXTRAPOLATION

The leaching rate will rapidly decrease to zero as the system approaches equilibrium.

TABLE XIII-2, LONG TERM LEACHING SCENARIO B

SETTING OF MASTER VARIABLES

- Groundwater flowing around the waste
- Mobile contaminant
- Any composition of groundwater
- Any matrix permeability

CONTROLLING LEACHING MECHANISMS

Leaching is limited by the rate of diffusion of the mobile contaminant in the pores of the matrix. There is no surface mass transfer resistance. It is assumed that the rate of groundwater renewal at the interface is sufficient to maintain a zero surface concentration and that the waste form is semi-infinite. Equation 3.3 is used to calculate the leaching rate:

$$L = C_T \left( \frac{D_e^{1/2}}{\pi t} \right) \quad 3.3$$

SETTING OF SECONDARY VARIABLES

$$C_T = 0.0384 \text{ mol/L}$$

$$D_e = 10^{-5} \text{ or } 10^{-6} \text{ cm}^2/\text{sec}$$

The range in diffusivities accounts for the variation of the molecular diffusion coefficient from species to species and for the tortuosity of the matrix.

CALCULATED LEACHING RATES

Time (years)	Leaching Rate (mmol/m <sup>2</sup> ·d)	
	$D_e = 10^{-6}$	$D_e = 10^{-5}$
0.01	33.3	105.4
0.05	14.9	47.1
0.1	10.5	33.3
0.5	4.7	14.5
1.0	3.3	10.5
5.0	1.5	4.7
10.0	1.1	3.3

The depth of penetration of the leaching front can be calculated using Equation 5.2



$$\left( \frac{C_p - C_1}{C_0 - C_1} \right) = \operatorname{erf} \left( \frac{z}{2(D_e t)^{1/2}} \right) \quad 5.2$$

where  $C_1$ , the surface concentration is set equal to zero.

Using the maximum value of  $D_e$ ,  $10^{-5}$  cm<sup>2</sup>/sec and the penetration criterion that the concentration at a point changed by 2% with respect to its initial value, we calculate that leaching starts affecting the centre of the 2 m slab after about 10 years.

#### EXTRAPOLATION

After 10 years, the rate will be lower than those calculated for a semi-infinite medium because the concentration at the middle of the 2 m slab will start decreasing.

TABLE XIII-3, LONG TERM LEACHING SCENARIO C

SETTING OF MASTER VARIABLES

- Groundwater flowing around the waste
- Low pH groundwater
- Insoluble contaminant
- Any matrix permeability

CONTROLLING LEACHING MECHANISMS

The leaching rate is initially controlled by the amount of acid available to neutralize the waste form matrix. It is assumed that (i) cement ANC is used up before metals are solubilized (ii) only a fraction of the total contaminant concentration is available for leaching and (iii) the matrix does not entirely dissolve. As a result of assumption (iii) diffusion of ions between the groundwater - waste form interface and the leaching front will eventually become rate limiting.

SETTING OF SECONDARY VARIABLES● Rate of Acid Contacted

Leachant velocity:  $\frac{50 \text{ m}^3}{\text{m}^2 \cdot \text{year}}$

Acid concentration:  $10^{-3} \text{ mol/L}$

+ Rate of acid contacted:  $137 \frac{\text{mmol}}{\text{m}^2 \cdot \text{d}}$

● ANC of the Matrix

ANC of hydrated portland cement:  $15 \frac{\text{meq}}{\text{g dry cement}}$   
(Section 7.2.2)

Cement dosage: 0.2 - 0.6 kg/kg of waste  
(Côté and Hamilton, 1983)

Volume increase as a result of solidification: 20 to 100%  
(Côté and Hamilton, 1983)

+ 150 to 250  $\frac{\text{kg dry cement}}{\text{m}^3 \text{ treated waste}}$

$$+ 2.25 \times 10^6 \text{ to } 3.75 \times 10^6 \frac{\text{meq}}{\text{m}^3 \text{ waste form}}$$

use  $2.5 \times 10^6$  for calculations

• Availability for leaching

Measured leaching efficiency varies from 10% to 50%  
(Table 7.4)

CALCULATE LEACHING RATES

leaching rate = rate of matrix neutralization  $\times$  contaminant concentration  $\times$  leaching efficiency

$$\left[ \frac{\text{m}^3}{\text{m}^2 \cdot \text{d}} \right] \times \left[ \frac{\text{mmol}}{\text{m}^3} \right] \times [ \quad ]$$

for leaching efficiency = 10%

$$\text{leaching rate} = \frac{137}{2.5 \times 10^6} \times 3.84 \times 10^4 \times 0.10 = 0.21 \frac{\text{mmol}}{\text{m}^2 \cdot \text{d}}$$

for leaching efficiency = 50%

$$\text{leaching rate} = \frac{137}{2.5 \times 10^6} \times 3.84 \times 10^4 \times .5 = 1.05 \frac{\text{mmol}}{\text{m}^2 \cdot \text{d}}$$

The leach rate is constant, function of the rate of acid contacted until diffusion through the leach layer becomes rate limiting.

EXTRAPOLATION

It is assumed that diffusion through the leached layer becomes rate limiting after 1 year.

SETTING OF MASTER VARIABLES

- Groundwater flowing around the waste
- Neutral groundwater
- Insoluble contaminant
- Any matrix permeability

CONTROLLING LEACHING MECHANISMS

This situation corresponds to the long term leaching test conditions (Section 7.4). Leaching rates are controlled by diffusion in the waste matrix. There is chemical equilibrium between the soluble and the insoluble fractions of the contaminant. Equation 3.3 is applicable with an effective diffusion coefficient given by Equation 3.8.

SETTING OF SECONDARY VARIABLES

Value of  $D_e = 10^{-12}$  to  $10^{-13}$   $\text{cm}^2/\text{sec}$

selected from Table 7.6 or from Equation 3.8 and 3.5 assuming a  $D$  value of  $10^{-6}$  and  $K_d$  values of  $10^6$  or  $10^7$ .

Those  $D_e$  values derived from the long term leaching tests include the effect of availability for leaching.

CALCULATED LEACHING RATES

Time (years)	Leaching Rate $D_e = 10^{-13}$	$\text{mmol}/\text{m}^2 \cdot \text{d}$ $D_e = 10^{-12}$
0.01	0.01054	0.03333
0.05	0.00471	0.01491
0.1	0.00333	0.01054
0.5	0.00149	0.00471
1	0.00047	0.00149
10	0.00033	0.00105

EXTRAPOLATION

The rates can be extrapolated since they are so low that even after 100 years, the center of a 2 m thick slab would not be affected by leaching.

SETTING OF MASTER VARIABLES

- Groundwater flowing through the waste
- Any composition of groundwater
- Soluble contaminant
- Low waste permeability

CONTROLLING LEACHING MECHANISMS

Leaching takes place via convective transport. The groundwater flows through the waste following Darcy's law and is subjected to a hydraulic gradient varying between 1.0 to 5.

SETTING OF SECONDARY VARIABLES

slab = 2 m thick

CALCULATION OF LEACHING RATES

Darcy's law

$$\frac{q}{A} = ki \quad \frac{\text{m}^3}{\text{m}^2 \cdot \text{sec}}$$

where  $q$  = flow rate  
 $A$  = surface area  
 $k$  = coefficient of permeability  
 $i$  = hydraulic gradient

$$L = k i \times C_p \times 3600 \times 24 \times 10^6$$

where

$C_p$  = pore concentration

$$k = 10^{-8}$$

$$C_p = 0.1 \text{ mol/L}$$

$$i = 1.0 \text{ to } 5.0$$

$$C_p = 0.1 \text{ mol/L pore solution}$$

$$L (i = 1.0) = 86.4 \text{ mmol/m}^2 \cdot \text{d}$$

$$L (i = 5.0) = 432 \text{ mmol/m}^2 \cdot \text{d}$$

### EXTRAPOLATION

Calculate the time for the front to go through

$$\frac{q}{A} = k i$$

for  $i = 1.0$

$$\frac{q}{A} = 10^{-8} \times 1.0 \times 3600 \times 24 \times 365$$

$$\frac{\text{m}}{\text{sec}} \times \frac{\text{sec}}{\text{h}} \times \frac{\text{h}}{\text{d}} \times \frac{\text{d}}{\text{year}}$$

$$= .315 \text{ m/year} \rightarrow 0.315 \text{ year}$$

similarly, for  $i = 5.0$

$$\text{duration} = 1.268$$

TABLE XIII-6, LONG TERM LEACHING SCENARIO F

Conditions similar to scenario E except for permeability =  $10^{-6}$  m/sec as a result of a failure of the physical containment system.

Leaching rate is directly proportional to permeability and thus 100 times larger.

Duration of leaching is inversely proportional to permeability and thus 100 times smaller.

SETTING OF MASTER VARIABLES

- Groundwater flowing through the waste
- Immobile contaminant
- Low matrix permeability
- Any composition of groundwater

CONTROLLING LEACHING MECHANISMS

Leaching takes place via convective transport. Darcy's law is applicable. Only the fraction soluble is transported. The groundwater also washes off the ANC (faster in the cases where the leachant has a low pH. Because of the low permeability, the process is so slow that interface phenomena (Scenario C) should control. There will eventually be a breakthrough.

SETTING OF SECONDARY VARIABLES

permeability  $10^{-8}$  m/sec

- ANC (from scenario C):  $2.5 \times 10^6$  mmol/m<sup>3</sup>

flow rate (from scenario E)

$$i = 1.0 \quad Q = 0.35 \frac{\text{m}^3}{\text{m}^2 \cdot \text{year}}$$

$$i = 5.0 \quad Q = 1.575 \frac{\text{m}^3}{\text{m}^2 \cdot \text{year}}$$

- rate of acid added:

$$\begin{aligned} \text{for } i = 1.0, \quad & .315 \frac{\text{m}^3}{\text{m}^2 \cdot \text{year}} \times 10^{-3} \frac{\text{M}}{\text{L}} \frac{1000 \text{ L}}{\text{m}^3} \frac{1000 \text{ mmol}}{\text{M}} \\ & = 315 \frac{\text{mmol}}{\text{m}^2 \cdot \text{year}} \end{aligned}$$

$$\text{for } i = 5.0, \quad 1575 \frac{\text{mmol}}{\text{m}^2 \cdot \text{year}}$$



LEACHING RATES

$$L = K_i C_p \quad 3600 \times 24 \times 10^6 \text{ (from scenario E)}$$

$$\text{assume } C_p = 10^{-5} \text{ mol/L}$$

$$L (i=1.0) = 10^{-8} \times 1.0 \times 10^{-5} \times 3600 \times 24 \times 10^{-6}$$

$$= 0.0086 \frac{\text{mmol}}{\text{m}^2 \cdot \text{d}}$$

$$L (i = 5) = 0.0432 \frac{\text{mmol}}{\text{m}^2 \cdot \text{d}}$$

EXTRAPOLATION

Leaching will take place at a constant rate until all the ANC has been washed off and the metals start coming out.

$$\text{ANC} = 2.5 \times 10^6 \frac{\text{mmol}}{\text{m}^3} \qquad \text{acid added } 315\text{-}1575 \frac{\text{mmol}}{\text{m}^2 \cdot \text{year}}$$

$$\text{calculate depth neutralized per year}$$

$$i = 1.0 \quad \frac{315 \frac{\text{mmol}}{\text{m}^2 \cdot \text{year}}}{2.5 \times 10^6 \frac{\text{mmol}}{\text{m}^3}} = .00013 \text{ m/year}$$

$$i = 5.0 \qquad = .00063 \text{ m/year}$$

time for breakthrough to occur

$$i = 1.0, \quad \frac{2 \text{ m}}{.00013 \frac{\text{m}}{\text{year}}} = 15873 \text{ years}$$

$$i = 5.0, \quad = 3174 \text{ years}$$

TABLE XIII-8, LONG TERM LEACHING SCENARIO H

Conditions similar to Scenario except for permeability =  $10^{-6}$  m/sec as a result of failure of the physical containment systems.

Leaching rates are 100 x larger

$$\text{for } i = 1.0, \quad 0.86 \frac{\text{mmol}}{\text{m}^2 \cdot \text{d}}$$

$$\text{for } i = 5.0, \quad 4.32 \frac{\text{mmol}}{\text{m}^2 \cdot \text{d}}$$

Breakthrough time are 100 times faster

$$\text{for } i = 1.0, \quad 158 \text{ years}$$

$$\text{for } i = 5.0, \quad 31.7 \text{ years}$$